COBALT INDUCED CARDIOTOXICITY: A SUSPECTED ADVERSE EFFECT ASSOCIATED WITH COCR ALLOY ORTHOPAEDIC IMPLANTS

by

SARUNYA LAOVITTHAYANGGOON

2018

THE THESIS IS SUBMITTED IN PARTIAL FULFILMENT
FOR THE DEGREE OF

DOCTOR OF PHILOSOPHY IN BIOMEDICAL ENGINEERING

DEPARTMENT OF BIOMEDICAL ENGINEERING
UNIVERSITY OF STRATHCLYDE

Declaration of Author's Rights

This thesis is the result of the author’s original research. It has been composed by the author and has not been previously submitted for examination which has led to the award of a degree.

Signed:

Date:

Abstract

Cobalt toxicity, arising from the release of metal nanoparticles and ions during wear of Co/Cr metal-on-metal (MoM) hip implants has become a recognised internal source of Co poisoning. Co ions enter the bloodstream during wear and corrosion processes of MoM implants, and then travel throughout the body causing systemic toxicity. Cardiac toxic manifestations have been shown to be among the most prevalent systemic symptoms following exposure. In this thesis we have investigated the effects of short and/or long term $CoCl_2$ exposure on the Swiss 3T3 fibroblast cell line (3T3s) and primary adult cardiac fibroblasts (CFs) *in vitro.* We have measured effects on cell viability, morphology, proliferation, assessed intracellular Co uptake, and detected and quantified protein expression by western blotting. Further, we also studied the effects of chronic *in vivo* $CoCl_2$ treatment (4 weeks of daily 1mg/kg intraperitoneal injections) of rats carrying out echocardiography, and determining the Co distribution into various organs. The expression of potential transporter proteins, TRPC6, TRPM7, DMT1, and of CAMKIIδ, a serine/threonine kinase with pivotal roles in cardiovascular function through regulation of Ca^{2+} handling and excitation-contraction coupling, were also investigated. To complete the *in vitro* and *in vivo* studies, the molecular mechanism(s) underlying the overall changes were screened by RNA-Seq analysis, and gene expression was subsequently validated by quantitative real-time-PCR (RT-qPCR) and western blotting.

In terms of proliferation of 3T3 cells and CFs treated with $CoCl_2$, the CFs were much more sensitive than 3T3 cells with IC_{50} values for $CoCl_2$ in the range of ~20 µM in CFs and ~250 µM in 3T3 cells. Using phalloidin to stain the actin inside cells showed that in both types of cells actin fibres were disrupted, and the membrane formed blebs at high Co concentrations. Co uptake, evaluated at the cellular level by using inductively coupled plasma mass spectrometry (ICP-MS), revealed 3 to 4-times greater Co uptake into CFs than 3T3 cells at 48 h.

In vivo studies using echocardiography showed evidence of altered cardiac function in Co treated rats after 28 days exposure. Reduction of the percentage of fractional shortening (%FS), from 60.29±0.53%, to 54.01±0.90% n=6, $p<0.05$, (Co-treated compared to normal rats) occurred. This could imply early indications of cardiac

dysfunction. Co accumulated in the organs of the rats and significant increases in Co ion levels (compared with control untreated animals) were detected in liver, kidney and heart (1,839.86±177.30, 1,536.01±83.95, and 307.82±35.74 µg/L respectively) by ICP-MS after 7 days exposure. Liver and kidney are the primary organs of excretion, and higher concentrations than other organs might be expected. However, these data provide strong evidence that Co accumulates in the hearts of the treated rats and this may result in cardiac dysfunction.

Western blot analysis of CFs, and heart tissue lysates from animals treated with $CoCl_2$ for 28 days, showed a significantly increased level of protein expression for CaMKIIδ, TRPC6 and TRPM7. In contrast, in 3T3 cells, the expression of TRPs was decreased at high concentrations of Co. TRP transport channel proteins are likely to act as ubiquitous metal ion flux pathways, and may play a role in uptake of Co^{2+} into the heart enabling it to contribute to compromised heart function.

Gene expression analysis of *Camkiid*, *Dmt1*, *Trpc6*, *Trpm7*, and *Trpv1* using RNA-Seq and RT-qPCR, found all had increased expression levels in heart RNA after 28 days exposure. RT-qPCR analysis showed there were increased levels in 4 out of the 5 selected genes (*Camkiid*, *Dmt1*, *Trpc6*, and *Trpm7*) in CFs after 72 h Co treatment. In contrast, *Trpc6* mRNA expression was absent in 3T3 cells using RNA-Seq and RT-qPCR. These results suggest the differential uptake of Co^{2+} between CFs and 3T3 cells might be mediated through *Trpc6*.

Sequestration of Co into cardiac cells *in vitro* and *in vivo*, suggests that *in vivo* the metal may accumulate in the hearts of MoM patients with high circulating Co blood levels. This may lead to systemic adverse effects including cardiotoxicity. Inhibition or downregulation of Co uptake mechanisms into cardiac cells may offer a therapeutic intervention to minimise adverse effects of Co in patients with MoM implants. We recommend careful monitoring of cardiac function in MoM patients, in addition to the blood metal ion level monitoring and scans already instigated by MHRA.

Acknowledgements

I would like to express my deep gratitude and very great appreciation to Professor Helen Grant, for her guidance, valuable and constructive suggestions, continuous support, encouragement, infinite patience, and especially for putting pressure to keep pushing me to accomplish my goal. I really appreciate the warm welcome I have received. And I am sincerely grateful to Dr. Susan Currie and Dr. Rothwelle Tate for their valuable motivation and guidance throughout my PhD studies always finding time to help me and guide me. It has been a great pleasure to work with them, and the experience gained during this time has widened my vision.

I am particularly grateful for the assistance energetically given by Mrs. Catherine Henderson for helping me to carry out my experiments. Without Katie's great help, it would have been impossible to complete all experiments on time. I would also like to thank Mr. Brian Cartilage and the members of technical staff in the Biological Procedures Unit (BPU), Strathclyde Institute of Pharmacy & Biomedical Sciences (SIPBS) and our lab, as well as a number of lecturers for their assistance, advice and timely help throughout the PhD.

A big thank you goes to our group, Peter, Riduan, Ibrahim and Laura, for providing invaluable caring and support during my experiments. I am extremely thankful to Sara Gómez Arnaiz, my great buddy, who always provided encouragement and laughs and mostly for keeping me sane throughout the PhD.

I am enormously grateful to all Thai friends at the University of Strathclyde (Aom, Pam and Eddy, P'Koi, Pat, P'Ann, P'Amy, Seng&B and Wee Peak, Jet, Zite, N'A, N'Anne, N'Mai) for making me life easier in Glasgow. I am also tremendously thankful to P'Ple, my flatmate, who was always beside me, cheering up and being fully supportive all my PhD life. There are many good friends and colleague (in the UK and outside the UK) who are not mentioned here, but I wish them to know that they are an important part of my success.

I would like to acknowledge the Royal Thai Government and Thailand Institute of Scientific and Technological research (TISTR) for funding this PhD work.

Finally, Thanks Mom and Dad for bringing me into the world. I owe everything to my parents for what I am today and I forever place them on a pedestal. My parents, whose love, sacrifices, endless support, faith in me and patience have allowed me to achieve my goals. My brother (Pikky Bob) who in his own way has also been so supportive, and who takes care of our parents. And my brother does everything to keep the family joy and happy. My aunt (Toy) for the encouragement and supportive for everything I do. Thank you all from the bottom of my heart.

Contents

List of Tables

List of Figures

List of Abbreviations and Symbols

%	Percent
(A)	Adenine
(C)	Cytosine
(G)	Guanine
(GC)	Guanine-cytosine
(T)	Thymine
(xg)	gravity
µg	microgram
µg/L	micrograms per liter
µg/ml	micrograms per milliliter
µl	microliter
µM	micromolar
$^{\cdot}OH$	Hydroxyl radical
3T3	3T3 cell line
A	Absorbance
AEBSF	4-(2-Aminoethyl) benzenesulfonyl fluoride hydrochloride
AF	Atrial fibrillation
ANOVA	Analysis of variance
ANP	Natriuretic peptide
APS	Ammonium persulfate
ATP	Adenosine triphosphate
AW	Anterior wall
B2m	Beta 2 microglobulin
BGI	Beijing Genome Institute
BHI	Brain heart infusion
bp	Base pair
BP	Biological process
BrdU	bromodeoxyuridine
BSA	Bovine serum albumin
BW	Body weight
C	Celcius
Ca^{2+}	Calcium/
CaMKII	Calcium/calmodulin–dependent protein kinase II
CaMKIID/*Camkiid*	Calcium/calmodulin–dependent protein kinase II delta
CaMKIIδ	Calcium/calmodulin–dependent protein kinase II delta
CC	Cellular component
CD31	cluster of differentiation 31
cDNA	complementary DNA
CF	Cardiac fibroblast
CO	Cardiac output
Co	cobalt
CO_2	Carbon dioxide
CoCr	Cobalt Chromium
$CoCl_2$	Cobalt chloride
COMB	Combine
CFDA	Carboxyfluorescein diacetate

Cont	Control
Cr	Chromium
Ct	Cycle threshold
CV	Crystal violet
D	Day
DAG	Diacylglycerol
DAPI	4',6-diamidino-2-phenylindole
DCT1	Divalent cation transporter
DEPC	Diethyl pyrocarbonate
DM	Diabetes mellitus
DMEM	Dulbecco's modified eagle's medium
DMSO	Dimethyl sulfoxide
DMT1	Divalent metal transporter 1
DNA	Deoxyribonucleic acid
dNTP	Deoxynucleotide
DRG	Dorsal root ganglion
DTT	Dithiothreitol
DW	Distilled water
ECACC	European collection of cell cultures
ECL	Enhanced chemiluminescent
ECM	Extracellular matrix
EDD	End-diastolic diameter
EF	Ejection fraction
ESD	End-systolic diameter
FBS	Fetal Bovine Serum
FITC	Fluorescein isothiocyanate
FRKM	Fragments per kilobase of exon per million fragments mapped
FS	Fractional shortening
g	Gram
GAPDH/*Gapdh*	Glyceraldehyde-3-phosphate dehydrogenase
GC	Gas chromatography
gDNA	Genomic DNA
GO	Gene Ontology
GRd	Glutathione reductase
GSEA	Gene Set Enrichment Analysis
GSH	Glutathione
h	Hour
H_2O_2	Hydrogen peroxide
HepG2	Liver hepatocellular cells
HF	Heart failure
HIF	Hypoxia-inducible factor
HRP	Horseradish peroxidase
HSG	Human submandibular gland cell line
Hz	Hertz
i.p.	Intra-peritoneal
IC_{50}	Half maximal inhibitory concentration
ICP-MS	Inductively coupled plasma mass spectrometry
IgG	Immunoglobulin G

IL-1β	Interleukin 1 beta
IL-6	Interleukin 6
IL-8	Interleukin 8
kDa	Kilodalton
KEGG	Kyoto Encyclopedia of Genes and Genomes
kg	Kilogram
LA	Left atrial
LC3	Microtubule-associated protein light chain 3
LV	Left ventricular
LVEDD	Left ventricular end-diastolic diameter
LVESD	Left ventricular end-systolic diameter
LVPW	Left ventricular posterior wall
LVPWd	Left ventricular posterior wall end diastole
LVPWs	Left ventricular posterior wall end systole
MF	Molecular function
mg	Milligram
mg/kg	Milligrams to kilograms
MHRA	The Medicines and Healthcare products Regulatory Agency
min	Minute
ml	Milliliter
MM	Master mix
MoM	Metal-on-metal
mM	Millimolar
mnth	Month
mRNA	Messenger RNA
MTT	(3-(4,5-Dimethylthiazol-2-yl)-2,5-Diphenyltetrazolium Bromide)
mΩ	Milliohm
NA	Numerical aperture
NCBI	National Center for Biotechnology Information
Ndfip1	Nedd4 family interacting proteins
Ndfip2	Nedd4 family interacting proteins
NEAA	Non-essential amino acids
Nedd4	Neural precursor cell expressed developmentally down-regulated protein 4
NHS	The National Health Service
NJR	The National Joint Registry
nm	Nanometer
NR	Neutral red
Nramp2	Natural resistance-associate macrophage pretein 2
O_2^-	Superoxide radicals
OD	Optical density
Oligo(dT)	Oligo deoxythymine
ox-CaMKII	oxidised-CaMKII
P/S	Penicillin&Streptomycin
P2X7	Purinoceptor 7
PBS	Phosphate-buffered saline
PC12	Rat pheochromocytoma cell

p-CaMKII	Phospho-CaMKII
PCR	Polymerase chain reaction
PE read	Paired-end read
PI	Propidium iodide
Pgk1	Phosphoglycerate kinase 1
ppb	Parts per billion
ppm	Parts per million
p-value	Probability value
PW	Posterior wall
QC	Quality control
Ref	Reference
RNA	Ribonucleic acid
RNase	Ribonuclease
ROS	Reactive oxygen species
Rpl13a	Ribosomal protein L13a
rpm	Round per minute
RT	Room temperature
RT(-)	Minus-reverse transcriptase
RT(+)	Plus-reverse transcriptase
RT-PCR	Reverse transcription polymerase chain reaction
RT-qPCR	Quantitative reverse transcription polymerase chain reaction
SAB	Sabouraud's medium
Sc	Scandium
SD	Sprague Dawley
SD	Standard deviation
SD rats	Sprague Dawley rats
SDS	Sodium dodecyl sulfate
SDS-PAGE	Sodium dodecyl sulfate polyacrylamide gel electrophoresis
SE read	Single-end read
sec	Second
SEM	Standard Error of Measurement
SEP	Separate
Srp14	Signal recognition-particle 14 KDa
SV	Stroke volume
Tbp	TATA-Box Binding Protein
TEMED	N,N,N′,N′-Tetramethylethylenediamine
Temp	Temperature
TMB	Tetra-methylbenzidine
TNF	Tumor necrosis factor
TNF-α	Tumor necrosis factor alpha
TRP	Transient receptor potential
TRPC6/ *Trpc6*	Transient receptor potential cation channel, subfamily C, member 6 or transient receptor potential canonical 6
TRPM7/ *Trpm7*	Transient receptor potential cation channel, subfamily M, member 7, or transient potential melastatin-7
TRPV1/ *Trpv1*	Transient receptor potential cation channel, subfamily V, member 1 or transient receptor potential vanilloid 1

TUNEL	Terminal deoxynucleotidyl transferase (TdT) dUTP Nick-End Labeling
UCSC	University of California
UDG	Uracil-DNA glycosylase
V	Volt
v/v	Volume/Volume
Vm	Vimentin
VWF	Von Willebrand Factor
w/v	Weight/Volume
W	Watt
wk	Week
yr	Year
αSMA	Alpha smooth muscle actin

Chapter 1. INTRODUCTION

1.1 General Uses of Cobalt-based alloys

Cobalt based alloys have been in use for several decades in a variety of applications, including super alloys in the food industry, aerospace industry, industrial gas turbines, marine application, medical devices and pigments in commercial and industrial ceramic and glass. The crystallographic nature of the alloys, its reaction to tension, the strengthening effects of chromium, tungsten and molybdenum, the production of metallic carbides, and the resistance of chromium to corrosion, are the main factors that determine the alloy characteristics. CoCr (ASTM F-75 and ASTM F-1537 with similar weight ratio compositions, Co:Cr:Mo 60:30:7) is widely used in the making of orthopaedic and dental implants. It has unique strength which makes it preferable in manufacturing of medical instruments, superalloys, magnetic alloys, and low-friction bearing materials. Co in the form of fine powder is used in the production of carbide cements, diamond cutting tools, and metal spraying ingredients. The largest use of Co is in superalloys that are used in gas turbine aircraft engines (ATSDR, 2004).

1.1.1 Food and Drink applications

In the food industry, Co has been used particularly in the brewing industry, "Co in the form of cobaltous chloride was added to beer to stabilize and improve the appearance of its foam" (Kesteloot *et al*., 1968). It has been used as a defoaming agent for beer, and has been added to beer production in Belgium since 1959. This continued until March 1967, when it was stopped after incidences of toxicity from this agent. According to a study by Kesteloot, there are 42 different brands of beer available in Belgium, and over 80 percent have been investigated to determine the amount of Co. The result found that there are approximately 1 ppm of pure Co in the product from most breweries. Consequently, it was suggested that people who drink beer on a daily basis might consume average on 0.05 mg of Co/kg bw/day (assuming 70 kg body weight) (Kesteloot *et al*., 1968).

The adverse reactions of Co were reported in the 1960s, when Canadian and Belgian heavy beer drinkers (8-25 pints/day) developed heart diseases, nausea, vomiting, and there were some cases of death. This was related to the addition of Co salts in specific beer brands to stabilise foam formation. Exposure rates in these patients were

identified at 0.04-0.14 mg of Co/kg. In 1972, 28 beer drinkers were reported by the Veterans Administration Hospital in Minneapolis, to have Co toxic reactions in the heart. The diagnosis showed left ventricular failure, cardiogenic shock, acidosis, pericardial effusion and polycythemia as a result of Co ingestion at a dose of up to 10 mg/day (Alexander, 1972).

Later on, Co ingestion led to erythropoietic effects, when it was used as a dietary supplement. Co containing supplements are presently offered commercially in the US. Co at a 1 mg daily dose was marketed to boost health by increasing the metabolism of fats and carbohydrates, and synthesis of proteins, providing an erythropoietic effect and increased physical energy (Finley *et al*., 2012). The British Expert Group on Vitamins and Minerals (EGVM) identified the safe daily dose of Co at lower than 1400 µg (EGVM, 2003). In contrast, the European Food Safety Authority (EFSA) has evaluated the maximum safe daily dose at 600 µg of Co (EFSA, 2009). However, Co^{2+} ions have been potentially misused in sport as an alternative to recombinant human erythropoietin (rHuEpo) doping. Some athletes seek a substance that can enhance athletic performance by increasing red blood cell (RBC) production to better oxygenate blood, and this correlates with the aerobic capacity. Consequently better endurance is obtained and decreased muscle fatigue (Jelkmann, 2012). However, reports indicated that the side effects include muscle contractions, infection of the upper respiratory system, hyperviscosity of the blood, headache, hypertension, and thrombosis (Raine, 1988). Furthermore, red cell aplasia (PRCA) was identified after long term intake (Pollock *et al*., 2008).

1.1.2 Medicine applications

1.1.2.1 Anaemia

Co stimulates homopoiesis, and is a good alternative treatment for anaemic patients with iron deficiency. The prescribed daily dose was 1 mg of Co /kg. In addition, Co was used as a remedy for other diseases such as renal failure, rheumatoid arthritis and sickle-cell anaemia. This medical practice was terminated recently because of the reported side effects of Co (Jelkmann, 2012).

It was found that people treated for anaemia who were exposed to 0.5 mg/kg for a few weeks showed effects on the thyroid, and one case study of anemia treatment found vision problems following treatment with 0.3 mg Co/kg for 6 weeks (ATSDR, 2004). Thus, regular treatment long term with Co may affect the body, with side effects including nausea, vomiting, neuropathies, heart failure, hypothyroidism and goiter (Jelkmann, 2012). A fatal case was reported for a hemodialysis patient who was treated with Co (50 mg/day) for a three month period. The postmortem analysis revealed a concentration of 1.65 µg/g of Co in myocardial tissue, which was 25 to 80 times higher than in relevant controls. An additional fatality was reported for a hemodialysis patient who was a 17 year old female. Death was explained as a result of rapid progressive dilated cardiomyopathy after an exposure of $CoCl_2$ at 50 mg daily dosage for a nine month period. Autopsy results showed 45 fold elevated Co concentration in her myocardial tissue compared to normal (Manifold *et al.*, 1978). Dietitians suggest a daily dosage of 0.1 µg of inorganic Co (ATSDR, 2004). The total Co content of the human body averages 1.1 mg of inorganic Co, which will be stored mainly in muscles (43%), in bones (14%) and in other tissues (Yamagata, Murata and Torii, 1962; Underwood, 2012). Interestingly, the comparison of Co exposure level between beer drinkers and patients on anaemia treatment showed that the level of Co exposure in beer drinkers was less than in the anaemia therapy patients but the adverse effects in beer drinkers were more pronounced. Beer drinkers with low protein diets were more seriously affected by adverse effects on the heart than people with a normal protein diet (Alexander, 1972, ATSDR, 2004), indicating that malnutrition is an important contributing factor.

1.1.2.2 CoCr alloy

In the 20th century, Co-Cr alloy was used in biomedical manufacturing (Hyslop *et al*., 2010). The first Co-Cr use was a prosthetic heart valve that was implanted in 1960 (Tarzia *et al.*, 2007). The metal is used in manufacturing of the stem component (femoral stem) for artificial joints, both for replacement hips and knees.

Multiple types of metallic alloys (stainless steel, titanium and Co-based alloys) were applied in the joint replacement industry given by ISO 5832-4 and ISO 5832-12 standards. Co-based alloys have a higher wear resistance when compared with other

materials (Sieber *et al*., 1999). They have good mechanical properties and excellent corrosion resistance, because an oxide layer protects the device surface.

Other biomedical applications of Co are in coronary stents, pacemakers and suture wires and in the dental field, where Co-Cr is a popular metal alloy in various applications. It is used for the production of a metallic structure or framework for removal of dentures, used as metallic substructures for structuring of porcelain based implant frames, and as a reliable feature for prostheses, dental fillings, crowns and bridges. The increasing utilisation of Co-Cr alloys in dental devices is a response to their physico-mechanical properties, enabling them to resist abrasion, and low budget cost. In conclusion, in addition to traditional dietary sources, Co exposure occurs through contamination of the environment, dietary supplements, occupational exposures and implanted medical devices.

1.2 Source of exposure and routes of exposure

1.2.1 Exposure from external sources

1.2.1.1 Oral intake from food

The main source for Co consumption is food. The average Co intake per day is estimated to be 5 to 40 µg, mainly from food containing vitamin B12. Examples of food with high Co content (0.2-1.0 µg Co/g) are fish, leafy green vegetables, and fresh cereals. Low-Co containing food includes meat, dairy products, processed cereals, and sugar, which contain 0.01 to 0.03 µg of Co per gram (Hokin *et al*., 2004).

Moreover, small amounts of Co exposure come through drinking water(ATSDR, 1992). The cause of Co contamination in meat is feeding stuff. Animal feeding stuffs are routinely supplemented with Co (II) compounds leading to human exposure. The European Food Safety Authority (EFSA) reported that “the estimated population average intake of Co was reported to be 0.005–0.04 mg Co/day in the USA, 0.011 mg Co/day in Canada, 0.012 mg/day in the UK and 0.029 mg Co/day in France”(EFSA, 2012).

There are no recommended acceptable daily intake (ADI) amounts for Co by the Food and Drug Administration (FDA). The Co level found in the suggested daily dosage of vitamin B12 in the US, was 2.5 µg (IOM, 1998).

Co intake orally in humans and animals, caused unwanted complications in cardiovascular, hematological, respiratory, gastrointestinal, renal, dermal, hepatic, and endocrine systems, and in some cases led to death (Table1-1). Absorption of Co through the gastrointestinal system, depends on the form and dose of the ingested Co. This was witnessed in anaemic and normal patients. The most sensitive effect occurring after Co exposure in humans is to increase the number of RBCs (polycythemia), in both normal and anaemic patients. After ingestion of beer containing Co there were severe effects on the CVS, including cardiomyopathy and death, which occurred in addition to GI effects (such as nausea and vomiting) and hepatic damage. The most frequently associated cardiovascular problems were left ventricular failure, reduced myocardial activity and response, enlarged heart, tachycardia, heart shock, intracellular disturbances, and pericardial effusion (ATSDR, 2004).

In March 1965, an international meeting in Brussels on non-obstructive cardiomyopathies referred to the risk of heart disease in chronic beer drinkers(Kesteloot *et al*., 1966). In 1966 in Canada and the US, there were reports of acute myocardial disease leading to high death rates, related to Co containing beer consumption (Morin and Daniel, 1967). Around 40-50% of patients with beer-Co cardiomyopathy died within a few years. But “Acute mortality” (death within 2-3 days of admission) accounted for 18% of the deaths “ and 23-41% of residual patients had a cardiac disability and abnormal electrocardiograms (Alexander, 1972). However, the early symptoms of the beer-drinkers occurred in the respiratory tract, accompanied by nausea, vomiting and diarrhoea and also liver injury by central necrosis. Elevated levels of liver enzymes such as glutamic oxaloacetic transaminase(SGOT), glutamic pyruvic transaminase(SGPT), and lactate dehydrogenase (LDH), were also observed (Morin *et al*., 1971), and raised levels of bilirubin were reported.

Table 1-1 Toxicity studies on Co after oral exposure.

Dose	Species/Descriptions	Side effect	Reference
-	14 patients / Beer drinkers	Myocardosis, death, 11 thyroids showed irregular follicle morphology and decreased follicular size	(ATSDR, 2004)
0.04-0.14 mg Co/kg/day , over yr	50 patients/ Beer drinkers	Pulmonary oedema, induced cardiac failure	(Morin *et al*., 1971)
	-/Co therapy	Increase in the weight of the thyroid gland (enlargement, hyperplasia and increased firmness**)**	(Chamberlain, 1961, Little and Sunico, 1958, Washburn and Kaplan, 1964)
-	4 cases of sickle-cell anaemia/ Co therapy	Thyroid gland enlargement, but when Co treatment is terminated this can be reversed.	(Gross *et al*., 1955)
0.16-1.0 mg Co/kg/day daily (as $CoCl_2$), 3-32 wks	Anephric patients (with resulting anaemia)/ Co therapy	Increased red blood cell count, leading to less necessity of blood transfusion	(Duckham and Lee, 1976b, Taylor and Marks, 1978)
-	Sickle-cell anaemia or renal amyloidosis patients/ Co therapy	Developed goiter, altered thyroid gland and death	(Kriss *et al.*, 1955)
$CoCl_2$ solution, approx 6.5 h	Children aged 19 mnths-old/ Co therapy	Vomiting, gastric lavage, and/or supportive therapy, death	(Jacobziner and Raybin, 1961)
$CoCl_2$ solution, approx 7 h	Children aged 6 yrs-old/ Co therapy	Neutropenia (fewer neutrophils than normal in the blood)	(Mucklow *et al*., 1990)

Table 1-1 Toxicity studies on Co after oral exposure(cont.).

Dose	Species/Descriptions	Side effect	Reference
1.3 mg Co/kg/day daily (as $CoCl_2$), 4 series of treatment, 6 wks each	-/Co therapy	Visual problems such as impaired choroidal perfusion and optic atrophy	(Licht *et al*., 1972)
30.2 mg Co/kg/day (as $CoCl_2$), 3 mnths	Rat	Decreased in the weight of lung, an increase in heart weight	(Mohiuddin *et al.*, 1970)
20 mg Co/kg/day (as $CoSO_4$) with and w/o ethanol, 5 wks	Guinea pig	Cardiomyopathy (such as increased heart weight; disfigured mitochondria; abnormal electrocardiography(EKGs); lesions involving the myocardium, pericardium, and endocardium)	(Mohiuddin *et al*., 1970)
12.4 mg Co/kg/day (as $CoCl_2$), 3 wks	Male rat	Cardiac impairment showing as multi location myocytolysis, associated with erosion of myofibrills	(Morvai *et al.*, 1993)
161 mg Co/kg	Sprague-Dawley rats	Effect on liver, heart, kidney and GI tract and death	(Domingo *et al*., 1984).
42 mg Co/kg (as CoF_2)	Rat and/or mice	Alteration of the proximal tubules, kidney effect	(Speijers *et al*., 1982)
10 mg Co/kg/day (as $CoCl_2$), 5 mnths	Rat	Enlargement of liver, alteration of the proximal tubules, kidney effect	(Murdock, 1959).
10–18 mg Co/kg/day, 4–5 mnths	Rat	Alteration of the proximal tubules, kidney effect	(Holly, 1995)
26–30.2 mg Co/kg/day (as $CoSO_4$ or $CoCl_2$), 2-3 mnths)	Rat	Degenerative heart lesions	(Grice *et al*., 1969)

h, hour; wk, week; mnth, month: yr, year; Dietary intake: 5–40 mg Co/day(Hokin *et al.*, 2004)

1.2.1.2 Inhalation Exposure

Metal industries, such as mining, refining and smelting of metals, Co based dye production, and manufacturing of chemicals containing Co products, occasionally generate contamination from Co in the air. Workers who work in that area have a high risk of occupational exposure.

Air in metal producing factories was analysed for Co content ranging between 1 to 300 µg/m^3, whereas the normal range is 0.4 to 2.0 ng/m^3(ATSDR, 2004). It has been reported that workers who work in an area for 6 h that contains 0.038 mg Co/m^3 (around 100,000 times that of normal ambient air) had problems with the respiratory tract, effects on the lungs, asthma and pneumonia symptoms and wheezing. Diamond polishers have developed respiratory effects such as lung dysfunctions due to inhalation of Co, the NOAEC or "No observed adverse effect concentration" was determined to be 0.0053 mg/m^3 (Nemery *et al.*, 1992). An minimal risk level (MRL) for chronic-duration inhalation exposure was 0.0001 mg Co/m^3 from this study(Nemery *et al*., 1992). The American Conference of Governmental Industrial Hygienists (ACGIH) established a threshold limit value (TLV) for Co, which was 0.02 mg/m^3, an 8-h time-weighted average (TWA) (ACGIH, 2004). An 8 h permissible limit (PEL) of 0.1 mg/m^3 was defined by the Occupational Safety and Health Administration (OSHA). In addition, the National Institute for Occupational Safety and Health (NIOSH) suggests an 8 h TWA of 0.05 mg/m^3(NIOSH, 2001).

Moreover, there are many literature reports of case studies about inhalation toxicity or occupational exposure (see Table1-2).

Table 1-2 Toxicity studies on Co after inhalation exposure.

Dose	Species/Descriptions	Side effect	Reference
Not Reported. Case study (no level of Co)	194 workers/ Diamond polishers	Respiratory effects	(Nemery *et al*., 1992)
0.038 mg Co/m^3, 6 h	Industrial workers/ -	Asthma and pneumonia symptoms and wheezing	(ATSDR, 2004)
0.005 mg Co/m^3, 0.007 mg Co/m^3	Hard metal workers/ a Co-tungsten carbide alloy	Asthma and skin rashes	(ATSDR, 2004)
0.125 mg Co/m^3	82 workers/ Co refinery	Dyspnea, wheezing, skin lesions (eczema, erythema) and decrease RBCs and Hb	(Swennen *et al*., 1993)
0.0152 mg Co/m^3	Workers/ Diamond polishing industry	Decreased ventilation function	(Gennart and Lauwerys, 1990)
Not Reported. Case study (no level of Co)	Two young men/ Mineral assay industry	Cardiomyopathy (effect on the ventricle) and enlargement of the hear	(Horowitz *et al*., 1988, Barborik and Dusek, 1972, Jarvis *et al*., 1992)
Not Reported. Case study (no level of Co)	a man, 41-yrs old/ -	Cardiac failure and high accumulation Co level in heart, liver, spleen and kidney	(Barborik and Dusek, 1972)
Not Reported. Case study, exposed 10 ± 5 yrs)	30 hard metal workers/-	Cardiomyopathy (effect on the ventricle) and enlargement of the heart, abnormality of chest x-rays, decrease in exercise right ventricular ejection fraction (EF)	(Horowitz *et al*., 1988)

Table 1-2Toxicity studies on Co, Inhalation exposure(cont.)

Dose	Species/Descriptions	Side effect	Reference
Not Reported. Case study	12 hard metal workers/-	Memory loss, nerve mediated deafness and decreased visual acuity	(Jordan *et al*., 1990, Meecham and Humphrey, 1991)
cobalt aluminate and cobalt-zinc silicate Case study (no level of Co)	61 female workers/ plate painter	Thyroid (abnormality of thyroid function level- T3 level) and allergic dermatitis (eczema and erythema), dermatitis(immunosensitisation)	(Prescott *et al*., 1992)
19 mg Co/m^3 or greater as $CoSO_4$ over 16 days	Rat and mice	Congestion in the vessels of the brain/meninges	(Bucher *et al*., 1990)
11.4 mg Co/m^3, over 13 wks	Rat and/or mice	Cardiomyopathy	(Kerfoot *et al*., 1975)
0.1 mg Co $dust/m^3$ for 6 hours/day, 5 days/wk for 3 mnths.	Miniature swine	Electrocardiogram abnormalities in reflect ventricular impairment	(Kerfoot *et al*., 1975)

h, hour; wk, week; mnth, month: yr, year; Normal range 0.4-2.0 ng/m^3 (EFSA, 2009) and manufacturing range 1 to 300 $\mu g/m^3$ (ATSDR, 2004).

1.2.1.3 Dermal exposure

Another route of Co exposure in human is dermal exposure. Skin sensitisation and bronchial asthma caused by both dermal and inhalation exposure to Co was reported in workers (Kim *et al*., 2006).

There are many studies of dermal exposure of Co, the most commonly observed effect is dermatitis. People who have body piercings with Co- containing devices showed an increased rate of dermatitis (Ehrlich *et al*., 2001). The allergic properties of Co can be found mainly from metal exposure rather than the metal salts. People who have Co allergy do not suffer from eczema after exposure to the soluble Co salts to their hands after daily exposure (Nielsen *et al*., 2000). But in some cases, oral Co exposure causes eczema and dermal dermatitis of the hand by Co-sensitisation after dosing orally with 1 mg $CoSO_4$ tablet per day (0.014 mg/kg/day) for 3 weeks(ATSDR, 2004).

Following dermal exposure to Co-containing metal implants, the prevalence of sensitivity is low; it is only 3.8% of patients that require implant replacement (Swiontkowski *et al*., 2001). In animals, single and multiple dermal exposure of rats, BALB/c mice and guinea pigs to varying concentration of $CoCl_2$ in dimethylsulfoxide (DMSO) or in ethanol affects the local lymph node assay by increasing cell proliferation in a dose response manner (Ikarashi *et al*., 1992).

1.2.2 Exposure from an internal body source

Co exposure is commonly reported in the literature, related to orthopaedic implants, pacemakers and also dental implants. Around 13% of people are sensitive to Ni, Co or Cr (Merritt and Rodrigo, 1996, Goh, 1986, Kiez-Swierczynska, 1990), so the development of metal sensitivity after implantation is common.

Over the last decade, the use of CoCr alloys related to orthopaedic implants, pacemakers and also dental implants has created an entirely new source of internal Co exposure. In particular, a common type of orthopaedic knee and hip replacement devices contain metal-on-metal bearings, ISO 5832-12 ASTM F-1537 and ISO 5832-4 ASTM F-75. The amount of metal in dental usage is very small when compared with these metal bearings and does not represent an issue. On the other hand, the use of Co

hard metal alloys as biomaterials in orthopedic joint replacement causes serious concerns because of their widespread use and the susceptibility of the patients.

Hip replacement is one of the most successful elective surgeries, with a large number of patients satisfied with the results since it improves the quality of life substantially. But there are limitations associated with it. In that regard, the greatest problem has only been uncovered in recent years and is related to the release of metal nanoparticles and ions from CoCr alloy hip implants.

The National Joint Registry (NJR) monitors the performance and effectiveness of the different types of surgery, improving clinical standards and also reporting the risks as well as benefits of replacement surgery in the orthopaedic sector. The NJR reports present the collected information on all hip, knee, ankle, elbow and shoulder replacement operations surgery in England, Wales, Northern Ireland and the Isle of Man. We therefore know that several thousands of these replacements take place in the UK every year.

Specifically, the 14th Annual Report of National Joint Registry (NJR) in 2017 reported the outcome data in relation to a variety of replacements. The total number of records in this registry is approximately 2.35 million since it was established in 2002. From the database of patients with implants in the 14th Annual Report during 1 April 2003 and 31 December 2016, the number of primary replacements were 890,681 total hip replacements, 975,739 in knee, 3,899 in ankle, 23,608 in shoulder and 2,196 in elbow replacements. The ratio of women to men having joint replacements was 60:40 and the average age is 69 in primary surgery.

The failure rates of metal-on-metal (MoM) articulations in resurfacing and in a variety of stemmed replacements, show higher rates than other bearings, ranging from between 14% and 27% at ten years for the worst performing hip implant types. However, the overall use of revision in resurfacing implants shows a reduction to 8%-9% during this period. Figure 1-1 shows the structure of resurfacing and stemmed hip replacements. The cumulative number of cases from 2003-2016 which are available to investigate is 97,341 cases of hip replacement. During this 13 year period (2003-2016),

the probability of hip revision following failure in all types, including MoM, within the first year after primary surgery is approximately 17%, and cases recorded include dislocation, fracture, infection and also aseptic loosening, with the majority being in the group of patients who were ≥75 years old at the time of operation(NJR, 2017).

In patients with long-term implants local accumulation of metal ions surrounds the prosthetic joint and they develop metallosis. Metallosis results in various complications such as implant failure, organ and tissue death or bone destruction that leads to revision surgery. Metallosis, including Co poisoning, has been reported with a 5% estimated incidence of total joint implant patients (hip, knee joints, shoulders, wrist and elbow joints). The incidence of adverse effects in hip joints is greater in women than men (Oliveira *et al*., 2015). The reason for this sex difference in adverse effects is mainly due to mechanical properties of smaller diameter hips.

1.2.2.1 Background to the hip joint.

The largest weight bearing joint in the body is the hip, which is composed of a ball and a socket joint, linked to the head of the thigh bone (femur), and to the socket forming a connection with the acetabulum in the pelvic bone (Figure1-1). Hyaline cartilage lines the acetabulum and the head of the femur. It provides a smooth surface for a gliding path during continuous movement of the bone protecting against erosion and wearing down of the bones. The connection of the ball-and-socket is bands of tissue, called ligaments that provide stability to the joint. The synovial membranes and layers of hyaline cartilage have synovial fluid to lubricate the joint (Navarro-Zarza *et al*., 2012).

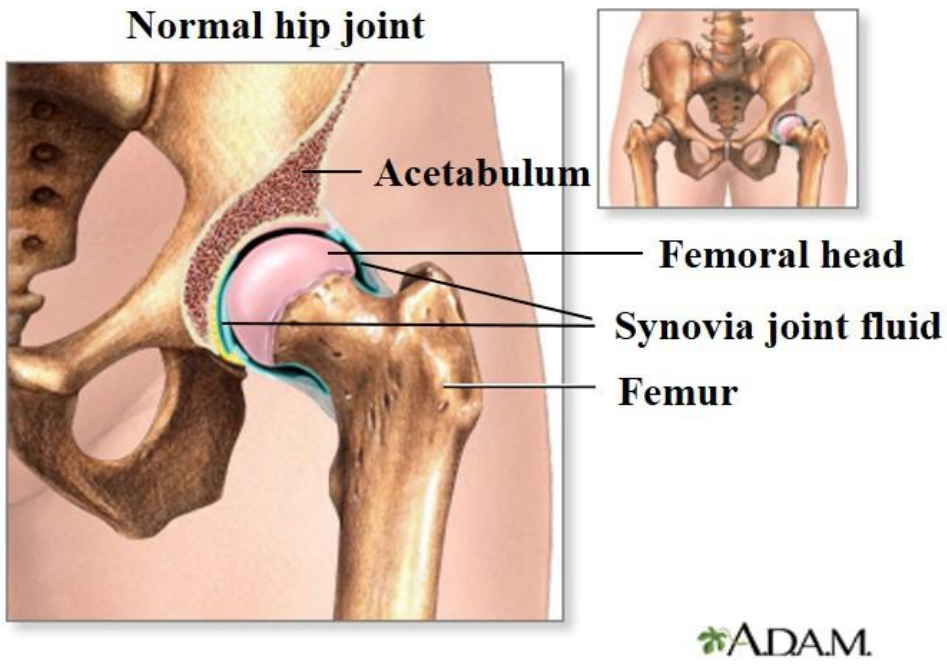

Figure 1-1 Anatomy of the normal hip joint and bones of pelvis, including acetabulum. (adapted from Pennstatehershey.adam.com, 2018).

1.2.2.2 Hip Replacement surgery

Hip replacement is recommended for treating and reducing chronic pain caused by any type of arthritis (rheumatoid arthritis, osteoarthritis, post-traumatic arthritis), hip fractures, avascular necrosis, ankylosing spondylitis and benign and malignant bone tumors. In the mid to late 1960s, the development of artificial hip prostheses was begun by Sir John Charnley, a British orthopaedic surgeon (Gomez and Morcuende, 2005). Total hip arthroplasty (THA) or total hip replacement (THR) is a hughly successful orthopaedic surgery to help patients with any hip pain condition.

THA is an orthopaedic surgery that involves removal of the acetabular cartilage and subchondrial bone and then insertion of the artificial implant (made of plastic, ceramic or metal). They are ball and socket joints (Figure 1-2). Two basic ball and socket components are designed and made from a combination of bearing (articulating) surface materials, including ceramic-on-ceramic (CoC), metal-on-plastic (MoP), and metal-on-metal (MoM). The type of metal used to make orthopaedic implants includes stainless steel, titanium alloys, and Co-Cr alloys. The image (Figure 1-3) below shows the two types of surgical procedures (total hip replacement surgeries: THA or THR) and hip resurfacing procedures. Hip resurfacing is a surgical replacement alternative to THA that only replaces the articulating surfaces and preserves the proximal femoral bone. It is specially used with younger and active patients who have retained adequate bone composition, and always uses a MoM articulation with CoCr alloy.

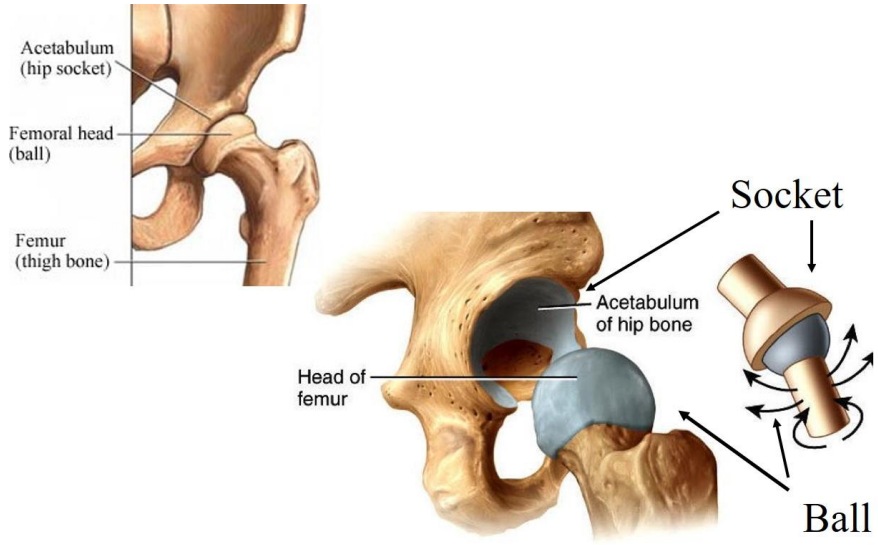

Figure 1-2 Ball and Socket Joints. (adapted from defenderauto.info, 2018).

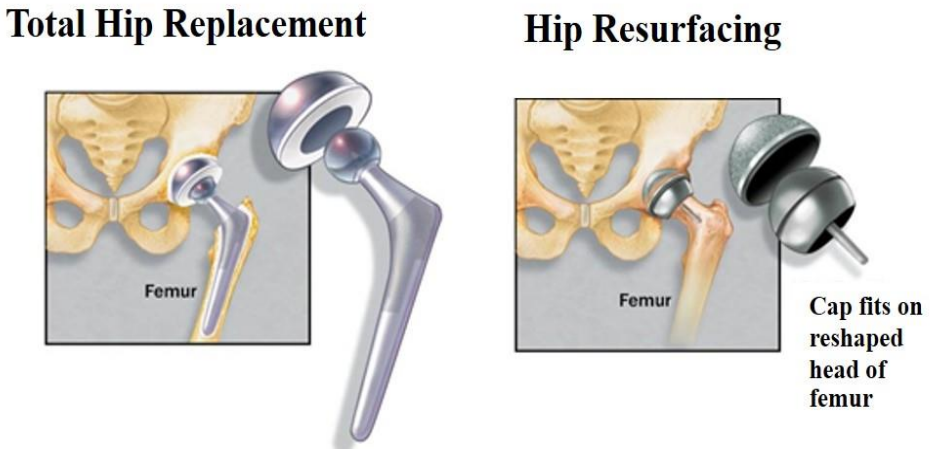

Figure 1-3 Total hip replacement: THA and hip resurfacing. (adapted from Mayo Clinic, 2018).

There are various reasons for THA failure such as fracture of the implant, aseptic loosening, infection, wear, and dislocation(Malchau *et al*., 2002). The development of hip resurfacing with MoM articulations led to a reduction of failure in high-activity younger patients (Learmonth *et al.*, 2007). These joints were less likely to dislocate. The most common cause of failure in aseptic loosening of resurfacing implants is adverse reactions to metallic debris and ions (Luo *et al.*, 2005).

Both male and female patients have high revision rates of Metal-on metal (MoM) hip replacements when compared with other materials (plastic or ceramics). The National Joint Registry for England and Wales reported the failure rate to be around 13.98% in hip resurfacing MoM implants while ranging from 3.8% to 5.9% for other fixation types (cemented, uncemented, hybrids and reverse hybrid) not including MoM bearing implants(NJR, 2017).

1.2.2.3 Internal Exposure Toxicity

MoM implants leach both Co and Cr ions. Co ions are more soluble, and travel through the bloodstream to cause systemic toxicity, whereas Cr ions tend to bind locally, causing local toxicity. Following exposure, Co caused adverse reactions in terms of systemic effects such as heart problems (cardiomyopathy and heart failure), visual, auditory and cognitive impairment, nerve problems, thyroid gland function effects and skin rashes.

Without a doubt, MoM leads to increased Co and Cr levels in many body fluids and elevated Co levels of any fluids (blood, joint fluid and urine) can be correlated with adverse effects. From a study of Langton and coworkers, 278 cases were reported that related the early failure from adverse reactions to metal debris (MoM) with high Co blood levels. In total 40 out of 278 patients or 14% of all cases reported, it was found that the Co levels were greater than 20 μg/L. All 40 cases reported have found metallosis (metal staining in local tissue) and had to undergo revision surgery (Langton *et al.*, 2013). Whereas, Tower described from his studies (214 patients) with both articular surface replacement implants ((ASR); DePuy, Warsaw, Indiana) and other types of metal-on-metal hips, that ten patients (around 5%) had a serum Co level of more than 20 μg/L and suffered from metallosis, with cardiac and neurological

symptoms. An improvement in symptoms and decreased Co level was reported on revision surgery(Tower, 2010, Oldenburg *et al*., 2009).

The elevated Co serum level in patients with hip implants can be more that 100-fold that of physiologic levels (0.032-0.29 μg/L) (De Smet *et al*., 2008). There have been cases of particularly high blood ion concentrations. For example, a case study in State of Alaska Epidemiology Bulletin reported 2 patients, both 49-years-old, who had received a MoMHA for osteoarthritis. The report showed that in one, the development of adverse reactions such as bilateral axillary rashes at 3 month post-op, unaccustomed shortness of breath at 8 months, central nervous sytem (CNS) problems (anxiety, headaches, irritability, tinnitus and hearing loss) occurred after 18 months and loss of peripheral visual acuity after 36 months. The monitored Co serum level in this patient was 122 μg/L. In the other case, effects on hearing loss, groin pain, rashes, mental fog, memory loss, vertigo and breathlessness were reported after 12 months, and cardiac problems (diastolic dysfunction) after 18 months. For this patient the Co level before revision was 23 μg/L. and after revision the Co level had decreased to 11 μg/L, and the symptoms were improved (McLaughlin, 2010).

High concentrations of Co (22.92μg/L) and Cr (19.43 μg/L) in the blood from a patient 37 yrs after THA McKee–Farrar MoM hip prosthesis implantation (Wretenberg, 2008), and Co (138μg/L) and Cr (39μg/L) in a 41-year-old patient after 3 months surgery with a bilateral MoM Birmingham Hip Resurfacing (BHR) (Fritzsche, Borisch and Schaefer, 2012) were reported. Increases of Co and Cr levels in blood has been reported in patients with CoCr implants, and this is related to a balance between ion release, kidney excretion, binding and systemic distribution giving rise to toxicity of metal ions both locally and in the systemic circulation (Clarke *et al*., 2003, Dunstan *et al*., 2005, Daniel *et al*., 2007a, Antoniou *et al*., 2008, Tkaczyk *et al*., 2010, Bisseling *et al*., 2011, Lavigne *et al*., 2011, Friesenbichler *et al*., 2012, Penny *et al*., 2013).

The Co concentration in whole blood and serum in these papers were reported to be from 398 μg/L to 625 μg/L. All of the symptoms improved after revision, and the blood Co level was significantly decreased to the normal physiological range (Oldenburg *et al*., 2009, Ikeda *et al*., 2010, Pelclova *et al*., 2012, Rizzetti *et al*., 2009). Another five

cases reported peak Co levels ranging from 15 μg/L to 83 μg/L, with poor wear of MoM bearing couples, and similar adverse symptoms as reported previously. Elevated risk of local problems secondary to metal debris production were reported with various MoM designs of THR(Mao *et al*., 2011, Tower, 2010, Tower, 2012).

Interestingly, serum Co levels of most MoM implant patients are higher than those in industrial workers exposed to Co and this leads to subclinical cognitive and cardiac impairment. Severe neurological and cardiac impairments are associated with arthroprosthetic patients who have serum Co exceeding 60 μg/L (Tower, 2010, Steens *et al*., 2006, Oldenburg *et al*., 2009, Rizzetti *et al*., 2009, Ikeda *et al*., 2010). Machado reported six cases of patients with ASR in the right hip, who were otherwise healthy had no historical alcohol consumption and who presented with a combination of endocrine problems, cardiac and neurological syndromes. They showed worsening dyspnoea, exertional chest tightness, severe global systolic dysfunction and a severely dilated left atrium. (Machado *et al*., 2012). From the literature, data indicated that, the Cr and Co levels that are present in plasma and tissues from patients with MoM implants at revision surgery are between 5-100 μg/L and 5-300 μg/L, respectively (Sampson and Hart, 2012). A wide range of Co levels have been reported in whole blood, serum, synovial fluid and other fluids as shown in Table 1- 3.

Table 1-3 Toxicity studies on Co, Internal exposure, Metal ion levels measured in body fluids from patients.

Implant	Body fluids	Co level	Follow up	Side effect	Reference
MoMHA for osteoarthritis	Serum 49-yrs-old	122 µg/L	3 mnths 8 mnths	Bilateral axillary rashes Shortness of breath	(McLaughlin, 2010).
MoMHA for osteoarthritis	Serum 49-yrs-old	23 µg/L : 11 µg/L	12 mnths 18 mnths 40 mnths (revision)	Mental fog, memory loss, vertigo, hearing loss, groin pain, rashes, and breathlessness Diastolic dysfunction	(McLaughlin, 2010).
THR	Whole blood 46-yrs-old,	6,521 µg/L		Fatigue, weakness, hypothyroidism, cardiomyopathy, polycythaemia, visual/hearing impairment, cognitive dysfunction, neuropathy and death.	(Zywiel *et al*., 2013).
Hip replacement/CoCrMo femoral head (Revision of ceramic on ceramic hip-ceramic socket kept but replaced with metal head : MoC)	Serum	398 µg/L (Post-op) 36 µg/L (after 8 wks Post-op) <1 µg/L(after 14 wks Post-op)	2 yrs	Loss of vision (Atrophy of optical nerve, retinopathy with malfunction of the macula), hearing impairment, numbness of the feet and dermatitis head and neck After post-op : Increasing impairment of vision (able to recognise outlines and colour but not read),	(Steens *et al*., 2006)
MoP articulations	Whole blood	625 µg/L	3 mnths	Headaches, cognitive, fatigue, hypothyroidism, hearing loss, cardiac abnormalities (LVH and interstitial fibrosis and polyneuropathy.	(Oldenburg *et al*., 2009)
MoP articulations	Whole blood	>400 µg/L	2 yrs	Hearing loss, partial loss of vision and polyneuropathy	(Ikeda *et al*., 2010)

Table 1-3 Toxicity studies on Co, Internal exposure (Metal ion levels measured in body fluids from patients(cont.).

Implant	Body fluids	Co level	Follow up	Side effect	Reference
MoP articulations	Serum	506 μg/L	14 mnths	Hypothyroidism, hearing loss, cardiac abnormalities and polyneuropathy.	(Pelclova *et al*., 2012)
MoM Arthroplasty (5 case report)	Serum/ Joint fluid	15 to 83 μg/L (Serum), 3200 to 3300 μg/L (Joint fluid)	-	Anxiety, tinnitus, deafness, blindness, cognitive decline, headaches, convulsions, fatigue, weakness, peripheral neuropathy, heart failure, and hypothyroidism.	(Mao *et al*., 2011, Tower, 2010, Tower, 2012)
ASR implant (24 case reports)	Serum	more than 20 μg/L	-	Neurological and cardiac symptoms	(Tower, 2012)
BHR arthropathy (5 case reports)	Serum	64-74 μg/L	23 mnths	Pain and noise at the hip, anxiety, depression, tinnitus, hearing loss, cognitive decline, cranial neuropathy and cardiomyopathy	(Tower, 2012)
THA MoM (84 ys old male)	Whole blood	22.92 μg/L	37 yrs	No symptoms	(Wretenberg, 2008)
MoM resurfacing (26 patients)	Whole blood	4.5 to 10.6 μg/L	Median 27 mnths	Painful but no specific reports	(Hart *et al*., 2009)
MoM resurfacing (Failed: 7 patients)	Whole blood	112.64 μg/L	Mean 51 mnths	No specific reports	(Hart *et al*., 2010)

Table 1-3 Toxicity studies on Co, Internal exposure (Metal ion levels measured in body fluids from patients(cont.).

Implant	Body fluids	Co level	Follow up	Side effect	Reference
Rupture ceramic head (replacement metal head, MoP)	Whole blood	549 µg/L	2 mnths	Progressive visual and hearing loss with near blindness and deafness, brain MRI with hyperintensity of optic nerves and tracts, peripheral neuropathy mild distal sensory motor disturbances, mild lower limb nerve amptitude reduction, visually evoked response (VER) irregular cortical visual responses, wheelchair bound because of lower limb hyposthenia, hypothyroidism	(Rizzetti *et al*., 2009)
Symptomatic MoM, both THA and resurfacing (92 patients)	Synovial Fluid	1104 - 1127 µEg/L	Mean of 36 mnths	-	(Davda *et al*., 2011)
Bilateral MoM resurfacing followed by unilateral MoM THA (41-yrs-old, pregnant)	Whole blood, aspirate of pseudotumor	138 µg/L (Whole blood) , 258 µg/L (aspirate pseudotumor)	3 mnths after revision surgery	No symptoms	(Fritzsche, Borisch and Schaefer, 2012)

Normal Co physiological level <0.25 µg/L (0.005µM)(Langton *et al*., 2008), MoMHA, Metal-on-metal hip arthroplasty; MoM, Metal-on-metal; MoP, Metal-on-polyethylene; THA, Total hip arthroplasty; THR, Total hip replacement; ASR, Articular Surface Replacement; BHR, Birmingham hip resurfacing; Post-op, Post operation; wk, week; mnth, month: yr, year;

In June 2012, MHRA recommended that following MoM, patients should have their Co blood level measured annually for 5 years post-operation. It also recommended measuring Co levels in patients who report pain or abnormal symptoms from hip replacement. In particular, they stated that patients who showed combined levels of Co and Cr in the blood > 7 μg/L (ppb), should be followed up in the next three months. In addition to the measurement of metal levels in patients, there are other factors to consider for long term biological safety of all types of MoM hips. Four categories of patients were suggested by MHRA of 1) patients with symptoms associated with loose MoM bearings, 2) patients with adverse outcome (including component position or small component size) from radiological features, 3) patients with concerns regarding the MoM bearing and 4) patients with high expected rates of failure with diabetes or renal failure. When a THA or resurfacing fails, the artificial joint is then revised, and an alternative articulation inserted instead, but this is a risk of morbidity to the patient (MHRA, 2012).

1.2.2.4 How is the Co released? : CoCr wear particles

Co and Cr ions are released by wear in the form of CoCr particles. The wear particles from the MoM implants are the same composition as the CoCr alloy in the nanometer size range. The composition reflects the MoM biomaterial (Germain *et al*., 2003). The average particle size range is 30 to 100 nm (Catelas and Wimmer, 2011). Debris of different forms are present such as colloidal complexes, free metallic ions, inorganic metal salts or organic forms (hemosoiderin) and lastly, wear particles.

When the MoM implant device produces metal particles and ions by wear processes and corrosion, the circulating metal ions from the surface of the prosthetic may enter the blood stream and circulate in the body and then accumulate in the heart liver, kidney, heart, lymp system, spleen and other organs of the body (Case *et al.*, 1994; Urban *et al.*, 2000). A proportion of metal ions will be eliminated by urine and faeces. The nanoparticle size allows diffusion throughout the body and may cause interaction with many different cell types(Lucarelli *et al*., 2004).

Over time, soluble and particulate wear debris will induce proinflammation and may cause inflammation and hypersensitivity. This will result in cytokine production and

facilitate an adaptive immune response that leads to bone modelling, to aseptic loosening and implant failure. Metallic debris spreads into the vascular system (Kwon *et al*., 2009), and it has been reported that entry into cells of nanometer sized wear particles occurs by endocytosis or pinocytosis (Shukla *et al*., 2005).

On the other hand, larger particles can stimulate phagocytosis such as by macrophages (Shukla *et al*., 2005, Trindade *et al*., 2001). Phagocytosed wear particles could be distributed within the lymphatic system and systemic vascular system. Macrophages may be able to process the particles, and this may lead to activation of T cells through antigen presentation. Also, the particles could interact directly with proteins or other intracellular molecules and interfere with normal biological processes (Hallab and Jacobs, 2009). The metal particles may cause osteolysis by immunological mechanisms involving hypersensitivity. There are markedly different inflammation patterns between the MoM articulations and MoP articulations (Athanasou, 2016).

The major difference between Co and Cr in the context of reactions to MoM debris is their solubility. Co is more soluble than Cr and the latter usually remains at the implantation area and tissue surrounding around the implants (Merritt and Brown, 1996). Moreover, if these particles are small enough, this will lead to the development of passivation, which is the low diffusion of metal ions through the passive film which covers and protects the implant surface(Metikoš-Huković and Babić, 2007).

It can be concluded that the two main mechanisms that could determine the rate of release of metal ions into the body are localised corrosion and passivation behaviour. Both corrosion and passivation are consequences of the composition and pH of the surrounding solution (Al-Kharafi, Badawy and Al-Ajmi, 1999; Lee and Choi, 2003). A low pH environment accelerates metallic corrosion and is linked to an increase of inflammation caused by exposure to debris (Rajamäki *et al.*, 2013). In Posada and coworkers's *in vitro* studies, an acidic environment caused a significant increase in Co and Cr ion release from CoCr alloys (Posada *et al.*, 2014).

A cell-mediated hypersensitivity response as part of the immunological effect was induced by orthopaedic metals. In addition, particulate wear debris and corrosive

materials increase the metal ion level, which causes the release of proinflammatory mediators, cytotoxicity, DNA damage and oxidative stress(Hallab *et al*., 2005). These factors cause changes in the biological activity of the cells and enlargement of mitochondria. (Lohmann *et al*., 2000). Metal ions (Co(II) and Cr(III)) released from orthopaedic implants cause cytotoxicity and induce apoptosis and/ or necrosis in cells(Huk *et al*., 2004). Generation of reactive oxygen species eg. superoxide radical (O_2.) and the hydroxyl radical (.OH) by metal ions cause oxidative damage and lead to damage to DNA. Some studies reported that orthopaedic metal ions, notably Co(II) Ni(II), Cr(VI) and Ni(II), inhibit DNA repair after both alterations in signal transduction and gene expression (Witkiewicz-Kucharczyk and Bal, 2006, Chen and Shi, 2002).

1.2.2.5 Metal ion levels in patients with CoCr hip implants.

The commonly used sample to monitor Co and Cr concentrations in the body is whole blood (Liu *et al*., 2011). In long term deposition studies, the metal content will be elevated in serum and urine of patients with implants(Jacobs *et al*., 2001). The concentration of metal ions in the serum corresponds only to the extracellular component.

Metal ion analysis of whole blood and serum seem to be the routine follow-up for MoM implants, and it is well documented that blood and serum Co are powerful tools in the diagnosis of sensitivity / specificity and are indicators of abnormal wear (Sidaginamale *et al.*, 2013; De Pasquale *et al.*, 2014).

Andrews *et al* documented that the physiological levels of Co and Cr are normally less than 0.25 µg/L (Andrews *et al*., 2011) and the reference blood value of Co in normal people in all ages is within the range 0.0- 20.0 nmol/L (nM). In patients who have implants (MoM implants) it should be less than 119 nmol/L. In 2012, MHRA produced guidelines on MoM hip implants recommending that Co and Cr in the blood of patients with implants should be less than 119 nmol/L total metal ions (or 7 parts per billion, ppb, µg/L) for resurfacings (MHRA, 2012).

There is no doubt that elevated levels of Co and Cr are measured in both blood (whole blood and serum) and joint fluid after implantation. Co and Cr blood levels after MoMHR of up to 4.6 µM and 2.3 µM, respectively were measured by Langton *et al* (2008) and in synovial fluid levels of 30 µM and 25 µM, respectively(Kwon *et al*., 2011). Many authors found levels of Co in the blood in the range from 2 to 25 parts per billion, ppb, µg/L (34 to 424 nmol/l or nM) of Co (Mcminncentre.co.uk, 2018). Although this is used as a coarse guide for studies of local resurfacings that related adverse reactions to device implants, the above levels do not indicate that systemic toxicity will occur.

The relationship between toxicity and levels of metals including the length of time exposed to the metal is not yet clear. Consequently, no established agreement exists between level of metal release and systemic problems. In addition, further studies to set up the relationship between metal ion level and development of toxicity are required (Learmonth *et al.*, 2007).

1.2.2.6 How is Co handled in the body? : Toxicokinetics of the Co Ion (ADME).

Acute Co toxicity occurs at larger doses, wheareas lower doses can cause long term toxicity. Histological studies found that Co particles were concentrated and localised to macrophages, which were located within the bronchial wall and interstitium close to terminal bronchiole (Brune *et al*., 1980). Co can also be spread through the lymphatic and vascular systems.

In terms of metal implants, corrosion, wear, and other medical factors produce metal debris and wear particles, which lead to soluble Co metal ions being released into the systemic circulation. Grey-black discoloration after deposition of wear particles and metal ions in the joint space elicits a localized chronic inflammatory reaction. After Co exposure, the metal concentration in serum and blood is potentially high, but rapidly decreases to minimal levels within 24 h, as Co is up taken by tissues. The primary organs that accumulate the Co ions and compounds are liver, kidneys, heart, stomach, and intestines in laboratory animal studies (Simesen, 1939; Greenberg, Copp and Cuthbertson, 1943; Ayala-Fierro, Firriolo and Carter, 1999). It is also stored in the skeleton and muscle in a time dependent manner(Czarnek, Terpilowska and Siwicki, 2015).

The highest Co levels are accumulated in the liver and the kidney, the primary organs of excretion. A study published by Jansen and colleagues, showed that Co was distributed into the liver and kidney after i.v injection of $CoCl_2$ in two human volunteers (Jansen *et al.*, 1996). In animal studies, Co accumulated in the liver (22.8%), kidneys (10.2%), and intestines (3.16%) 2 h after $CoCl_2$ exposure (i.v injection in rats) (Gregus and Klaassen, 1986; Patrick, Batchelor and Stirling, 1989). After 100 days daily exposure of Co (i.v injection $CoCl_2$) in rats, it was observed in spleen, followed by heart and then bone (Thomas *et al*., 1976). After absorption the Co was eliminated from the body in both the urine and faeces.

A human study reported that 40% of total dose of inorganic Co after intravenous injection was eliminated within the first 24 h, another 70% within the first week, around 20% within one month and the remainder 10% after one year (Letourneau *et al.*, 1972; Smith, Edmonds and Barnaby, 1972; Alexandersson, 1988).

Afolaranmi and co-workers showed distribution of Co throughout the body in rodents. In one paper, Co was injected into rats daily intraperitoneally to monitor its distribution, and in the other nanoparticles of CoCr alloy were administered via air pouches in mice. In the latter study levels of Co, Cr and Mo were measured and found to peak in blood and organs after 48 h, with the content of kidney being highest(Afolaranmi *et al.*, 2012).

1.2.2.7 Toxicity of Co at high blood levels

Red blood cells carry Co and an accumulation of Co within red blood cells will be eliminated within their 120 day lifespan, and thus the level of Co in blood should return to normal. Monitoring of Co toxicity can be determined in the peripheral blood and body fluids such as urine. As noted previously, the level of Co in the human body should be less than 0.25 µg/L (Andrews *et al*., 2011). There are many papers that study the relationship between the level of Co in body fluids and its adverse effects. For example Mucklow reported one case study of a 6 year-old boy who took a drink containing 2.5 g $CoCl_2$. The plasma Co level was 7.23 µmol/L (425.29 µg/L) after 7 h, and 0.09 µmol/L (5.29 µg/L) one month later compared with reference value (<0.02

µmol/L). Development of abnominal pain and vomiting was observed (Mucklow *et al.*, 1990).

Another two case studies from occupational exposure were reported by Alexanderson where workers in the Swedish hard metal industry, had been exposed to an airborne Co level of 0.09 mg/m^3. The Co levels found in the blood were 178.1 nmol/L (10.48 µg/L), causing impaired pulmonary function(Alexandersson and Lidums, 1979). The mean Co level in the blood of plate painters after they had been exposed to an airborne Co concentration of approximately 0.05 mg/ m^3 was 36.7 nmol/L (2.16 µg/L), which caused a few abnormalities of electrocardiograms, significantly higher pulse rate and also swelling of the mucosa in the bronchiole, because of the irritating effect of dust or droplet aerosols(Raffn *et al*., 1988). In another case report in 1972, a 49 year-old man had a blood Co level of 234 µg/L with symptoms such as bilateral deafness (sensorineural) and visual failure (optic atrophy) (Meecham and Humphrey 1991). As noted previously, the incidence of Co poisoning occurring in implant patients is increasing. Some examples are shown in Table 1-3.

1.2.2.8 Do the adverse effects disappear and improve after revision?: Co levels before and after revision

By comparing the durations of time that patients had been wearing implants (Table 1-4), it was found that the incidence of revision rates increased as time elapsed. The revision rate of THR is also more than the revision rate of resurfacing. Comparing the revision rate by region showed that the rate of revision was similar in all regions, as shown in Table 1-5. Moreover, the rate of failure of MoM implants, is affected by the size of the head of the device - an increased head size of the device decreased failure rate (Rodriguez and Rathod, 2012; Kostensalo *et al.*, 2013; Zijlstra *et al.*, 2017) and also females have more chance of failure than males (Smith *et al*., 2012). This is based on female patients having a smaller acetabulum, and so requiring a smaller diameter implant.

Table 1-4 Revision rates by age for THR and Resurfacing.

Mean Time Since Implant (Months)	Range of Revision Rates in Implant for THR (Point Estimates, %)	Range of Revision Rates in Implant for Resurfacing (Point Estimates, %)
6- <12	0.50	0.0-2.7
12- <24	0.3-16.0	0.01-15
24- <36	2.06-16.4	0.0-3.2
36- <48	1.0-7.6	0.0-5.6
48- <60	0.50-2.0	5.5-8.7
60- <72	0.0-15.0	0.05-14.6
72- <84	1.0-6.0	6.8-31
84- <96	1.0-5.3	4.3
≥96	3.7-16.7	6.1-73

Table 1-5 Revision rates by region for THR and Resurfacing.

Region	Range of Revision Rates in Implant for THR (Point Estimates, %)	Range of Revision Rates in Implant for Resurfacing (Point Estimates, %)
United States	1-16	0.0-15
United Kingdom	3.7-13.8	0.0-9.3
Europe (non UK)	1.8-8.83	2.703.6
Japan	0.0-16.4	31
Australia	15	0.86-73
Canada	2.0	3.40-7.0
Others	0.3-3.4	1.6-4.6

Reprinted from “Executive SummaryMemorandum: Metal-on-metal hip implant systems” (Earlstevens58.files.wordpress.com, 2018).

Table 1-6 shows the circulating Co levels in patients before and after revision surgery. The patients who were monitored showed obviously decreased metal ion levels during the first two months, but mostly within the first weeks after revision surgery. Continuing reduction of metal ion levels occurred to reach to base line levels over a period of two years(Mcminncentre.co.uk, 2018).

Table 1-6 Comparison of serum metal ion levels prior to MoM implant revision and after revision.

Implant Type	Before Revision (in brackets µg/L)	After Revision (in brackets µg/L)	References
THR	Pt1: at 6 mnths 167.8 µg/L Pt2: at 18 mnths 37.22 µg/L	Pt1: at 5 mths 7.77 µg/L Pt2: at 2 yrs 23.1 µg/L, : at 5 yrs 1.66 µg/L	(Beldame *et al.*, 2009)
THR or Resurfacing	307.1±99.72 µg/L, N = 25	6.56 ± 1.13 µg/L (after revision)	(Ebreo *et al.*, 2011)
THR and Resurfacing	Pt1: at 36 mmths 122 µg/L (peak level) Pt2: no reported.	Pt 1 : 83 µg/L in serum : 2.2 µg/L in CSF : 3200 µg/L in joint fluid (after revision) Pt 2 : 23 µg/L in serum, : 3300 µg/L in joint fluid (1 yr after revision)	(Tower, 2010)
THR	230 nmol/L (13.53)	77 nmol/L (4.53) 4wks after revision	(Machado *et al*., 2012)
THR (MoP revision)	Pt1: 410 nmol/L (24.12) Pt2: 258 nmol/L (15.18)	Pt1: 60 nmol/L (3.53) 8wks after revision : 9 nmol/L (0.53) in CSF : 4218 nmol/L (248.12) in joint fluid Pt2: 42 nmol/L (2.47) 8wks after revision	(Mao *et al*., 2011)
THR (ceramic femoral head and PE inlay)	625 µg/L in WB 165,000 µg/L in urine	34 µg/L in WB 149 µg/L in urine 80 µg/L in WB after 4-yrs 38.1 µg/L in urine after 4-yrs	(Oldenburg *et al*., 2009)

Total hip Replacements; PE, Polyethylene; MoP, Metal-on Polyethylene; Pt, Patient; WB, Whole blood; CSF, Cerebrospinal fluid; wk, Week; mnth, Month; yr, Year

1.2.2.9 Cardiotoxicity from Metal-on-metal implants.

Systemic toxic manifestations with CoCr alloy implants, including cardiac and neurological symptoms were observed in patients following implant use. Some studies showed a variation of average Co ion concentrations for different types of replacement orthopaedic implants, but it is still not obvious if there is any correlation between ion levels and different implant types. Howerver, high Co levels were detected after implantation of the Metasul LDH; Zimmer, the ASR, the ASR XL, and the Ultamet; DePuy. (Hartmann *et al.*, 2013; Jantzen *et al.*, 2013; Randelli *et al.*, 2013). Cardiotoxic effects related to Co toxicity reported in the orthopaedic literature, are the presence of hypertension, low voltage on the echocardiogram (ECG), pericardial effusion, reduced cardiac ejection, interstitial fibrosis, left ventricular hypertrophy (LVH), and modest histological changes indicating cardiomyopathy. Prentice described heart function in 35 asymptomatic MoM implants patients with a mean of 8 years after implantation compared with 35 conventional hip replacement patients. The results reported that after 8 years post implantation patients showed a reduction of 7 % in the left ventricular ejection fraction, and 6% larger left ventricular end diastolic diameter in MoM implants, compared with the conventional type of hip replacements (Prentice *et al.*, 2013).

However, in 2017, Berber and coworkers recently reported a case study of 90 patients with MoM hip implant who underwent detailed cardiovascular system examination using the best available technologies, including MRI, Cardiac magnetic resonance imaging(CMR) or Echocardiography(ECG or EKG), and Blood Bio-marker measurement. The results showed no level of Co and Cr in the blood that corresponded to induction of cardiotoxic effects in MoM hip implant patients. There was a very weak correlation between fractional shortening (FS) and Co blood level(Berber *et al.*, 2017). Nevertheless, Table 1-7 shows Co-induced heart diseases in the orthopaedic literature that were attributed to Co-based alloy implants.

Table 1-7 Clinical reports of cardiac adverse effects associated with cobaltism in patients with Co-based alloy prostheses.

Age/Sex	Co level (µg/L)	Cardiac syndrome reported	Type of implants	References
56/M	625(WB)	Moderate systolic dysfunction, sinus tachycardia/LVH, interstitial fibrosis	MoP	(Oldenburg, Wegner and Baur, 2009)
56/M	506(S)	LVH, pericardial effusion	Metal implant (Co, Cr and Ti)	(Pelclova *et al.*, 2012)
75/M	13.5(S)	Coronary artery disease, HF, EF 21%	MoM ASR	(Machado, Appelbe and Wood, 2012a)
46/M	6521 (WB)	Cardiomyopathy, Fatal	SH MoM	(Zywiel *et al.*, 2013)
59/F	287.6-398.6(S)	Pericardial effusion, Cardiomyopathy	MoM THA	(Allen *et al.*, 2014)
75/M	352.6(S)	Pericardial effusion, EF 32%, global hypokinesia	MoM THA	(Giampreti, Lonati and Locatelli, 2014)
55/M	880(S)	EF 25%, global Hypokinesia	MoP	(Dahms *et al.*, 2014)
54/M	120(S)	Biventricular dysfunction, Cardiomyopathy, HF	MoM	(Samar *et al.*, 2015)
69/F	199	HF, fatal	LH MoM (36mm)	(Martin *et al.*, 2015)
69/F	200-300 (S)	LV/RH dysfunction, MRI Hyperenhancement, pericardial effusion	ASR(+2 mm MoM liner)	(Khan *et al.*, 2015)
54/M	189(S)	LV/RH dysfunction, MRI Hyperenhancement	MoM THA	(Mosier *et al.*, 2016)
46/M	156(WB)	Idiopathic cardiomyopathy, HF, EF 20%	SH MoM	(Charette, Neuwirth and Nelson, 2017)
60/F	424-642(WB)	Reduced EF35-40%. Global LV hyperkinesia	MoP	(Fox *et al.*, 2016)
58/F/	169(S)	Dilated cardiomyopathy	THA CoCr	(Moniz, Hodgkinson and Yates, 2017)

An EF cutoff for sustainable performance is below 40% (Bhatia, Tu and Lee, 2006); HF, Heart failure; LV, Left ventricular; LVH, left ventricular hypertrophy; WB, Whole blood; S,Serum; EF, ejection fraction; ASR XL, Acetabular Surface Replacement; CoC, Ceramic on ceramic; SH MoM, Small head (≤32mm) MoM; LH MoM, Large head (≤32mm) MoM; CoP, Ceramic on polyethylene; MoP, metal-on-polyethylene.

In conclusion, there is accumulating evidence that Co may causes cardiac problems at high circulating blood levels. But no correlation has been found between the two and there may also be extraneous health nutrition and lifestyle factors that influence development of the cardiac problems. However, if Co is toxic to the heart, it must enter the cardiac cells by some mechanism, involving an uptake sysem.

Also the variation in implant materials is unable to account for the risk of cardiac problems. However, Australian Orthopaedic Associated National Joint Replacement Registry (AOANJRR) reported that there was an incidence of heart failure in hospitalisation found in ASR XL with large-head (LH : > 32 mm) MoM implants (AOANJRR, 2017). Such patients certainly showed as defined raised blood levels of Co (Hart *et al.*, 2011; Gill *et al.*, 2012; Chang *et al.*, 2013; Hartmann *et al.*, 2013; Jantzen *et al.*, 2013; Randelli *et al.*, 2013). There is also possible increased risk of heart problems during long term monitoring but this may be partly due to increased clinical vigilance (Gillam *et al.*, 2017).

1.2.3 Proteins and transporters that facilitate Co uptake -How does Co^{2+} enter into the cells?

Co ions are divalent similar to calcium, and therefore Co and other trace divalent metal ions may enter cells through Ca channels. The Co ion plays a vital role as a structural constituent of numerous proteins, including enzymes and transcription factors, and it is therefore likely that an uptake mechanism has evolved in cells.

Over a decade, plasma membrane ion channels and/or transporters and the characterisation of their physiological functions have been the subject of much research. This is essential for Ca^{2+}, as it plays a vital role in both signalling and membrane trafficking (Michelangeli, Ogunbayo and Wootton, 2005; Zampese and Pizzo, 2012).

Transient receptor potential (TRP) proteins belong to the TRP superfamily of Ca^{2+}-permeable channels with diverse tissue distribution, subcellular localisation, and physiological functions, and may play a role in Co uptake. Mammalian TRP can be divided into 6 subfamilies; TRP canonical (TRPC1–6), TRP vanilloid (TRPV1–6),

TRP melastatin (TRPM1–8), TRP Ankyrin (TRPA1), TRP polycystic (TRPP1–3), and TRP mucolipin (TRPML1–3), and there are a total of 28 members.

Most of the TRP channels are located in the plasma membrane and function as the driving force for Ca^{2+} and Mg^{2+} transport. These channels and transporters regulate and mediate the ion influxes across membranes controlling homeostasis, membrane potential, catabolite export, and membrane trafficking (Dong, Wang and Xu, 2010; Morgan *et al.*, 2011). TRP channels are also permeable to trace metal ions and play an important role in their physiological uptake. After release from wear debris, Co and Cr ions, may be taken up through these TRP channels into cells and this may lead to adverse reactions. However, the mechanism by which these metal ions enter into cells is still under research. TRP ion channels represent important metal transporting proteins by movement of ions according to electrochemical gradients.

There are limited studies about Co uptake into cells. Chigurupati showed that $CoCl_2$ affects the basal concentration of Ca^{2+} and mediates the overexpression of TRPC6 channels at the level of mRNA and protein levels in glioblastoma (Chigurupati *et al.*, 2010). A variety of divalent cations, including trace metal ions such as Co^{2+}, Mn^{2+} and Zn^{2+} permeate the TRPM7 channel in Human embryonic kidney cells (HEK-293) and Hamster Chinese ovary (CHOK1) cells (Monteilh-Zoller *et al.*, 2003; Li, Jiang and Yue, 2006; Topala *et al.*, 2007).

Another transporter potentially involved in transport of divalent cations like Co is divalent metal ion transporter 1 or DMT1. Expression of DMT1 is found in adult mammalian tissue and it is known to actively transport Fe well as other metal ions, such as Zn, Mn, Co, Cd, Cu, Ni, and Pb, via a proton-coupled mechanism(Gunshin *et al.*, 1997). DMT1 appears to mediate the entry of iron from the extracellular environment and/or from recycling endosomes(Shawki *et al.*, 2015). Co^{2+} ions are predicted to enter cells via this transporter, and it may play a role in intestinal, nasal and pulmonary absorption (Illing *et al.*, 2012).

Moreover, the interaction of DMT1 with excessive Fe and Co uptake increased its activity, and led to a production of the reactive oxygen species that caused cellular

damage (Howitt *et al.*, 2009). Although, there is still poor understanding of Co uptake by DMT1, this transporter would be suggested as one of the transporters that may also be involved in cardiac tissue.

1.2.3.1 CaMKII protein and cardiovascular disease-a possible target for the effect of Co^{2+} on the heart.

Ca^{2+}/calmodulin(CaM)-dependent kinase II (CaMKII) is a serine/threonine kinase that is located in a wide range of tissues, and it phosphorylates a broad range of protein substrates(Hudmon and Schulman, 2002). It mediates vital cellular functions (excitable and non-excitable tissues), including physiology/pathophysiology of every organ, especially the heart, and contributes to the cardiovascular system in both a homeostatic and activity-dependent manner (Schulman, 2004). CaMKII is expressed as a multimeric protein that is comprised of 12 subunits (Hoelz, Nairn and Kuriyan, 2003). Its function is linked to CaM binding functions and it is known that the mechanism of CaMKII activation requires Ca^{2+}/CaM binding(Saucerman and Bers, 2008).

CaMKII is an important potential target protein to study in investigations of the actions of Co that are associated with cardiotoxicity. In the cardiovascular system, CaMKII is an important marker implicated in cardiac problems such as cardiac hypertrophy. It plays a key role in development of cardiac hypertrophy and dilated cardiomyopathy (Zhang *et al.*, 2003). CaMKII, in addition to its oxidised(oxidised CaMKII) and phosphorylated (phospho CaMKII) post translational modifications, all play a fundamental role in pathological effects and are central in cardiovascular disease, including heart failure and arrhythmias. Overexpression and high activity of the endogenous CaMKII is reported in a variety of animal models of cardiac hypertrophy and failure (Zhang and Brown, 2004). Ablation of CaMKIIδ has prevented cardiac hypertrophy and remodeling in mice experimental models (Backs *et al.*, 2009). Many studies have implicated the role of CaMKII in terms of vascular remodeling, angiogenesis, enhanced activation of vascular dysfunction and disease (Yousif *et al.*, 2008; Li *et al.*, 2011; Singer, 2012; Scott *et al.*, 2013). It is involved in the mediation of the effects of several pharmacological/physiological signalling molecules and could therefore be a potential target for the actions of Co^{2+}.

Moreover, the relationship between CaMKII and the TRP channel, especially in TRPC6 has been studied. CaMKII plays a role in modulation of Ca^{2+} permeable TRPC6 channels at CaMKII phosphorylation site Thr487, which is responsible for the activation of TRPC6 channel by receptor stimulation. This mechanism is also located in vascular mooth muscle cells (Shi *et al.*, 2013). Additionally CaMKII also plays a vital role in a variety of other TRP channels participating in Ca^{2+} homeostasis/dynamics in the cell such as TRPV1 and TRPC6 (Jung *et al.*, 2004; Li *et al.*, 2008).

1.2.3.2 TRP channels related to cardiovascular disease.

TRP channels are linked to many diseases such as cardiovascular disease, respiratory disease, neurodegenerative and inflammatory processes. The members of the canonical TRP (TRPC) have been studied in cardiomyopathies, which are one of the frequent symptoms caused by adverse effects of implants.

TRPC ion channels are important in Ca^{2+}signalling. High expression of Trpc1, Trpc3 and Trpc6 genes are seen in heart disease, and the TRPC channels contribute to remodeling of the heart (Rowell, Koitabashi and Kass, 2010). TRPC6 –mediated Ca^{2+} entry plays as a key role in a calcium-dependent regulatory loop that leads to pathologic cardiac remodeling via the calcineurin-NFAT signalling regulator(Kuwahara *et al.*, 2006). TRPC6 is an essential component of receptor-activated cation channels, and it is a mediator of receptor-activated Ca^{2+} entry into smooth muscle cells(Soboloff *et al.*, 2005). Mutation of TRPC6 may contribute to pulmonary arterial hypertension(Yu *et al.*, 2009; Garcia-Rivas *et al.*, 2017). Under stretch conditions, TRPC6 activity may be evaluated by measuring extracellular Ca^{2+} influx through the TRPC6 channels in atrial endocardial endothelium cells that are located between the myocardium and the circulating blood (Nikolova-Krstevski *et al.*, 2013). Blockage of TRPC3 and TRPC6 receptors by inhibitors (GSK2332255B and GSK2833503A; against TRPC3 and TRPC6 , respectively) provides evidence to support this, by the inhibition of hypertrophy and dysfunction in cardiac disease in studies of HEK293T cells, derived from human embryonic and neonatal kidneys (Seo *et al.*, 2014). Abnormalities in intracellular Ca^{2+} signalling contribute to sustained pathological cardiac hypertrophy and heart disease.

TRPM7 channels also play a predominant role in Ca^{2+} and Mg^{2+} cellular and systemic homeostasis by their ability to transport metal ions (Nadler *et al.*, 2001; Monteilh-Zoller *et al.*, 2003). Researchers have investigated the characteristics of these channels in a variety of cell types, including the heart(Gwanyanya *et al.*, 2004), brain (Aarts *et al.*, 2003), and intestine (Kim *et al.*, 2009). Recent studies show that TRPM7 may be a key player in cardiovascular disease, embryonic development, and cancer(Fleig *et al.*, 2014).

TRPV1 plays a vital role in the activation of cardiovascular disease, including congestive heart failure, atherosclerosis, cardiac fibrosis, systemic hypertension and vascular remodeling (Randhawa and Jaggi, 2017). Horton demonstrated the effects of a TRPV1 antagonist (BCTC (4-(3-Chloro-2-pyridinyl)-N-[4-(1,1-dimethylethyl) phenyl]-1-piperazinecarboxamide) in cardiac hypertrophy and heart failure in mice(Horton, Buckley and Stokes, 2013). Thus TRP proteins are involved in the transport of cations (Ca^{2+} and Mg^{2+}) and metal ions, and may play a role in uptake of Co^{2+} ions into tissue such as cardiac tissue.

1.2.4 Cardiac Fibroblasts

To assess the potential for toxicity effects of Co especially in heart, initial experiments have screened the *in vitro* toxic responses of Co in a standardised cell line (3T3 cell line) and in primary cardiac fibroblasts (CFs). The mechanism(s) responsible for toxicity of Co ions are poorly understood.

In the heart, cardiac fibroblasts are essential for maintaining structural, mechanical, and electrical functions (Souders, Bowers and Baudino, 2009; Bergmann *et al.*, 2015). In addition to cardiac fibroblasts, the heart is composed of cardiomyocytes, smooth muscle cells, and endothelial cells. Two main cell types in the myocardium are cardiac myocytes and cardiac fibroblasts. The majority of the total cell population in the heart are cardiac fibroblasts which constitute 30-70%, whereas the cardiac myocytes are less than 50% of the total cell population in the heart. The proportion of each cell type varies among species and changes during maturation and in disease (Zak, 1974; Nag, 1980; Adler, Ringlage and Böhm, 1981; Banerjee *et al.*, 2007; Romano *et al.*, 2009). Fibroblasts are cells with a structural function, synthesising components of the

extracellular matrix. They are accordingly associated with various forms of connective tissue. The developing cardiac fibroblast originates from different sources eg. epicardium, endocardium, and the neural crest (Doppler *et al.*, 2017).

CFs are flat, spindle-shaped cells with multiple processes and are the only cell type in the heart lacking a basement membrane(Accornero *et al.*, 2011). The role of cardiac fibroblasts is that they are the primary cell type responsible for the synthesis, deposition, and degradation of matrix proteins, and they therefore play a critical role in the development and maintenance of functional heart tissue, for example, in cell proliferation, cell migration and ECM deposition(Zhang, Su and Mende, 2012).

The size, shape, and function of the myocardium changes in response to alterations in mechanical and/ or electrical signals, which are a common feature in many cardiovascular diseases (including hypertension, coronary artery disease, valvular defects, genetic disorders and arrhythmia disorders (Swynghedauw, 1999). Thus, CFs have a major role in development of diseases, and remodelling responses to injury or toxic events. Cardiac fibroblasts can be programmed *in vivo* to respond to their native environment, which might promote survival, maturation, and coupling with neighboring cells. If Co causes damage to the heart, this function of CFs is likely to be important at the remodelling repair stages hence, the rationale for choosing to examine these cells in this study.

1.3 Aims of the present study

As soon as adverse effects from metal orthopaedic implants were suspected, for example on the cardiovascular system, case reports became available and information on the incidence of adverse effects in patients undergoing hip replacement has continuously increased.

The relationship between metal levels in blood, loosening of prostheses and occurrence of bystander adverse effects is still unclear, since different individuals may present different responses to similar ion levels. Safe Co ion levels have not been established to help decide whether a revision surgery would be necessary to prevent adverse effects. Therefore, the available information is not enough to protect patients and lessen the adverse effects from metal orthopaedic implants made from CoCr alloy.

To focus on this problem, we have investigated the effects of Co ions at concentrations similar to those released from MoM implants on rat heart *in vivo*, cardiac cells *in vitro* and 3T3 cell cultures by means of general toxicity assays, in addition to molecular techniques and cardiac function monitoring.

In terms of toxicity *in vitro*, we tried to find out Co doses that cause a negative impact on cells measured by different cytotoxicity assays, which resulted in testing out much higher doses compared to the Co blood levels seen in patients with metal-on-metal implants. It is important to note though that patients present a diverse susceptibility to Co ions in blood. Catalani *et al*. suggested that using high doses of Co could be necessary in order to observe toxic effects, which might develop earlier in certain patients due to their particular susceptibilities (Catalani *et al.*, 2012).

Conversely, the concentration used for long term testing is associated with that seen in patients. The latter resulted in toxic effects but not in a fatal outcome so it is plausible that low Co levels induce weak toxicity that later develops into more profound effects according to exposure time, which tends to be up to several years in patients.

The objectives of the individual studies comprising this thesis are to:

: Assess the toxicity of Co ions *in vitro* between two cell types, a standardised cell line (3T3 cell line) and primary cardiac fibroblasts (CFs), by exploring cytotoxicity, cell staining (live/dead and morphology change), cell proliferation and cellular uptake.

: Explore the changes in protein and gene expression (western blotting, RNA-Seq and RT-qPCR) *in vitro* after cells have been treated with Co ions.

: Assess the general toxicity of Co ions *in vivo* on male Sprague-Dawley rats, by exploring the effects of exposure to daily administration for 7 and 28-days. Cardiac function (left ventricular end diastolic/systolic diameter and fractional shortening) and Co distribution in the various organs were measured.

: Explore the changes in protein and gene expression (western blotting, RNA-Seq and RT-qPCR) in heart homogenate *in vivo* after animals were treated with Co ions.

: Explore *in vivo* and *in vitro* alterations in RNA gene expression in rat heart and both cell types which could correspond to the interaction between genes and Co ions. This will help to determine novel physiological pathways linked to potential adverse responses to Co ions in MoM implant patients.

Chapter 2. GENERAL METHODS

2.1 Introduction

This chapter contains general methods which were applied in several parts of the thesis. These are separated into two parts, composed of *in vitro* and *in vivo* protocols. Some more specific methods are detailed in the relevant results chapters.

2.2 *In vitro*: Cells

2.2.1 Sterilisation procedures

Aseptic technique was used for cell culture experiments. All apparatus in cell culture work was sterilised by autoclaving for 30 min at 120°C and where possible disposable plasticware was used. All cell culture work was carried out under a laminar-air-flow cabinet maintained by Crowthorne Hi-Tec Service Ltd., Glasgow UK, which controlled aseptic conditions. Prior to and after using a laminar flow cabinet, the cabinet was thoroughly sprayed and cleaned with 70% ethanol. Plastic apparatus was micro-waved for 5 min. at 800 W. All solutions including growth culture media were routinely checked for contamination by adding 1-2 ml of solution to 20 ml of brain heart infusion (BHI) and Sabouraud's medium (SAB), and then incubating at 37°C for 72 h. If there is contamination, the solution becomes turbid, alternatively the solution remains clear. Sabouraud's medium (SAB) which is used to test for fungal contamination and brain heart infusion (BHI) which is used to test for bacterial contamination, were both obtained from Oxoid Ltd., Basingstoke, UK.

2.2.2 Type of Cells

The following cell types were used throughout the research:

: Standardised 3T3 cell line (3T3 cell) , mouse Swiss albino embryo fibroblasts (European Collection of Cell Cultures(ECACC); Wiltshire, UK).

: Primary adult cardiac fibroblast (CFs), isolated from Sprague Dawley rat hearts.

2.2.3 Culturing of the 3T3 cell line (3T3s)

The standardised and immortalised 3T3 cell line was derived from mouse Swiss Albino embryo fibroblasts and obtained from the European Collection of Cell Cultures (ECACC). The cell line grows adherent to the flask surface, and was stored frozen under liquid nitrogen.

The 3T3 cell line was routinely grown in 10 ml complete medium, Dulbecco's Modified Eagle's Medium (DMEM) (Lonza, Slough, UK) plus 10% (v/v) Foetal Bovine serum (FBS): 1% (v/v) Penicillin & streptomycin (5000 μg/ml) and 1% (v/v) Non-essential amino acids (NEAA) (all from Life Technologies; Paisley, UK) in 25 cm^2 flasks (Nunc A/S; Roskilde, Denmark).

Confluence in 3T3 cell cultures occurs 2-3 days after seeding. Cells were passaged at a ratio of 1:5 every 3 days. The complete medium was discarded from the flask, the adherent cells were washed twice with 5 ml versene to remove all particle or waste and traces of serum from the old medium. After that, 1-2 ml of 0.05% (w/v) Trypsin (Life Technologies; Paisley, UK) was added; cells were incubated for 3-5 min and checked under the phase contrast microscope (Nikon Corporation, Japan) for detachment. The trypsin acted to detach the adherent cells from the flask surface by protease action. The flask was tapped to help any remaining cells to detach. Subsequently, the complete medium with the presence of FBS was added to stop the reaction of trypsin.

2.2.4 Isolation of primary cardiac fibroblast (CFs)

Primary cardiac fibroblasts derived from adult rat heart were isolated by a Chunk digestion method (Martin *et al*., 2014, Lawan *et al*., 2011).

2.2.4.1 Preparation of solutions used

All solutions were freshly prepared prior to isolation and all chemicals and reagents were purchased from Sigma-Aldrich; Dorset, UK.

2.2.4.1.1 Krebs–Henseleit (Krebs) buffer (non-Ca^{2+} containing) pH 7.4

This solution was prepared for making digestion buffer and washing buffer and contained 120 mM NaCl, 5.4 mM KCl, 0.52 mM NaH_2PO_4, 20 mM Hepes, 11.1 mM glucose, 3.5 mM $MgCl_2$, 20 mM Taurine and 10 mM Creatine; (all Sigma-Aldrich; Dorset, UK) made up to 500 ml of MilliQ water. The pH of Krebs was adjusted to 7.4 using 0.1 or 0.5 M NaOH and then filtered-sterilised with a 0.22 µm syringe filter (Merck Millipore, Ireland) prior to use.

2.2.4.1.2 Washing Buffer

50 ml washing buffer was prepared using Krebs–Henseleit (Krebs) buffer pH 7.4, with added 0.5 ml 1mM EGTA and 1 ml 2X Penicillin & streptomycin (5000 Unit/ml-5000 µg/ml). The solution was filtered-sterilised with a 0.22 µm syringe filter prior to use.

2.2.4.1.3 Digestion Buffer

50 ml digestion buffer was prepared using Krebs–Henseleit (Krebs) buffer pH 7.4, 40 mg Collagenase Type II and 1.5 mg Protease XIV. The solution was filtered-sterilised with a 0.22 µm syringe filter prior to use.

2.2.4.1.4 Isolation Medium and Growth Medium

Isolation medium and growth medium were prepared using Dulbecco's Modified Eagle's Medium (DMEM) plus 20% (v/v) Foetal Bovine serum: 2% (v/v) Penicillin & streptomycin (5000 µg/ml) and 1% (v/v) Non-essential amino acids (NEAA).

2.2.4.2 Isolation of Cardiac fibroblast from adult rat' heart: Procedures

Primary cardiac fibroblasts were isolated from male Sprague Dawley rat hearts (weight of rats, 200-300 g). Rats were bred in house, Strathclyde University. They were kept in cages with sterilised wood shavings as bedding at 24 ± 2°C in a 12 h light/dark cycle and fed with standard diets and tap water *ad libitum*.

All work was carried out in sterile conditions using the biological safety cabinet. The rat was euthanised by sodium pentobarbitone injection intraperitoneally (i.p.) at 60 mg/ kg. The skin of the chest was sprayed with ethanol, then the chest cavity opened. The heart was carefully excised from the cavity using sterilised scissors and placed into a 20 ml sterile tube containing 10-15 ml pre-warmed (37°C) washing buffer.

Fibroblasts were dissociated from the tissue via digestion in Krebs (non-Ca^{2+} containing) containing 0.8mg/ml collagenase type II (Life Technologies, Paisley) and 0.03mg/ml protease XIV (Sigma-Aldrich, Dorset, UK). The digestion steps were repeated 3-4 times until the tissue was completely digested. After each digestion step, the solution was centrifuged at 600rpm (462g) for 3 min and the supernatant containing the isolated cells collected. After complete digestion, supernatants were pooled and centrifuged for 10 min at 2000rpm (5,143g). Once the supernatant from this final centrifugation was discarded, the cell pellet was re-suspended in culture medium, plated into a T75 flask and incubated at 37^{o}C for 4-5h. At this time remaining myocytes were removed by replacement with fresh culture medium and cells left for 2 days until a further medium change. Cells were grown to sub-confluency then passaged or plated for use. These primary cells were used from passages 1-2. This whole procedure is illustrated in Figure 2-1.

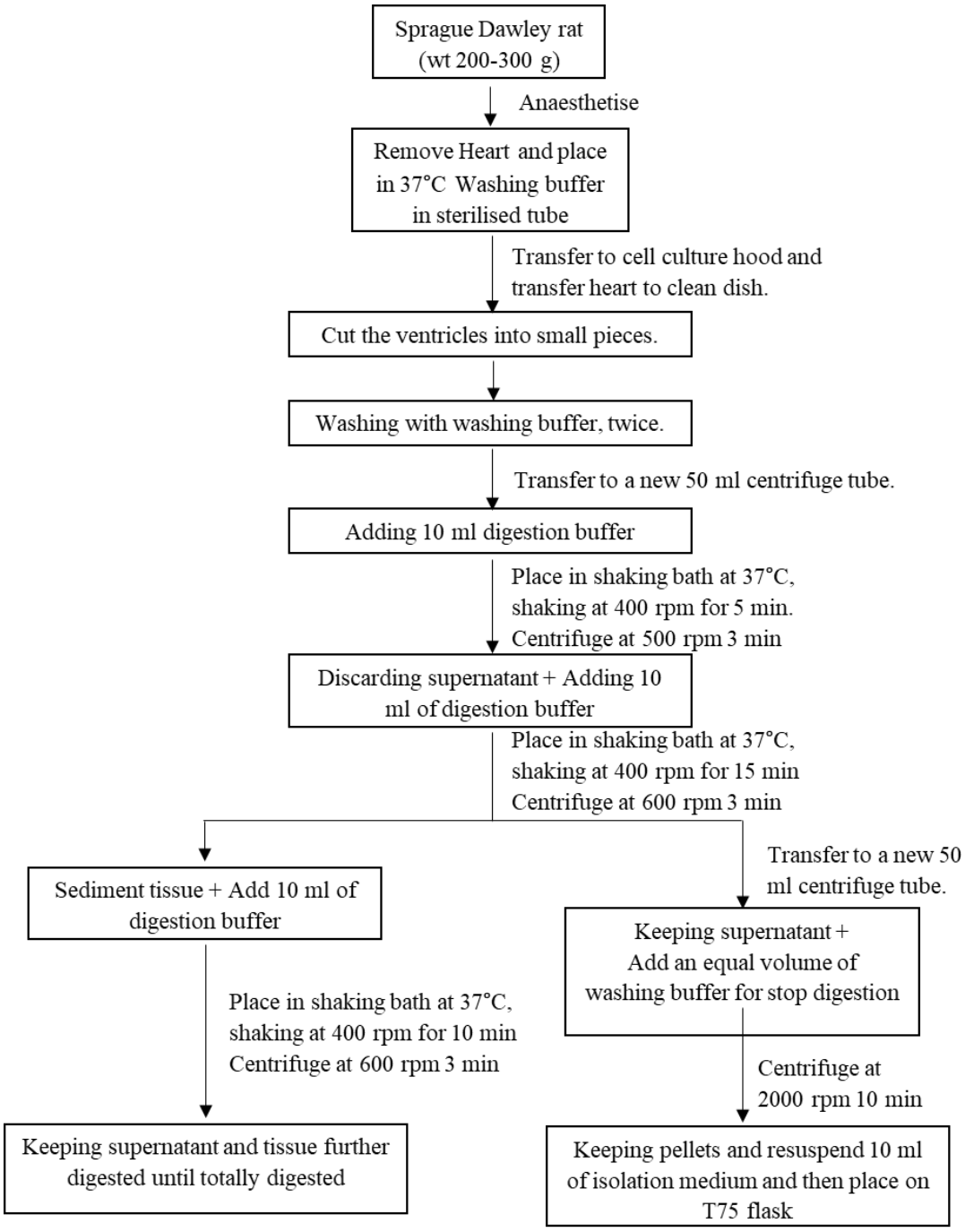

Figure 2-1 Isolation of cardiac fibroblasts from adult rat' hearts.

2.2.5 Culturing of Primary cardiac fibroblast (CFs)

Primary cardiac fibroblasts (CFs) were only used up to passage 2 for experiments because de-differentiation starts to occur after passage 2. Culturing of CFs was as previously described in section 2. 2. 3 except using TrypLE Express (Life Technologies; Paisley, UK) instead of 0.05% (w/v) Trypsin in trypsinisation. The TrypLE Express is a special protein digestive enzyme for gentle cell detachment of adherent cells such as primary cardiac cell fibroblasts from the flask surface, which is suitable for primary cardiac fibroblast when comparing with 0.05% (w/v) Trypsin.

2.2.6 Immunochemistry of the characteristics of CFs

The majority of the total cell numbers in the heart are fibroblasts and they account for approximately 70% of all cells in the healthy adult heart (Souders *et al.*, 2009). However, the number of fibroblasts in the heart is not stable and it responds dynamically to the development of disease and aging (Snider *et al.*, 2009, Biernacka and Frangogiannis, 2011). Normally, fibroblast cell types have been difficult to positively identify. Fibroblasts can take on a wide array of shapes in different tissues and are identified based on the spindle shape combined with vimentin-positive staining. This is the mesenchymal marker. Absence of staining for epithelial cell types can also be proven (muscle cells, astrocytes and hematopoietic cells) (Chang *et al.*, 2002).

Cells were counted using a haemocytometer (Marienfeld; Germany), seeded in a sterilised glass coverslip and placed on a 35 mm^3 culture dish (Nunc A/S; Roskilde, Denmark) at a density of 10^4 cells/cm^2 or $1.6x10^4$ cells/ml, and incubated 37°C, 5% CO_2 for 24 h. After incubation, cells were then washed with phosphate –buffered saline (PBS) pH 7.4. The cells were fixed with ice cold methanol (MeOH) for 10 min. After that, cells were permeabilised using 0.01% Triton x-100/PBS for 10 min and then blocked with 1% (w/v) bovine serum albumin (BSA) in PBS for 1 h at room temperature. Then, primary antibody (Anti-vimentin antibody (Vim3B4); Abcam; UK) was added (1:400), and then incubated at 4°C overnight. After incubation, culture dishes were washed three times with cold PBS and treated with the secondary antibody (FITC-conjugated donkey anti-mouse IgG, 1:1000, Abcam; UK) at room temperature for 1 h in the dark. Culture dishes were then washed again three times with cold PBS.

This was followed by staining with DAPI (4',6-diamidino-2-phenylindole), which was added to each culture dish, and they were then kept in the dark for 5 min. Finally, the coverslips were washed with PBS and then mounted onto slides with Mowiol® (Sigma-Aldrich; Dorset, UK). The slides were then viewed using a Carl Zeiss Axio Imager microscope (Carl Zeiss MicroImaging GmbH, Germany) under a 20X lens (NA 0.50). Fluorescence was excited using a mercury lamp and emission was recorded using fluorescein isocyanate (FITC)/DAPI filter block (493/358 nm; 528/461 nm) for vimentin and DAPI. Fluorescence was stable allowing digital images to be captured using AxioVision v.4.6 (Zeiss, Germany).

2.2.7 Preparation of Co ion solutions

Cobalt (II) Chloride hexahydrate ($CoCl_2.6H_2O$) (Sigma-Aldrich; Dorset, UK) was used to make up the Co (II) stock solution for the experiments. Co (II) solutions were made freshly every time cells were passaged and incubated. Freshly weighed $CoCl_2.6H_2O$ was dissolved in deionised water on the day of the experiment, and then filtered-sterilised with a 0.22 µm syringe filter to give 100 mM. Subsequent dilutions were made in growth medium for required concentrations, as follows

Short term toxicity testing: 0 - 1000 µM

Long term toxicity testing: 0 - 5 µM

Cell Proliferation: 0 – 500 µM and 0-25 µM

Cell Staining: 0, 250 µM and 500 µM

Cellular Co uptake: 0 - 300 µM

Western blotting: 0 - 100 µM

RNA-Seq and RT-qPCR: 0, 1 and 10 µM

Concentration of Co ions within solution may be reported using different units, depending on the conventions accepted within particular disciplines. To allow easy comparison of the results within this thesis with existing literature, a conversion table has been provided in the Appendix, Table A1-1.

2.2.8 Exposure of 3T3s and CFs to Co ions

3T3 cell lines (cultured as described in section 2.2.3) and isolated primary cardiac fibroblasts (prepared as described in section 2.2.4 and 2.2.5) were counted using a haemocytometer, seeded in a 96-well plate or 35 mm^2 culture dish at a density of a 10^4 cells/cm^2 or $1.6x10^4$ cells/ml, and incubated for 24 h. Cultures were then treated with a range of Co (II) solutions (as described in section 2.2.7) in complete medium, at 37°C, 5% (v/v) CO_2 for exposure times, as follows:

Short term toxicity testing, cell staining and Co uptake: 24, 48 and 72 h.

Short term cell proliferation: 48 and 72 h.

Long term toxicity testing: 28 days (as described below)

For the long term toxicity study, the experiment was started on a Thursday, when a flask (75 cm^2) containing a confluent 3T3 cells was passaged. The 3T3 cells were counted by haemocytometer and seeded in six sterile T25 cm^2 flasks labelled as control (0 µM), Co1 (0.001 µM), Co2 (0.01 µM), Co3 (0.1 µM), Co4 (1 µM), Co5 (5 µM). The cells in suspension were reseeded into each of the six flasks at densities of $7x10^3$ cells/cm^2 or $1.75 x10^3$ cells/ml. These flasks were incubated at 37°C, 5% CO_2 for four days until the next Monday. This point marked the start of the first week. On Monday, the cells in the six flasks were each reseeded at a density of $7x10^3$ cells/cm^2 to form four separate samples. One was a T25 flask, another was a 96 well plate and the remaining two were 35 mm^2 culture dishes. These were incubated further with the Co for further three days until Thursday. At this point, the cells from the 96 well plate and the two 35 mm^2 culture dishes were collected. The viability of the cells in the 96 well plate was measured by using a combined viability assay and the cells in both 35 mm^2 culture dishes were stained for live/dead cells and actin-filament fluorescence staining. Finally, the stained cells were observed under the Zeiss Microscope (Carl Zeiss MicroImaging GmbH; Germany). For the remaining T25 flask (at every Co dose), the cells were reseeded with freshly prepared Co (II) in the respective Co concentration in growth medium and then incubated further. This marked the start of wk2. The whole procedure was repeated every Thursday and Monday, giving Co exposure for 28 days to measure long term toxicity of Co in 3T3 cells. See flow chart on Figure 2-2 for a description of this experimental design.

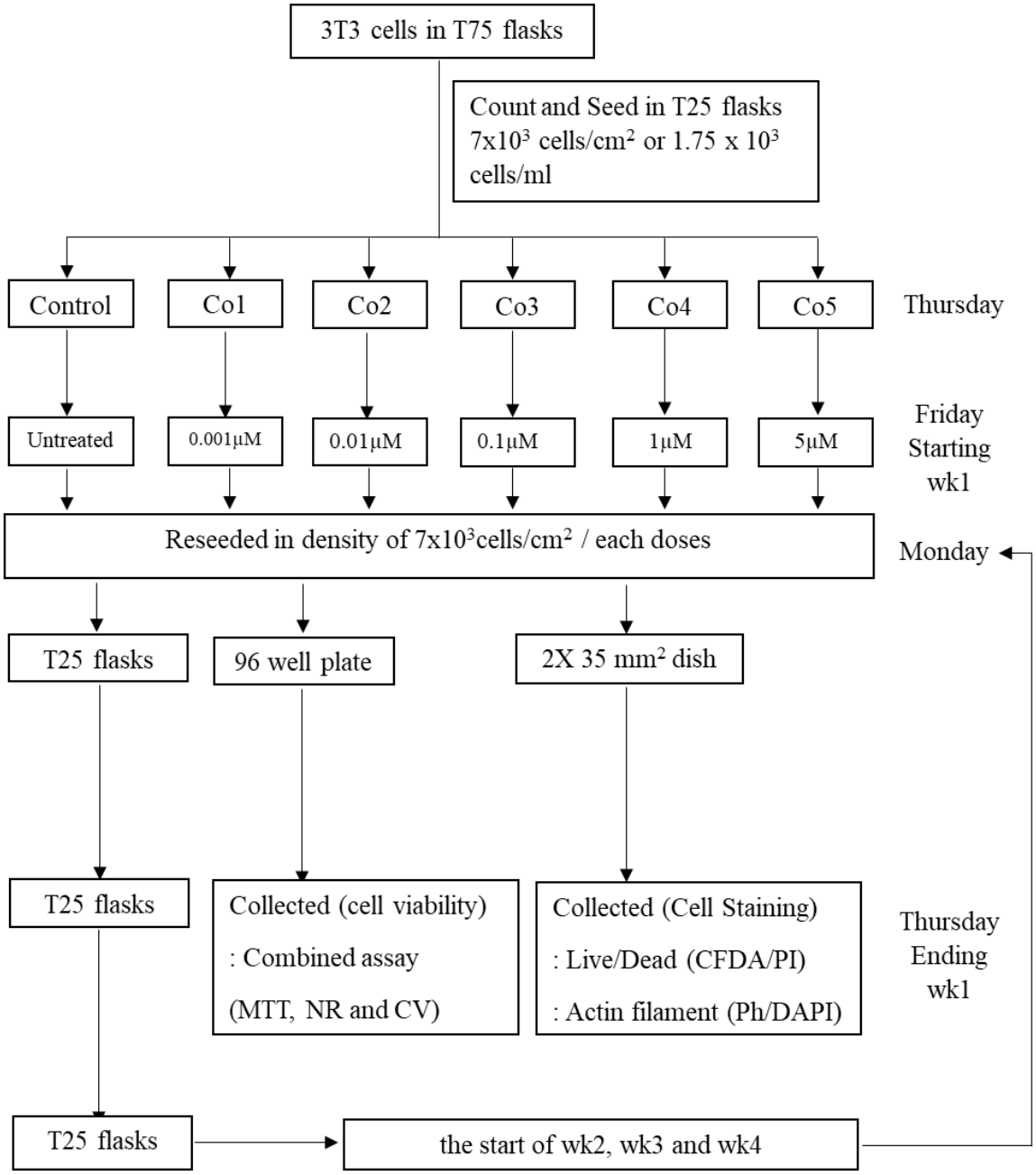

Figure 2-2 Experimental design for long term toxicity testing on 3T3 cell line.

2.2.9 MTT assay for cell viability

MTT is one of the most common methods for detection of cytotoxicity following exposure to toxic substances. The mechanism of the MTT assay involves intracellular substrate (MTT) reduction, both by mitochondrial and cytosolic enzymes. MTT (3-(4, 5- Dimethylthiazol- 2- yl) - 2, 5- Diphenyltetrazolium Bromide) is a water soluble tetrazolium salt, which is cleaved of the tetrazolium ring by succinate dehydrogenase and other reductase enzymes. The purple formazan product is largely impermeable to cells and therefore accumulates within healthy cells (Mosmann, 1983). Berridge and Tan stated that reduction of MTT can be mediated by both NADH or NADPH within the cells (Berridge and Tan, 1993).

The 3T3 cells were cultured (as described in section 2.2.8) in a 96 well plate. A range of Co (II) solutions (200 µl, 0- 1000 µM) were added to the cells and they were incubated for 24, 48 and 72 h, and then washed out. MTT (50 µl, 4 mg/ml in PBS pH 6.75) and cell culture medium (150 µl) were added to each well. The cells were then incubated at 37°C and 5% CO_2 for an additional 4 h. The medium containing MTT was discarded, and intracellular MTT formazan that had been produced was extracted with 150 µl DMSO following 15 min agitation. The absorbance was measured at 540 nm immediately using a Thermo Scientific Multiskan Ascent spectrophotometer plate reader. The toxicity of $CoCl_2$ was measured by the 50% inhibitory concentration (IC_{50} of MTT reduction), comparing the absorbances in control wells which were not exposed to Co, with each of the treated wells. IC_{50} was calculated by linear regression.

2.2.10 Neutral Red Assay (NR) for cell viability

The Neutral Red (NR) assay is also a common method for determining cell viability (Fautz, Husein and Hechenberger, 1991; Morgan *et al.*, 1991). Living cells take up the neutral red dye. Nonionic passive diffusion helps the cationic dye diffuse through cell membranes, and it is concentrated within the lysosomes. The lysosomes bind the dye by electrostatic hydrophobic bonds to anionic and phosphate groups of the lysosomal matrix.

The 3T3 cells were cultured and treated with Co as before. NR stock solution (4 mg/ml in PBS pH 7.4) was diluted at a ratio of 1:100 with complete medium and added to

each well. The cells were then incubated at 37°C and 5% CO_2 for an additional 3 h. The medium containing NR was discarded and cells washed with PBS, pH 7.4. After that the cells were extracted with 200 µl of destain of the following composition (50% (v/v) ethanol, 1% (v/v) glacial acetic acid and 49% (v/v) distilled water) and shaken on a plate shaker for 1 h. The absorbance was measured at 540 nm immediately using a Thermo Scientific Multiskan Ascent spectrophotometer plate reader. The toxicity of $CoCl_2$ was indicated by 50% inhibitory concentration (IC_{50}), comparing absorbances in Co treated and control wells.

2.2.11 Crystal Violet (CV) Assay for cell viability

Crystal violet (CV) or gentian violet is a triphenylmethane dye, which provides a simple, rapid, and inexpensive colorimetric assay for detecting cell viability (Gillies, Didier and Denton, 1986). Crystal Violet stains viable cells that adhere to their culture vessel, and intact cells are stained by this dye. The cells are first fixed for example in methanol or glutaraldehyde thus allowing the stain to permeate. CV stains nuclei a deep purple colour, permitting their visualisation. There are some limitations to this method because crystal violet (CV) only detects adherent cells. Lysed cells simply detach from the vessel surface and are not stained by CV.

The 3T3 cells were cultured and treated with Co as before. 200 µl of 4% (v/v) Formalin was then added to fix cells for at least 30 min. The fixative was then removed, and the cells washed 3 times with PBS, pH 7.4 before adding the CV in distilled water (50µl, 1 mg/ml in DW) for an additional 20 min at room temperature. The stained cells were washed with PBS three times. After that the cells were extracted with 200 µl of 0.1% Triton-x100 (0.1% in PBS) and shaken on a plate shaker overnight. The absorbance of light was measured at 540 nm immediately using a Thermo Scientific Multiskan Ascent spectrophotometer plate reader. The toxicity was indicated by 50% inhibitory concentration (IC_{50}), by comparing absorbance in Co treated and control wells. The experimental design for the separate viability assays is shown in Figure 2-3.

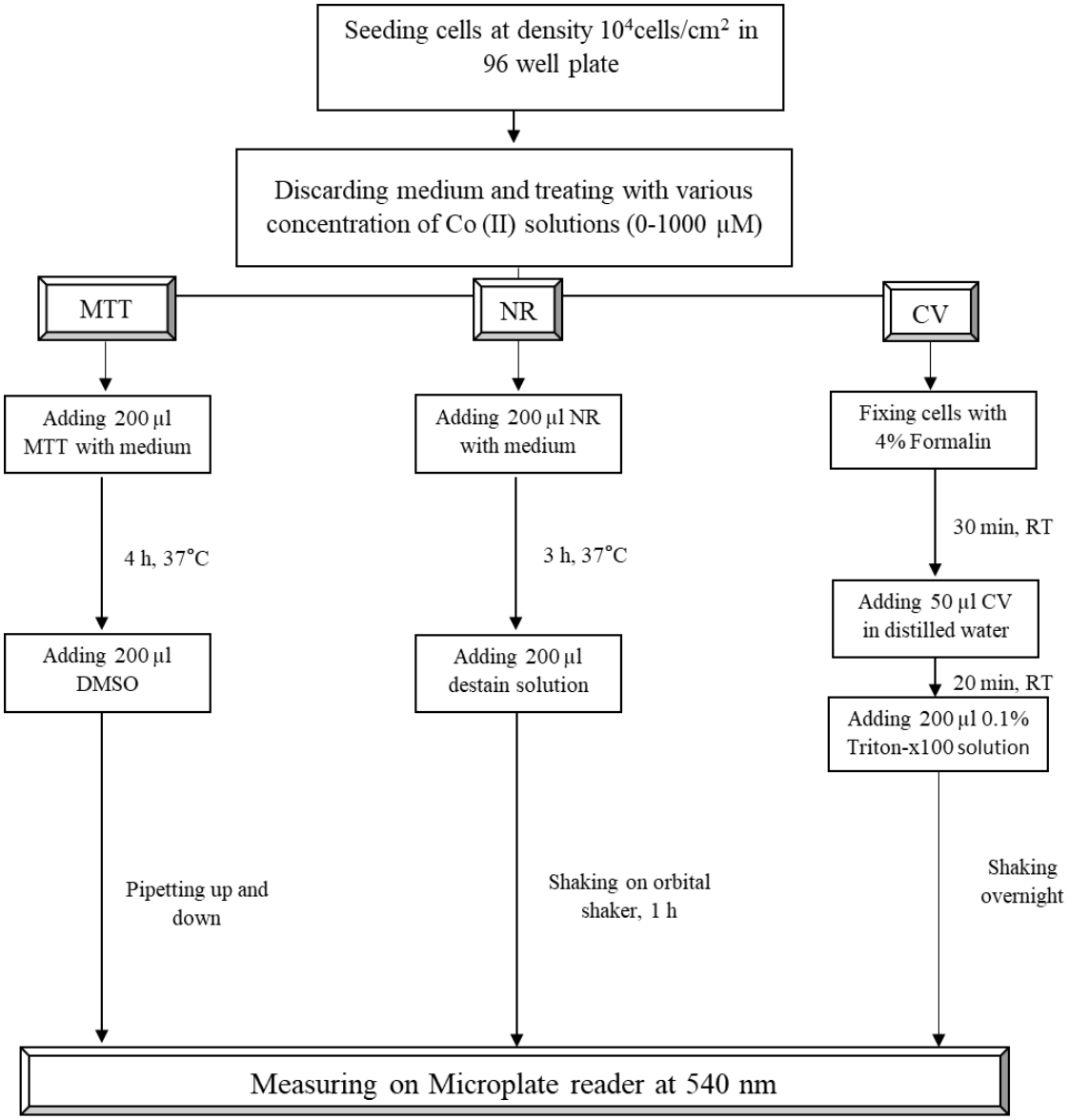

Figure 2-3 Experimental design of cytotoxicity testing using separate assay (MTT, NR and CV).

2.2.12 Combined assay (MTT, NR and CV) for cell viability

The combined assay is composed of the three simple assays, neutral red, MTT and also crystal violet. Each assay can be measurement by spectrophotometric measurement at absorbance 540 nm, on the same 96 well plate. The results from the combined assay were validated by comparison with each assay carried out individually.

The 3T3 cells and CFs were cultured and treated with Co as before. NR stock solution (4 mg/ml in PBS pH 7.4) was diluted at a ratio of 1:100 with complete medium and added to each well. The cells were then incubated at 37°C, 5% CO_2 for an additional 2 h. After that 50 µl MTT (4 mg/ml in PBS pH 6.75) was added and the plate incubated for a further 1 h. After incubation for a total of 3 h, the medium containing NR and MTT was discarded and cells washed quickly with 200 µl of 1% formalin in PBS. Then 150 µl of extraction solution of the following composition (1% glacial acetic acid solution containing 30% ethanol) was added and samples allowed to stand for 20 min at room temperature. The extraction solution was transferred to a new 96 well plate for measuring the neutral red cytotoxicity. The absorbance of light was measured at 540 nm immediately using a Thermo Scientific Multiskan Ascent spectrophotometer plate reader. The toxicity was indicated by 50% inhibitory concentration (IC_{50}) as before. After transferring the extract the wells were washed quickly with extraction solution and 100 µl Isopropanol was added and agitated for 10-15 min or until clear. The absorbance measurements were read at 540 nm. The toxicity was indicated by 50% inhibitory concentration (IC_{50}) as before. Finally, 200 µl of 4% Formalin was added to fix the cells for at least 30 min. Formalin was then removed and the cells washed three times with PBS pH 7.4 before adding the CV in distilled water (50µl, 1 mg/ml in DW) for an additional 20 min at room temperature. The stained cells were washed with PBS at 3 times. After that, these cells were extracted with 200 µl of 0.1% Triton-x100 (0.1% in PBS) and shaken on the plate shaker overnight. The absorbance was read at 540 nm. The toxicity was indicated by 50% inhibitory concentration (IC_{50}) as before. The flow chart on Figure 2-4 illustrates the experimental design.

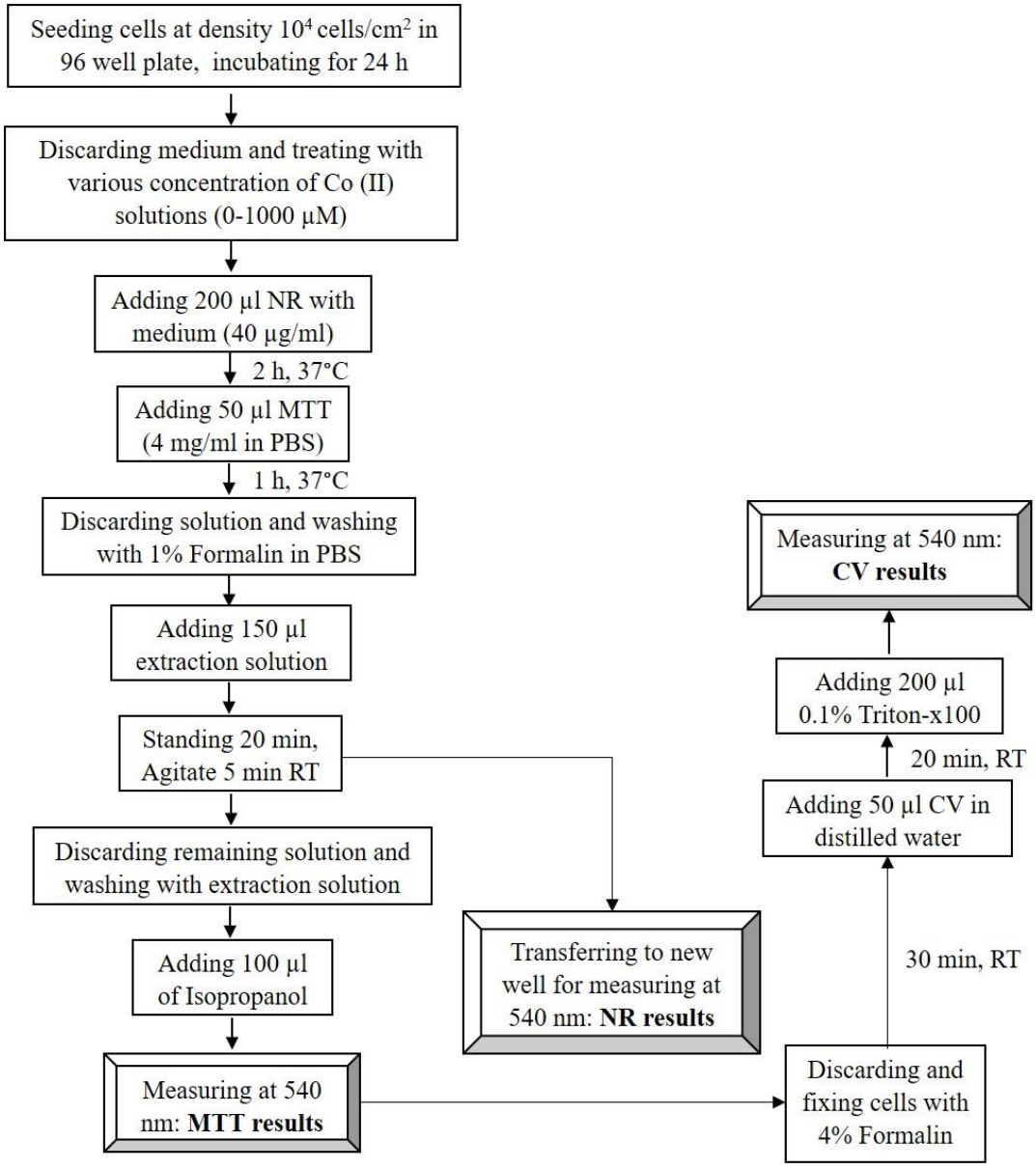

Figure 2-4 Experimental design of cytotoxicity testing by using the combined assay (MTT, NR and CV).

2.2.13 Analysis of cell viability via microscopy (CFDA and PI)

In order to assess the effects of Co on cell viability, cells were stained with Carboxyfluorescein diacetate (CFDA) and Propidium Iodide (PI). The double staining fluorescent techniques such as Propidium iodide coupled with CFDA were used to evaluate live and dead cells treated with Co. CFDA is a stain for determining cell membrane integrity. It is hydrolysed by intracellular esterases to the fluorescent carboxy fluorescein which is retained in the intact cell and shows as green fluorescence (Haugland, 2005). PI is impermeable to intact plasma membranes, but it easily penetrates the plasma membrane of dead or dying cells and intercalates with DNA or RNA forming a bright red fluorescent complex. PI does not pass into living cells, and is commonly used to detect dead cells in a population (Bank, 1987, 1988)

The 3T3 cells and CFs were seeded in a 35 mm^2 culture dish at a density of 10^4 cells/cm^2 or $1.6x10^4$ cells/ml, and incubated for 24 h. A range of Co (II) solution concentrations (2 ml, 0, 250 and 500 µM) were added to the cells and incubated for 24, 48 and 72 h. After the incubation time, the medium was discarded and the monolayer washed twice with PBS pH 7.4 and then PI (Sigma-Aldrich; Dorset, UK) added (20 µg/ml in PBS, pH 7.4) to each dish and they were incubated in the dark for 1 min. After that the PI was removed and discarded to a waste bottle and the cells washed three times with PBS pH6.75 prior to staining with CFDA (Sigma-Aldrich; Dorset, UK). The CFDA stain was incubated for 5-15 min in the dark, and then the cells washed again with PBS pH 6.75. The cells were then viewed using a Carl Zeiss Axio Imager microscope under a 20X water immersion lens (NA 0.50). Fluorescence was excited using a mercury lamp and emission was recorded using fluorescein isocyanate (FITC)/Rhodamine filter block (485/535 nm; 546/617 nm) for CFDA and PI. Fluorescence was stable allowing digital images to be captured using AxioVision v.4.6 (Zeiss; Germany). Analysis of images was carried out with both AxioVision 4.6 and the freeware ImageJ v.1.47q (http://rsbweb.nih.gov/ij/download.html).

2.2.14 Analysis of cell morphology via microscopy (Phalloidin and DAPI)

In order to assess the effects on cell morphology actin was stained. Phalloidin is a bicyclic peptide belonging to a class of phallotoxins, and is isolated from the death cap mushroom (*Amanita phalloides*). This toxin selectively labels F-actin. FITC binding to the phalloidin provides green fluorescence. Phalloidin binds to actin filaments more strongly than to actin monomers. DAPI (4',6-diamidino-2-phenylindole) is a blue-fluorescent stain that binds strongly to A-T rich regions in double stranded DNA, and it is compatible with both live- and fixed-cell applications. It is cell wall permeable, and is popular for detecting the DNA in cell culture. Both membrane intact cells and membrane damaged cells can be stained with DAPI.

The 3T3 cells and CFs were seeded in a 35 mm^2 culture dish at a density of 10^4 cells/cm^2 or $1.6x10^4$ cells/ml, and incubated for 24 h. A range of Co (II) solution concentrations (2 ml, 0, 250 and 500 µM) were added to the cells and they were incubated for 24, 48 and 72 h. The cells were fixed (permeabilised) with 4% Formalin for at least 30 min, and then the fixative was washed off by rinsing three times with PBS pH 7.4. A small silicone ring was used to control the volume of Phalloidin, added to each dish, and 100 µl Phalloidin was added and incubated at 37°C in moist conditions at 1 h. After that the Phalloidin was discarded to a specific waste bottle, and then the sample washed three times with PBS pH 7.4. Then, 1 ml DAPI (0.6 nM) was added to each dish for 5-15 min and washed off with PBS pH 7.4 again. The cells were then viewed using a Carl Zeiss Axio Imager microscope under a 20X water immersion lens (NA 0.50). Fluorescence was excited using a mercury lamp and emission was recorded using a fluorescein isocyanate (FITC)/DAPI filter block (485/358 nm; 546/461 nm) for Phalloidin and DAPI. Fluorescence was stable allowing digital images to be captured using AxioVision v.4.6 (Zeiss, Germany). Analysis of images was carried out with both AxioVision 4.6 and the freeware ImageJ v.1.47q (http://rsbweb.nih.gov/ij/download.html).

2.2.15 Cell Proliferation Assay (BrdU assay)

Cell proliferation can be measured by various methods. In this study, the BrdU Cell Proliferation Assay was chosen and cell proliferation was determined by a non-isotopic BrdU Cell Proliferation Immunoassay kit (Calbiochem, Darmstadt, Germany). The kit provided all the agents and solutions required.

Bromodeoxyuridine (BrdU) is a non-isotopic immunoassay, using an analog of a DNA nucleotide - the thymidine analog BrdU (5-bromo-2'-deoxyuridine), which incorporates into the synthesised DNA of actively dividing cells and is detected with an anti-BrdU antibody. A second antibody linked to horseradish peroxidase (HRP) provides the detection system. The HRP catalyses the conversion of the chromogenic substrate tetra-methylbenzidine (TMB) from a colourless solution to a blue solution (or yellow after the addition of stopping reagent), the intensity of which is proportional to the quantity of BrdU incorporated into cells, which is a direct indication of cell proliferation. The coloured reaction product is quantified using a plate reader. See Figure 2-5 for a diagrammatic representation of this assay.

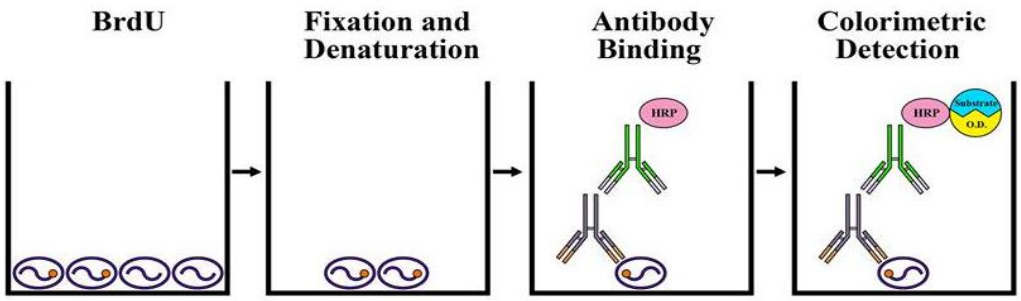

Figure 2-5 BrdU Cell Proliferation Assay.

All solutions from the kit were placed at room temperature for around 1 h before using. The BrdU label was diluted into fresh growth medium at a ratio of 1:2000(20 µl of BrdU label were added into 4 ml of complete medium). The 100X Anti-BrdU Ab was diluted into antibody diluent at a ratio of 1:100 (60 µl of 100X Antibody- BrdU Ab were added into 6 ml of antibody diluent). The Peroxidase Goat Anti-Mouse IgG HRP Conjugate was diluted into Conjugate diluent (10 µl of Peroxidase Goat Anti- Mouse IgG HRP Conjugate were added into 10 ml of Conjugate diluent). The 20X wash concentrate buffer was diluted into distilled water at a ratio of 1:20 (25 ml of 20X wash concentrate buffer were added into 475 ml of distilled water).

The 3T3 cells and CFs were counted by haemocytometer and seeded in a 96 well plate at a density of $1.25x10^5$ cells/cm^2 or 10^5cells/ml (200µl/well), and incubated for 24 h. A range of Co (II) solutions (100 µl, 0- 1000 µM) were added to the cells and incubated for 48 and 72 h. Then, 4 h before the incubation period was complete, the BrdU label was added into each well and then washed out after the end of the incubation time (48 and 72 h). The cells were fixed with fixative/denaturing solution for an additional 30 min at room temperature, then the solution was discarded and the plate was tapped on paper towels to dry it. Following this step, Anti- BrdU Antibody was added into each well and the plates were incubated for 1 h. After that the Peroxidase Goat Anti-Mouse IgG HRP Conjugate was added to bind with Anti-BrdU Antibody for 30min at room temperature. Then, plates were washed to remove excess Antibody and Substrate solution, followed by stop solution which was added into each well under dark conditions at room temperature. The absorbance was finally measured (approximately within 1 h) using a Thermo Scientific Multiskan Ascent spectrophotometer plate reader at dual wavelengths of 450- 570 nm. Then cell proliferation was calculated by comparing the sample OD value with the control OD. The experimental design of this experiment is shown in the flow chart on Figure 2-6.

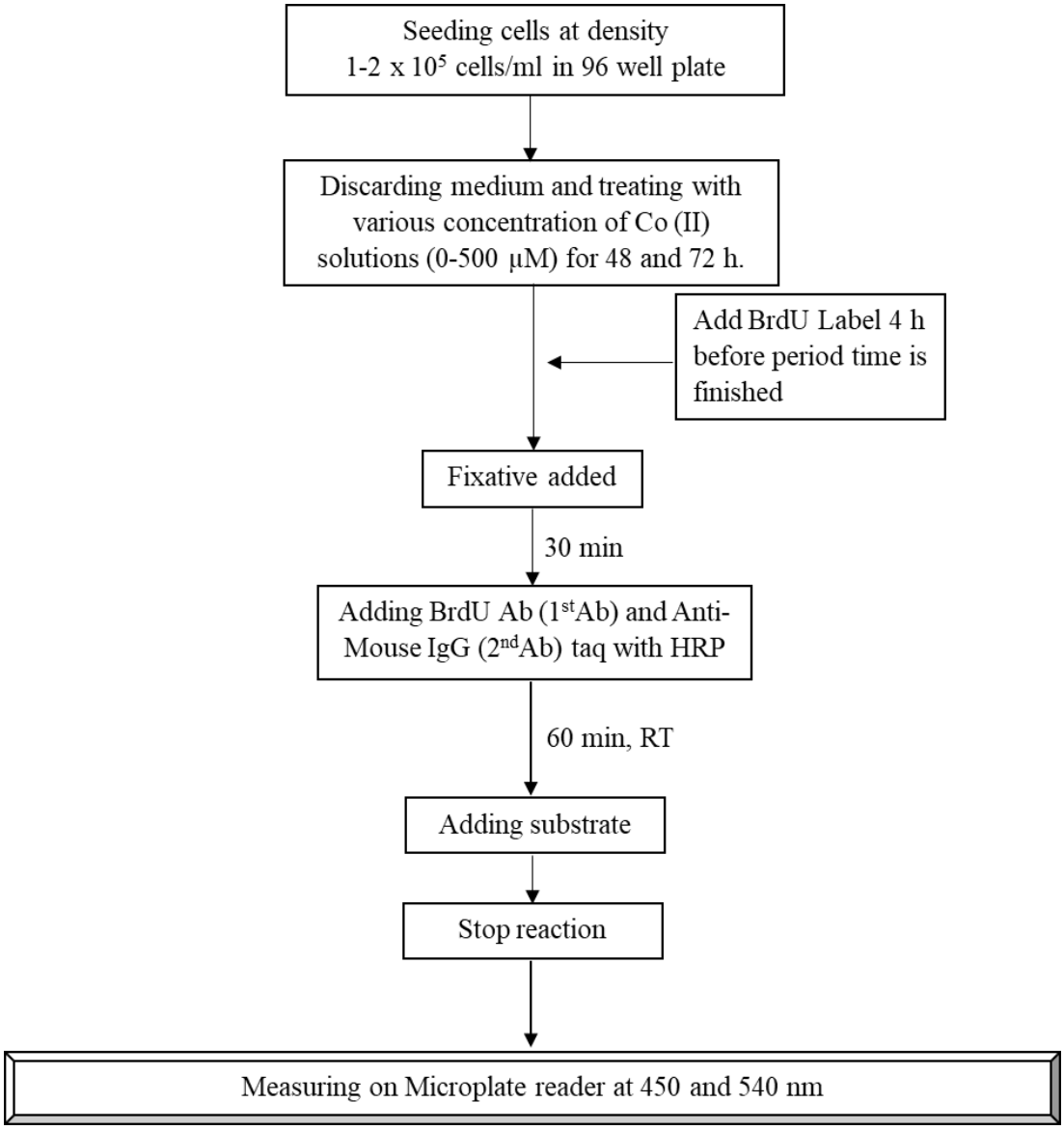

Figure 2-6 Experimental design of BrdU cell proliferation assay.

2.2.16 Inductively coupled plasma mass spectrometry (ICP-MS) Analysis of metal ion concentrations

The aim of these experiments was to investigate the uptake of $CoCl_2$ into the 3T3 and CF cells by measuring intracellular metal content using ICP-MS to investigate whether increased uptake into CFs accounted for the differences in the differential effect of Co in these cells.

2.2.16.1 Preparing the equipment, supplies and chemicals

All glass and plastic devices used in metal analysis were soaked in 2% (v/v) HNO_3 overnight. After that everything was rinsed twice with ultrapure water (18mΩ) and dried.

2.2.16.2 Cell Preparation and Treatment (3T3 cells and CFs)

In order to determine cellular up-take of the Co ions from the culture medium during incubation with $CoCl_2$ (cultured as described in Section 2.2.3 and 2.2.5), the 3T3 cells and CFs were seeded in a 35 mm^2 dish at a density of $7x10^3$ cells/cm^2, and incubated for 24 h at 37°C and 5% (v/v) CO_2. A range of Co (II) solutions (2 ml, 0-300 µM) was added to the cells and they were incubated for 24, 48 and 72 h.

Treatment with every concentration was carried out in triplicate and controls with no Co were also present. After the incubation time, the medium was discarded and the monolayer washed twice with PBS pH 7.4. After the second wash, PBS (1 ml/ dish) was added, cells scraped and transferred into an Eppendorf tube. Cells were centrifuged at 350xg for 5min. PBS was discarded and pellets were sonicated for 30 min at 45°C.Cell lysates were then resuspended in 1ml of ultrapure water (18mΩ) and stored at -20°C overnight. They were then allowed to thaw at room temperature and centrifuged at 16,100 g for 15min. The supernatant was transferred to a new 15 ml centrifuge tube. All samples were diluted 10-fold (1 ml of each sample was added to 9 ml of 2% (v/v) HNO_3). Co standards (range 0, 50, 100, 250, 500 and 1000 µg/l) were prepared by diluting 1000 mg/l (TraceCERT®, Sigma-Aldrich; Dorset, UK) with HNO_3. Samples were analysed using an Agilent 7700x octopole collision system ICP-MS (Agilent Technologies; Wokingham, UK) in helium gas mode using Scandium (Sc, 3 ppm) as internal standard. The quantification is based on the maximum signal for a particular isotope, also referred to as peak height. Five readings are taken, and

the result obtained is the mean value. This was performed by Department of Pure and Applied Chemistry, University of Strathclyde, Glasgow, UK. The experimental design is shown on the flow chart on Figure 2-7.

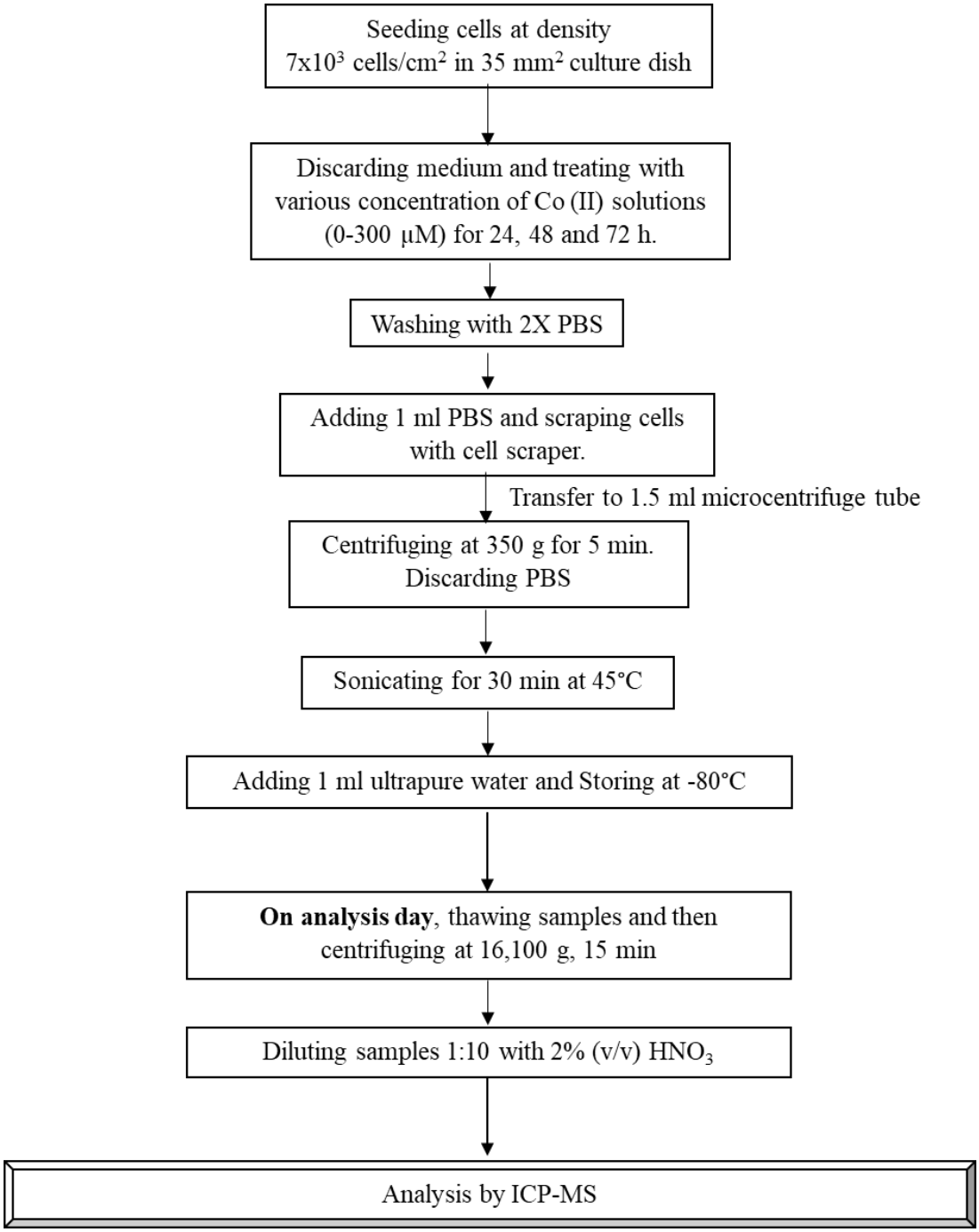

Figure 2-7 Experimental design of metal ion concentrations.

2.2.17 Western blotting

2.2.17.1 Cell preparation and Treatment (CFs) for immunoblotting

The CFs (cultured as described in Section 2.2.5) were counted by haemocytometer, seeded in a T25 flask at a density of 10^5cells/ml in 25cm^2, and incubated for 24 h at 37°C and 5% (v/v) CO_2. They were treated with various concentrations (0, 0.1, 1, 10 and 100µM) of Co. Cells were exposed to the treatments for 48 and 72h before being analysed by western blot.

At each culture end-point, culture medium was discarded. Cells were washed twice with PBS and 300 µl homogenisation buffer added [containing 0.1 M Sodium Phosphate buffer (NaPi) pH 7.6 and 1X protease inhibitor cocktail (500 µM AEBSF, 150 nM Aprotinin, 1 µM E-64, and 1 µM Leupeptin, Calbiochem, USA)]. After that cells were scraped using cell scraper. Cells were then homogenised using seven strokes of a motor driven Teflon-glass homogeniser. Homogenates were split into three 150µl aliquots to be stored at -80°C until used for Western blotting and one 50µl aliquot was used to measure the total protein content.

Homogenate samples were prepared at 1mg/ml in 1X sample buffer (containing 1.25 ml 4Xsample buffer, 0.35 g 1,4-Dithiothreitol (DTT) and 3.75 ml distilled H_2O; all Sigma-Aldrich; Dorset, UK) and boiled for 5min in sure-lock microcentrifuge tubes, prior to immunoblotting.

2.2.17.2 Measurement of total protein content

After homogenising the cells, the quantity of total protein was measured for each sample by Lowry assay (Lowry et al., 1951). For this purpose, solution A (2% (w/v) Na_2CO_3, 1% (w/v) $CuSO_4$ and 1% (w/v) NaK tartrate) and solution B (1:4 dilution of Folin's in distilled H_2O) were prepared. Bovine serum albumin standards (BSA) were made up in test tubes as shown in Table 2-1. 50 µl of each sample was diluted with 950 µl 0.5 M NaOH. 5ml of solution A were added to standards and samples, which were mixed and incubated at room temperature for 10 min. After this, 0.5 ml of solution B were added to each tube, then they were mixed and left again around 30-90 min. The absorbance was read at 725 nm using water as blank. The results for protein

concentration per well versus time in culture were then plotted. All chemicals were obtained from Sigma-Aldrich; Dorset, UK.

Protein Concentration (µg/ml)						
	0	**25**	**50**	**100**	**150**	**200**
BSA (ml)	0.000	0.125	0.250	0.500	0.750	1.000
0.5 M NaOH (ml)	1.000	0.875	0.750	0.500	0.250	0.000

Table 2-1 Protein standards.

2.2.17.3 Sodium dodecyl sulfate polyacrylamide gel electrophoresis (SDS-PAGE)

The running gel and the stacking gel made up as shown in Table 2-2. Samples (10-50 µg/well) were loaded in the wells, and the gels run at 130V for 1 h 30 min.

Solutions	Running Gel	Stacking Gel
Buffer 1 pH8.8	3 ml	-
Buffer 2	-	1.87 ml
Acrylamide	4 ml	0.75 ml
1.0%Ammonium persulfate (APS)	100 µl	75 µl
N,N,N′,N′-Tetramethylethylenediamine (TEMED)	15 µl	10 µl
Distilled Water	5 ml	4.87 ml

Table 2-2 Reagents for casting gels.

Western Blot

Proteins were then transferred to the nitrocellulose using transfer buffer (containing 25 mM Tris base, 190 mM Glycine, and 20% (v/v) Methanol; all Sigma-Aldrich; Dorset, UK) at 300 mA for 1 h 45 min.

Membranes were then blocked in NATT buffer (washing buffer containing 20 mM Tris base, 150 mM NaCl, and 0.1% (v/v) Tween 20 adjusted to pH7.4 with HCl) containing 5% Bovine serum albumin for 1 h 30 min at room temperature. The primary antibody in the dilution shown in Table 2-3 in 0.5% BSA in NATT, was added and then membranes were incubated overnight at 4°C. Membranes washed 6 times in NATT (15 min per wash) at room temperature. Secondary antibody was prepared in 0.5% (w/v) BSA in NATT (as shown in Table 2-3) and shaken with the membranes for 1h 30 min at room temperature. Membranes were incubated in chemiluminescence (ECL) reagent then exposed onto Autoradiography Film was used (Ultra Cruz™, USA) and developed using the Jpi Automatic X-RAY Film Processor Model JP-33 (Jpi Healthcare Co., Ltd.; Korea). Finally, the results were quantified with both a GS-800 Imaging Densitometer and the software Quantity One® (Bio-Rad; Hertfordshire, UK).

Protein Antigen	Species	Supplier of Primary Antibody	Primary Antibody Dilution	Secondary Antibody Dilution
CaMKIIδ	Rabbit	Eurogentec (Custom made)	1:1000	1:5000
phosphoThr286-CaMKIIδ	Mouse	Thermo Fisher Scientific	1:500	1:5000
oxidised-CaMKII	Rabbit	GeneTex	1:1000	1:5000
DMT1	Rabbit	Sigma-Aldrich	1:800	1:7500
TRPM7	Rabbit	Abcam	1:500	1:7500
TRPC6	Rabbit	Sigma-Aldrich	1:500	1:7500
GAPDH	Rabbit	Sigma-Aldrich	1:100,000	1:7500

Table 2-3 Dilution conditions for antibodies used in immunoblotting. All secondary antibodies were supplied by Sigma-Aldrich.

2.2.18 RNA sequencing (RNA-Seq) and Reverse Transcription Quantitative PCR (RT-qPCR).

2.2.18.1 Minimum Information for Publication of Quantitative Real-Time PCR Experiments (MIQE).

The Minimum Information for Publication of Quantitative Real-Time PCR Experiments (MIQE) guidelines were created to help ensure good practice in the molecular analysis of gene expression by RT-qPCR (Bustin *et al*., 2009 and Bustin 2010). These guidelines were used to help provide consideration for the appropriate design, documentation, and reporting of qPCR experiments for the necessary evaluation and publishing of qPCR results. An overview of the key criteria important to the reporting of the qualification and quantification of RT-qPCR that forms the basis of the MIQE guidelines is given in Figure 2-8. Where possible, the MIQE guidelines were followed in the current study for both the cell line and tissue gene expression work. The checklist of this work is found in Appendix, Table A4-1.

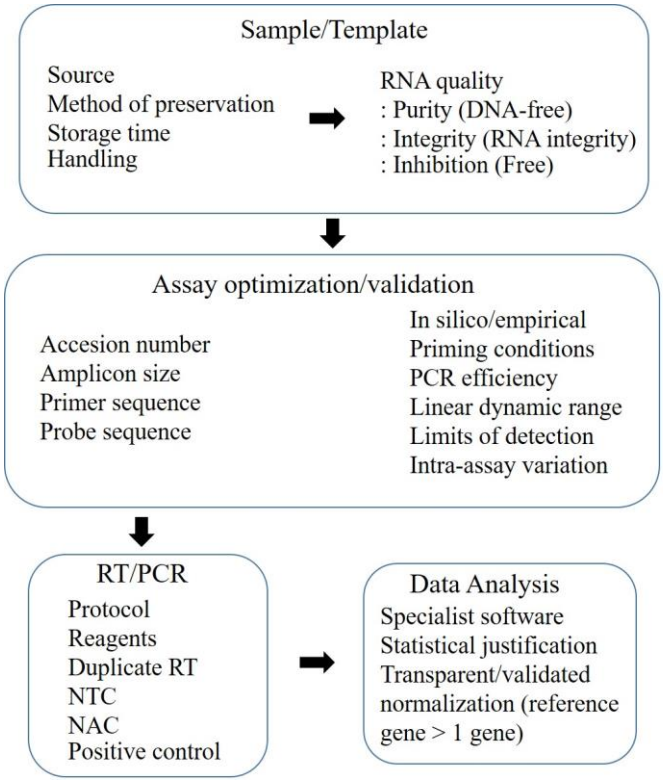

Figure 2-8 Overview all key criteria/ parameter of technical information step that determine the quality of qPCR data. Accession number: unique identifier of a nucleotide sequence. In silico: BLAST specificity analysis. NTC: no template controls (H_2O). NAC: no amplification controls (RT- controls) (adapted from Bustin 2009 and Bustin *et al*., 2010).

2.2.18.2 Isolation of total RNA from cell culture

Total RNA from 3T3 cells and CFs, was isolated using RNeasy Plus Mini Kit (Qiagen; Crawlay, UK) following the manufacturer's instructions. The kit provides all the required reagents, columns and tubes for the process. All steps carried out were as per the kit manual and an overview is given in Figure 2-10.

3T3 cells and primary cardiac fibroblasts were counted by haemocytometer, seeded in T25 flasks at a density of 10^5 cells/ml in 25 cm^2, and incubated for 24 h at 37°C and 5% (v/v) CO_2. A range of Co (II) solutions (0, 1, 10, and 100 µM) was added in complete medium, and cultures were treated for 72 h.

At each culture end-point, the culture medium was discarded. Cells were washed twice with PBS and then 600 µl of Buffer RLT Plus was added (containing buffer RLT plus 2-Mercaptoethanol (β-ME), provided in kit). Cells were lysed upon contact with the Buffer RLT Plus and detached from the surface of the flask. Homogenisation with a QIAshredder homogeniser spin column (Qiagen, Crawlay, UK) was used by pipetting the lysate directly into a QIAshredder spin column placed in a 2 ml collection tube and then centrifuging at maximum speed for 2 min prior to RNA extraction, as shown in Figure 2-9.

The homogenised lysed 3T3 cells and CFs were transferred to a gDNA Eliminator spin column. They were then centrifuged at 8000xg for 30 sec. After that the column was discarded, the flow-through was saved, and an equal volume of 70% (v/v) ethanol solution added. It was mixed thoroughly by pipetting up and down. The lysate/ethanol was taken into a RNeasy spin column placed in 2 ml collection tube and then centrifuged at 8000xg for 15 sec at room temperature. The flow-through liquid was discarded. The binding spin column was placed back into the collection tube to apply any remaining lysate/ethanol mixture to the column. The centrifugation was repeated as described above. 700 µl Buffer RW1 was added to the RNeasy spin column, and it was centrifuged at 8000xg for 15 sec at room temperature to wash the membrane, and the flow-through in the collection tube discarded. 500 µl of Buffer RPE was then added to the RNeasy spin column and then it was centrifuged again at 8000xg for 15 sec. The flow through was discarded and 500 µl of Buffer RPE was again added to the spin

column and then centrifuged for again at 8000xg for 2 min. After that the RNeasy spin column was placed into a new 2 ml collection tube and centrifuged at full speed (16,100 g) for 1 min to eliminate any possible carryover of Buffer RPE and any residual flow through remaining on the outside of the RNeasy spin column. The RNeasy spin column was placed in a new 1.5 ml collection tube and then 50 µl of RNase-free water added directly to the spin column membrane. This tube was spun at 8000xg for 1 min to elute RNA into the collection tube. The eluate was spun again by passing it through the same spin column membrane to get a final higher RNA concentration. 5 µl of the RNA was aliquoted for measuring the concentration of nucleic acid and purity of RNA. The remaining sample was stored at -80°C.

The extracted total RNA was then quantified and assessed for RNA purity using a NanoDrop 2000c spectrophotometer and the Nanodrop v3.7 software (Thermo Scientific; Wilmington, USA) with 2 µl of the RNA sample. The ratio of the absorbance readings at 260 nm and 280 nm (A260/A280) give an indication of protein contamination with pure RNA having an A260/A280 ration of 2.0. Salt contamination of the RNA sample can be assessed by the A260/A230 ratio which should also be around 2.0 for samples free from salts. Finally, RNA integrity was assessed in an aliquot of the RNA by determining the RNA Quality Indicator (RQI) number, which is automatically generated by the Experion Automated Electrophoresis System (Bio-Rad; Watford, UK) using an algorithm that compares three regions of an electrophoretic profile to a series of degradation standards.

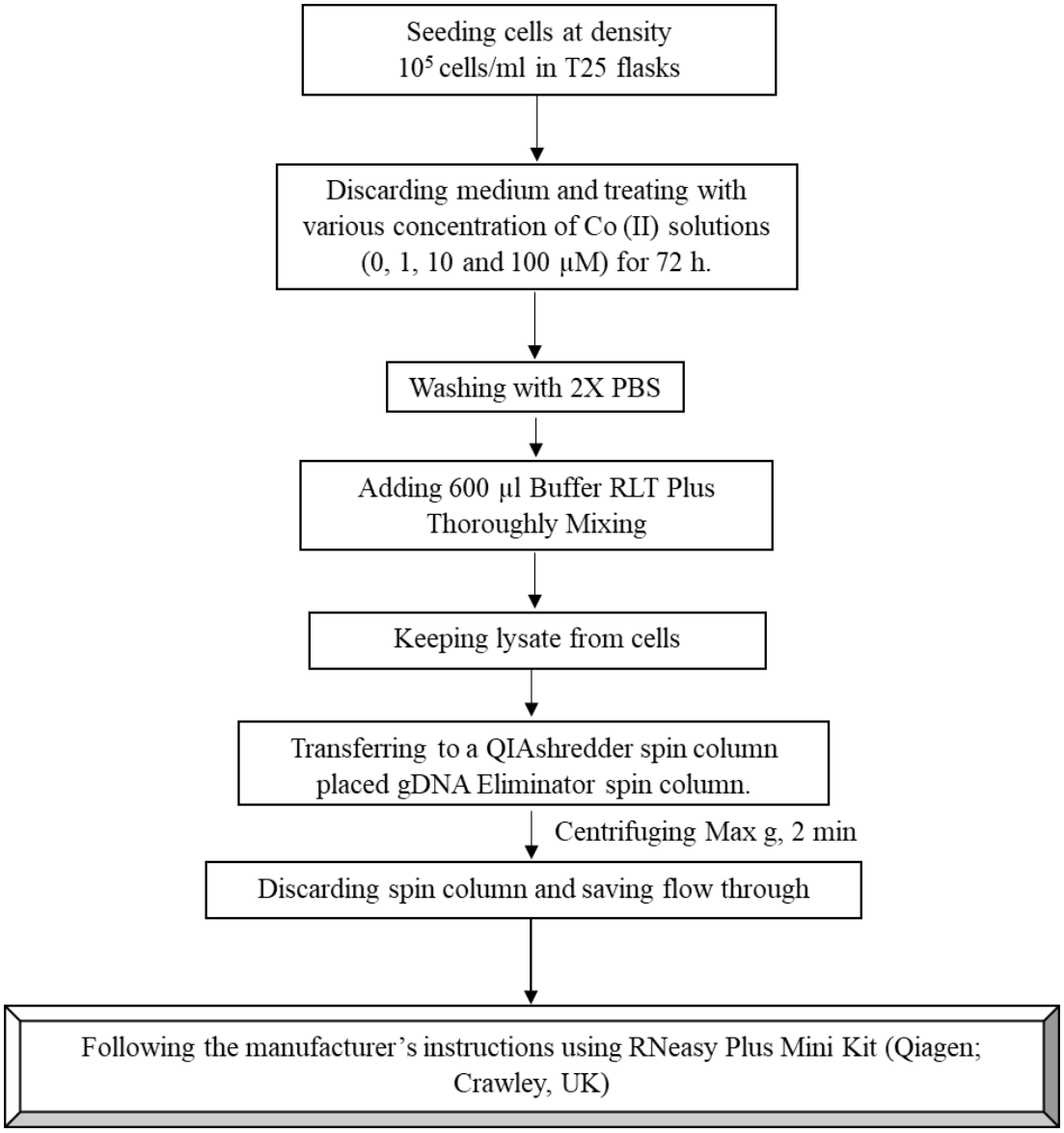

Figure 2-9 Sample preparation for Isolation of RNA from cell culture.

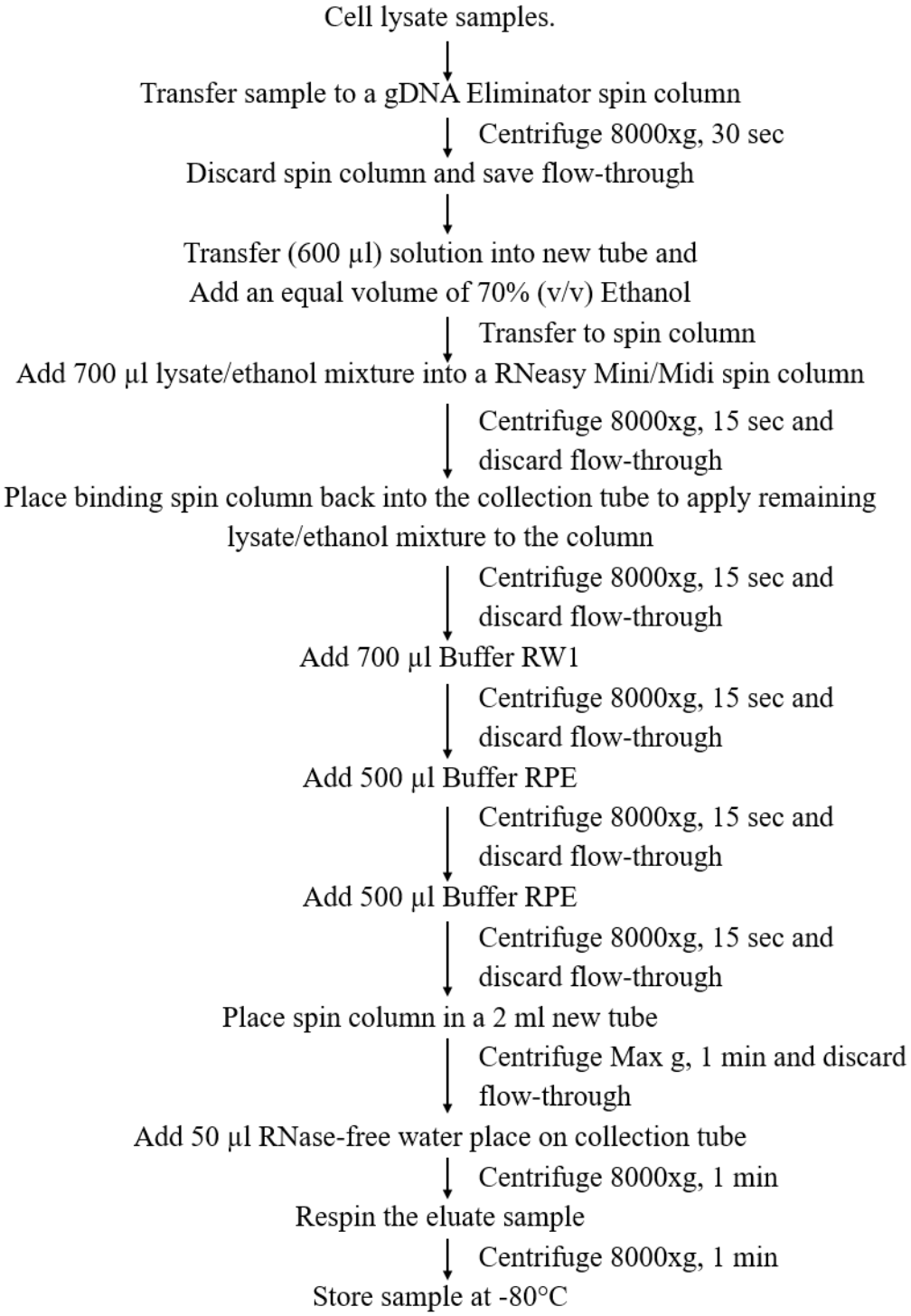

Figure 2-10 Overview of total RNA isolation from cell culture using RNeasy Plus Mini Kit (Qiagen; Crawley, UK).

2.2.18.3 RNA Sequencing

Total RNA isolated from the samples was also used in RNA-seq to examine the change in gene expression between control and Co treated samples at a transcriptome level. The RNA-Seq was performed and conducted on a contract basis by the BGI-Tech Solutions (Hong Kong) for gene expression quantification. Their RNA-Seq Quantification service was used with 20 Million clean reads, 50bp single end (SE) per sample on their BGISEQ-500 next generation sequencing platform. BGI-Tech conducted the necessary library construction, sequencing, and provided their standard bioinformatics analysis.

An overview of the bioinformatics pipeline carried out on the standard bioinformatics analysis by BGI-Tech is shown in Figure 2-11. Further analysis of the gene lists obtained from the standard bioinformatics analysis was conducted to elucidate genes, mechanisms, and pathways involved in the response to Co.

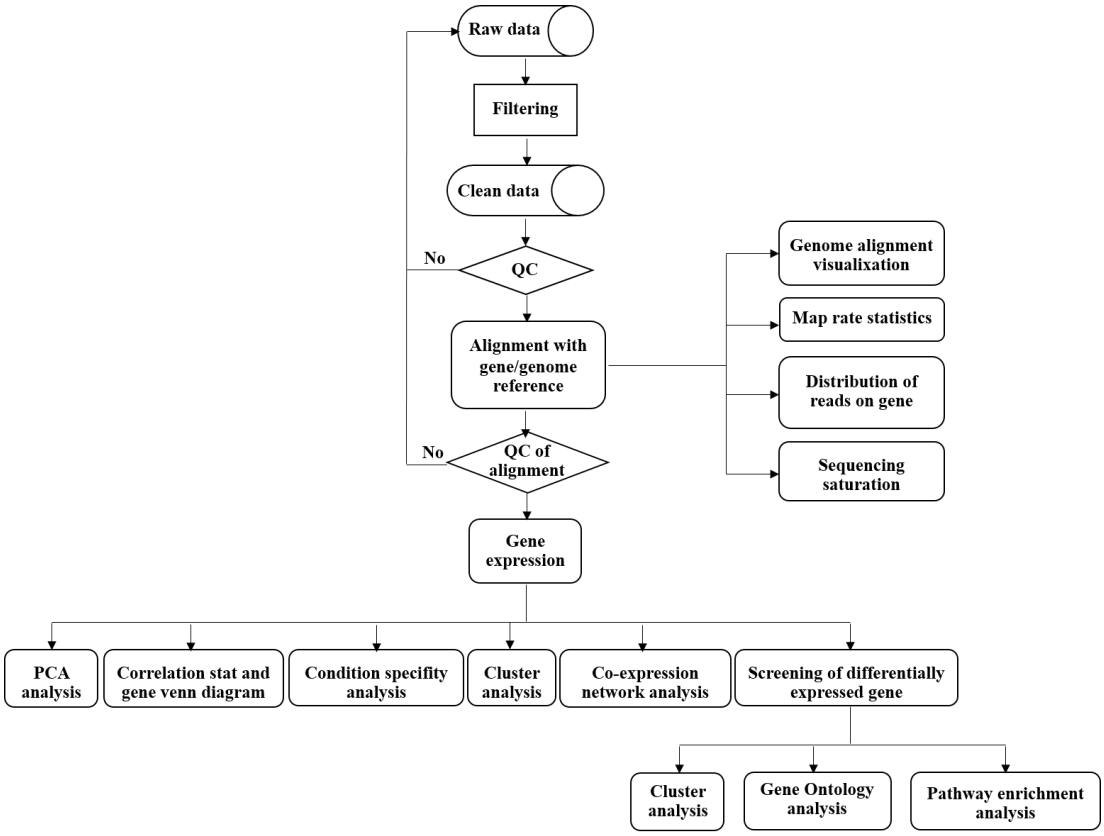

Figure 2-11 Bioinformatics analysis pipeline (the flowchart) from the BGI report. Primary sequencing data, called as raw reads, is subjected to quality control (QC) to determine if a resequencing step is needed. After QC, raw reads are filtered into clean reads which will be aligned to the reference sequences. QC of alignment is performed to determine if resequencing is needed. The alignment data is utilised to calculate distribution of reads on reference genes and mapping ratio. If alignment result passes QC, we will proceed with downstream analysis including gene expression and deep analysis based on gene expression (PCA/correlation/screening differentially expressed genes and so on). Further, we also can perform deep analysis based on DEGs, including Gene Ontology (GO) enrichment analysis, KEGG pathway enrichment analysis, cluster analysis, protein-protein interaction network analysis and finding transcription factor.

2.2.18.4 Gene Set Enrichment Analysis (GSEA)

Gene Set Enrichment Analysis (GSEA) is a bioinformatic tool for performing enrichment analysis(Subramanian *et al.*, 2005). GSEA is a computational method that determines whether an *a priori* defined set of genes shows statistically significant, concordant differences between two biological states. There are a number of research tools available to help identify genes that target specific gene transcripts such as GOrilla (Gene Ontology enRIchment anaLysis and visuaLizAtion tool)(Eden *et al.*, 2009), WebGestalt (WEB-based GEne SeT AnaLysis Toolkit)(Zhang, Kirov and Snoddy, 2005), BIND (Biomolecular Interaction network database)(Bader, Betel and Hogue, 2003), Cytoscape plug in (ClueGO + CluePedia + Clustermaker2) (Cline *et al.*, 2007; Bindea *et al.*, 2009) and DAVID (Huang, Sherman and Lempicki, 2008).

2.2.18.5 Gene Ontology (GO)-based enrichment analysis

Gene Ontology (GO), is standardised gene functional classification system, which offers a dynamically-updated controlled vocabulary, as well as a strictly defined concept to comprehensively describe properties of genes and their products in any organism. It is a commonly used approach for studies of large scale genomic or transcriptomic data. GO has three ontologies: molecular function, a cellular component, and biological process. GO enrichment analysis provides all GO terms that are significantly enriched in a list of DEGs, comparing then to a genome background, and it filters the DEGs that correspond to specific biological functions.

In this analysis, GOrilla (Gene Ontology enRIchment anaLysis and visuaLizAtion tool) was used to interpret the genes in all ontologies. GOrilla is a web-based application that identifies enriched GO terms in ranked lists of genes, without requiring the user to provide explicit target and background sets. GOrilla is publicly available at: http://cbl-gorilla.cs.technion.ac.il. This is particularly useful in many typical cases where genomic data may be naturally represented as a ranked list of genes (e.g. by level of expression or of differential expression). GOrilla employs a flexible threshold statistical approach to discover GO terms that are significantly enriched at the top of a ranked gene list. The appropriate background gene list, used in the mapping of the RNA used in the mapping of the RNA-Seq data, was obtained from the University of California, Santa Cruz (UCSC) Genome Browser (http://genome.ucsc.edu/).

2.2.18.6 Kyoto Encyclopedia of Genes and Genomes (KEGG) –based pathway enrichment analysis

Another way to analyse the gene expression is based on pathway enrichment. Pathway-based analysis helps to further understand the biological functions of genes (Jin *et al.*, 2014). The Kyoto Encyclopedia of Genes and Genomes (KEGG) is a commonly used major public pathways-related database, which can be used to assist in the pathway enrichment analysis of DEGs(Kanehisa and Goto, 2000)

The direct and indirect determination factors of each pathway are employed to demonstrate the regulation mechanisms among KEGG pathways. A pathway clustering analysis was performed on the DEGs to construct and visualise a pathway network, using the (ClueGO + CluePedia + Clustermaker2) plug- in Cytoscape software, according to KEGG pathway (http://apps.cytoscape.org/apps/).

2.2.18.7 PCR Primer Design

Primer design is a very important step for PCR studies as the specificity and stability of the oligonucleotide primers can significantly impact on the performance of the PCR resulting in inefficient amplification.

Molecular information on each gene of interest was obtained via a search of the National Center for Biotechnology Information (NCBI) gene database (https://www.ncbi.nlm.nih.gov/gene/). The NCBI Reference Sequence (RefSeq) of each gene was used as the template for the primer design for each PCR assay. The PCR primers were designed using the NCBI tool Primer-BLAST (https://www.ncbi.nlm.nih.gov/tools/primer-blast/)(Ye *et al.*, 2012). The webpage parameters for primers selection were: oligonucleotide primer length between 20 and 25 nucleotides; a melting temperature (Tm) with a minimum of 57°C and a maximum of 63°C (ideal melting temperature is 60°C); percentage of guanine-cytosine (GC) of between 50-60%; and as the primers are intended for SYBR-Green RT-qPCR, the primer sets were designed to produce a short amplicon of between 140-150 bp in size for all of the targets in the study. To minimise the risk of the primers generating an amplicon from any genomic DNA carried over from the RNA isolation, where possible, the primers were designed to be seperated by an intron or span exons. The primer sequences and their Tms, and amplicon sizes are summarised in Table 2.4

Gene	Primer sequences (5'->3'), (nucleotides)		Tm	Amplicon size (bp)
B2m (Rat: CFs)	Sense	TGA CCG TGA TCT TTC TGG TGC (21)	60.61	150
	Anti-Sense	TTT GAG GTG GGT GGA ACT GAG (21)	59.86	
Camkiid (Rat: CFs)	Sense	AGA CGT GAA AGC ACG AAA GC (20)	59.42	147
	Anti-Sense	TCC ACT AAG TTG CCC AAT GCT (21)	56.92	
Slc11a2 (*Dmt1*) (Rat: CFs)	Sense	AGA TGT GGA GCA TCT GAC AGG (21)	59.51	140
	Anti-Sense	TCC AGC CTA TTC CGT TGG AG (20)	59.17	
Srp14 (Rat: CFs)	Sense	CTG CTG ACG GAG TCG GAA C (19)	60.44	149
	Anti-Sense	GGT TTA GTG CGA CCA TCA TAC TTC (24)	59.73	
Tbp (Rat: CFs)	Sense	AGA TCC AAA ATA TTG TAT CCA CCG (25)	56.87	149
	Anti-Sense	GAT CAA CGC AGT TGT TCG TGG (21)	60.40	
Trpc6 (Rat: CFs)	Sense	TAT CTG CTG ATG GAC GAG CTG (21)	59.66	147
	Anti-Sense	AGC CAA CCT TCT TCC CTT CTC (21)	56.65	
Trpm7 (Rat: CFs)	Sense	TGA AAC ATG TGG GTG CTG CT (20)	60.47	149
	Anti-Sense	TCG TAA CCA ATC CGG CAA CA (20)	59.96	
Trpv1 (Rat: CFs)	Sense	TCC GAG GGA TTC AAT ATT TCC TGC (24)	60.75	140
	Anti-Sense	CTC CTT GCG TTG GCT GAA GT (20)	60.89	
B2m (Mouse: 3T3s)	Sense	GAT GTC AGA TAT GTC CTT CAG CAA G (25)	59.53	148
	Anti-Sense	CAT GTC TCG ATC CCA GTA GAC G (22)	60.03	
Camkiid (Mouse: 3T3s)	Sense	CCG GTT CAC CGA CGA GTA TC (20)	60.25	144
	Anti-Sense	TGA TGG TCC CTA GCA GAA AGC (21)	59.79	
Slc11a2 (*Dmt1*) (Mouse: 3T3s)	Sense	AGG ATG TGG AGC ACCTAA CG (20)	59.46	148
	Anti-Sense	GCA ATC CTC CAG CCT ATT CCA T (22)	60.22	
Srp14 (Mouse: 3T3s)	Sense	CTC AAG AAA TAT GAC GGT CGC AC (23)	60.00	142
	Anti-Sense	TCA CTT CTT TGG AGC TCA CCA C (22)	60.49	
Tbp (Mouse: 3T3s)	Sense	TGA GAG CTC TGG AAT TGT ACC G (22)	59.83	140
	Anti-Sense	TCA TGA TGA CTG CAG CAA ATC G (22)	59.65	
Trpc6 (Mouse: 3T3s)	Sense	CCC AGC TTC CGG GGT AAT G (19)	60.15	140
	Anti-Sense	CGT TCT TCC TCA ATA GAC AGG CT (23)	60.12	
Trpm7 (Mouse: 3T3s)	Sense	GCA CTG CTG AAA GGT ACT AAT GC (23)	60.18	149
	Anti-Sense	AGA GCA TCA AGC ATA GCC TGT (21)	59.51	
Trpv1 (Mouse: 3T3s)	Sense	TCC GAG GGA TCC AGT ATT TCC T (22)	60.09	141
	Anti-Sense	ACT CCT TGC GAT GGC TGA AG (20)	60.39	

Table 2-4 Primer sequences, melting temperatures (Tm), and amplicon size as provided and calculate by NCBI Primer BLAST.

Complementary DNA (cDNA) Synthesis for reverse-transcribed PCR, Tetro cDNA Synthesis Kit (Bioline, USA) was used to generate cDNA from mRNA isolated from the samples using an Oligo (dT)18 primer. The kit provides all of the reagents required including oligo (dT)18, 10mM dNTP mix, 5xRT buffer, 200 u/µl Tetro Reverse transcriptase, Ribosafe RNase Inhibitor, and DEPC-treated water and the cDNA synthesis was carried out as in the manufacturer's instructions

"RT+" cDNA from total RNA was generated by preparing the mix on ice in a RNase-free reaction tube for each sample, containing 1 µg of Total RNA sample, 1 µl of Oligo(dT)18, 1 µl of dNTP mix, 4 µl of RT buffer, 1 µl of Reverse transcriptase, and DEPC-treated water to a total volume of 20 µl and mixed gently by pipetting. "RT-" samples were similarly prepared but without reverse transcriptase. Such reactions would provide a check for any persisting contaminating genomic DNA as a PCR carried out using an aliquot of the "RT-" as the template should not generate any PCR products as there is no cDNA present. If PCR using the "RT-" sample as template does produce a PCR product then this could be as a result of carryover contaminating genomic DNA. Both "RT+" and "RT-" were incubated at 45°C for 30 min and followed by a termination of the reaction by heating at 85°C for 5 min. The tubes were chilled on ice, briefly centrifuged to collect the contents at the bottom, and then stored at -20°C until required.

2.2.18.8 SYBR Green quantitative real-time PCR

Determination and analysis of the expression levels of selected gene in the heart tissue and cell samples was conducted using SYBR Green-based quantitative real-time PCR RT-PCR. This method is reliant on SYBR® Green dye binding to double-stranded DNA and when this occurs its fluorescence increases 1000-fold over that of unbound SYBR Green. As such SYBR green is useful in monitoring the accumulation of double-stranded PCR products in quantitative real-time PCR at every cycle. The oligonucleotide primers and the creation of the cDNA templates used for these experiments are described in Sections 2.2.18.7 and 2.3.8.4.

PowerUp™ SYBR® Green Master Mix; MM (Applied Biosystems™, USA) was used for dye-base quantitative real-time PCR to set the individual SYBR green primer sets.

With SYBR green present in the reaction, binding between SYBR dye and double stranded PCR products results in an increase on fluorescence intensity proportioned to the amount of PCR product produced.

Triplicate technical replicate real-time PCR reactions were run for each sample. For each reaction, 20 µl reaction contained 2 µl of 10 pmol/ µl Forward primer , 2 µl of 10 pmol/ µl Reverse primer, 10 µl of PowerUp master mix, 5 µl H_2O, and 1 µl of template (H_2O control, RT+ or RT-) was added to the MicroAmp™ Fast Optical 96-Well Reaction Plate (Applied Biosystems™, USA). The reaction reagents were mixed thoroughly by pipetting, trying to avoid air bubbles, and the wells sealed with MicroAmp™ Optical Adhesive Film Kit (Applied Biosystems™, USA).

The reaction plate was subjected to a brief, low-speed centrifugation spin to ensure all the reaction was collected at the bottom of the wells. After that the reaction plate was loaded into a StepOnePlus Real-Time PCR system (Applied Biosystems™, USA). Thermocycling conditions were set for a Fast Cycling Mode as shown on Table 2.5, which was completed with the melting curve stage to detect any issues with misprimimg or multiple amplicons. Threshold cycle (Ct) values from the amplication curves were recorded and used for normalised target gene expression from PCR by the StepOnePlus software (v2.1).

Table 2-5 PCR thermal cycling and melting curve stage conditions.

Fast Cycling Mode (For StepOnePlus™ instrument and Primer Tm≥60°C)			
Step	**Temperature**	**Duration**	**Cycles**
UDG Activation	50°C	2 min	Hold
AmpliTaq DNA Polymerase Activation	95°C	2 min	Hold
Denature	95°C	3 sec	40
Anneal/Extend	60°C	1 min	
Melting curve stage	95°C	15 sec	Ramp rate 1.6°C/sec
	60°C	1 min	

The delta-delta Ct (ΔΔCt) method was used to calculate the relative changes in the gene expression of the samples determined from RT-qPCR experiments (Livak and Schmittgen, 2001). The ΔΔCt method normalises the Ct values of the target gene to the Ct values of the reference gene to determine the fold changes (Up and down

regulation) in the gene expression between the control and treated samples using following formula:

- The difference between the Cts for the target gene and the reference gene for the treated and the control samples (ΔCt)

  : ΔCt1 = Ct (Target Gene-treated) - Ct (Ref Gene-treated)

  : ΔCt2 = Ct (Target Gene-control) - Ct (Ref Gene-control)

- The difference between the ΔCts between the treated and control gene samples (ΔΔCt):

  : ΔΔCt = ΔCt1 (Treated) - ΔCt2(control)

- Fold change (FC) in treated sample obtained using the followeing equation:

  Normalised target gene expression level = The fold change = $2^{(-\Delta\Delta Ct)}$

Target; Target gene (e.g, *Camkiid, Dmt1, Trpc6, Trpm7, and Trpv1*)

Ref; Reference gene (e.g. *Tbp, Srp14*, or *B2m*)

The appropriate reference gene for each experiment was (e.g. Gene expression changes in 3T3 cells following Co treatment), was determined using RefFinder which identified the most stable gene under each experimental condition.

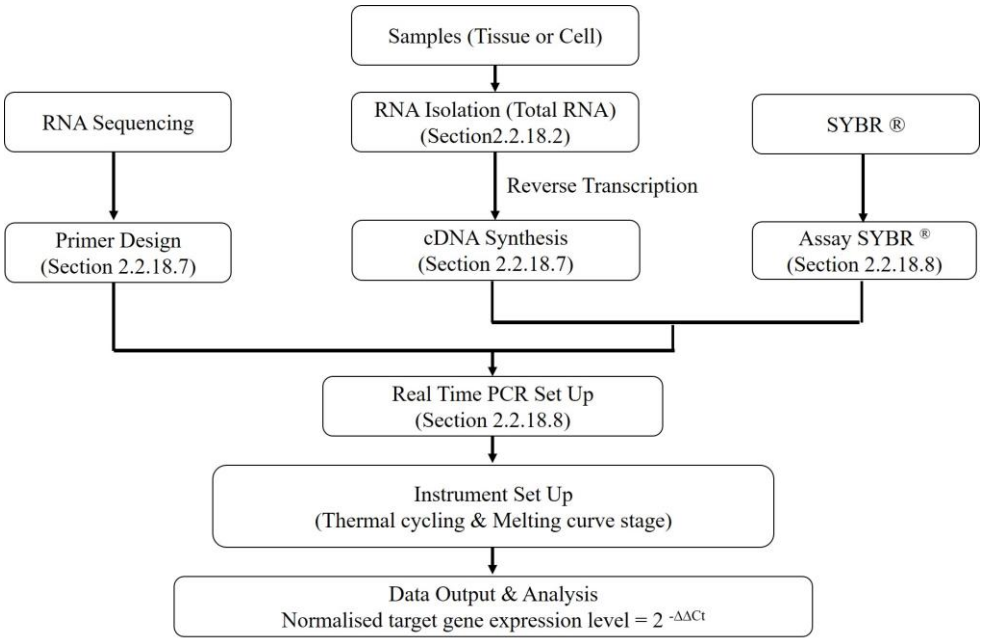

Figure 2-12 Overview of RT-qPCR from cells and heart tissue.

2.3 *In vivo* experiments to measure distribution and toxicity of Co in rats

2.3.1 Animal Housing

All the animal studies were conducted under a valid Home Office project licence (PPL 60/4341). Adult male Sprague–Dawley rats (150–250 g) in-bred in the Strathclyde University Animal Unit had access to water and food (supplied by Special Diet Services, Bicester, UK) *ad libitum.* Procedures complied with the ARRIVE guidelines and conformed to the Guide for the Care and Use of Laboratory Animals published by the US National Institutes of Health (NIH Publication No. 85-23, revised 1996) and Directive 2010/63/EU of the European Parliament.

2.3.2 Preparation and exposure of rats to Co ion

Cobalt (II) Chloride hexahydrate ($CoCl_2.6H_2O$) was used to make up the Co (II) stock solution for the experiment. Co (II) solutions were made freshly every week and then were injected daily by intraperitoneal administration (i.p.) at 1mg/kg. Freshly weighed $CoCl_2.6H_2O$ was dissolved in sterilised deionised H_2O on the day of preparation, and then filtered-sterilised with a 0.22 µm syringe filter to give 1 mg/ml. Daily injections were administered by Animal Unit staff, and the weights and general health of animals monitored daily.

Male Sprague–Dawley rats each weighing approximately 200 g were given intra-peritoneal (i.p.) injections of distilled water (n=3) or 1mg/kg $CoCl_2$ (n= 6) in distilled water daily for 7 days and 28 days. Cardiovascular parameters were examined by echocardiography examination and animals were then euthanised by CO_2 asphyxiation. Blood was collected by cardiac puncture and specific organs (liver, brain, spleen, heart, lungs, kidneys and testes) were removed, weighed and then collected for further analysis as described in section 2.3.4 and 2.3.5.

2.3.3 Echocardiographic Examination

An echocardiogram is an ultrasound of the heart. Echocardiography objectively and quantitatively evaluates the effects of Co on cardiac function. The most commonly used echocardiographic parameter of ventricular performance is fractional shortening (%FS), which measures the degree of shortening of the left ventricular diameter between end-diastole and end-systole. Fractional shortening is used as an estimate of myocardial contractility. The measurement can be judged by comparing control normal rats with the treated animals. Echocardiography was performed by Claire McCluskey and Margaret MacDonald, Strathclyde Institute of Pharmacy & Biomedical Sciences (SIPBS), University of Strathclyde.

Echocardiographic assessment of left ventricular (LV) function was performed both 1 and 4 weeks after the start of the treatment. Animals were briefly anaesthetised in a Perspex chamber. Isofluorane was given by inhalation via a specially designed nose cone at 3% in oxygen delivered at 2 l min^{-1} for induction, and after 2-3 min, rats were placed supine on a facemask receiving 1.5-2% isofluorane in oxygen at 0.5-1 l min^{-1} for maintenance. Initially, fur was removed by application of a topical depilatory cream to the neck and upper chest area. For the echocardiography of the heart, two-dimensional short axis views and M-mode measurement was performed at the level of the papillary muscle using the MIUS HDI 3000CV echocardiography system, a 13MHz linear array transducer and ultrasound transmission gel. When all structures were displayed correctly the picture was zoomed into and the M-mode record was acquired. The measured parameters in M mode were systolic and diastolic left ventricular (LV) wall measurements (including anterior wall (AW) and posterior wall (PW) measurements, LV end systolic dimension (LVESD) and LV end diastolic dimension (LVEDD). Fractional shortening (%FS) was assessed from M mode traces. These parameters were considered as the basic set of parameters. The percentage of fractional shortening is calculated by the following formula;

$$\%\text{Fractional Shortening (FS)} = [\text{LVEDD} - \text{LVESD}/\ \text{LVEDD}] \times 100$$

An average of three measurements of each variable was used for each animal.

2.3.4 Animal observation: Body weight and organ weight

Body weights were recorded daily (in the morning). Recording body weight during Co treatment provides an indicator of the general health status of the rats that may be relevant in the interpretation of toxic effects.

At termination of the studies (7 and 28 days), the rats were weighed (on the morning of necropsy), and euthanised by CO_2 asphyxiation. The rats were not fasted prior to necropsy, but the possibility that some organ weight changes can occur over the course of the day is acknowledged, and has been reported previously for liver (Rothacker *et al.*, 1988). Following necropsy, specified organs were examined, dissected free of fat and weighed using calibrated balances (Precisa Instruments Ltd.; Switzerland). Organs with any macroscopic abnormality (such as those with discolouration, those that were damaged during necropsy, or those with evidence of confounding disease) were excluded from the evaluations described in this report to minimise the influence of these changes on organ weights. The ratios between organ weight and body weight for each organ were recorded.

2.3.5 Storing samples from the in vivo study

2.3.5.1 Blood samples

Whole blood samples were collected by cardiac puncture in collection tubes, containing 1000 IU/ml heparin at a dilution 1:10 (Sigma-Aldrich; Dorset, UK) and delivered to the laboratory on the same day of collection. Upon arrival at the laboratory, blood samples were divided into 500 µl aliquots. To minimise RNA degradation, 1.2 ml of RNA*later*® (Life Technologies; Paisley, UK) was added to each sample. Samples were incubated overnight at 4°C and then stored at -80°C until use. Another 500 µl aliquot of heparinised blood was placed in 15 ml polypropylene tubes prior to metal analysis by ICP-MS.

2.3.5.2 Organ samples

The rats were euthanised by CO_2 asphyxiation and specific organs (liver, brain, spleen, heart, lungs, kidneys and testes) were dissected into collection tubes. Heart tissue was weighed, washed with Krebs solution to remove clotted blood and divided into 3 parts: 150 mg of left ventricle (LV) for homogenisation; 100 mg of tissue were placed in a 15 ml polypropylene tube for metal analysis and lastly; 100 mg tissue were weighed

for RNA analysis. To minimise RNA degradation, 0.5ml of RNA*later*® was added to each sample. Samples for RNA isolation were incubated overnight at 4°C and then stored at -80°C until use. Other organs (liver, brain, spleen, lungs, kidneys and testes) were collected in the same way as heart tissue.

2.3.6 ICP-MS Analysis of metal ion concentrations in organs

With regard to the study of the disposition of Co in patients who have received a metal implant, there is very little literature. In order to help predict the disposition of Co ions in patients after their release from MoM implants, the organ distribution pattern of Co ions in rats after an intra-peritoneal (i.p.) injection of 1 mg/kg $CoCl_2$ was studied.

Blood samples from cardiac puncture, and also samples of specific organs (liver, brain, spleen, heart, lungs, kidneys, testes), were removed and collected for study of the *in vivo* distribution of Co in rats.

2.3.6.1 Preparing the equipment, supplies and chemicals

As described in section 2.2.16.1

2.3.6.2 Blood and organ Preparation

Blood samples and portions of each organ were digested by acid digestion. 0.5 ml of blood or 100 mg of each organ were placed into a 15 ml tube and then 0.5 ml of HNO_3 (70%v/v) added. After that the tubes were placed into a hot block at 103°C for 20 min, then 0.25 ml of hydrogen peroxide (H_2O_2, 30% (w/v)) was added and the digestion continued for another 20 min. The digested samples were cooled down and then transferred into a new 15 ml polypropylene tube and stored at -20°C prior to metal analysis.

2.3.6.3 ICP-MS Analysis of metal ions

The samples were then allowed to thaw at room temperature and all samples were diluted 40-fold (0.25 ml of each sample were added to 9.75 ml of ultrapure water (finally 1% (v/v) HNO_3 in samples). Co standards were prepared as indicated previously. Samples and standards were analysed using an Agilent 7700x octopole collision system ICP-MS as for the *in vitro* cell samples.

2.3.7 Preparation of heart tissue for western blotting

The hearts were washed thoroughly in ice-cold Ca^{2+}-free Krebs solution. The left ventricle (LV) was dissected and weighed. 5 volumes of ice cold homogenisation buffer was added [containing 20 mM Tris-base buffer, 1 mM DTT, 1X protease inhibitor cocktail (500 µM 4-(2-Aminoethyl) benzenesulfonyl fluoride hydrochloride; AEBSF, 150 nM Aprotinin, 1 µM trans-Epoxysuccinyl-L-leucylamido(4-guanidino) butane; E-64, and 1 µM Leupeptin)] and this tissue minced finely on ice prior to homogenisation using an Ultra-Turrax T8 (IKA®, UK) hand-held homogeniser. Homogenates were split into three aliquots to be stored at -80°C until use and one 50 µl aliquot was used to measure the total protein content.

2.3.8 RNA Sequencing (RNA-Seq) and Reverse Transcription Quantitative PCR (RT-qPCR).

2.3.8.1 Isolation of total RNA from heart tissue

Total RNA was isolated the sample tissues using RNeasy Plus Universal Midi Kit (Qiagen; Crawley, UK) following the manufacturer's instructions. The kit provides all the required agents and tubes for the process. All steps carried out were in the kit manual and an overview is given in Figure 2-14.

At the end of the Control and Co treatment period, the rat heart was dissected and then placed in a RNase/DNase-Free collection tube. The tissue was then snipped into small pieces using scissors. To help stabilise the RNA and protect it from degredation, the tissue was submerged in RNAlater (Qiagen; Crawley, UK) overnight at 4°C, after which the samples were stored at -80°C until required for RNA extraction as Figure 2-13.

Briefly, the heart tissue was disrupted and homogenised by using a Mixer Mill MM301 bead mill (Retsch GmbH, Haan, Germany). 100 mg of each tissue sample was added to a 2 ml microcentrifuge tube containing a 6mm steel cone ball with 500 µl Qiazol lysis reagent. The tubes were then placed in the mixer mill tube rack and clamped securely in the mixer mill. The mixer mill was set up at to shake at 30.0 Hz for 1 min where the cone ball would vigorously to break up and homogenise the tissue. This was repeated up to 3 times until the tissue was completely disrupted and free from clumps. Then the lysate was transferred to a new 15 ml tube and where a further 4 ml of Qiazol

lysis reagent was added. This was vortexed and placed on the bench at room temperature for 5 min and followed by the addition of 500 µl gDNA Eliminator solution and shaken vigorously for 15 sec. 1 ml chloroform was added to each tube. The tube was shaken vigorously for 15 sec, placed on the bench at room temperature for 2-3 min, and then centrifuged at 4500 x g for 15min at 4°C. The upper aqueous phase containing RNA was transferred to a new tube where an equal volume of 70% Ethanol solution added and mixed thoroughly by pipetting up and down. 4 ml of this lysate/ethanol mixture, was transferred into a RNeasy Midi spin column placed in a 15 ml collection tube and then centrifuged at 4500 x g for 5 min at room temperature. The flowthrough liquid was discarded. The RNA-binding RNeasy spin column was placed back into the collection tube to apply any remaining lysate/ethanol mixture to the column. The centrifugation was repeated as described above. 4 ml Buffer RWT was added to the RNeasy spin column, and it was centrifuged at 4500 x g for 5 min at room temperature to wash the column and the flowthrough discarded. 2.5 ml Buffer RPE was added to the RNeasy spin column and then centrifuged at 4500 x g for 2 min. The flowthrough was discarded and 2.5 ml of Buffer RPE was again added to the spin column. The column was centrifuged again at 4500 x g for an extended spin for 5 min to conduct the final wash and remove any residual wash buffer. The RNeasy spin column was placed into a new 15 ml collection tube and 150 µl RNase-free water added directly to the spin column membrane. This tube was spun at 4500 x g for 3 min to elute RNA from the column into the collection tube. The eluate again was passed through the same spin column membrane to get a maximise the recovery of RNA. 5 µl of RNA was aliquoted for measuring the concentration and integrity as described previously and the remaining sample was stored at -80°C.

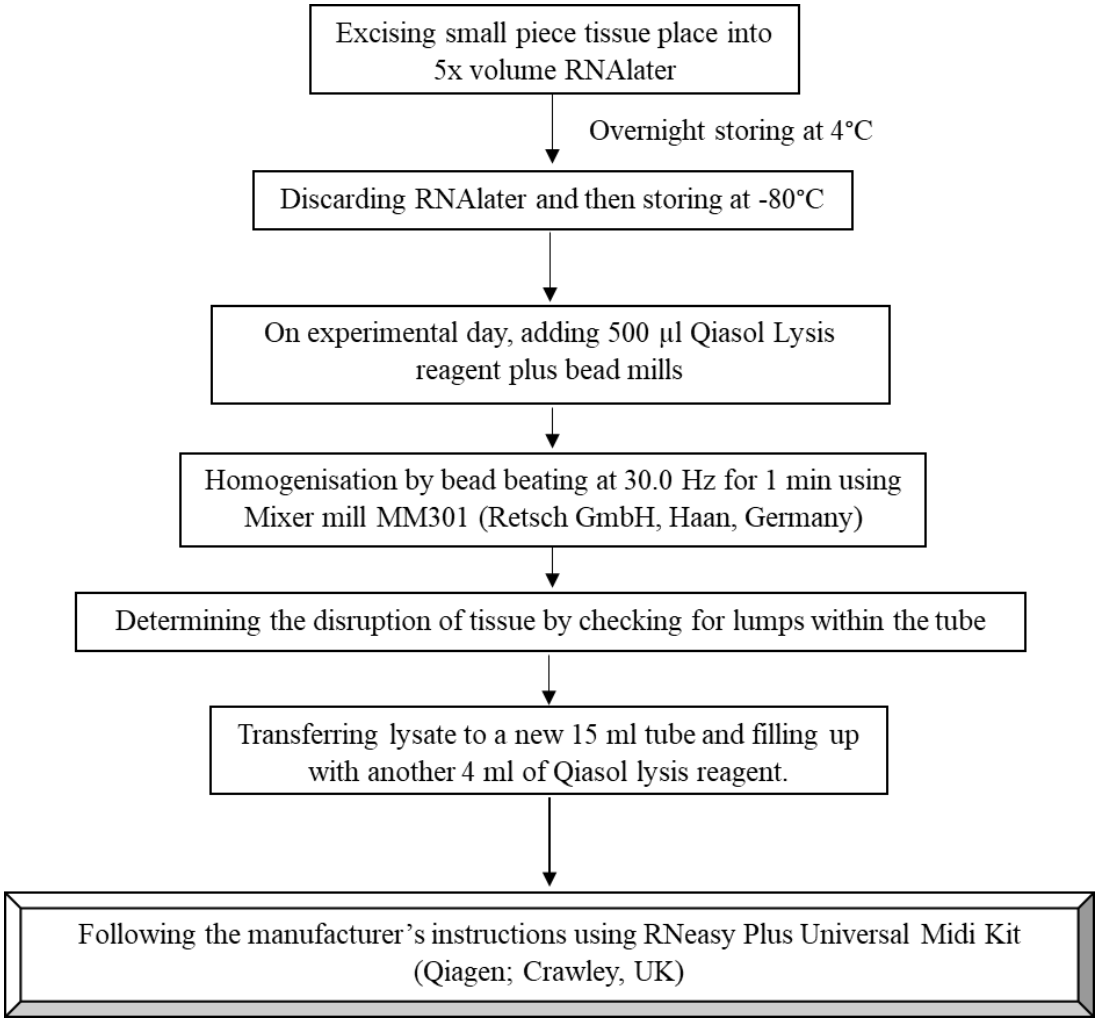

Figure 2-13 Sample preparation for Isolation of RNA from tissues.

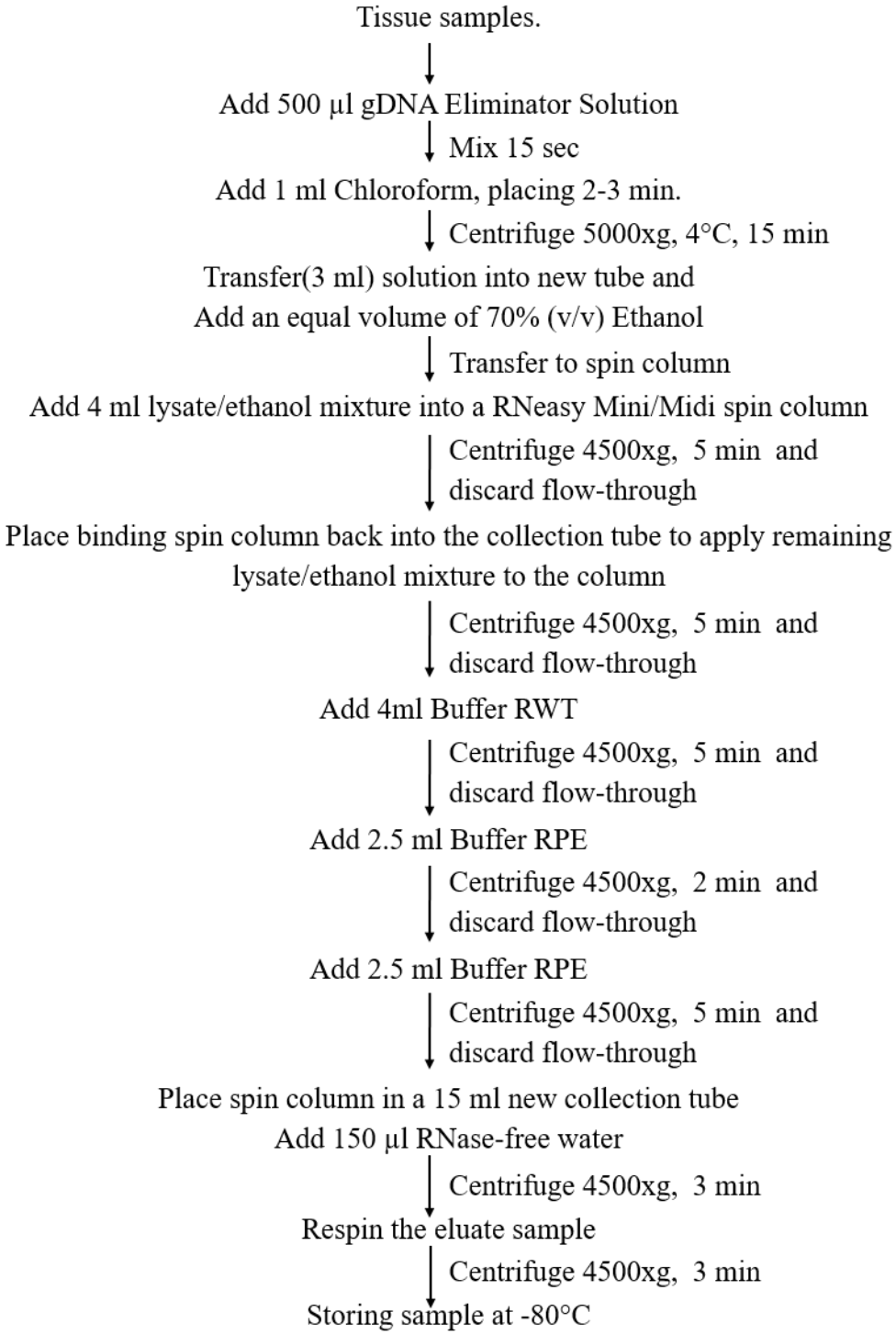

Figure 2-14 Overview of total RNA isolation from tissue using RNeasy Plus Universal Midi Kit (Qiagen; Crawlay, UK).

2.3.8.2 RNA Sequencing

As described in section 2.2.18.3

2.3.8.3 Gene Set Enrichment Analysis (GSEA)

As described in section 2.2.18.4

2.3.8.4 PCR Primer Design

To prepare the primer set for PCR, firstly we need to design the primer. Primer design is a very important step for reverse transcription-qPCR (RT-qPCR). All steps carried out as described in section 2.2.18.7. Primer sequences, Tm, and amplicon size are summarised in Table 2-4 and Table 2-6 (addition).

Gene	Primer sequences (5'->3'), (nucleotides)		Tm	Amplicon size (bp)
Pgk1	Sense	CTG GGA ACA AGG TTA AAG CTG AG (23)	59.50	148
	Anti-Sense	GCC TTC TGT GGC AGA TTC AC (20)	59.19	
Rpl13a	Sense	GCC TAC CAG AAA GTT TGC TTA CC (23)	59.81	147
	Anti-Sense	TTC CTT AGC CTC AAG AGC TGC (21)	60.07	

Table 2-6 (addition) Primer sequences, melting temperatures (Tm), and amplicon size as provided and calculate by NCBI tool Primer BLAST.

2.3.8.5 SYBR Green quantitative real time PCR

As described in section 2.2.18.8

Target; Target gene (eg, *Camkiid, Dmt1, Trpc6, Trpm7* and *Trpv1*)

Ref; Reference gene (eg. *B2m, Rpl13a* and *Pgk1*)

Chapter 3. EFFECTS OF COBALT IONS ON 3T3s AND CFs (SHORT TERM)

3.1 Introduction

Aseptic loosening of a hip implant is the leading cause of failure and need for subsequent revision surgery, and may occur months or years after implantation. There are potentially several reasons for loosening, such as mechanical overload, physiologic bone resorption, or a combination of both at the bone–implant interface. Loosening may occur early, through failure of initial ingrowth of bone into the prosthesis or poor cementing technique. A major cause of adverse tissue response is release of prosthesis wear particles and it is an important contributor of bone loss around the implant (Luo *et al*., 2005).

As mentioned in Chapter 1, metal ions which are released from implant wear debris can lead to either toxic or allergic responses. However, the mechanisms of toxicity of metal particles and ions are poorly understood. This raises concerns about the long term effects of exposure to metal debris particularly as younger, more active patients are being offered MoM joint replacement for end-stage bone disorders (Rao *et al.*, 2012). The metal ions Co (II) and (III) are the most cytotoxic which are released from orthopaedic implants inducing apoptosis and /or necrosis in cells. Corrosion products including CoO, Cr_2O_3 and $CrPO_4$ also show moderate cytotoxicity (Huk *et al*., 2004).

Many recent studies have examined ion release from CoCr alloys in different *in vitro* conditions. In the current study, the mouse 3T3 fibroblast cell line (3T3 cells) was used as a fibroblast cell line to compare with isolated primary cardiac fibroblasts from adult rat heart (CFs). Both types of cells were used to study the toxicity of Co, at a range of concentrations as described in section 2.2.7.

Both cells were exposed to Co ions to order to evaluate the toxicity of Co in terms of changes in cell morphology, viability, proliferation and cellular uptake. Both the 3T3 cell line and CFs were exposed to various concentrations of cobalt (II) chloride ($CoCl_2$) for different times and toxicity was measured using MTT, neutral red, crystal violet and a combined assay with all 3 tests, and also cell staining was used to study the viability and morphology changes and actin distribution. Determining cell proliferation by the BrdU Elisa method, and also cellular uptake using ICP-MS was also included. Finally, western blotting was carried out which is a widely used

technique to detect specific proteins in a sample of cell lysate. Insight into the mechanism of Co induced toxicity to cells *in vitro* was being sought by the experiments in this chapter.

3.2 Aims

3.2.1 To develop and validate a combined assay for cytotoxicity that would allow us to obtain data on MTT reduction, NR uptake and CV staining on a single sample.

3.2.2 To evaluate the in vitro cytotoxicity of Co in both a standard widely used fibroblast cell line, 3T3 cells, and in primary cultures of cardiac fibroblasts (CF) isolated from adult rat hearts.

3.2.3 To determine whether Co had an in vitro cytostatic effect by measuring cell proliferation after exposure in both 3T3 cells and CF.

3.2.4 To measure uptake of Co in vitro in both types of cells using a specific, sensitive inductively coupled plasma mass spectrometry (ICP-MS) method.

3.2.5 To investigate mechanisms of in vitro toxicity using immunoblotting to detect and compare expression of selected proteins in both cell types after exposure to Co.

3.3 Results

3.3.1 Isolation of Cardiac fibroblasts from adult rat heart

Primary cardiac fibroblasts were cultured from adult rat heart for over 8-10 days. Figure 3-1(taken using a Motic AE31 Trinocular Inverted Microscope together with a Moticam 10 camera and the Motic Images Plus 2.0 software) shows the monolayer of primary cardiac fibroblasts on day0-day8. Cultures reached 50% to 80% confluence between days 8 and 10, and did not expand significantly after this period. Cells were confluent and sufficient for experiments by day 8. Cells were not left in culture for more than 15 days.

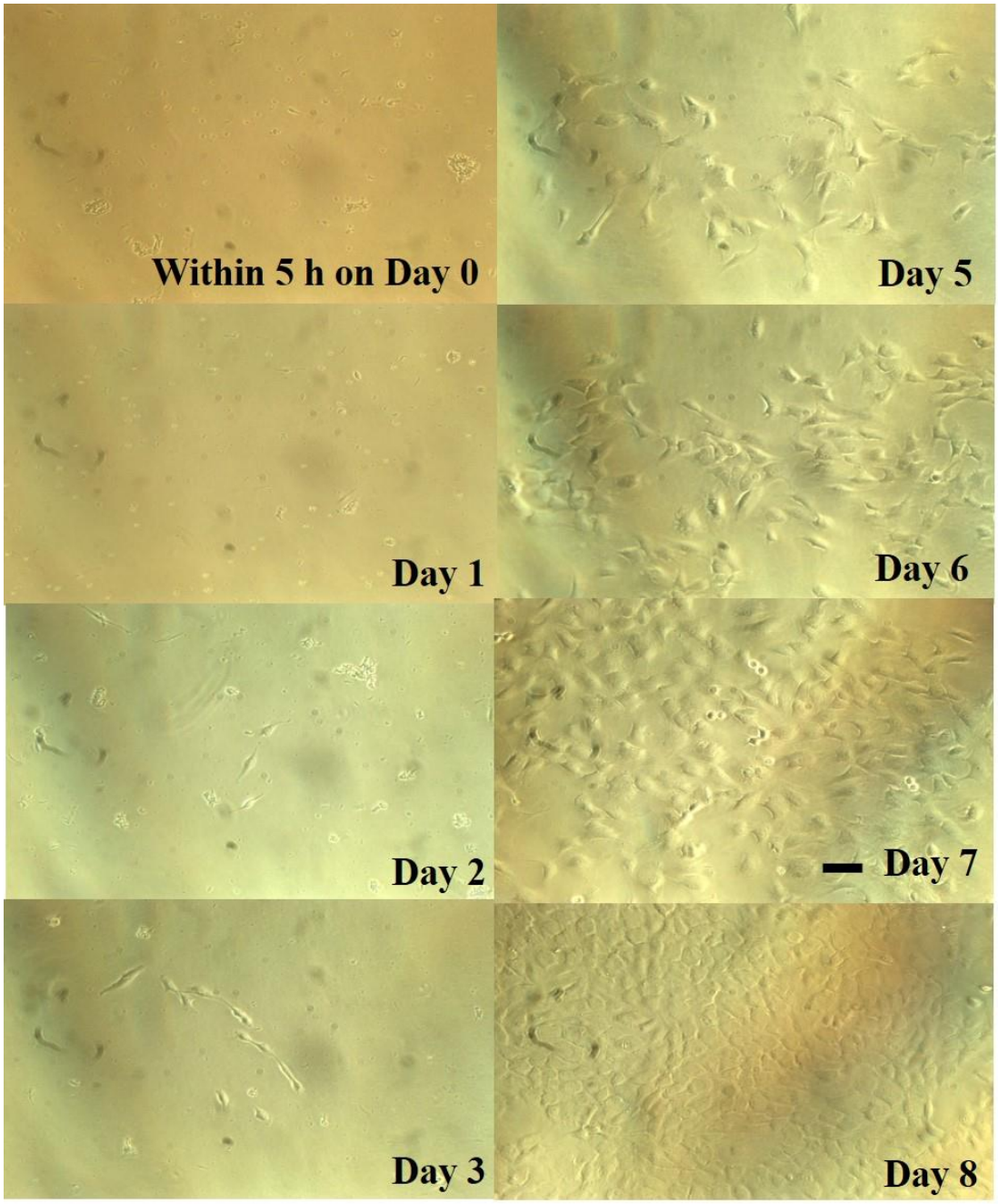

Figure 3-1 Primary cardiac fibroblasts (CFs) isolated from adult rat's heart on Day0-Day8. Phase contrast microscopy of CFs examined after culture on Day0-Day8 (Bar= 20 µM). The images were obtained using 10X objective lens.

3.3.2 Immunofluorescence assessment of Fibroblasts

Immunofluorescence of cultured fibroblasts shows that the vimentin antibody positively stained cardiac fibroblasts as would be expected for a non-selective fibroblast marker. Together with a spindle-shaped morphology, strong staining is a reliable stable marker for fibroblasts. However, the non-selective nature of this marker requires that additional staining is performed (see below). The image shown in Figure 3-2 shows staining of primary cardiac fibroblasts using anti vimentin antibody (Vim3B4). The green colour indicates vimentin antibody staining of the protein that belongs to the intermediate filament family, and is needed for maintaining cell shape, integrity of the cytoplasm, and for stabilising cytoskeletal interactions.

Since vimentin is not highly specific for fibroblasts, we also stained for other proteins known not to be expressed in these cells. We used an antibody to CD31 and Von Willebrand Factor (VWF), which are known to stain endothelial cells. Antibodies to CD31, VWF, were negative for staining in the fibroblasts and positive in the endothelial cells (see Figure 3-2, Panel b-d). Also αSMA was negative for staining in the fibroblasts and postitive in the smooth muscle cells. We thus conclude that, in formalin –fixed cells, the vimentin antibody, but not CD31, VWF and αSMA, stain for fibroblasts.

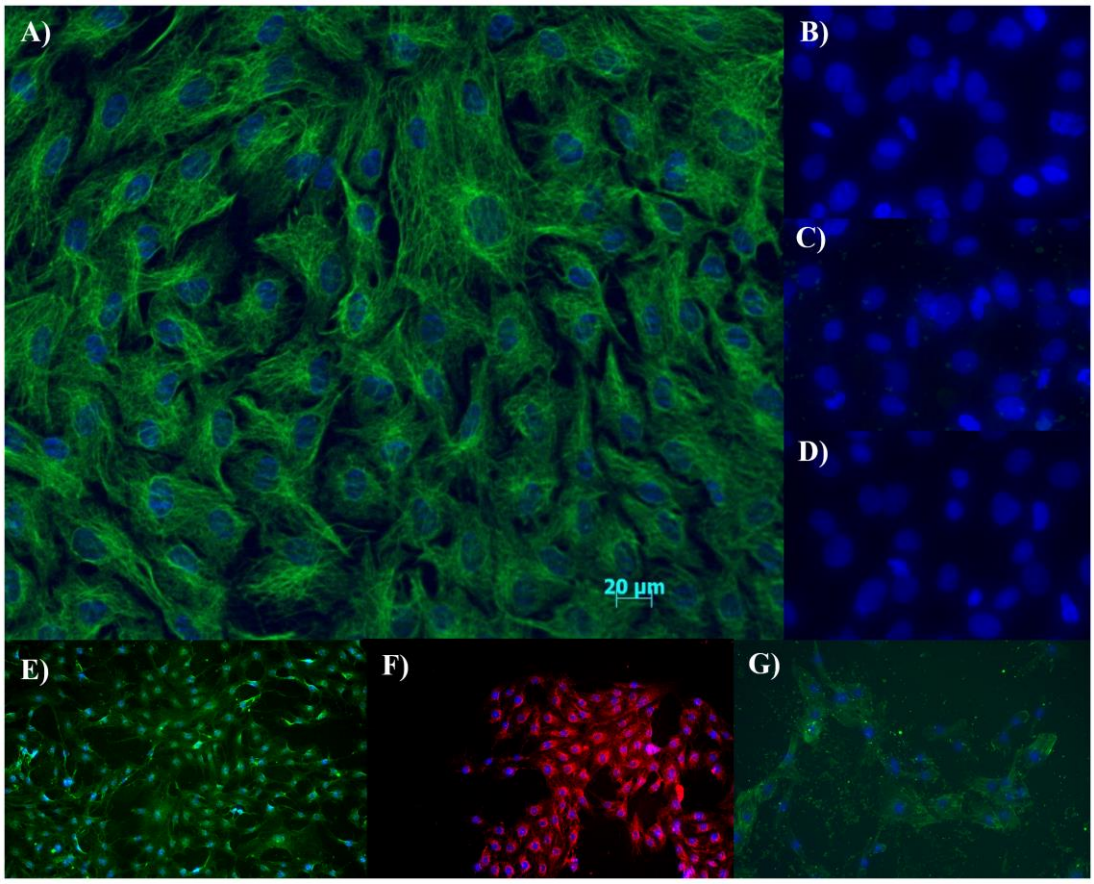

Figure 3-2 Antibody staining in formalin-fixed cultured fibroblasts. Growing CFs, primary cardiac fibroblast, fibroblast-like, in growing and quiescent states were fixed with formalin (Bar = 20 µM). Double staining of (A) Vimentin (Vm)/DAPI (B) CD31/DAPI (C) Von Willebrand Factor (VWF)/DAPI and (D) alpha smooth muscle actin (αSMA)/DAPI. And double staining of (E) VWF /DAPI and (F) CD31/DAPI in endothelial cell and (G) αSMA/DAPI in smooth muscle cells. Cardiac fibroblast simultaneously stained with vimentin antibody conjugated with FITC and with DAPI**.** Nuclei are stained blue with DAPI **.**Antibody staining is shown in green and red from FITC plus substrate. Panel A-D were obtained using 20X objective lens. Panel E-G were obtained using 10X objective lens. Endothelial cell donated by Dr Christopher McCormick, Biomedical Engineering, University of Strathclyde. Smooth muscle cell by Dr. Paul Coats, Strathclyde Institute of Pharmacy & Biomedical Sciences (SIPBS), University of Strathclyde.

3.3.3 Cytotoxicity testing

3.3.3.1 Separate assays; MTT, neutral red and crystal violet: 3T3 cell line

The results of the experiments demonstrating the percentage of cell viability of treated 3T3 cells and the various concentrations of $CoCl_2$, 0-1000 µM, after 24, 48, and 72h results are shown in Figure 3-3, Figure 3-4 and Figure 3-5, using three separate assays; MTT, neutral red and also crystal violet.

As is illustrated in Figure 3-3, and measured by MTT assay, at 24 h, the number of cells was constant, and therefore cells were not significantly affected by $CoCl_2$ exposure for this time. At 48 h, there were not any significant changes following 0-200 µM-treatment. However, significant differences were evident after exposure to concentrations greater than 200 µM, and these enabled us to calculate the IC_{50} value (see Table 3-1). At 72 h, the results showed the same pattern as at 48 h. The results also show time-dependent effects of $CoCl_2$ treatment.

Figure 3-4 shows that as measured by NR assay, after 24, 48 and 72 h exposure, the number of viable cells had decreased after treatment with $CoCl_2$ (0-1000 µM) at all exposure times. It was possible to calculate IC_{50} values (see Table 3-1).

The results from the crystal violet assay have the same pattern as the MTT and neutral red data. This enabled us to calculate IC_{50} value (see Table 3-1).

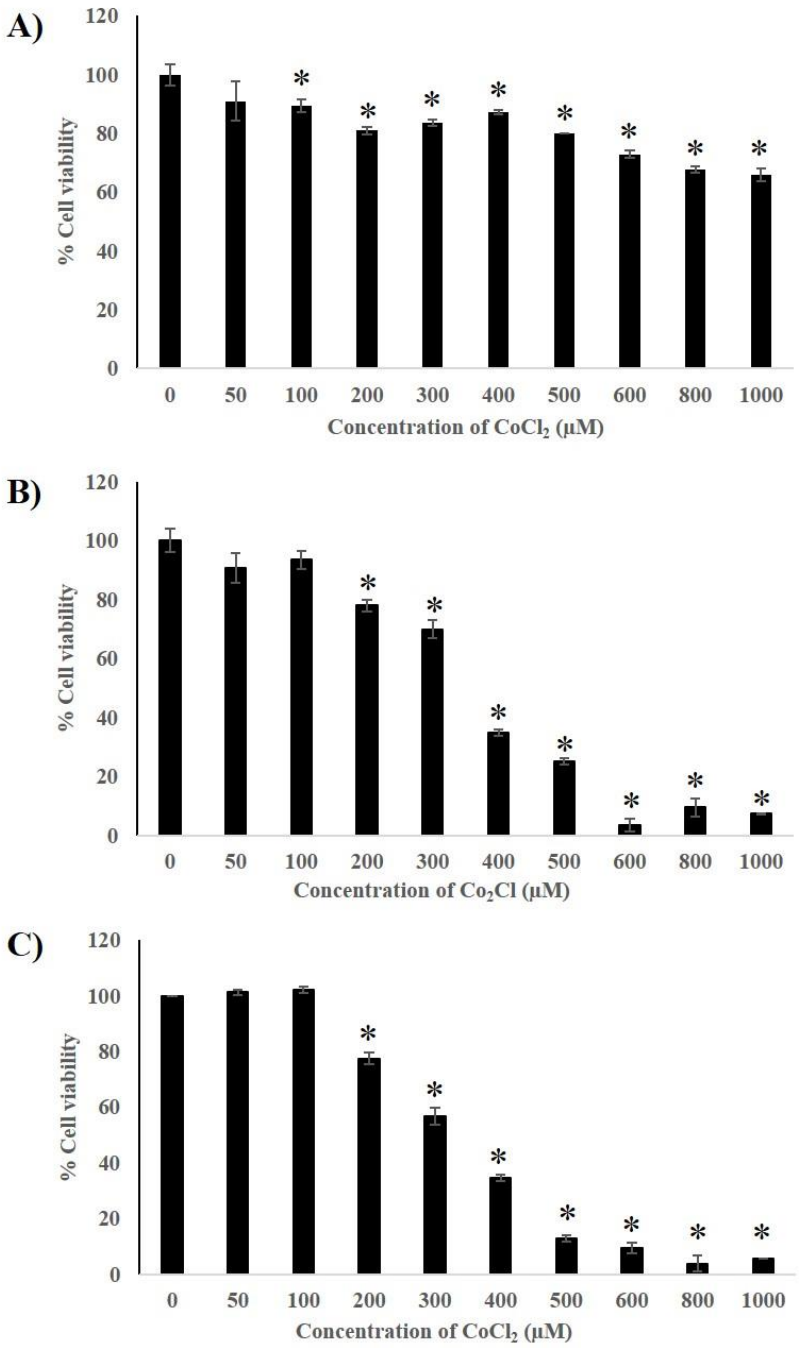

Figure 3-3 $CoCl_2$ reduces viability of 3T3 cells using MTT assay. Cell viability was reduced in a dose-dependent manner with $CoCl_2$ (0-1000 µM) treatment over (A) 24 h (B) 48 h and (C) 72 h, as measured by MTT assay. The cell viability was markedly reduced at both 48 and 72 h compared to 24 h. Statistical analysis was carried out using one-way-ANOVA with post hoc Dunnett's comparison (n = 3, *$p<0.05$ with a significant difference to control)**.**

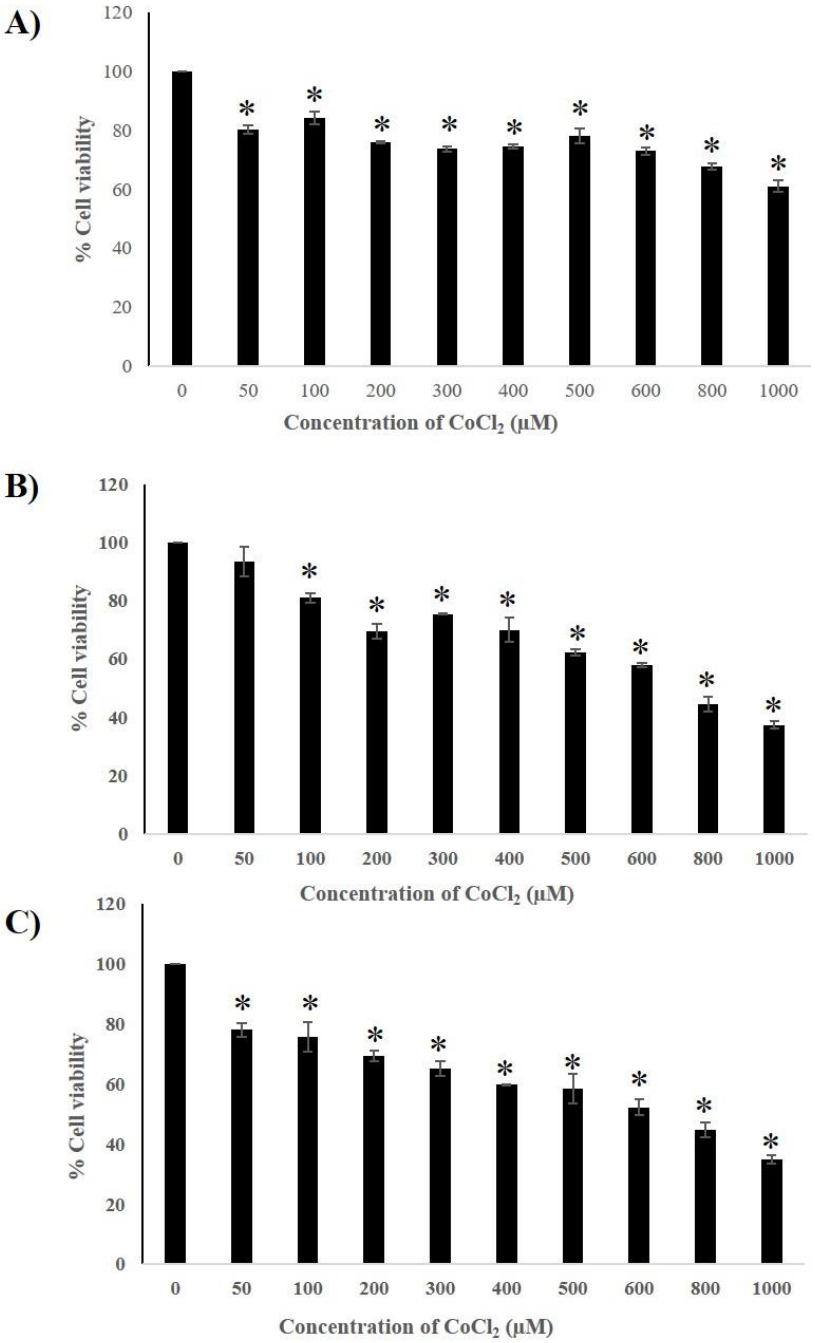

Figure 3-4 $CoCl_2$ reduces viability of 3T3 cells using NR assay. Cell viability was reduced in a dose-dependent manner with $CoCl_2$ (0-1000 µM) treatment over (A) 24 h (B) 48 h and (C) 72 h, as measured by NR assay. The cell viability was significantly reduced at both 48 and 72 h compared to 24 h. Statistical analysis was carried out using one-way-ANOVA with post hoc Dunnett's comparison (n = 3, *$p<0.05$ with a significant difference to control).

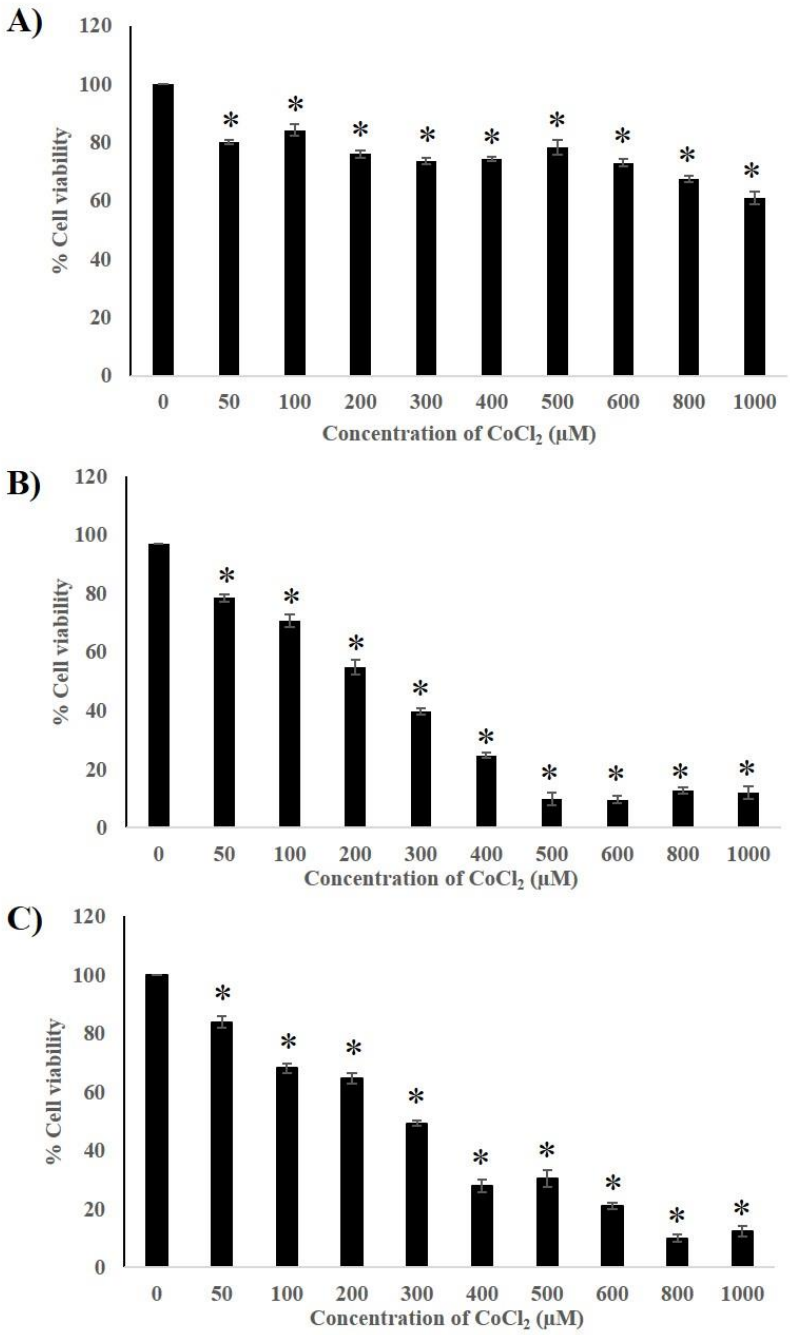

Figure 3-5 $CoCl_2$ reduces viability of 3T3 cells using CV assay. Cell viability was reduced in a dose-dependent manner with $CoCl_2$ (0-1000 µM) treatment over (A) 24 h (B) 48 h and (C) 72 h, as measured by CV assay. The viable cell was obviously decreased at both 48 and 72 h compared to 24 h, as the same pattern with MTT measuring in Figure 3-3. Statistical analysis was carried out using one-way-ANOVA with post hoc Dunnett's comparison (n = 3, $*p<0.05$ with a significant difference to control).

The percentage cell survival rates shown in Figure 3-3, Figure 3-4 and Figure 3-5 were inversely correlated to the concentration of $CoCl_2$, in a dose and time-dependent manner with $CoCl_2$ (0-1000 µM) treatment over 24, 48 and 72 h exposure, as measured by three separated assay (MTT, NR and CV assay), when compared with control, leading to IC_{50} value evaluation (see Table 3-1).

The half maximal inhibitory concentrations (IC_{50}) of $CoCl_2$ were >1000 µM, 341.0 ± 11.37 and 311.05 ± 7.57 µM at 24, 48 and 72 h, respectively, using the MTT assay. With the NR assay, it was calculated the IC_{50} values were >1000 µM, 770.83±5.78 and 654.18±13.78 µM at 24, 48 and 72 h, respectively. Lastly, the results from the CV assay have the same pattern as the MTT and NR data. By 24 h, the number of cells was slightly decreased, and there were significant changes at both 48 and 72 h. The IC_{50} of $CoCl_2$ was >1000 µM, and was 331.31±5.67 and 292.14±7.86 µM at 24, 48 and 72 h, respectively. The IC_{50} values of treated cells at 48 and 72 h with $CoCl_2$ was significantly different when compared with 24 h treated cells, but not significantly different between 48 and 72 h treated group.

There are differences between these three simple assays in terms of the IC_{50} of $CoCl_2$. The results can be separated into two assay groups using IC_{50} values, the first group is composed of the data from the MTT and CV assays and the second group is the NR assay data. The results show that MTT and CV assays have similar IC_{50} values for $CoCl_2$ (300-400 µM, at 48 and 72 h respectively) and the NR assay data show higher values of IC_{50} for $CoCl_2$ (600-800 µM, at 48 and 72 h respectively). The IC_{50} of $CoCl_2$ as measured by MTT and CV assay were significantly lower the IC_{50} of $CoCl_2$ as measured by NR assay.

Table 3-1 The IC_{50} value of $CoCl_2$ on the 3T3 cell line by separate assays and the combined assay.

TIME	IC_{50} of $CoCl_2$ (µM)					
	24 h		48 h		72 h	
	SEP	COMB	SEP	COMB	SEP	COMB
MTT	>1000	>1000	341.00±11.37$^{*,\wedge}$	370.89±14.67$^{*,\wedge}$	311.05±7.57$^{*,\wedge}$	348.53±4.76$^{*,\wedge}$
NR	>1000	>1000	770.83±5.78$^{*,\#}$	741.18±8.97$^{*,\#}$	654.18±13.78$^{*,\#}$	703.76±15.56$^{*,\#}$
CV	>1000	>1000	331.31±5.67$^{*,\wedge}$	376.95±6.78$^{*,\wedge}$	292.14±7.86$^{*,\wedge}$	309.66±6.95$^{*,\wedge}$

Data represent mean ± SEM and Statistical analysis was carried out using one-way-ANOVA with post hoc Dunnett's comparison (n = 3, $^{*}p<0.05$ with a significant difference to control, $^{\#}p<0.05$ with a significant difference to MTT assay, $\wedge p<0.05$ with a significant difference to NR assay). h, hours; SEP, separate assays; COMB, combined assay. There were no significant differences between the combined assay and separate assays for each respective time point.

3.3.3.2 Combined assays; MTT, neutral red and crystal violet: 3T3 cell line after treatment with $CoCl_2$

The combined assay was composed of the same three simple assays, neutral red, MTT and also crystal violet. The results show the responses of the 3T3 cell line after being treated with various concentrations of $CoCl_2$, over 0-1000 µM and the toxicity of $CoCl_2$ was indicated by 50% inhibitory concentration (IC_{50}) as shown in Table 3-2.

Using the combined assay method the half maximal inhibitory concentration (IC_{50}) of $CoCl_2$ on the 3T3 cell line using the MTT assay was over 1000 µM, and was 370.89±14.67 and 348.53±4.76 µM at 24, 48 and 72 h, respectively. For the NR assay, the data show IC_{50} value was over 1000 µM, and was 741.18±8.97 and 703.76±15.56 µM at 24, 48 and 72 h, respectively. Lastly, the data for crystal violet was over 1000 µM, and was 376.95±6.78 and 309.66±6.95 µM at 24, 48 and 72 h, respectively.

The comparison between the IC_{50} value of each assay and combined assay is shown in Table 3-1 and Figure 3-6. Looking at Table 3-1, the values for the IC_{50} obtained using the separate and combined assays showed no statistically significant differences. Thus, the combined method is appropriate to use to replace the separate assays. Especially in primary cardiac cells, which have a limited number of cells available, the combined assay can help to generate more data. Overall, the combined assay is an option that can help reduce the time, and cost of testing and limitations of cell numbers.

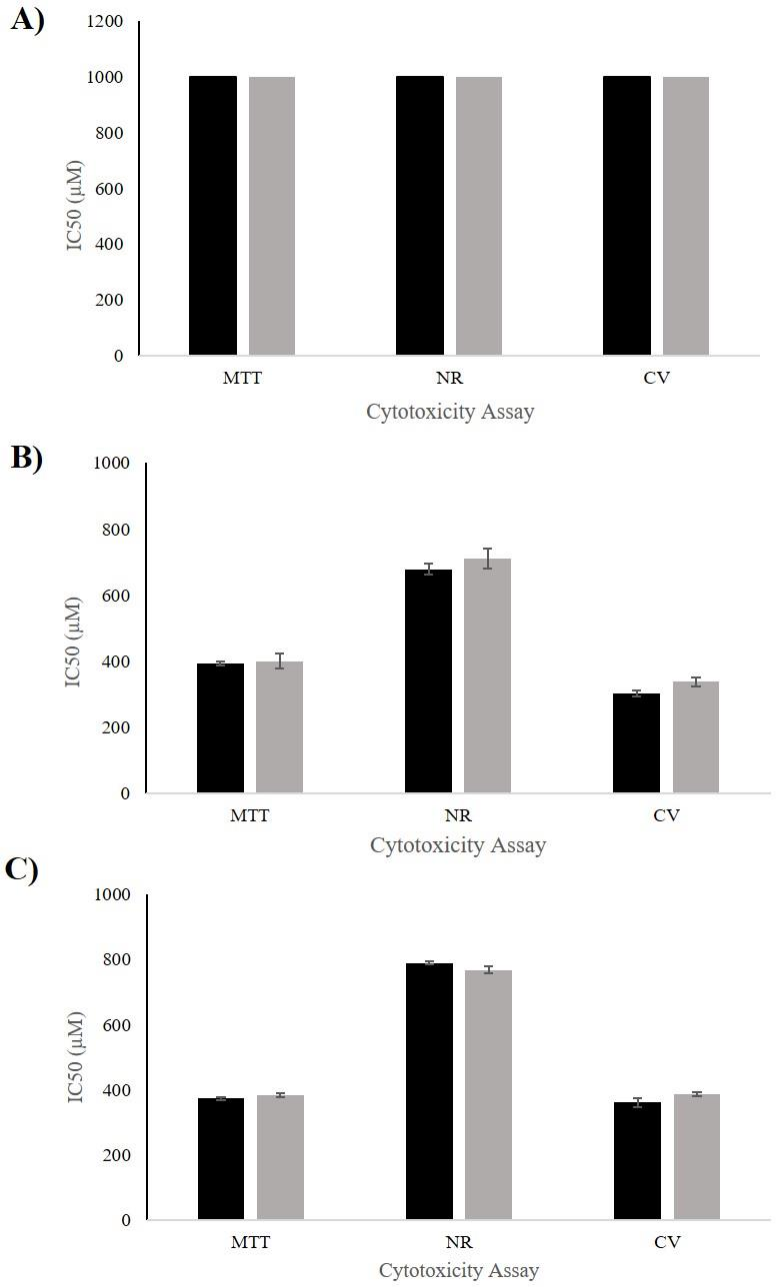

Figure 3-6 Comparison of cytotoxicity assay figures of IC_{50} values of Co by time dependence on 3T3 cell line using separate assays and combined assays. (A) 24 h (B) 48 h and (C) 72 h. Measurements of IC_{50} of $CoCl_2$ were calculated from separate cytotoxicity (black) and combined cytotoxicity (grey) asays, which are composed of MTT, neutral red (NR) and crystal violet (CV). There were no significant differences between the combined assay and separate assays for each respective time point (using two-sample t-test). Both MTT and NR assay are significant, $p<0.05$ different to NR assay for each respective time ($p<0.05$ using one-way-ANOVA with post hoc Dunnett's comparison).

3.3.3.3 Combined assays; MTT, neutral red and crystal violet: Cardiac fibroblasts after treatment with $CoCl_2$

From the results of the combined assay on the 3T3 cell line, it can be seen that the combined assay can be an alternative appropriate method for detecting the toxicity of Co, because the results were similar on both separate and combined assays. The results show the cytotoxicity of CFs after being treated with various concentrations of $CoCl_2$, over 0- 1000 µM, and the toxicity of $CoCl_2$ was indicated by 50% inhibitory concentration (IC_{50}) as shown in Table 3-2.

The half maximal inhibitory concentrations (IC_{50}) of $CoCl_2$ on CFs by MTT assay was over 1000 µM, 384.54±6.78 and 400.27±22.83 µM at 24, 48 and 72 h, respectively. For NR assay, the data show that the IC_{50} value was over 1000 µM, and was 768.40±10.87 and 710.73±29.05 µM at 24, 48 and 72 h, respectively. Lastly, the data for crystal violet were over 1000 µM, and was 387.43±5.46 and 337.55±14.54 µM at 24, 48 and 72 h, respectively.

Table 3-2 The IC_{50} of $CoCl_2$ on CFs by combined assay.

TIME	24 h	48 h	72 h
MTT	>1000	384.54±6.78$^{*,\wedge}$	400.27±22.83$^{*,\wedge,}$
NR	>1000	768.40±10.87$^{*,\#}$	710.73±29.05$^{*,\#}$
CV	>1000	387.43±5.46$^{*,\wedge}$	337.55±14.54$^{*,\wedge}$

Data represent mean ± SEM and Statistical analysis was carried out using one-way-ANOVA with post hoc Dunnett's comparison (n = 3, $^{*}p<0.05$ with a significant difference to control, $^{\#}p<0.05$ with a significant difference to MTT assay, $\wedge p<0.05$ with a significant difference to NR assay). MTT, MTT assay. NR, neutral red assay; CV, crystal violet. There were no significant differences between 48 and 72 h exposure time.

CFs after being treated with $CoCl_2$ show similar results as the 3T3 cell line. The results are shown in Figure 3-7. Moreover, the comparison of the three assays (MTT, NR and CV) found that both MTT and CV can detect the level of cytotoxicity of $CoCl_2$ on 3T3 cell line and CFs, more readily than NR because the IC_{50} values in both MTT and CV assays were lower than the IC_{50} value of NR. In the same fashion in the 3T3 cell line and in the CFs, the effect of $CoCl_2$ was time and dose dependent manner.

The value of IC_{50} on 3T3 cells was almost equal to the value of IC_{50} for CFs. as shown in Figure 3-7. In conclusion, there was no significant difference in the effect of $CoCl_2$ between the 3T3 cell line and CFs.

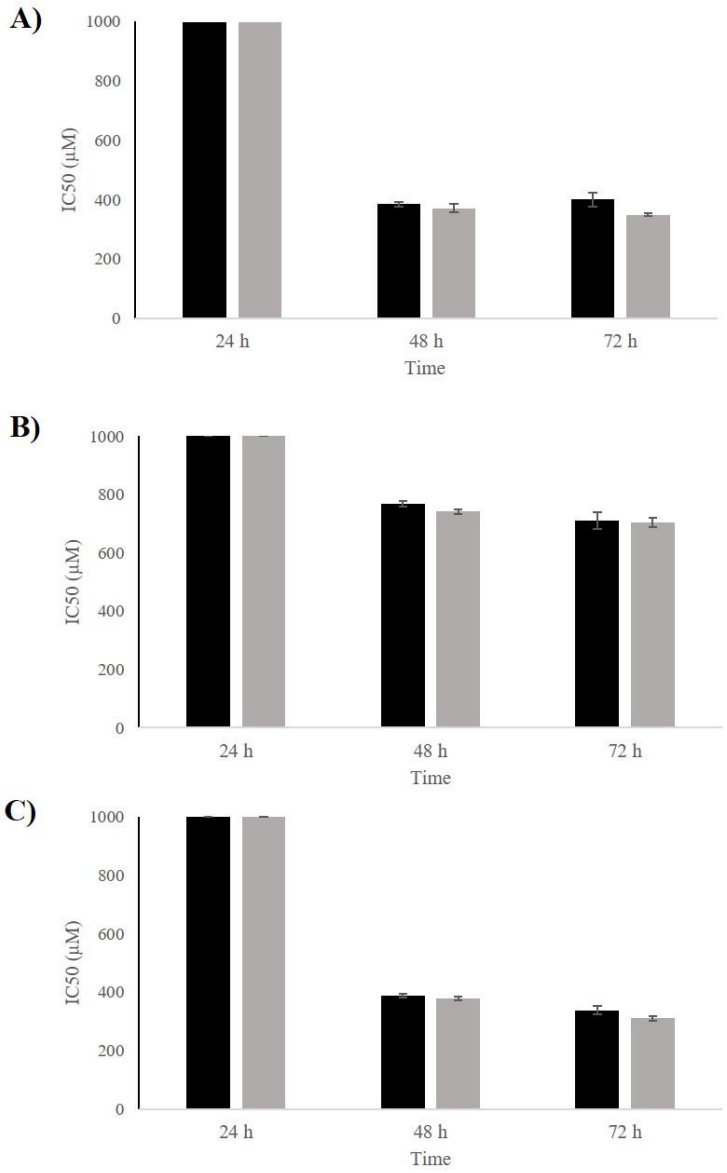

Figure 3-7 $CoCl_2$ effects on 3T3 cell line and primary cardiac fibroblast (CFs) as measured by the combined assay. The combined assays show IC_{50} value of 3T3 cells and CFs after being treated with various concentrations of $CoCl_2$ (A) MTT assay (B) Neutral red assay and (C) crystal violet assay (combined assay method). A toxic response was measured by all three assays, the responses were not statistically different when comparing between both cells, and the responses of the 3T3 cells (black) and the CFs (grey) were similar as measured by each assay. There were no significant differences between the 3T3 cells and CFs for each respective assay using two-sample t-test, n=3, $p<0.05$. (Appendix, Table A2-1)

3.3.4 Cell Proliferation assay.

3.3.4.1 Cell Proliferation assay by BrdU cell proliferation assay

Cell proliferation of CFs and the 3T3 cell line was inhibited after exposure to increasing doses of $CoCl_2$ (0-500 µM), as described in Figure 3-8.

The BrdU results showed a significant difference in the response to $CoCl_2$ (over 0-500 µM) in terms of the proliferation of 3T3 cells and CFs. All results are statistically different from their respective control values of untreated cells at each time point. Exposure of cardiac fibroblasts to $CoCl_2$ (48/72h) caused marked inhibition of DNA replication, as measured by BrdU incorporation assay, with effects of more than 80% inhibition of DNA synthesis when they were treated at concentrations of $CoCl_2$ of over 0-500 µM. The proliferation of CFs decreased dramatically to almost 20 percent by 25 µM $CoCl_2$ and then gradually fell to nearly 0 at 150 µM $CoCl_2$ after 48 and 72 h exposure. The IC_{50} values for inhibition of CF cell proliferation by $CoCl_2$ were 16.90 ± 1.57 and 16.78 ± 1.59 µM at 48 and 72 h, respectively. Whereas, in contrast proliferation of 3T3 cells was inhibited to a lesser extent by $CoCl_2$ with IC_{50} values of 272.68 ± 1.16 and 225.03 ± 4.15 µM at 48 and 72 h.

The IC_{50} values for proliferating CFs are significantly lower than those for 3T3 cell lines, and this suggests that CFs are more sensitive to the effect of $CoCl_2$ than 3T3 cell lines. There were no significant differences between 48 and 72 h exposure time using two-sample t-test in either cell types.

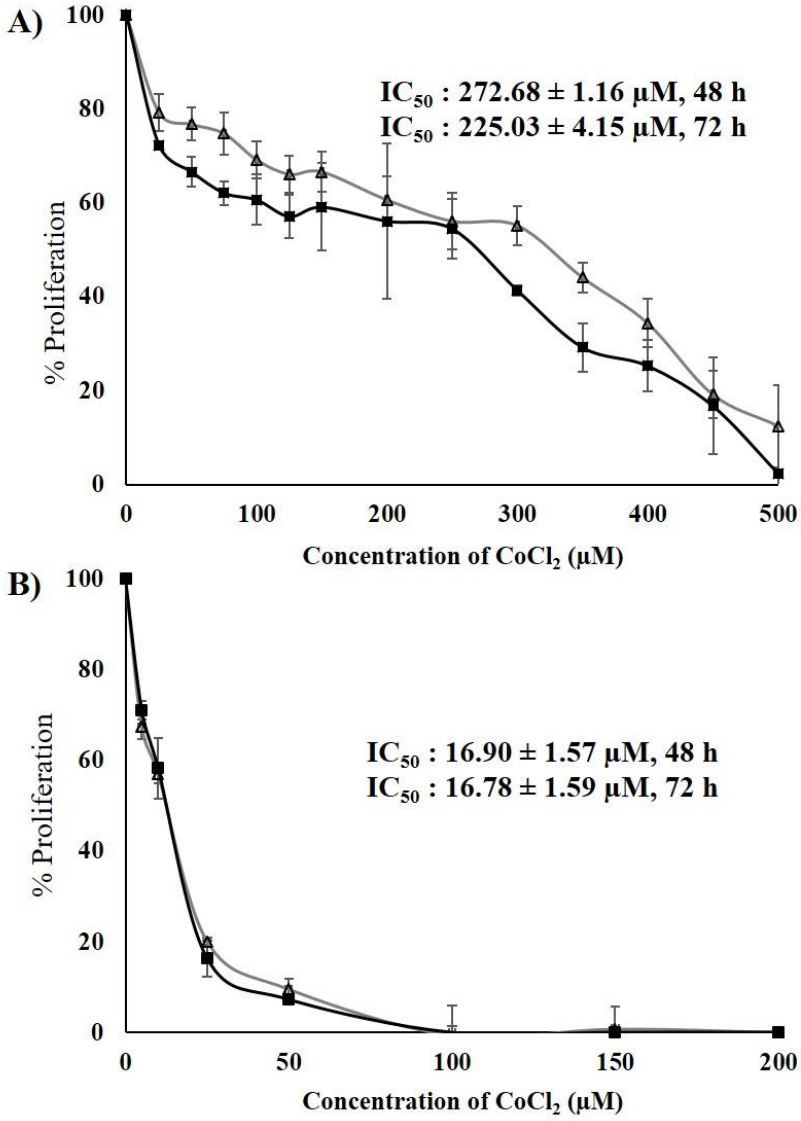

Figure 3-8 Dose and Time dependent inhibition of the cell proliferation by Co exposure. Treatment of (A) 3T3 cells and (B) CFs with $CoCl_2$ (0-500µM) decreased cell proliferation as detected by BrdU Cell Proliferation Assay at 48 h (black) and 72 h (grey). Untreated cells of the appropriate type were used as control. All results are statistically different from their respective control values of untreated cells using one-way-ANOVA with post hoc Dunnett's comparison (n = 3, $*p<0.05$ with a significant difference to control). There were no significant differences between 48 and 72 h using two-sample t-test. (N.B Note difference in x-axes scales)

3.3.4.2 Cell viability for low dose toxicity of $CoCl_2$ using MTT Assay

The two graphs below provide data about the viability of cells when treated with low doses of $CoCl_2$ (Figure 3-9). The results of the MTT assay are consistent, showing that $CoCl_2$ had no effect on viability of either 3T3s or CFs at low concentrations of $CoCl_2$ (0.00625 – 25 µM) for 24, 48 and 72 h.

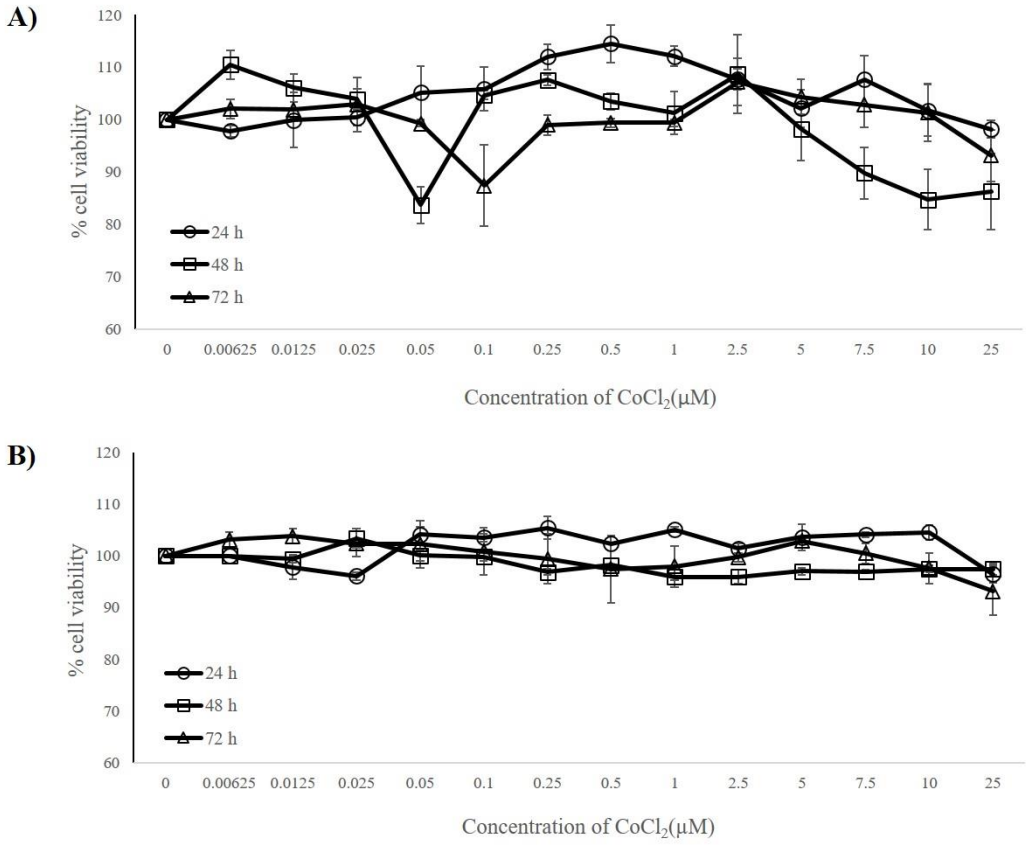

Figure 3-9 Cell viability test of the effect of low concentrations of Co on 3T3 cells and CF by using the MTT assay. Both (A) 3T3 cells and (B) CFs were treated with low concentrations of $CoCl_2$ (0.00625 – 25 µM) after incubation for 24, 48 and 72 h. Results of MTT assay of 3T3 cells and CFs did not reveal any significant difference in cell viability by treatment with low concentration of $CoCl_2$ at all exposure time. ANOVA followed by Dunnett's test (n = 3, $p<0.05$).
N.B. Equivalent in vivo blood cencentraions in patients 0.025 µM is 60 µg/L and 1 µM is 240 µg/L.

3.3.5 Staining for Live and Dead cells using CFDA and PI after treatment with $CoCl_2$

3.3.5.1 3T3 cell line -staining with CFDA and PI after treatment with $CoCl_2$

Figure 3-10 shows the staining of cells. Living cells were detected as green from CFDA, and dead cells were stained red from PI. The picture shows that when increasing the duration of the test, the number of cells increased, especially in untreated cells. However, when increasing the concentration of $CoCl_2$, the red colour representing dead cells increased at all exposure times (24, 48 and 72 h). The CFDA and PI provided a direct observation of the proportion of living and dead cells. The control group exhibited the least number of dead cells and the greatest number of living cells, on staining. Other treated cells showed a relatively higher proportion of dead cells than control group. However, some dead cells were lost during washing of the dish, and also there are morphology changes in the cells. For example, the boundary of treated cells (cell membrane) was less sharp when compared with normal cells. There were also vacuoles occurring within the treated cells as shown by red arrows at both 250 and 500µM of $CoCl_2$ treated samples.The nuclei in cells were destroyed and broken into small fragments in many cells and these are shown by the blue arrows.

3.3.5.2 Cardiac Fibroblasts (CFs) -staining with CFDA and PI after treatment with $CoCl_2$

Following treatment with 0, 250 and 500 µM $CoCl_2$, Figure 3-11 shows representative fluorescence images of live and dead cells for each treatment condition before and after $CoCl_2$ exposure. It is readily apparent that the characteristics of staining of viable cells and dead cells on CFs are similar to the 3T3 cell line. Fluorescence microscopy distinguished viable (green) and dead (red) cells**.** The number of cells increased after increasing time for untreated cells. The number of cells was also inversely related to the concentration of $CoCl_2$ (250 and 500 µM) at all exposure times (24, 48 and 72 h). Also, irregular shapes of cells were found in the treated cells, and the membrane of cells were not smooth when compared with untreated cells. The vacuoles and cell debris also occurred in some treated CFs as well as in the 3T3 cell line (see Figure 3-11).

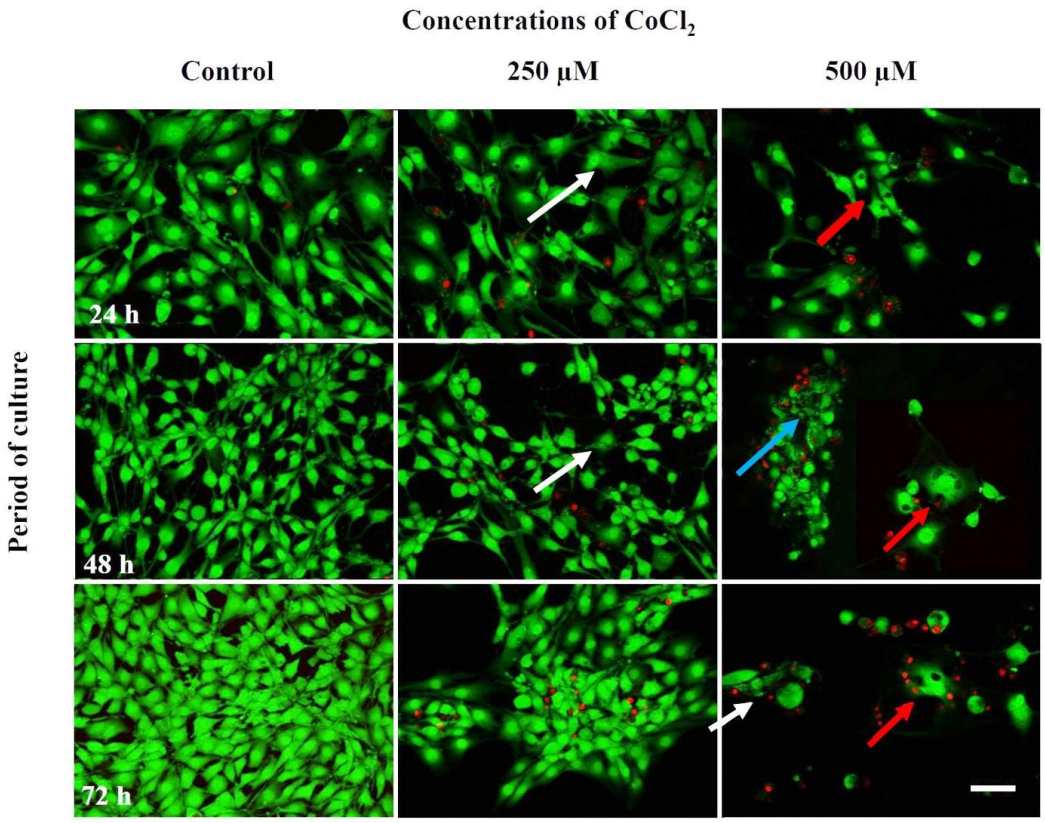

Figure 3-10 Viability of the 3T3 cell line cultured with various concentrations of $CoCl_2$. Live-Dead cell staining of 3T3 cell line on 35 mm^2 culture dish after being treated with various concentrations of $CoCl_2$; untreated cells, 250 and 500 µM after 24, 48 and 72 h (Bar= 40 µm). Live and dead cells simultaneously stained with carboxyfluorescein diacetate (CFDA) and with propidium iodide (PI). CFDA staining of live cells (green) and PI staining of nucleus in dead cells (red). Red arrows show vacuoles occurring in cell. White arrows show cell debris. Blue arrow shows broken nuclei. The Images were obtained using 20X objective lens. Some figures are magnified in the Appendix, Figure A3-1.

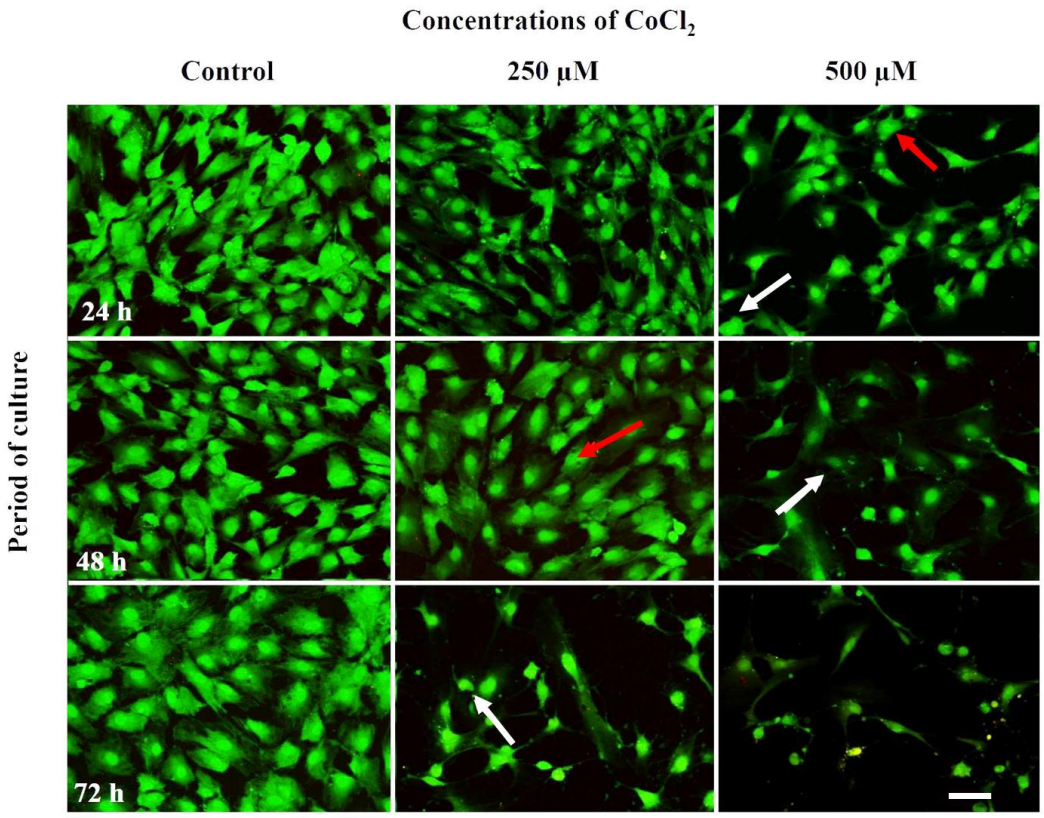

Figure 3-11 Viability of cardiac fibroblast (CFs) cultured with various concentrations of $CoCl_2$. Live-Dead cell staining of CFs on 35 mm^2 culture dish after being treated with various concentrations of $CoCl_2$; untreated cells, 250 and 500 µM after 24, 48 and 72 h (Bar= 40 µm). Live and dead cells simultaneously stained with carboxyfluorescein diacetate (CFDA) and with propidium iodide (PI). CFDA staining of live cells (green) and PI staining of nucleus in dead cells (red). Red arrows showing vacuoles occurring in cell. White arrows show cell debris. The images were obtained using 20X objective lens.

3.3.6 Staining for Actin using Phalloidin-FITC in 3T3 cells and cardiac fibroblasts treated with $CoCl_2$

3.3.6.1 3T3 cell line-staining with Phalloidin-FITC and DAPI after treatment with $CoCl_2$

Figure 3-12 shows the distribution of actin filaments used to detect the morphology of the 3T3 cell line after treatment with $CoCl_2$. The normal distribution of actin was observed in untreated cells at 24, 48 and 72 h, which were uniformly stained. There was no change in the size of the nucleus and elongated cells were present as normal in untreated cells. After being treated with $CoCl_2$, at 250 and 500 µM, broken actin filaments were found in cells as shown by the white arrows, and also loss of the shape of cells as shown by the yellow arrows. Interestingly, it can be observed that the arrangement of actin within the normal cells is to surround the nucleus of the cell. Whereas the actin distribution in treated cells was not normal; it was not surrounding the nucleus but arranged around the cell border. Specifically, actin filaments in 3T3 cells treated with $CoCl_2$ appear changed with a slightly decreased actin staining intensity relative to untreated cells. The membrane formed blebs, and ballooned out in treated cells (red arrow). The bleb formation is supporting the suggestion that $CoCl_2$ causes cell apoptosis.

3.3.6.2 Cardiac Fibroblasts (CFs) -staining with Phalloidin-FITC and DAPI after treatment with $CoCl_2$

The distribution of actin filaments was also used to detect the morphology of CFs that had been treated with $CoCl_2$. As shown in Figure 3-13, the normal distribution of actin was observed in untreated cells at 24, 48 and 72 h, which were uniformly stained. No change in the size of nuclei was detected after $CoCl_2$ exposure. But the arrangement of actin in treated CFs was distributed around the border of the cells, and not close to the nuclei. Actin filaments in CFs treated with $CoCl_2$ were disrupted with greatly decreased F-actin staining intensity. The bleb formation occurred in treated cells, 500 µM of $CoCl_2$, at 24, 48 and 72 h. There was no change in the size of the nucleus and the integrity of actin appear to be compromised.

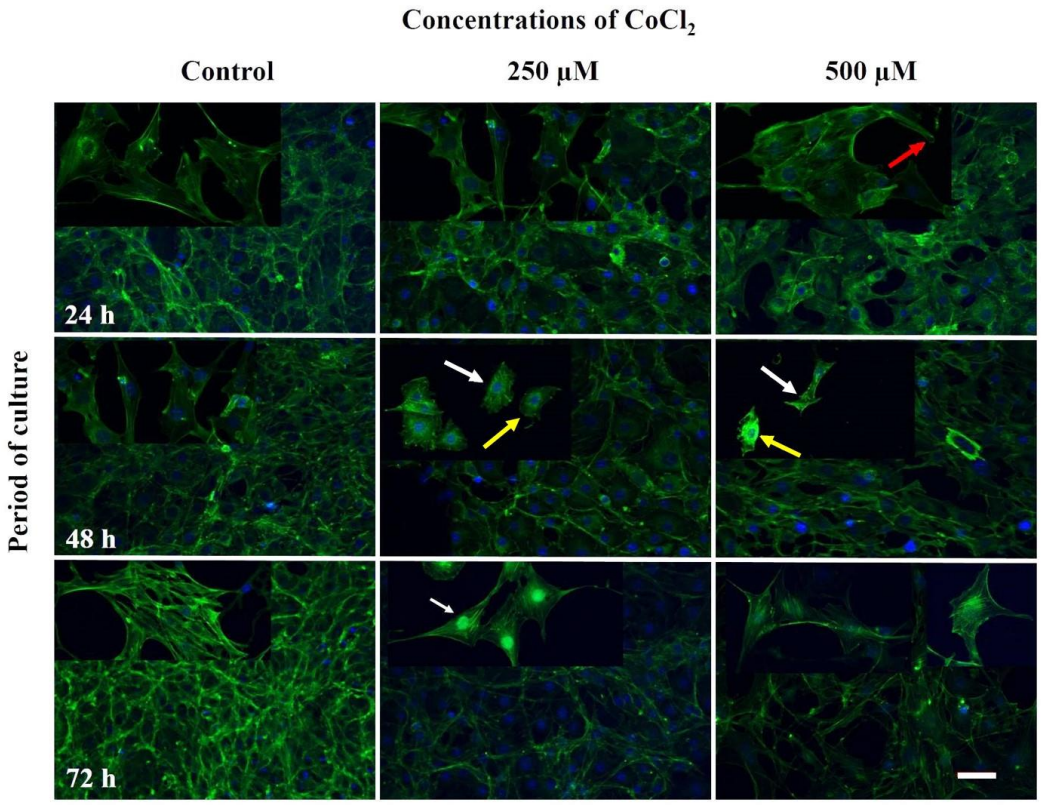

Figure 3-12 Staining of F-actin filaments of the 3T3 cell line cultured with various concentrations of $CoCl_2$. Actin cytoskeleton staining of 3T3 cells on 35 mm^2 culture dish after being treated with various concentrations of $CoCl_2$; untreated cells, 250 and 500 µM after 24, 48 and 72 h (Bar= 40 µM). Changes in actin cytoskeleton were verified by Phalloidin-FITC staining of actin fibres (green) and DAPI staining of the nucleus in cells (blue). Red arrows show blebbed cells. White arrows show broken cytoskeleton in cells. Yellow arrows show irregular cell shape. Image were obtained using a 20X objective lens. All images were captured using identical exposure settings.

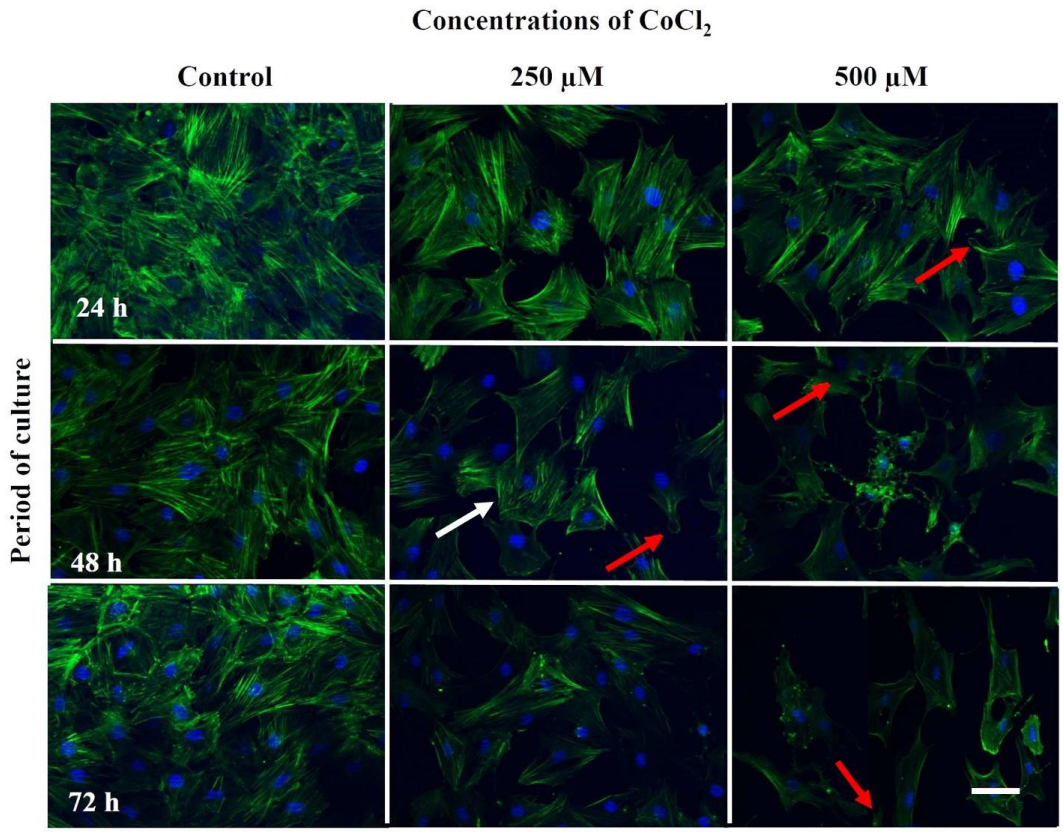

Figure 3-13 Staining of F-actin filaments of cardiac fibroblasts (CFs) cultured with various concentrations of $CoCl_2$. Actin cytoskeleton staining of CFs on 35 mm^2 culture dish after being treated with various concentrations of $CoCl_2$; untreated cells, 250 and 500 µM after 24, 48 and 72 h (Bar= 40 µM). Changes in the actin cytoskeleton were verified by Phalloidin-FITC staining of actin fibres (green) and DAPI staining of the nucleus in cells (blue). Red arrows show blebbed cells. White arrows show broken cytoskeleton in cells. Images were obtained using a 20X objective lens. All images were captured using identical exposure settings. Some figures are magnified in the Appendix, Figure A3-2.

3.3.7 Co uptake in 3T3 cells and in CFs during treatment with $CoCl_2$

Clinical studies report blood Co levels in ppb or µg/L, and also the data obtained from ICP-MS measurements is expressed as ppb or µg/L. Results shown here specify the concentration of Co added to the culture as both µM and ppb units in order to easily understand and compare the data.

Table 3-3 and Figure 3-14 show the results of the experiments demonstrating the level of cellular Co ion uptake in 3T3s and CFs treated with various concentrations of $CoCl_2$, 0-300 µM, after 24, 48, and 72 h exposure, using ICP-MS. It can be seen in both Figure 3.14 and Table 3.3 that with increasing medium concentration of $CoCl_2$, the intracellular Co concentration of both 3T3s and CFs increased. After 24, 48 and 72 h the results show that the range of intracellular Co ions ranges between 0-50 ppb in 3T3s and 0-120 ppb in CFs, at all exposure times (24, 48 and 72h). Intracellular levels in both 3T3 cells and CFs increase linearly with the concentration of $CoCl_2$ and the duration of exposure time.

At 24 h, ICP-MS data show significant Co uptake into both cell types at only concentrations of 100 µM, and above. Whereas for 48 and 72 h exposure, there is significant Co uptake into both cell types starting from a concentration of 25 µM. In order to avoid toxicity limiting uptake, it was decided to limit the concentration of $CoCl_2$ used in these experiments to less than the IC_{50} value (as shown in Table 3-1 and 3-2) of each cell. So 300 µM of $CoCl_2$ was the highest concentration, which was used to treat both 3T3 cells and CFs.

When the Co uptake between 3T3 cells and CFs was compared, the data showed that the uptake of Co into CFs was significantly higher when compared with 3T3s at the same concentrations. Co uptake into CFs was greater than into 3T3s and this may at least partly explain the difference in toxicity between the two cell types.

Figure A3-3 compares the uptake of Co versus proliferation for both CFs and 3T3 cells. The slope of the lines show dissimilar gradients, suggesting that a dissimilar mechanism of action may be present in both cell types in terms of the effect on proliferation.

Table 3-3 Comparison of Cellular ion uptake in 3T3s and CFs treatment with $CoCl_2$ for up to 72h.

	Concentration of $CoCl_2$											
µM(mg/L)	**0 (0)**		**25 (5.90)**		**50 (11.80)**		**100 (23.79)**		**200 (47.59)**		**300 (71.38)**	
cell	3T3s	CFs	3T3s	CFs	3T3s	CFs	3T3s	CFs	3T3s	CFs	3T3s	CFs
24h (µg/L)	0.61±0.04	0.63±0.35	0.44±0.04	0.82±0.21	0.75±0.18	1.12±0.21*	2.16±0.37*	5.07±0.43$^{*,\#}$	8.90±0.08*	28.82±1.52$^{*,\#}$	15.31±2.05*	28.24±0.28$^{*,\#}$
48h (µg/L)	0.00	0.30±0.22	0.63±0.15*	1.79±0.35$^{*,\#}$	0.81±0.00*	0.88±0.05*	2.48±0.07*	4.37±0.06$^{*,\#}$	15.93±0.89*	58.99±2.67$^{*,\#}$	23.73±2.05*	75.65±1.17$^{*,\#}$
72h (µg/L)	0.00	0.21±0.04	1.28±0.13*	1.36±0.15*	2.64±0.13*	2.40±0.31*	7.17±0.33*	8.09±0.40*	25.64±0.88*	71.57±3.92$^{*,\#}$	47.26±8.11*	118.66±7.72$^{*,\#}$

The concentrations of Co added to the culture medium in order to measure uptake are given in both µM and mg/L. Co ion uptake units are µg/L. Data represent mean ± SEM; Statistical analysis was carried out using one-way-ANOVA with post hoc Dunnett's comparisons (n = 3, $*p<0.05$ with a significant difference compared to controls) and using two-sample t-test (n=3, $^{\#}p<0.05$ between 3T3 cells and CFs). 3T3s, 3T3 cells; CFs, cardiac fibroblasts. There were also significant differences between 24, 48 and 72 h exposure time in all treated cells**.**

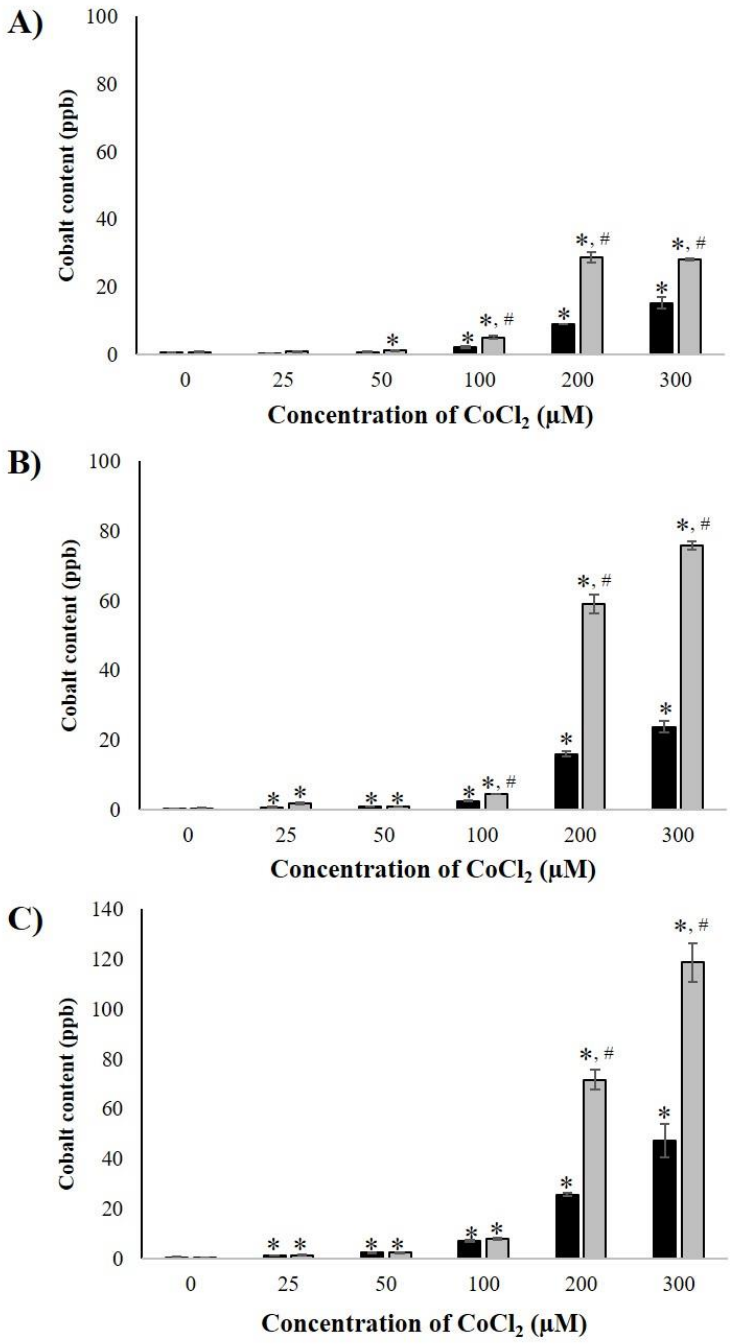

Figure 3-14 Comparison of cellular ion uptake in both 3T3s and CFs. Cells were exposed for (A) 24, (B) 48, and (C) 72 h to various concentration of $CoCl_2$, 0-300 µM. Intracellular levels in both 3T3 cells (black) and CFs (grey) increase linearly with the concentration of $CoCl_2$ and the duration of exposure time. Results are expressed as mean values ±SEM. Statistical analysis was carried out using one-way-ANOVA with post hoc Dunnett's comparison (n = 3, $*p<0.05$ with a significant difference to control) and using two-sample t-test (n=3, $^{\#}p<0.05$ between 3T3 cells and CFs).

3.3.8 Western blotting to evaluate the expression of potential target proteins in 3T3 cells and CFs treated with $CoCl_2$.

Western blotting was used to detect the effect of Co treatment on the presence of CaMKII (Total CaMKIIδ, phospho-CaMKII and oxidised-CaMKII), and ion transporters (DMT1 and Transient receptor potential (TRP; TRPM7 and TRPC6)). 3T3 cells and CFs were treated with 0, 0.1, 1, 10 and 100 µM $CoCl_2$ for 48 and 72 h. The cell lysates were analysed by SDS-PAGE (10% Tris-Glycine) based on 50 µg total protein/lane on the Bio-Rad Criterion Cell system, transferred to a PVDF membrane and then probed with all the target proteins. GAPDH (cat. No. Ab37168; 1:7500; Abcam, UK) was used as a loading control**.**

3.3.8.1 Expression of CaMKII

CaMKII is well known to modulate various mechanisms underlying cardiovascular dysfunction therefore it was of interest to check whether altered levels of this enzyme were evident following $CoCl_2$ treatment. We examined the effects of $CoCl_2$ on CaMKIIδ and ox-CaMKII and p-CaMKII expression in CFs. The data in Table 3-4, Figure 3-15, and Figure 3-16 show the expression of the proteins as a ratio of the optical density of the bands of the protein of interest / optical density of GAPDH. An increase in this ratio compared with control indicates increased expression. We tested the effects of $CoCl_2$ at concentrations of 0.1, 1, 10 and 100 µM for 72 h, and found that the expression of CaMKIIδ increased in a concentration dependent manner to a ratio of 3.38 ± 0.32, 3.91 ± 0.22, 3.35 ± 0.03 and 2.77 ± 0.08 fold at doses 0.1, 1, 10 and 100 µM, respectively compared with a ratio of 2.49 ± 0.03 in controls. The effects on CaMKIIδ expression were different after treatment with 100 µM of $CoCl_2$ at 48 h where the ratio decreased 2.66 ± 0.04 fold compared with 3.40 ± 0.23 in controls. The effects observed at 72 h showed a maximum up-regulation at 1 µM of $CoCl_2$, which was a ratio of 3.91 ± 0.22 fold compared with 2.49 ± 0.03 in controls.

For ox-CaMKII, results show significantly increased expression of ox-CaMKII only when cells were exposed for 72h to concentrations of $CoCl_2$ of 1, 10 and 100 µM. The maximum effects were observed at 10 µM of $CoCl_2$ for 72 h. Lastly, western blotting cannot determine the p-CaMKII expression in CF on both untreated and treated CFs. The p-CaMKII is not abundantly present in the primary CF. When there were no signal

or bands present, the test result is interpreted as negative. The cause of no bands can also arise due to many reasons related to antibody, antigen or buffer used. In this case, antigen from another source can be used to confirm whether the problem lies with the sample or with other factors. Whole heart homogenate was used as positive control to confirm the factor that might be cause any problem with the process by running in the same gel and membrane. Another reason for absence of visible bands is low concentration of protein or absence of antigen and in this experiment protein loading was increased up to 50 µg per lane. No band for p-CaMKII was observed.

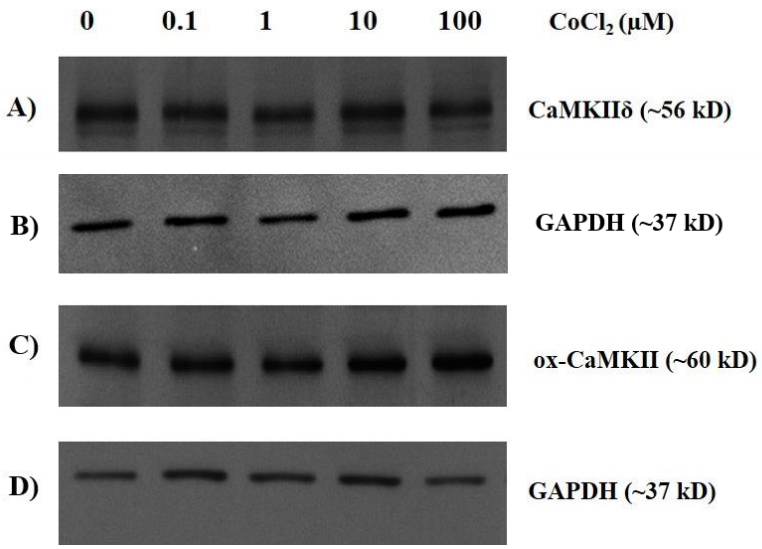

Figure 3-15 Effects of $CoCl_2$ on CaMKIIδ and ox-CaMKII expression after exposure in cardiac fibroblasts (CFs). Results of expression of (A) CaMKIIδ, (C) ox-CaMKII and (B and D) GAPDH **.** Cardiac fibroblasts were exposed to the different concentrations of $CoCl_2$ 0, 0.1, 1, 10 and 100 µM for 72 h **.**Total cell extracts were analysed by western blot for CaMKIIδ and ox-CaMKII with specific antibodies **.**CFs mean cardiac fibroblast, CaMKIIδ means Total-CaMKIIδ, ox-CaMKII means oxidised CaMKII**.**

Table 3-4 Quantitative analysis of CaMKIIδ and ox-CaMKII protein expression in cardiac fibroblasts (CFs) after treatment with Co. $CoCl_2$ treatment induced CaMKII and ox-CaMKII expression in cardiac fibroblasts (CFs) at 72 h. Protein expressions were determined by western blotting in cell lysates. CFs treated by $CoCl_2$ at various concentration (0, 0.1, 1, 10 and 100 μM) for different time points (48 and 72 h).

Sample	CaMKIIδ	ox-CaMKII
48 h		
$CoCl_2$ 0 μM	3.40 ± 0.23	2.25 ± 0.34
$CoCl_2$ 0.1 μM	3.13 ± 0.10	2.33 ± 0.30
$CoCl_2$ 1 μM	3.51 ± 0.16	2.41 ± 0.40
$CoCl_2$ 10 μM	3.23 ± 0.26	2.14 ± 0.44
$CoCl_2$ 100 μM	2.66 ± 0.04*	1.72 ± 0.28
72 h		
$CoCl_2$ 0 μM	2.49 ± 0.03	2.11 ± 0.02
$CoCl_2$ 0.1 μM	3.38 ± 0.32*	2.41 ± 0.17
$CoCl_2$ 1 μM	3.91 ± 0.22*	2.48 ± 0.05*
$CoCl_2$ 10 μM	3.35 ± 0.03*	2.81 ± 0.09*
$CoCl_2$ 100 μM	2.77 ± 0.08*	2.27 ± 0.10*

Data represent mean ± SEM and Statistical analysis was carried out using one-way-ANOVA with post hoc Dunnett's comparison (n = 3, *$p<0.05$ with a significant difference to untreated cells). h, hours; CaMKIIδ, Total-CaMKIIδ; ox-CaMKII, oxidised CaMKII. The expression values are shown as the ratio between the density values for the protein of interest and the density value of GAPDH. An increase in this ratio compared with the control value would indicate induction, and a decrease inhibition.

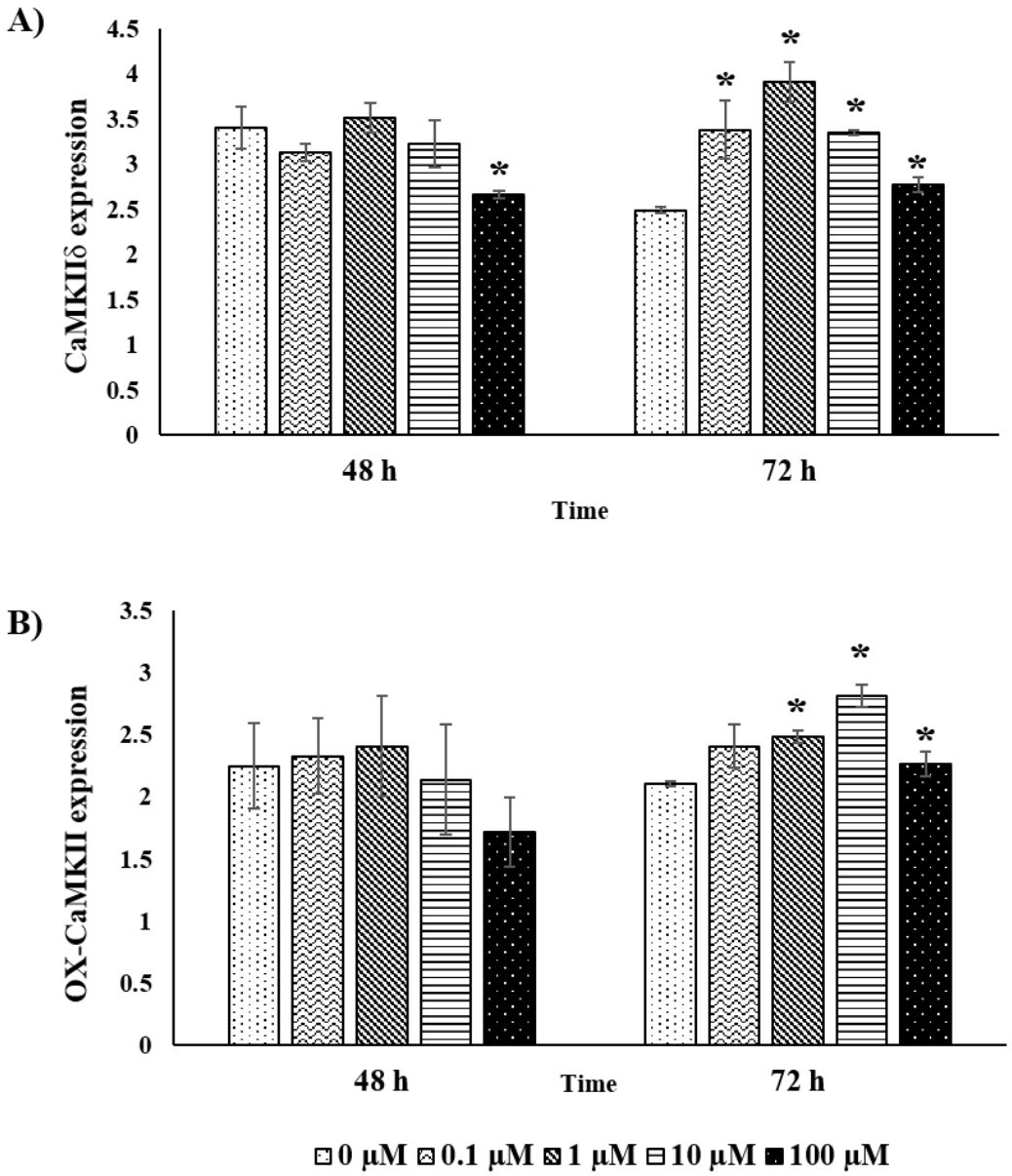

Figure 3-16 Relative expression of CaMKIIδ and oxidised-CaMKII (ox-CaMKII) in cardiac fibroblasts (CFs) after treatment with $CoCl_2$. Western blotting demonstrating the expressions of (A) Total-CaMKIIδ and (B) ox-CaMKII after treatment with $CoCl_2$ (0, 0.1, 1, 10 and 100 µM) for 48 and 72 h in both cardiac fibroblasts (CFs), compared with control groups. Statistical analysis was carried out using one-way-ANOVA with post hoc Dunnett's comparison ($n \geq 3$, $*p<0.05$, treatment group vs. control group). Expression values are shown as the ratio of the density values of the protein of interest and the density value of GAPDH. An increase in this ratio compared with the control value would indicate induction, and a decrease inhibition.

3.3.8.2 Expression of potential Co transporters.

We investigated whether Co treatment caused changes in expression of the transporter DMT1 in CFs using western blotting. CFs were treated with various concentrations (1, 10 and 100 µM) of $CoCl_2$ at different times (48 and 72h). Results are in Figure 3-17 and Table 3-5, and they demonstrated that $CoCl_2$ down-regulated DMT1 expression as assessed following normalisation with the internal control (GAPDH). Expression of all transporters of interest are expressed as the ratio of the density of the transporter compared with that of GAPDH. Protein expression of DMT1 was significantly decreased to 0.73± 0.11 and 0.69± 0.08 after treatment with 1 and 10 µM $CoCl_2$ for a 48 h period, respectively (see Table 3-5). Having found that DMT1 expression in CFs was down-regulated by Co treatment, its expression in the 3T3 cell was not determined after Co treatment.

Next, western blots were carried out to investigate the effect of $CoCl_2$ on the expression levels of TRPM7 and TRPC6 in CFs, and it was found that both TRPC6 and TRPM7 expression is much higher after Co treatment than in untreated CFs. The expression of both TRPC6 (at Co concentrations of 1, 10 and 100 µM after both 48 and 72 h) and TRPM7 (at Co concentrations of 0.1, 1 and 10 µM after both 48 and 72h) are significantly increased. Having discovered the upregulation of TRPC6 and TRPM7 in CFs after Co treatment, their expression in the 3T3 cells and CFs was compared after Co treatment.

Co treatment of CFs with 1, 10 and 100 µM, at 48 h significantly enhanced the expression TRPC6 to 1.18 ± 0.05, 1.21 ± 0.07 and 1.30 ± 0.11, respectively compared with 1.09 ± 0.03 in the control. Similarly, at 72 h in CFs also enhanced the expression of TRPC6 by 0.93 ± 0.00, 1.01 ± 0.08 and 1.11 ± 0.1, repectively compared with 0.72 ± 0.11 in the control. Whereas in the 3T3 cell line, $CoCl_2$ significantly down-regulated the expression of TRPC6. Expression was 0.43 ± 0.02 at 100 µM for 48 h, 0.47 ± 0.03 and 0.41 ± 0.01, at concentrations of 10 and 100 µM for 72 h treatment, as shown in Table 3-5. Controls were 0.59 ± 0.04 at 48h and 0.52 ± 0.01 at 72h.

Co treatment of CFs also significantly enhanced expression of TRPM7 to 0.63 ± 0.01, 0.61 ± 0.00, 0.59 ± 0.01 and 0.39 ± 0.03 at concentrations of 0.1, 1, 10 and 100 µM

after 48 h treatment, respectively compared with 0.50 ± 0.00 in the control, and 0.54 ± 0.01, 0.64 ± 0.00 and 0.57 ± 0.01 compared with the control (0.50 ± 0.00) at concentrations of 1, 10 and 100 µM after 72 h, respectively. On the other hand, Co treatment of 3T3 cells show different results when compared with the CF data. In contrast, the expression of TRPM7 in 3T3 cells was diminished by Co treatment 0.26 ± 0.02 at 100 µM compared with 0.41 ± 0.01 in the control after 48 h and 0.40 ± 0.00, 0.40 ± 0.00, 0.45 ± 0.02 and 0.39 ± 0.00 at concentrations of 0.1, 1, 10 and 100 µM after 72 h, respectively compared with 0.53 ± 0.03 in the control, as shown in Table 3-5 and Figure 3-18.

It is noted that the expression of TRPC6 and TRPM7 was markedly up-regulated following presence of $CoCl_2$ in CFs, whereas the expression was markedly down-regulated for both proteins in 3T3 cells especially at high concentrations (10 and 100 µM) of $CoCl_2$. Low concentrations of $CoCl_2$ (0.1 and 1 µM) can affect the cardiac fibroblasts and induce expression of TRPC6 and TRPM7 whereas in 3T3 cells there is no effect with the low $CoCl_2$ doses (see Figure 3-19).

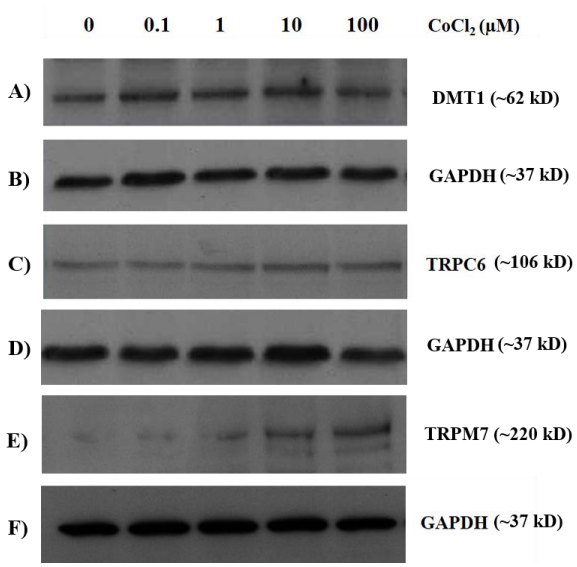

Figure 3-17 Effects of $CoCl_2$ treatment on Co transporter (DMT1, TRP channels (TRPC6 and TRPM7)) expression in CFs. Results of expression of **(**A**)** DMT1, **(**C**)** TRPC6**,**)E (TRPM7 and)B, D and F(GAPDH**.** Protein expressions were determined by western blotting**.** Cardiac fibroblasts were exposed to the different concentrations of $CoCl_2$ **(**0, 0**.**1, 1, 10 and 100 µM**)** for 72 h**.** Total cells extracts were analysed by western blot for Co transporter with specific antibodies**.** CFs cardiac fibroblasts, Divalent metal transporter **(**DMT1**)**, TRPC6 means Transient receptor potential/canonical receptor subtype 6; TRPM7 means Transient receptor potential/melastatin receptor subtype 7**.**

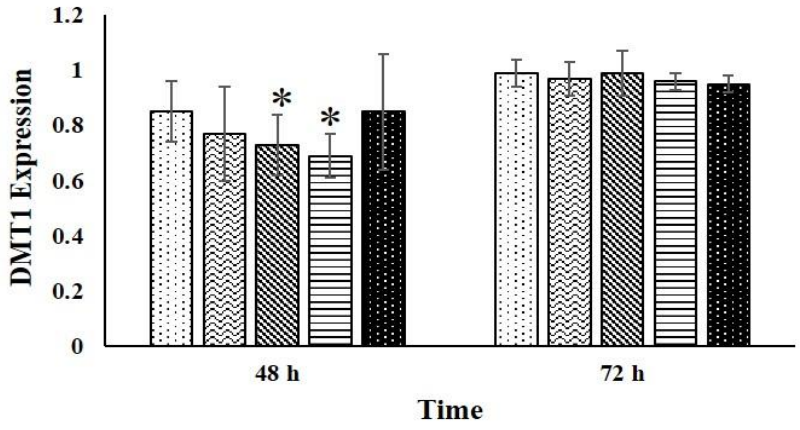

Figure 3-18 Relative expression of DMT1 in cardiac fibroblasts (CFs) after treatment with $CoCl_2$. Western blotting demonstrating the expressions of DMT1 after treatment with $CoCl_2$ (0, 0.1, 1, 10 and 100 µM) for 48 and 72 h in cardiac fibroblasts (CFs), compared with control group. Statistical analysis was carried out using one-way-ANOVA with post hoc Dunnett's comparisons ($n \geq 3$, $*p<0.05$, treatment group vs. control group). Expression was expressed as the ratio of the density for DMT1 compared with the density value of GAPDH.

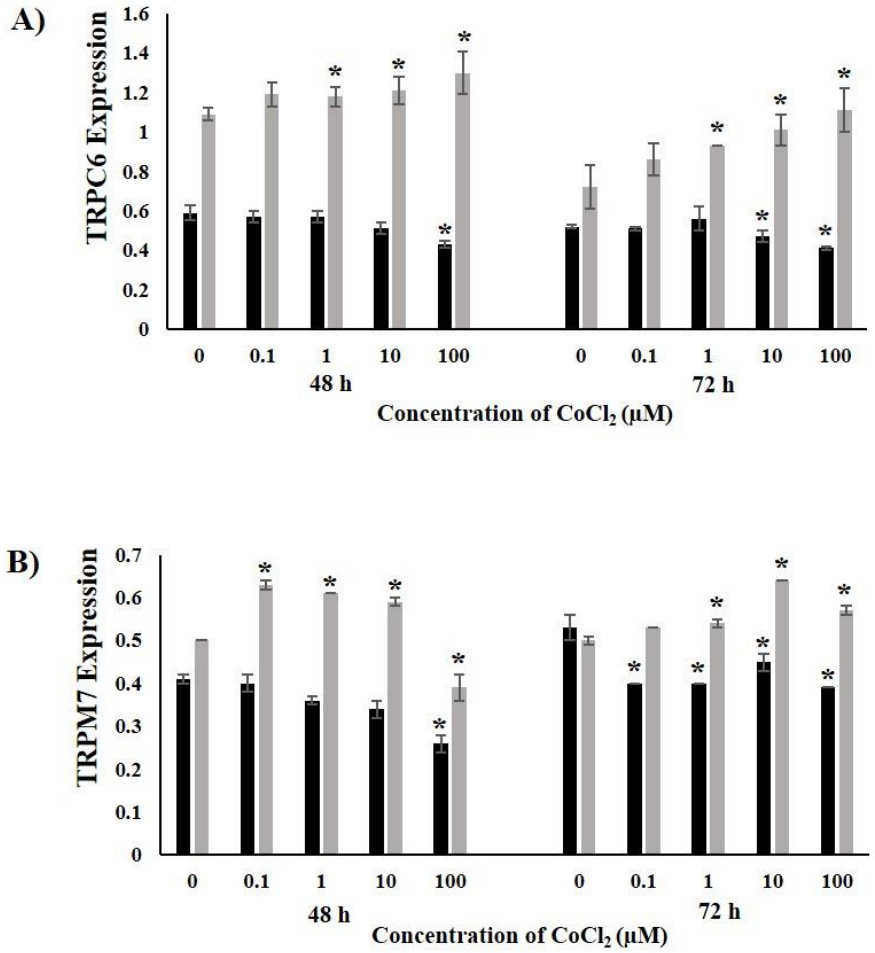

Figure 3-19 Relative expression of TRPC6 and TRPM7 in Cardiac fibroblasts (CFs) and 3T3 cell line (3T3s) after treatment with Co for 24 and 72 h. Expression is expressed as optical density of the transporter band of interest over the optical density of GAPDH band. Western blotting demonstrating the expressions of (A) TRPC6 and (B) TRPM7 after treatment with $CoCl_2$ (0, 0.1, 1, 10 and 100 µM) for 48 and 72 h in both cell types, CFs (grey) and 3T3 cells (black), compared with control groups. (Mean ± SEM) Statistical analysis was carried out using one-way-ANOVA with post hoc Dunnett's comparison ($n \geq 3$, *$p<0.05$, treatment group vs. control group). There were significant differences between the 3T3 cells and CFs for each protein expression result using two-sample t-test, n=3, $p<0.05$.

Table 3-5 Quantitative analysis of DMT1, TRPC6 and TRPM7 protein expression after Co treatment in CFs and 3T3 cells. $CoCl_2$ treatment effect on DMT1, TRPC6 and TRPM7 expression in cardiac fibroblasts (CFs) and 3T3 cell line (3T3s). Protein expressions were determined by western blotting. Both CFs and 3T3s treated by $CoCl_2$ in various concentration (0, 0.1, 1, 10 and 100 µM) at different time points (48 and 72 h).

Sample	DMT1		TRPC6		TRPM7	
	CFs	3T3s	CFs	3T3s	CFs	3T3s
48 h						
$CoCl_2$ 0 µM	**0.85 ± 0.11**	**n.d.**	**1.09 ± 0.03**	**0.59 ± 0.04**	**0.50 ± 0.00**	**0.41 ± 0.01**
$CoCl_2$ 0.1 µM	**0.77± 0.17**	**n.d.**	**1.19 ± 0.06**	**0.57 ± 0.03**	**0.63 ± 0.01***	**0.40 ± 0.02**
$CoCl_2$ 1 µM	**0.73± 0.11***	**n.d.**	**1.18 ± 0.05***	**0.57 ± 0.03**	**0.61 ± 0.00***	**0.36 ± 0.01**
$CoCl_2$ 10 µM	**0.69± 0.08***	**n.d.**	**1.21 ± 0.07***	**0.51 ± 0.03**	**0.59 ± 0.01***	**0.34 ± 0.02**
$CoCl_2$ 100 µM	**0.85 ± 0.21**	**n.d.**	**1.30 ± 0.11***	**0.43 ± 0.02***	**0.39 ± 0.03***	**0.26 ± 0.02***
72 h						
$CoCl_2$ 0 µM	**0.99 ± 0.05**	**n.d.**	**0.72 ± 0.11**	**0.52 ± 0.01**	**0.50 ± 0.01**	**0.53 ± 0.03**
$CoCl_2$ 0.1 µM	**0.97 ± 0.06**	**n.d.**	**0.86 ± 0.08**	**0.51 ± 0.01**	**0.53 ± 0.00**	**0.40 ± 0.00***
$CoCl_2$ 1 µM	**0.99 ± 0.08**	**n.d.**	**0.93 ± 0.00***	**0.56 ± 0.06**	**0.54 ± 0.01***	**0.40 ± 0.00***
$CoCl_2$ 10 µM	**0.96 ± 0.03**	**n.d.**	**1.01 ± 0.08***	**0.47 ± 0.03***	**0.64 ± 0.00***	**0.45 ± 0.02***
$CoCl_2$ 100 µM	**0.95 ± 0.03**	**n.d.**	**1.11 ± 0.11***	**0.41 ± 0.01***	**0.57 ± 0.01***	**0.39 ± 0.00***

Data represent mean ± SEM and Statistical analysis was carried out using one-way-ANOVA with post hoc Dunnett's comparisons (n = 3, *$p<0.05$ with a significant difference to untreated cells). DMT1, Divalent metal transporter; TRPC6, Transient receptor potential/canonical receptor subtype 6; TRPM7, Transient receptor potential/melastatin receptor subtype 7; n.d = Not determined. Expression of the transporters are expressed as a ratio of the optical densities of the transporter bands compared to the optical density of GAPDH bands.

3.3.9 Summary of major findings

In this chapter, the *in vitro* effects of Co on cell viability, cell proliferation, and cell morphology, and its intracellular uptake were measured, and immunoblotting of CaMKII, DMT1 and TRP channel (TRPC6 and TRPM7) proteins carried out in both the standard 3T3 cell line and primary cardiac fibroblasts (CFs). The main findings of this study are:

- Primary cardiac fibroblasts were identified based on their spindle shape combined with positive staining for the fibroblast marker vimentin and the absence of staining for endothelial and smooth muscle cell markers.
- The acute or short term toxicity showed that the $CoCl_2$ was toxic in a time- and dose- dependent manner after treatments at 48 and 72 h of both cell types as measured by cell viability and cell morphology.
- High concentrations of $CoCl_2$ caused different effects on cell proliferation (by BrdU assay) between both cell types. The assessment of proliferation suggested that CFs were more sensitive to $CoCl_2$ treatment than 3T3s.
- Low concentrations of $CoCl_2$ (0-25 µM) did not seem to have an effect on viability for either 3T3 cells or CFs after 48 and 72h exposure.
- Uptake of $CoCl_2$ into CFs was greater than into the 3T3 cells, and this may at least partly explain the difference in toxicity between the two cell types.
- CaMKII protein expression was affected in CFs by $CoCl_2$. Expression of CaMKII was increased and that of oxidised CaMKII increased.
- DMT1 protein expression was affected in CFs by $CoCl_2$. DMT1 expression was decreased.
- TRP channel (TRPC6 and TRPM7) protein expression was affected in CFs and 3T3s by $CoCl_2$. Of particular relevance was induction of expression of both TRP channel proteins in CFs, but not in 3T3 cells, where the expression of TRPs were decreased at high concentrations of Co.

3.4 Discussion

One of the most significant orthopaedic issues in recent years has been the adverse effects of metal ion release from CoCr alloy hip implants with a metal-on-metal (MoM) articulating surface. Since 2007 several prominent device manufacturers have been forced to issue recalls and withdraw their MoM implants including Depuy, Smith and Nephew and Stryer Orthopaedics. Use of MoM devices was at its peak in 2006, but by 2013 they accounted for only about 1.1% of hip implants inserted (Corten and MacDonald, 2010; Jiang *et al.*, 2011; Posada *et al.*, 2015). Although, in 2010 the Depuy ASR MoM implant was withdrawn from the market, and recalls have taken most of the defective designs off the market, it is estimated that there are still 49,000 patients with these implants in situ in the UK alone (NHS Choices, 2012).

These arthroprosthetic patients can be affected by an internal source of Co exposure, and are prone to the Co-induced symptoms of haematological, cardiac, thyroid, hepatic and neuropathic conditions. This problem has given rise to the term arthroprosthetic Cobaltism in which the most commonly observed symptoms are cardiomyopathy, hypothyroidism and neurological problems (Tower, 2010; Mao, Wong and Crawford, 2011; Zywiel *et al.*, 2013). Cardiomyopathy was recognised as an adverse effect of Co in Canada in the 1960s when it caused the deaths of at least 20 people after a brewing company added $CoSO_4$ or $CoCl_2$ to beer as an antifoaming stabiliser (Morin and Daniel, 1967). Post-mortem examination showed Co in the myocardium (Machado, Appelbe and Wood, 2012). So, it is therefore important to understand and attempt to minimise or prevent toxic events caused by the metal ion release. This is especially relevant for Co, which tends to remain mobile, as there are greater Co concentrations than expected in blood, and Co in remote organs has been reported (Afolaranmi *et al.*, 2012).

Much of the work in this thesis was carried out in cell culture in either 10 or 20 % FBS. Tvermoes *et al* (2015) showed that 95% of the Co at this concentration is bound to serum proteins, primarily albumin, in human volunteers. It is therefore likely to be extensively bound in our *in vitro* experiments. Human plasma contains approximately 7.6% proteins of which albumin is the most predominant (Martini *et al.*, 2015). The Co is likely to be highly bound both in culture medium, and in the rat blood circulation

in vivo, and the fraction free will be less than 8% of the total serum concentration (Nandedkar *et al*, 1972).

To be sure that the cells we isolated were CFs a cardiac marker should be used to detect the type of cells. However, the fibroblast cell population is still the least characterised cell type in the heart compared with other cell populations, and no specific markers of cardiac fibroblasts exist. However, numerous studies of isolated fibroblasts have been conducted, and various molecular tools (Immuhistochemistry, immuno blotting and RT-PCR) have been used to identify them, but most markers are either nonspecific or insufficiently sensitive. In this experiment, the main method for identifying fibroblasts is by vimentin marker. Isolated primary cardiac fibroblasts positively stained with this marker. Vimentin is recognised as a non-specific marker of fibroblasts.

Vimentin is a protein that is present in the intermediate filament proteins, and has been the most widely used fibroblast marker. However, vimentin antibody can positively detect this protein in various cells. For example, the entire endothelial lineage also expresses vimentin. Additionally, smooth muscle cells, myoepithelial cells, pericytes, and neurons contain intermediate filaments and therefore also express vimentin (Camelliti, Borg and Kohl, 2005). In this case, we used markers that might be specific for the related cardiac cell types, a smooth muscle cell marker and an endothelial cell marker. Testing the isolated primary cardiac fibroblasts with both specific markers for the other cell types found that primary cardiac fibroblast were negative for endothelial cell and smooth muscle cell markers. They did not express smooth muscle cell (alpha actin) or cardiac endothelial cells marker (CD31 and Von Willebrand Factor (VWF)). Those specific markers are positively expressed on smooth muscle cells and endothelial cells (Skalli *et al.*, 1986; Bachetti and Morbidelli, 2000). Thus, we are confident that the cells that we isolated were indeed cardiac fibroblasts.

Following the isolation of primary cardiac fibroblasts, they were used to study short term cytotoxicity comparing the toxic responses of Co with a standard fibroblast cell line (3T3 cell line). In the current study, it has been shown that $CoCl_2$ was toxic to both 3T3s and CFs in a time- and dose- dependent manner. The results obtained show that the IC_{50} values of $CoCl_2$ on both 3T3s and CFs after 48 and 72 h exposure, as

determined by the MTT and CV assays, have similar values that are between 300 and 400 µM $CoCl_2$ (see Table 3-1, Table 3-2 and Figure 3-7).The high $CoCl_2$ concentration proved to be cytotoxic for both 3T3s and CFs. In comparison, the $CoCl_2$ IC_{50} values measured by NR assay after 48 and 72 h exposure were more than 700 µM. The MTT and CV assays are more sensitive than the NR assay in the detection of the cytotoxicity. This was especially the case for the MTT assay; this metabolic assay was more sensitive than the NR assay, indicating that failure to maintain metabolic homeostasis could drive the cell to death.

From literature data, the IC_{50} values of Co cytotoxicity in the current study are similar to many of the values in the animal cells in previous *in vitro* studies(Yang *et al.*, 2004; Mahey *et al.*, 2016). Human submandibular gland cells (HSG) show Co induced cytotoxicity and fragmentation of chromatin in both a time and dose dependent manner. Co also inhibits Bcl-2 protein expression on human B lymphoblastoid cells, and this is a protein family involved in the regulation of apoptotic cell death (Tsujimoto, 1998). $CoCl_2$ also induced apoptosis of rat pheochomocytoma cells (PC12) involving the mitochondria-mediated pathway(Zou *et al.*, 2001). Moreover, Akita et al report that $CoCl_2$ induces cytotoxicity and cell death and DNA ladder formation in human submandibular gland cells (HSG) cells in both a dose and time dependent manner by suppression of Bcl-2 expression and mRNA (Akita *et al.*, 2007). Furthermore on other cell types (glia cells, epithelial cells, and cervical cells), $CoCl_2$ also causes cytotoxicity, with IC_{50} values ranging between 100-500 µM (Kim *et al.*, 2003; Yang *et al.*, 2004; Fleury *et al.*, 2006; Bresson *et al.*, 2013). The range of some of the IC_{50} found in several literature papers is tabulated (see Table 3-6).

To understand why this difference in the sensitivities of the 3 assays was observed in our experiments, it is important to appreciate the differences between the viability measurements made by the three assays. Appendix 2 directly compares IC_{50} values of 3T3s and CFs in all three assays by combined assay. Comparing three assays for cytotoxicity testing, both the MTT and the CV assays have similar sensitivities to detect the effect of Co, whereas the NR assay shows less sensitivity for Co effect. So the sensitivity of both of MTT and CV assays are significantly different when compared with the response of NR assay.The MTT assay detects the metabolic activity

Table 3-6 The IC_{50} values of various cell types after cobalt chloride exposure.

IC_{50} values	Assay	Cell types	References
~ 200 µM, 24 h	WST-1 (Reductase activity)	Human submandibular gland cells (HSG)	(Akita *et al.*, 2007)
470 µM, 24 h	MTT assay (Reductase activity)	Human cervical cancer HeLa cells	(Kim *et al.*, 2003)
~ 440 µM, 72 h	CellTiter-Glo assay (ATP measurement)	Human lung cells (BEAS-2B: epithelial cell)	(Ortega *et al.*, 2014)
170 µM, 72 h	MTT assay (Reductase activity)	Human osteoblast-like cells (MG-63)	(Fleury *et al.*, 2006)
400 µM, 24 h	MTT assay (Reductase activity)	C6 rat glioma cells	(Yang *et al.*, 2004)
500 µM, < 36 h	CV assay	Rat pheochomocytoma cells (PC12)	(Zou *et al.*, 2001)

of the cells during reduction of the tetrazolium dye. It is dependent not only on reductase activities, but also on availability of NADH/NADPH. Whereas, NR binds to the lysosomes in the cells, and indicates the cell number directly without metabolism, and CV permeates the lipid membranes, cross links the proteins of cell membranes, and stains the protein and DNA in the cells. Perconti and co-workers have reported that mitochondrial dysfunction might be one of the pathways that is involved in Co toxicity (Perconti *et al.*, 2012). In this context Asawary and Karian assessed the direct impact of $CoCl_2$ induced oxidative stress on cardiac mitochondria. $CoCl_2$ treatment of the interfibrillar and the subsarcolemmal membrane of isolated mitochondria had a prominent effect, by increasing the level of lipid peroxidation and decreasing levels of reduced glutathione, which confirmed the induction of oxidative stress in the process (Ayswarya and Kurian, 2016). The reduction of MTT in many cell types occurs predominantly in the mitochondria (Karovic *et al.*, 2007; Ayswarya and Kurian, 2016). In the former study the mitochondria appeared to be a main target site for Co toxicity, and the authors showed depletion of the mitochondrial membrane potential and release of apoptogenic factors (Karovic *et al.*, 2007). If this organelle is specifically targeted by Co that may account for the particular sensitivity of the MTT assay. Furthermore, oxidative conditions generated by Co may deplete availability of NADH/NADPH required for MTT reduction in the cells. It is unclear what leads to the marked sensitivity of the CV assay for Co toxicity. CV detects the toxicity of Co, by binding

to proteins and DNA of attached therefore viable cells (Feoktistova, Geserick and Leverkus, 2016).

We further compare the cytotoxicity results with cell staining visualised by the Zeiss Axio Imager Microscope images. The cell staining with CFDA and PI for live and dead cells, showed that there was an increasing number of red cells in the samples treated with $CoCl_2$. This links to the metabolic data from cells treated with this ion, after incubation with high concentrations of $CoCl_2$ for longer incubation periods (48 and 72 h). The detrimental effects of $CoCl_2$ were observed in both 3T3 cells and CFs.

The current experiments show evidence that Co induced apoptosis in both 3T3 and CF cells. Using Phalloidin- FITC to stain actin, the untreated cells show normal distribution of actin within the cells where it can be observed surrounding the nuclei of cells. In contrast, the treated cells showed a different distribution where the actin is concentrated around the border of the cells, and is not surrounding the nucleus. Moreover, the treated cells had blebs on their membranes, especially at 500 µM Co exposure. Cell death processes may often show distinct characteristics like blebbing or vacuolisation of the cytoplasm. The blebs represent the process of cell apoptosis and are caused by localised decoupling of the cytoskeleton from the plasma membrane (Fackler and Grosse, 2008). Further experiments to prove the occurrence of apoptosis would include analysis of DNA degradation (TUNEL and DNA damage assays), caspase detection assays (for example, caspases 3 and 7), mitochondrial permeability assays, Annexin V detection assay and also an integrated microfluidic cell array (Martinez, Reif and Pappas, 2010; Wlodkowic *et al.*, 2011).

Important effects of Co could also be caused by metal-induced activation of hypoxia-inducible factor (HIF), which is present in almost all animal cells. For example, $CoCl_2$ treatment at a range of 50-750 µM induced apoptotic death of cardiomyocytes and other cells though hypoxia-inducible factor-1-alpha(HIF-1α)-dependent stabilisation of p53 protein (Long *et al.*, 1997; Yao *et al.*, 2008; Naito *et al.*, 2010; Yue *et al.*, 2012; Sajjad *et al.*, 2014). The changes in cell morphology we observed do not prove the presence of apoptosis and the results might also be interpreted as autophagy (Romano *et al.*, 2009; Bauckman, Owusu-Boaitey and Mysorekar, 2015). Autophagy is said to

be a pro-survival mechanism based on the auto-digestion of the cell and it is strongly linked to lysosomes (Tait, Ichim and Green, 2014), which in turn, store metal ions and play an important role in iron homeostasis (Kurz, Terman and Brunk, 2007). Further experiments to prove the occurrence of autophagy would include analysis of transmission electron microscopy, half-life assessments of long-lived proteins, detection of LC3 maturation/aggregation, fluorescence microscopy, and colocalisation of mitochondrial- or endoplasmic reticulum–specific markers with lysosomal proteins (Tasdemir *et al.*, 2008). The results assembled in the current experiments are not sufficient to conclude the mechanism(s) responsible for toxic response of Co ions in terms of apoptosis or autophagy.

The Bromodeoxyuridine (BrdU) Elisa assay is specific for detection of newly synthesised DNA of actively dividing cells (Figure 2-5), and it was used to compare cell proliferation rates after exposure to Co in both cell types (see Figure 3-8). There were different effects of Co on BrdU cell proliferation. Considering the data between the two cell types, the assessment of proliferation suggested that CFs were more sensitive to $CoCl_2$ treatment than 3T3 cells. In the former, after either 48 h or 72 h exposure to Co there was ~80% reduction in proliferation with 25 µM $CoCl_2$ and almost total inhibition of proliferation following exposure to 100-150µM $CoCl_2$, whereas 3T3 cells showed a slow decline in proliferation, occuring over the entire time period. The BrdU showed reproducible results with IC_{50} values for $CoCl_2$ in the range of 200-300 µM and ~20 µM on 3T3 cells and CFs, respectively. The IC_{50} proliferation values from the BrdU assay, show that on cardiac fibroblasts Co has a 10-fold greater effect than on 3T3 cells.

Inhibition of proliferation has been reported with several cell types following exposure to Co. For example, in human osteoblasts, Anissian and coworkers found that Co ions caused a dose dependent decrease in cell proliferation as measured by ^{3}H thymidine incorporation (Anissian *et al.*, 2002). Akbar and co-workers studied the effects of Cr(VI) and Co(II) on human lymphocytes, and found that cell proliferation and function (by cytokine release) were affected by nontoxic concentrations (Akbar, Brewer and Grant, 2011). The mechanism(s) responsible for Co induced cellular toxicity is/are likely to involve redox reactions. Co, which is redox active, can generate

reactive oxygen species (ROS), eg. superoxide radicals (O_2^-) and the hydroxyl radical ($^{\cdot}OH$) via a Fenton-driven reaction with hydrogen peroxide (H_2O_2). ROS induce oxidative damage to lipids, protein and also DNA (Leonard *et al*. 1998; Tewari *et al*. 2002; Fleury *et al*. 2006; Valko *et al*. 2006; Battaglia *et al*. 2009). (see Figure 3-20)

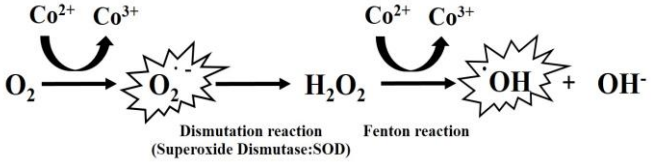

Figure 3-20 Schematic representation of possible mechanism of reactive oxygen specie generation from Co-mediated reactions.

There are some studies reporting that several redox active orthopaedic metal ions, notably Ni(II), Cr(VI) and Co(II), inhibit DNA repair, and alter signal transduction and gene expression on BALB/3T3 mouse fibroblast cells (Beyersmann, 2002; Chen and Shi, 2002; Witkiewicz-Kucharczyk and Bal, 2006). The observations of *in vitro* toxicity may have relevance where ions are released from metal devices. For example, Evans *et al* concluded that Co is highly toxic and released Co ions from CoCr alloys induce cellular damage in primary lines of fibroblast cells from the musculo-skeletal tissue of newborn rats (Evans and Thomas, 1986; Evans, 1994). Inhibition of proliferation in patients with long term exposure to Co ions may also occur and exposure is likely to be to lower Co concentrations that used in this study in this chapter. This will be discussed in chapter 4.

The 3T3 cells were more tolerant of $CoCl_2$ than CFs in terms of proliferation and that was further studied by measuring the intracellular Co uptake in both cell types by ICP-MS. The result showed that with increasing medium concentration of $CoCl_2$, intracellular Co concentration in both 3T3s and CFs increased, to a range of between 0-50 ppb and 0-120 ppb in both cell types, respectively. Uptake into CFs was greater than into the 3T3 fibroblasts, and at a concentration of 200 µM for example, the uptake into CFs is 3-fold higher at 24h, 4-fold higher at 48h and 3-fold higher at 72h than that into 3T3 cells. The higher uptake into CF cells will contribute considerably to the observed increased sensitivity of CF cells to Co induced inhibition of proliferation, although the responses to Co in terms of viability do not appear to be different between the two cell types, and may be induced by a different mechanism. Co may act at the

cell membrane to decrease viability, and thus the effect might be independent of uptake.

The BrdU proliferation assay measures DNA synthesis at the G1/S Phase (Begg *et al.*, 1985). Co has been reported to delay the progression of the G2/M phase in mouse embryonic stem cells(Lee *et al.*, 2013). It is plausible that Co could prevent the access of daughter cells to the next mitotic process due to numerous dividing cells caught into the G2/M stage. This could lead to a gradual decline in the number of daughter cells reinitiating the cell cycle, which could explain why Co could lead to inhibition of the proliferation but not to cell death, as demonstrated by the viability assays in both cell lines. The increased accumulation of intracellular Co in CFs might result in a large impact over cell proliferation in this instance.

From our data, cardiac cells are more sensitive to the effects of Co on proliferation. The effect of Co on DNA synthesis measured in this way may reflect nuclear toxicity, whereas the effects on cell viability measures a cytoplasmic/ membrane toxic effect. Although, we do not know the mechanism(s) involved Co may be more toxic to nuclear fractions in CFs than 3T3 cells.

Here we review the existing literature on mechanisms of Co cardiotoxicity and examine selected proteins that may be involved in Co transport and toxicity. In the present study this has been investigated *in vitro* with respect to cardiotoxicity using primary cultures of adult rat cardiac fibroblasts using immunoblotting to detect alterations in protein expression of key players that may be involved in cobalt transport (DMT and TRP channels) and cardiac dysfunction (CaMKII).

Firstly, CaMKII expression and activation via oxidation was determined by immunoblotting. CaMKII is critically involved in regulating Ca^{2+} homeostasis. CaMKII activation requires Ca^{2+}/CaM binding as an initiating step. Thus, the extent of CaMKII activation within a cell is likely to be at least partly dependent on local CaM concentrations, as has been proposed in cardiac myocytes (Saucerman and Bers, 2008). The role of the regulatory domain to CaMKII function is so integral, it is not surprising to discover that the known isoforms of mammalian CaMKII have nearly identical primary structure within the regulatory domain (Erickson, 2014). CaMKII

represents a vital key protein in the management of cardiac physiology and pathology (Erickson, 2014). It has been shown to contribute to a remarkably wide variety of cardiac pathologies, for example heart failure (HF). High expression levels of CaMKII are an established contributor to pathologies such as cardiac remodeling, and is widely thought to directly promote arrhythmia and contractile dysfunction during heart failure.

We found a significantly higher level of expression of CAMKIIδ and ox-CaMKII after Co treatment in CFs for 72 h, whereas within 48 h, the expression of the CaMKII isoform remained unchanged. However, we could not detect a band when membranes were probed with antibodies to phosphorylated CaMKII, which is one of the activated CaMKII forms. CaMKII is known to be a regulator of gene expression in cardiac cells (Ramirez *et al.*, 1997) and other cell types (Nghiem *et al.*, 1994; Yoshida *et al.*, 1995; Higuchi *et al.*, 1996; Wang *et al.*, 1996). Moreover, Ersilia showed evidence that selective inhibition of CaMKII expression resulted in the reduction of cardiac hypertrophy both in *in vitro* and *in vivo* models. Both acute and chronic manifestations of major heart diseases involve alterations in CaMKII. We hypothesised that if Co was damaging the heart cells, then the CaMKII system would be induced and activated (Cipolletta *et al.*, 2015). According to the results of our work Co induces increased expression of CaMKII *in vitro* (and *in vivo* after treatment of the rats) (see Chapter 5). Although the results showed significant changes, the changes observed in CaMKII may not be biologically significant compared with untreated cells. In studies in human tissue, which was obtained from patients undergoing orthotopic heart transplantation due to end-stage heart failure, an approximately 2-fold increase CaMKIIδ was reported in the failing human myocardium and a 3-fold increase in human heart failure (Hoch *et al.*, 1999; Kirchhefer *et al.*, 1999).

The mechanism of the cellular uptake of Co is not clear at present, and Colognato et al have suggested that both passive diffusion and receptor-mediated endocytosis are potential mechanisms in addition to specific transporter proteins (Colognato *et al.*, 2008). Moreover, other cellular transporter molecules, such as the transmembrane ionotropic receptor P2x7, and the divalent metal transporters especially DMT1, are suspected to be involved in Co uptake. The latter transporter, DMT1, plays a key role

in iron uptake by cardiac myocytes (Link, Pinson and Hershko, 1985; Tsushima *et al.*, 1999), and may also be important for Co transport.

Transporters likely to be important for Co transport are also likely to transport essential metals *in vivo* eg. iron. For example, DMT plays an important role in the efficacy of metal transport for Cd^{2+}, Fe^{2+}, Co^{2+} and Mn^{2+}, and also to a lesser extent for Zn^{2+}, Ni^{2+} and Va^{2+} (Gunshin *et al.*, 1997). This protein is normally used for iron (Fe^{2+}) transport, and this has been shown for example in duodenal enterocytes, in erythroid precursor cells and in the endosomal membrane (Fleming *et al.*, 1998; Mackenzie *et al.*, 2007; Ehrnstorfer *et al.*, 2014; Wolff *et al.*, 2014; Yanatori *et al.*, 2015).

Previous studies discussed the ubiquitin-dependent regulation of DMT1, and the role of the E3 ubiquitin-protein ligase Nedd4 family, Ndfip1 and Ndfip2 particularly, in this process (Foot *et al.*, 2016). Ubiquitination is well known for its role in regulating ion channels and transporters (MacGurn, Hsu and Emr, 2012). Howit and coworkers reported that the level of expression of DMT1 is regulated by the Ndfip1 level. Ndfip1 is an adaptor protein that recruits E3 ligases to ubiquitinate target proteins. When human neuronal cells were exposed to Fe and Co, Ndfip1 was upregulated (Howitt *et al.*, 2009) (Figure 3-21). Moreover, *in vitro* studies conducted on CHO cells stably transfected with Myc-tagged DMT1, overexpression of both Ndfip1 and Ndfip2 has lowered DMT1 activity (Foot *et al.*, 2008). $Ndfip2^{-/-}$ knockout female mice also showed an increase in DMT1 expression in the liver, with no change in male mice (Foot *et al.*, 2016).

Our results in cardiac fibroblasts demonstrate that DMT1 expression level decreased after $CoCl_2$ exposure for 48h. This might happen through the action of Ndfip regulators, which may interact with Co. Further evidence suggesting the involvement of DMT1 in Co uptake in CFs comes from the western blotting (Table 3-5).

In addition, Co, as a divalent ion, may share a calcium channel as one of the possible uptake routes (Simonsen, Harbak and Bennekou, 2012). Co has a similar structure to Ca^{2+} and Mg^{2+}. Co has the same hexagonal structure and coordinate with six water molecules in their first hydration shell, when their oxidation number is 2+ (Cullis and Verkleij, 1979; Guskov and Eshaghi, 2012). In contrast to the former, Co (II) may also

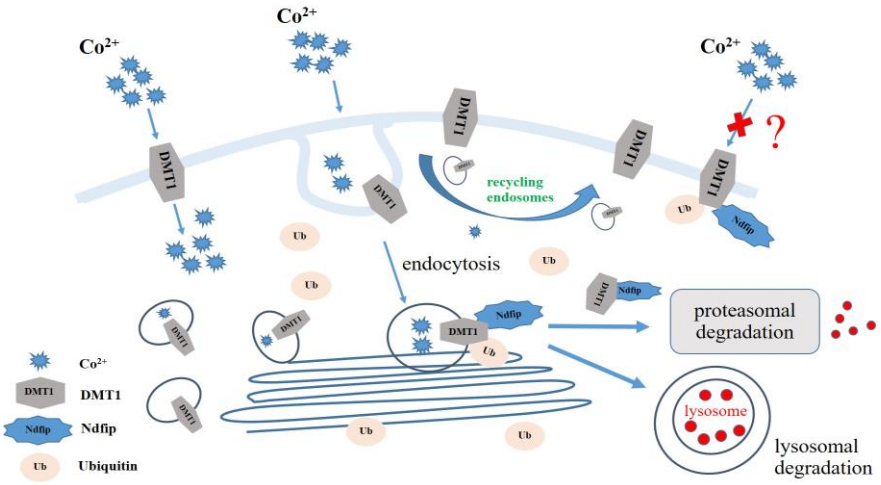

Figure 3-21 Postulated schematic illustration of Ndfips-mediated regulation of DMT1. DMT1 is known to be trafficked through recycling endosomes back to the plasma membrane or internalised and delivered to late endosomes. Golgi apparatus-localised Ndfips to mediate the degradation of DMT1 at the Golgi apparatus through the lysosomal pathway. By DMT1 can interact with Ndfips which leads to its ubiquitination and promotion of its degradation via the 26S proteasome and/or lysosome. (adapted from Figure S6 in Foot *et al*. 2008.).

have tetrahedral, square planar, trigonal or square bipyramidal, and octahedral (still the most common) ligand configuration (Hughes, 1981) and impersonation by Co as an ion that can be transported in a similar way to Ca^{2+} could be one of the ways for this metal to cross the membrane. Ca^{2+} transport is involved in several cellular processes (Berridge, Lipp and Bootman, 1999) and this is also the case with Mg^{2+}, which plays a vital role in the modulation of ion channels, receptors, G proteins, and effector enzymes (Volpe and Vezu, 1993; Romani and Scarpa, 2000). So an important factor participating in the uptake of trace metal ions is ion channels, and this may involve moving across an electrochemical gradient (Bouron, Kiselyov and Oberwinkler, 2015).

Some transient receptor potential (TRP) channels have been shown to be permeable to trace metal ions, and it has been demonstrated in some cases that TRP channels are important for the physiological uptake of trace metal ions (Ramsey, Delling and Clapham, 2006; Venkatachalam and Montell, 2007; Nilius and Owsianik, 2011). TRP channels allow the entry of Ca^{2+} into the cytosol. Most of them are located in the plasma membrane, but some are both in the plasma and in intracellular membranes. Moreover, more than ten TRP channels have been reported to be expressed in the heart

and vasculature of mammals including humans (Inoue *et al.*, 2006; Watanabe *et al.*, 2008). In addition, up-regulated TRP channels are believed to mediate the progression of electrical remodelling and the arrhythmogenesis in heart disease (Inoue, Jian and Kawarabayashi, 2009a). Among the seven isoforms (TRPC1– TRPC7), TRPC6 is the only TRPC channel known to transport physiologically relevant trace elements, specifically its uptake of iron (Fe^{2+} and Fe^{3+}) and Zn^{2+} has been studied (Mwanjewe and Grover, 2004; Gibon *et al.*, 2011). In PC12 cells TRPC6 channels permit entry of Fe^{2+} and Fe^{3+} independently of transferrin and its receptor (Mwanjewe and Grover, 2004).

The other TRP channel that we investigated is the mammalian subfamily (TRPM channel). These proteins comprise eight members (TRPM1-TRPM8), and the first TRP channel investigated with respect to trace metal permeation was TRPM7 (Nadler *et al.*, 2001; Monteilh-Zoller *et al.*, 2003). Mg^{2+} ions accumulate intracellularly and they regulate the channel activity. Studies have shown that TRPM7 channels are permeable to a wide variety of divalent cations, including physiologically important trace metal ions, such as Co^{2+}, Mn^{2+} and Zn^{2+}, which seems to permeate TRPM7 channels particularly well (Monteilh-Zoller *et al.*, 2003; Li, Jiang and Yue, 2006; Witkiewicz-Kucharczyk and Bal, 2006; Topala *et al.*, 2007). So it is possible that TRPC6 and TRPM7 which generate complexes to mediate physiological Ca^{2+} entry in fibroblasts, might also be involved in Co uptake into these cells.

In western blots showing the expression levels of TRPC6 and TRPM7 in CFs, we found that both TRPC6 and TRPM7 expression is high in the untreated control CFs and is higher after Co treatment. Expression of TRPC6 for example, is significantly increased at concentrations of 1, 10 and 100 µM Co after both 48 and 72 h exposure. The dose dependent manner of the induction suggests that both TRPM7 and TRPC6 are affected by Co treatment and may be responsible for Co uptake in the CF cells. As seen in the study of Chigurupati and coworkers, it was found that $CoCl_2$ at a dose 100 µM induced the expression of TRPC6 under hypoxic conditions in primary samples and cell lines derived from glioblastoma multiforme (Chigurupati *et al.*, 2010). However, the identity of the endogenous TRP channel involved in physiological conditions is still debated, -both in cardiac cells and in the CNS.

Nishida and colleagues reported the presence of TRPC1, TRPC3, TRPC6 and TRPC7 in primary cultures of rat cardiac fibroblasts (Nishida *et al.*, 2007b). TRPC6 regulates the contraction of the vascular and pulmonary smooth muscles (Dietrich *et al.*, 2005; Di and Malik, 2010; Earley, 2010; Earley and Brayden, 2010) and Ca^{2+} entry and subsequent signalling is closely associated with the initiation of fibrosis (Vennekens, 2011). All TRPC isoforms (TRPC1, TRPC3, TRPC4, TRPC5, TRPC6 and TRPC7) with the exception of TRPC2 are proposed to be involved in cardiac hypertrophy (Nishida and Kurose, 2008a; Watanabe *et al.*, 2008; Eder and Molkentin, 2011). In particular, TRPC6 appears to be essential for the development of cardiac hypertrophy (Kuwahara *et al.*, 2006). Also TRPM7 is abundantly expressd in cardiac fibroblasts and is a major Ca^{2+} permeable channel in both human and mouse cardiac fibroblasts (Du *et al.*, 2010). Furthermore, TRPM7 current density is up-regulated 3-5 fold in fibroblasts from patients with atrial fibrillation (AF) compared with sinus rhythm patients (Du *et al.*, 2010). TRPM7 is also up-regulated in cardiac myocytes from AF patients (Zhang *et al.*, 2012). The role of TRP calcium channels in Co toxicity in the heart is seldom studied and still remains unclear. The data discussed above indicate that TRPC6 and TRPM7 might be responsible for the regulation of the intracellular Co^{2+} ions content. The currently available literature data about the effect of Co ions on the expression of TRP channels are inconsistent and contradictory. Further experiments are needed to identify whether changes in TRP channel expression are functionally important in the heart and to assess the effects of increased channel expression, regulation of channel activity, and fibroblast activity in the heart with respect to deterioration of function in cases of Co toxicity.

The concentrations of Co studied in this chapter are higher than those encountered in the blood of patients with CoCr implants certainly. At the higher end of patient blood Co levels they are reported to have been exposed to 6,521 ppb (Zywiel *et al.*, 2013), and patients are now closely monitored to ensure levels remain below 7 ppb (MHRA, 2010). However, uptake into organs such as the heart may occur even at very low levels to elevate local intracellular Co levels, and this combined with exposure periods in excess of 40-50 years may lead to an underestimate of the actual risk from exposure to low Co levels. This should be kept in mind when considering the risk of Co toxicity.

Chapter 4. EFFECT OF LONG TERM COBALT ION TREATMENT ON 3T3 CELL LINES

4.1 Introduction

According to results in chapter 3 where short term toxicity testing of $CoCl_2$ *in vitro* on both 3T3 cells and cardiac fibroblasts was examined, there are some differences in the effects of Co between the two cell types, especially in cell proliferation and cellular uptake of the ion. The results from short term exposure (24, 48 and 72h) have shown there is greater accumulation of $CoCl_2$ in CFs and the inhibitory effect on cell proliferation in CFs is greater.

These experiments have determined the acute toxicity of high concentrations of Co. We are mainly concerned with the release of Co ions into the blood of patients wearing a metal-on metal prosthesis. These prostheses can be in place for up to 40-50 years, and the patients are therefore exposed long term to the effects of the released ions. The concentrations of Co commonly measured in patient blood when a MoM is in place are 0-6,251 µg/L or 0-25 µM. We therefore extended the *in vitro* exposure time to Co to 28 days, and used a range of Co exposures between 0-5 µM or 0-1,200 µg/L in order to observe the effect on cells.

In these experiments we only exposed 3T3 cells to Co, because the primary cardiac fibroblasts could not be maintained in culture for a longer period. Considering the different responses to the two cell types, this is a major limitation of the work in this chapter.

The cells were treated continuously for 4 weeks with the same concentration of $CoCl_2$ and were trypsinised and counted twice a week. The number of cells was compared to the number of cells cultured under control conditions using the combined cytotoxicity tests validated in chapter 3 of this thesis. It is essential to determine the potential effects of long-term exposure to metal ions and debris, since several previous studies have reported that long term toxicity from CoCr alloy is evident (Raghunathan *et al.*, 2007). This long term toxicity study should also indicate the potential effects of long-term exposure to metal ions in across cell types.

Two major long- term cytotoxicity patterns could be distinguished by measuring cytotoxicity using a combined assay (MTT, NR and CV) and staining cells to study the viability and morphology changes, and actin distribution in the cells.

4.2 Aims

To assess the effect of long term treatment with Co ions on an immortalised cell line (3T3 cell lines) *in vitro* by:

4.2.1 Combined assay (MTT, NR and CV assays) for viability after long term toxicity study (28 days).

4.2.2 Fluorescent microscopy to evaluate changes in morphology.

4.3 Results

4.3.1 Cytotoxicity testing of low dose, long term exposure to Co in 3T3 cells: Combined viability assay

In preliminary studies, reported in Chapter 3 the combined viability assays were compared with each assay carried out separately. Thus, the use of the combined assay protocol to test cytotoxicity was validated in this way.

Figure 4-1 illustrates the percentage of viable cells after being treated with various concentrations of $CoCl_2$ (0, 0.001 μM, 0.01 μM, 0.1 μM, 1 μM and 5 μM) over 4 weeks (Wk1, Wk2, Wk3 and Wk4). It is readily apparent that the combined assay results showed that $CoCl_2$ did not exert any significant effect on proliferation or viability of the 3T3 cells over the concentration range 0-5 μM. The viability of 3T3 cells was not significantly different from controls with the range of lower $CoCl_2$ concentrations used (0-5 μM).

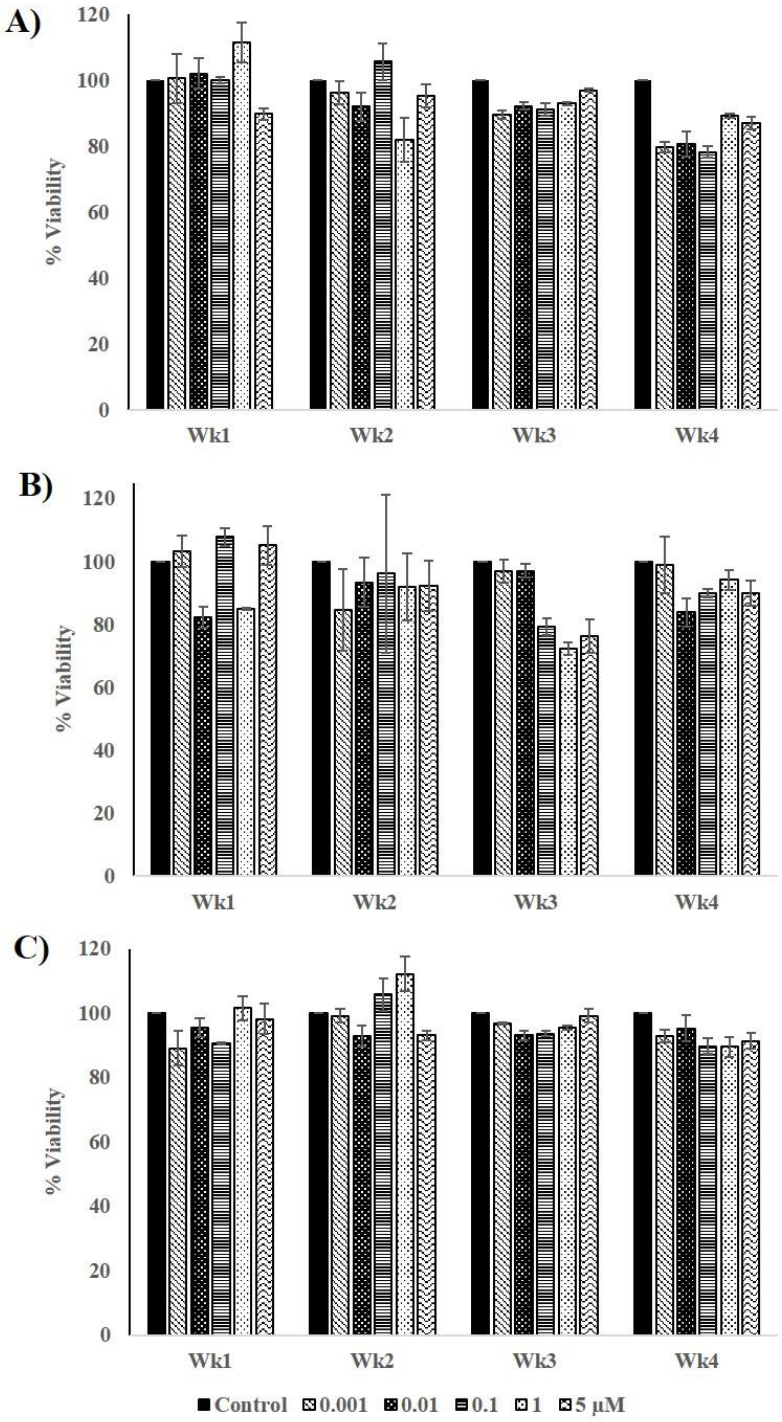

Figure 4-1 Viability of 3T3 cells after long-term exposure to Co. Cells were treated with various concentrations of $CoCl_2$, untreated control cells, 0.001 µM, 0.01 µM, 0.1 µM, 1 µM and 5 µM over a period of 4 wk (Wk1,Wk2, Wk3 and Wk4), and viability measured by (A) MTT (B) NR assay and (C) crystal violet assay from the combined assay. Note that cultures exposed to long-term $CoCl_2$ treatment present non-significantly different percentages of cell viability compared with untreated cells. Statistical analysis was carried out using one-way-ANOVA with post hoc Dunnett's comparison (n = 3, $*p<0.05$ with a significant difference to control).

4.3.2 Staining for Live and Dead cells using CFDA and PI after exposure to $CoCl_2$ at various concentrations for up to 28 days.

Almost all cells were labeled with the green CFDA colour, and PI did not show any red stained nuclei in treated cells at any timepoint or concentration of Co. There was no apparent cytotoxicity to 3T3 cells at any exposure period (Figure 4-2). No change in cell morphology was observed despite the fact that some vacuoles occurred in both control and treated cells and this might be due to the presence of aging cells. Some dead cells may have been lost during washing of the dish, but the remaining cells were viable at all concentrations and time exposures.

4.3.3 Staining for Actin using Phalloidin-FITC after exposure of cells to $CoCl_2$ at various concentrations for up to 28 days.

The normal distribution of actin was observed after treatment with all concentrations of $CoCl_2$ over a 2 wk period and also in the untreated cells at all the times of exposure (4wk). No change in the size of the nucleus was observed over the period of exposure. However, bleb formation was observed after cells were treated for 2 wk as seen in Figure 4-3 using a higher magnification (20x), 3T3 cells being treated with $CoCl_2$, at all doses (exception 0.1 µM) showed evidence of membrane formed blebs, and ballooned in treated cells (labelled with red arrows, Figure 4-4). The bleb formation supports the suggestion that $CoCl_2$ causes cell apoptosis.

As indicated in Figure 4-4, broken actin filaments were found in cells treated with $CoCl_2$ at 5 µM (as shown on Figure 4-4 by the white arrow) and also it can be observed that the arrangement of actin within the normal cells is to surround the nucleus of the cell, whereas the actin distribution in Co-treated cells was not normal; not surrounding the nucleus but arranged around the cell border as shown by the blue arrow. Moreover, it was observed that the green intensity within the cells due to actin staining was noticeably decreased (not quantified), which may indicate weakening of the actin filaments. Cells with different distribution of actin formed strong stress fibres at the cell edge, while disrupted actin assembly was observed at the cell centre.

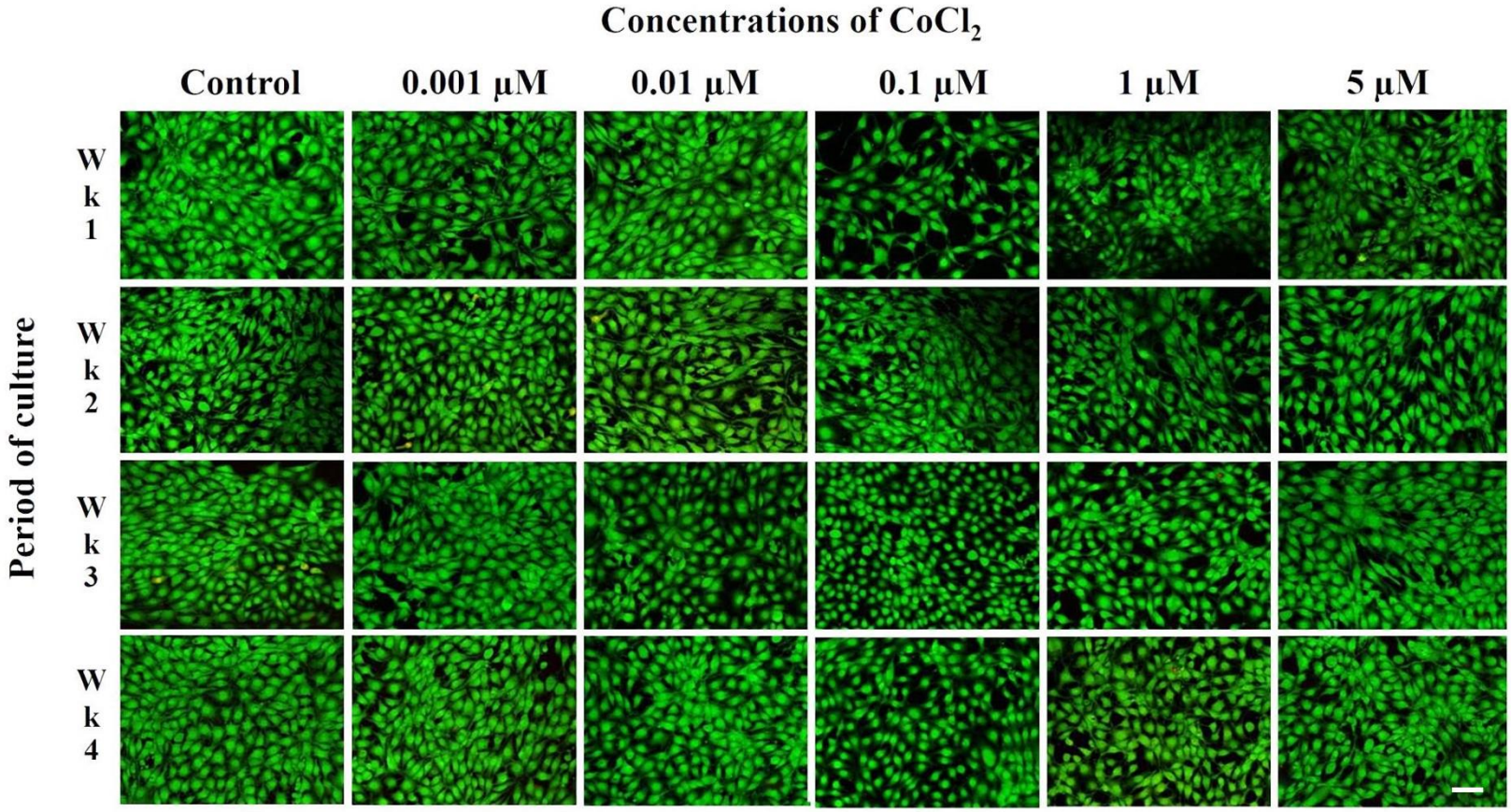

Figure 4-2 Live / Dead 3T3 cells observed by microscopy after 28 days treatment with various concentrations of $CoCl_2$. 3T3 cells were treated with various concentrations of $CoCl_2$ (untreated cells, 0.001 µM, 0.01 µM, 0.1 µM, 1 µM and 5 µM) for up to 4 wk (Wk1, Wk2, Wk3 and Wk4**)** (Bar =40 µM). CFDA staining of live cells **(green)** and PI staining of the nucleus in dead cells (red). The images were obtained using 20x objectives lens**.**

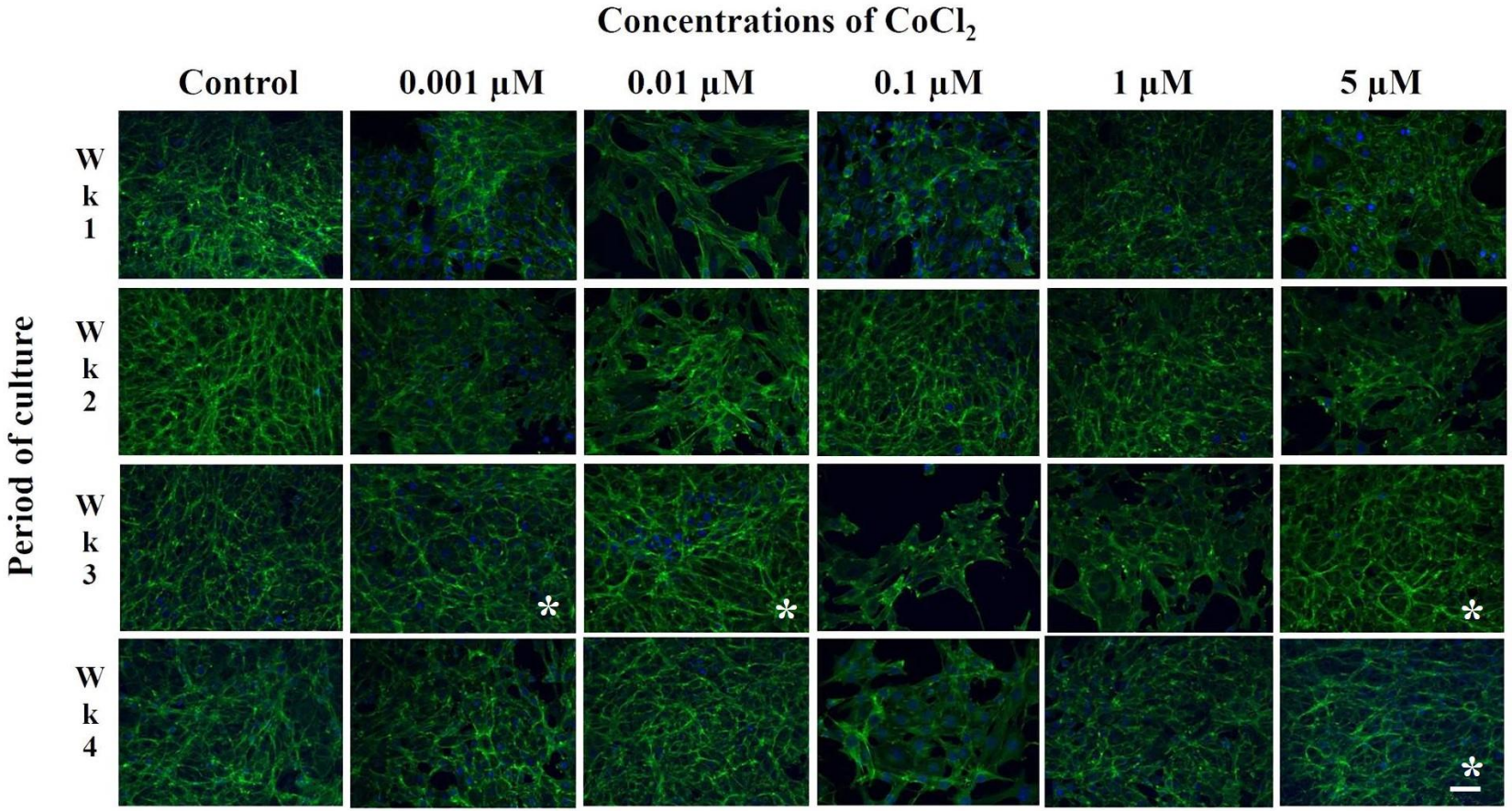

Figure 4-3 F-Actin filaments in 3T3 cells during prolonged treatment of cells with various concentrations of $CoCl_2$. 3T3 cells were treated with various concentrations of $CoCl_2$ (untreated cells, 0.001 µM, 0.01 µM, 0.1 µM, 1 µM and 5 µM) for up to 4 wk (Wk1,Wk2, Wk3 and Wk4) (Bar= 40 µM). Phalloidin-FITC staining of actin fibres (green) and DAPI staining (blue) of nuclei. Image were obtained using 20X objective lens. All images were captured using identical exposure setting. *is illustrated bleb formation, magnified view in **Figure 4-4**.

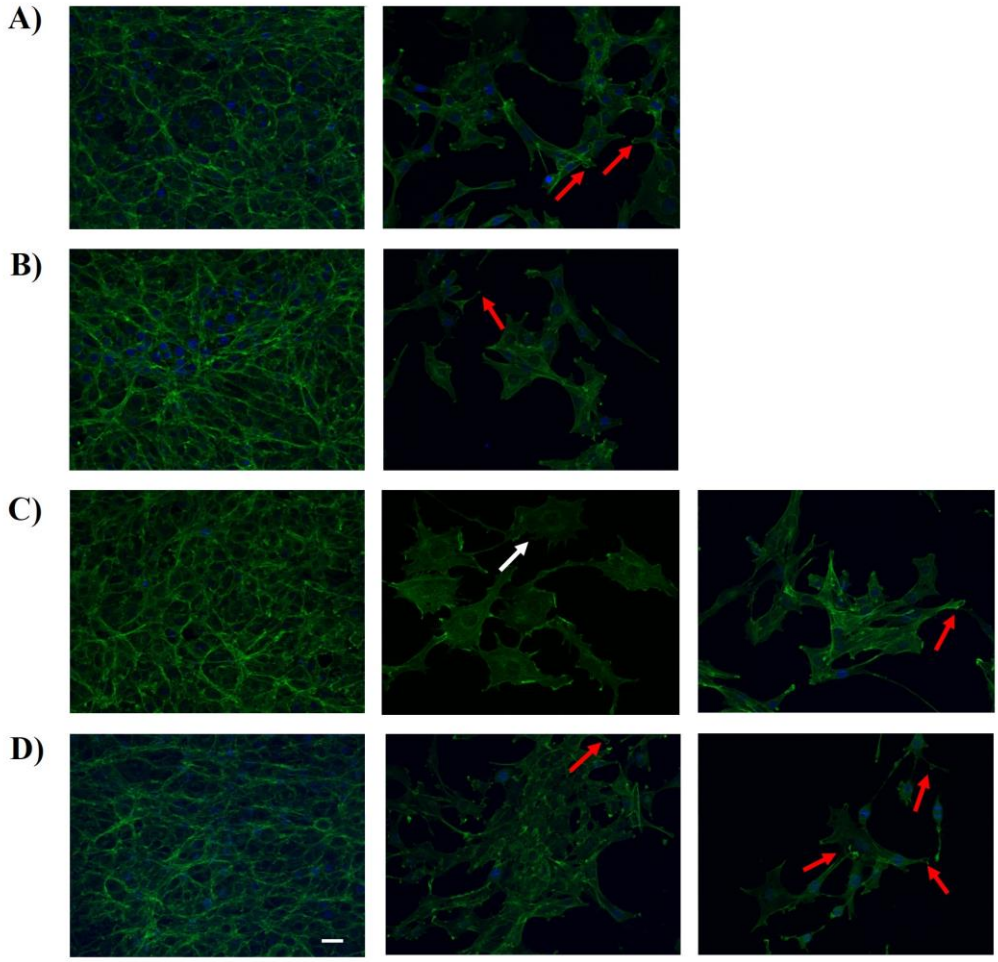

Figure 4-4 F-actin filament and nuclei staining of 3T3 cells Actin cytoskeleton staining of CFs on 35 mm^2 culture dishes after being treated with various concentrations of $CoCl_2$ for 4 wk. Changes in the actin cytoskeleton were verified by Phalloidin-FITC staining of actin fibres (green) and DAPI staining of nucleus (blue). At week 3 (A) 0.001 µM, (B) 0.01 µM, (C) 5 µM and (D) 5 µM for endpoint (wk4) show blebbed cells by red arrows. (Bar= 40 µM). Actin appears to be broken by the $CoCl_2$ at doses of 5 µM on Wk 3 (shown by the white arrow). 3T3 cells formed stress fibres at the cell edge. Images were obtained using 20X objective lens. All images were captured using identical exposure setting.

4.3.4 Summary of major findings

In this chapter, the potential for *in vitro* long term toxic effects of low concentrations of Co on cell viability, proliferation and morphology on the standardised cell line (3T3 cell line) has been studied. The main findings of this study are:

- The long term toxicity testing (28 days) showed that the $CoCl_2$ had little or no toxic effects at low doses over long periods of exposure as determined by measuring the percentage cell viability each week for 4 weeks.
- Due to the low toxicity observed, the half maximal inhibitory concentration (IC_{50}) of $CoCl_2$ cannot be calculated for these treatment periods and Co concentrations.
- No cell loss or cell death was detected at any of the concentrations and times with live/dead staining.
- Bleb formation was detected after a 3 wk period of exposure at some concentrations (0.001, 0.01 and 5 µM), and this represents a sign of cell apoptosis.
- Abnormalities of actin distribution in cells were also detected at some concentrations (0.001, 0.01, 1 and 5 µM) after a 3 wk exposure period. The actin was found at the membrane border of cells, and not surrounding the nucleus as it is in untreated control cells.
- Long term *in vitro* studies with Co exposure for up to 4 weeks show evidence for 3T3 cell death due to initiation of apoptosis after 3 weeks exposure to 5 µM Co.
- This concentration of Co is equivalent to 1,200 ppb, which is equivalent to concentrations of Co found *in vivo* in patients with CoCr alloy MoM implants in place (Langton *et al.*, 2008; Tower, 2010; Catalani *et al.*, 2012; MHRA, 2012; Zywiel *et al.*, 2013; Cheung *et al.*, 2016).

4.3.5 Implications of the in vitro long term toxicity study

- From our data: Fibroblasts may be reduced in number in the tissues of such patients, and perhaps processes of damage “repair” described as fibrosis may be inhibited *in vivo* by exposure to Co.

4.4 Discussion

MoM implants can be in situ for up to 30 years, slowly leaching both Co and Cr ions over this period. The Cr interacts predominantly with tissue local to the implant, but Co as previously stated, distributes through the body after entering the blood stream. Adverse reactions from Co and Cr take months or even years to manifest, and each person will experience the toxicity differently so it is important to consider long term damage in patients with MoM implants.

The physiology of the patient will affect the deposition of the ions and debris released during the life time of an implant. The rates of revision of hip replacements are unacceptably high, with 97,569 hips and 60,818 knees revised in total between April 2003 and December 2016 in the UK (excluding Scotland)(NJR, 2017). The major reason for revision is aseptic loosening often associated with wear. Thus, device failure occurs too frequently, and every avenue must be explored to increase device reliability and longevity.

The joint registry data have recently reported (NJR, 2017) a remarkable growth of revision surgeries involving metal-on-metal hip replacements and resurfacings, and it has already warned about a crucial need to develop research in this matter. Several studies have reported adverse tissue reactions resulting in failure of the implants. With a better understanding of the factors that influence the wear rate of the implants, adverse tissue reactions and subsequent implant failure can hopefully be reduced. In addition, patient selection and surgical technique affect the wear rate and the risk of tissue reactions involved.

Although several investigations have attempted to reduce implant adverse effects by the development of new materials in order to improve the patients' quality of life, the increasing number of revision rates for MoM implants remains. This is primarily a consequence of "pseudotumours"(Pandit *et al.*, 2008; Bisschop *et al.*, 2013; Munro *et al.*, 2014; van der Weegen *et al.*, 2014; Davis and Morrison, 2016), which arise from soft tissue changes due to adverse reactions to wear debris released from the metallic bearing surfaces.

The main catalysts for MoM implant failures are mechanically related aspects. Particularly femoral neck fractures, destruction of the femoral head, in addition to component loosening. Another contributing factor is the production of metal debris that leads to inflammation in the joint and the development of benign soft tissue tumours. The latter feature is also known as bearing related failures and might lead to osteolysis (McMinn *et al.*, 2011).

Although MoM devices normally succeed in recovering patients' mobility, they tend to become obsolete after 10-15 years of implantation. Furthermore, it is predicted that around 20% of the patients with MoM hip implants will undergo a revision surgery after a 10-13 year period, especially amongst patients enduring hips with larger head sizes (≥36mm) (AOANJRR, 2017).

The metal alloy used is a mixture of cobalt (Co), chromium (Cr) and molybdenum (Mo) composed of 58.9–69.5% Co, 27.0–30% Cr, 5.0–7.0% Mo (Liao *et al.*, 2013) that leach in the form of particulate matter due to the mechanical friction between the bearing components. These particles further deliver metallic ions, which overall are known to react adversely with the local tissue. In that regard, larger head size has demonstrated a larger quantity of nanoparticulate debris which increases the amount of released metal ions (Langton *et al*., 2012). Therefore, the size of the prosthesis is an important consideration with all MoM total hip replacements.

In light of this evidence, the MHRA updated its guidance on MoM implants in 2017 asking for a periodical follow-up. The recommendations given take into account risk factors such as whether the bearing components correspond to hip replacements or resurfacing, in addition to the femoral head size. It also establishes patients' discomfort (assessed by the Oxford Hip score), which may be associated with soft tissue reactions, and metal blood ion levels (MHRA, 2010). These early diagnoses will help to prevent local reactions shown as decreased mobility, limb weakness and even derived rash from hypersensitivity reactions to the metal ions. Moreover, there might be an opportunity to prevent the systemic effects reported in the literature, e.g. bone loss, neurological symptoms (Mabilleau *et al.*, 2008) and cardiomyopathies (Zywiel *et al.*, 2013).

Metal ion levels in blood are used as an indicator of systemic toxicity coming from the prosthesis given that the excessive metal debris production results in ions of two metal alloy components (Co and Cr) in the blood and urine of patients with CoCr alloy implants (Haddad *et al.*, 2011; MacPherson and Breusch, 2011).

Given the individual susceptibility to different levels of blood metal ions reported in the medical literature, there is not an exact Co ion blood level above which a patient must be considered for revision surgery. However, the patients with a symptomatic hip resurfacing or metal on metal hip replacement should be quickly referred for further investigation. The MHRA opinion in this matter recommends that patients with blood metal ion concentrations over 7 μg/L, should undergo MRI scans and Ultrasound scans in order to form a decision on whether a revision is needed for each particular patient (MHRA, 2010).

The National Joint Registry 14th Annual Report (2017) presents survey data on THR implants. Many more females (59.7%) than males (40.3%:) are reported to have hip primary procedures(NJR, 2017). The median age of females at which primary surgery was carried out was 69 (IQR 61-76) years, overall range 7-105 years (NJR, 2017). Conversely, females have higher rates of revision than their male counterparts (Mahomed *et al.*, 2003; NHS Choices, 2012). The 13 year revision rate for uncement MoP total hip replacements went up to 8.14% (females) vs. 7.26% (males). For comparison the MoM replacements are revised in 35.24%(females) and 22.04%(males), respectively (NJR, 2017).

In 2009, Glyn-Jones and colleagues also concluded in a case study with 1224 patients a significant risk of revision due to pseudotumours presented in women (Glyn-Jones *et al.*, 2009). They reasoned that this was likely due to the effects of osteoporosis (consisting on low bone density, bone thinning leading to fractures) caused by the menopause. These observations may partly explain why revision rates were higher in women.

The implantation of MoM hip replacements was recommended to patients with a predicted longer life span, since they are in general more active and this type of prosthesis allows for an increased range of movement. However, this fact now leads

to a worrisome scenario for many patients due to the unknown implications of long-term exposure to metal ions and wear debris. The recorded data from the National Joint Registry for England, Wales and Northern Ireland reveal that the incidence of revision rates in younger active patients may be greater than originally predicted (NJR, 2017). Moreover, in the last five year period NJR reported that around 10,000 to 30,000 patients less than 25 years old have undergone joint replacement (Sedrakyan *et al.*, 2014).

In general, MoM implants offer a greater range of motion that adapts better to the routine of young people who are normally more active and might participate in demanding exercises after the surgery.

Moreover, when comparing the lifespan of hip replacements between older and younger patients, it is apparent that the duration of use in younger people is more than elders, exceeding the usual 10 to 15 year span. Therefore, it is necessary to study the adverse long-term reaction to examine possible health implications.

Medical complications are another issue of high importance in relation to the revision surgery. Within this context, diabetes mellitus has been involved in deep infection in THR patients shortly after a revision surgery, although it does not seem to have a relationship with aseptic loosening or dislocation (Pedersen *et al.*, 2010).

Diabetes mellitus (DM) is associated with a number of micro- and macrovascular complications, (Almdal *et al.*, 2004; Booth *et al.*, 2006; Cade, 2008) and might also have an impact on bone remodelling, (Siqueira *et al.*, 2003; Kotsovilis, Karoussis and Fourmousis, 2006). Therefore, THR in DM patients may have serious medical implications. The increasing demand for total hip replacement and also the prevalence of diabetes among the population will result in a considerable number of diabetic patients with THRs. Other risk factors for deep infection in THR revisions are cardiovascular comorbidities prior to surgery (Pedersen *et al.*, 2010).

From the motives mentioned above, there are strong reasons to study the effects of long-term exposure of the patients to the metal ions. The variation of factors such as gender, added diseases and living standards, and moreover, the increasing life

expectancy due to improved technology, result in long term exposure in patients *in vivo* and are a concern wias regards extending a healthy lifespan for the patient.

Little research had been done on the long-term effects of metal ions so long term toxicity *in vitro* was investigated by exposing 3T3 cells to low doses of Co (0-5µM) for 28 days, with data collected every week. Chronic effects of exposure to Cr (VI) were studied in the same way by Raghunathan and colleagues on the clinically relevant human monocyte cell line (U937) over 4 weeks. During this period higher concentrations of Cr(VI) had a significant effect on glutathione (GSH) content and glutathione reductase (GRd) expression in the cells (Raghunathan *et al.*, 2007).

The range of $CoCl_2$ that we used in the current experiment (0-5 µM or 0-1,200 µg/l), relates to the concentration of Co in the blood of patients with implants (Langton *et al.*, 2008; Tower, 2010; Catalani *et al.*, 2012; MHRA, 2012; Zywiel *et al.*, 2013; Cheung *et al.*, 2016). Moreover, the lowest concentration of Co that was being used to treat 3T3 cells in the current study is similar to normal physiological levels of Co in human (<0.25µg/L or 0.005 µM)(Andrews *et al.*, 2011).

In the current study, we studied only the 3T3 cells. These cells are commercially available, and spontaneously immortalised with a stable growth rate. They can undergo more than 20 – 80 population doublings, retaining stable function of cells. Whereas primary cardiac fibroblasts have a finite life span, and lose their fibroblast phenotype after only 2-3 passages when they take on more of a myofibroblast phenotype. There are also commercially available cardiac fibroblasts provided from many companies, but these still have limitations. Although those cells are guaranteed through 5-8 population doublings that is not enough to enable us to prolong the exposure period to Co for long enough for the kind of study used in this thesis.

Longer incubation times with $CoCl_2$ retained the cell viability of 3T3s at 80% at all doses and time periods, as measured by combined assay (MTT, NR and CV assay). $CoCl_2$ was not toxic at low doses in terms of viability as determined by measuring the percentage of viable cells each week.

Lower concentrations of $CoCl_2$ were chosen for the chronic investigation, because these low concentrations mimic the patient blood concentration of Co in many people with MoM implants, and also these concentrations allow us to maintain the number of cells required for the period of exposure time. In the literature MoM implants have been proven by many authors to slowly release Co and Cr ions. In some cases these patients could be exposed to released metal ions for over 50 years (Afolaranmi *et al.*, 2008). This is much more than the relative period of exposure we used in our rat experiments. Rats live on average for 2 years, i.e. circa 105 weeks. The exposure time was 4 weeks, i.e. 20% of the life span of the animal. To mimic the length of exposure of human patients to Co, we would need to have exposed the rats to Co for approximately 1 year and this was not practically possible during the current project

Using Phalloidin-FITC to stain actin, broken actin filaments were found in cells being treated with $CoCl_2$ (5 μM) after 3 weeks of exposure**.** Abnormalities of actin distribution were also found in cells being treated with $CoCl_2$ after a 3 week exposure**.** The actin was found at the membrane border of cells, not surrounding the nucleus. Apoptotic blebs also appeared following a 3 week exposure.

The weakening of the actin cytoskeleton and plasma membrane connections causes membrane blebs (Cunningham, 1995; Doctor, Zhelev and Mandel, 1997), which indicate cleavage and phosphorylation of cytoskeletal proteins (Mills, Stone and Pittman, 1999). The presence of a disturbed actin cytoskeleton may indicate with impending cell death by $CoCl_2$ (Peters *et al.*, 2001) (as seen in Figure 4-4). Failure to maintain essential transmembrane gradients (Ca^{2+}, Na^{+}, K^{+}, etc) likely leads to Co-provoked cell death and occurs after the cytoskeletal abnormalities and the loss of integrity of the plasma membrane (Walker *et al.*, 1988).

The long term effects of Co on macrophages *in vivo* may also arise as a result of phagocytosis and intra-cellular corrosion of debris (Goode *et al.*, 2012). Such chronic exposure to ion releases *in vivo* can cause local soft tissue reactions that destroy muscle and bone and lead to chronic disability.

The bearing surfaces of MoM implants from CoCr alloys can produce wear and release nanometre-sized Co and Cr particles accompanied with the release of Co and Cr ions.

The interaction between the Co-Cr nanoparticles and ions from a hip implant causes adverse reactions by reducing cellular viability, activating the inflammatory response, inducing genotoxic effects (DNA damage and chromosome aberrations), and by immunotoxic effects via metal hypersensitivity reactions.

Desrochers and colleagues also reported that the principal mechanism for the failure of the implants could be chronic inflammation in the periprosthetic region induced by soluble ions generated from debris products, which could lead to osteolysis and aseptic loosening by the action of macrophages (Romesburg, Wasserman and Schoppe, 2010; Frigerio *et al.*, 2011; Desrochers, Amrein and Matyas, 2013). In that regard, Catelas and co-workers also demonstrated that Co and Cr ions exposure produced macrophage cell death at levels of 1-10 mg/l Co^{2+} and 0-500 mg/l of Cr^{3+} for 24 and 48 h (Catelas *et al.*, 2005).

Although Co and Cr ions have similar protein binding affinity, the proportion of binding depends on the added concentration ratio (Yang and Black, 1994). Equally, when a metal ion binds to a protein, it can be transported and either be stored or excreted (Sargeant and Goswami, 2007). Therefore, both metal ions can enter into the bloodstream and then get distributed to the lymph nodes, spleen, liver, heart and kidneys before being excreted in urine and and cause systemic toxicity. A proportion of these ions will bind to the tissues, and may indeed accumulate in selective tissues, as we have observed in our animal experiments. Under physiological conditions, Co has been reported to corrode quicker than Cr (Xia *et al.*, 2011). Therefore, Co ions readily leak and dissolve into the blood resulting in a prompt penetration of Co in the systemic circulation in contrast to Cr, as explained by the distinct blood ion content results seen in other studies (Afolaranmi *et al.*, 2012) where the peak Co level in blood was 77.0± 19.7µg/l at 48 h, compared with 35.5 ± 1.6 µg/l for Cr after *in vivo* equal treatment.

The immune system is activated by ions binding with native proteins (Jacobs *et al.*, 2001). The biological tissue responses range from vascularised granulomatous tissue formation along the bone-implant interface, influx of inflammatory cells such as macrophages and lymphocytes, bone resorption, osteolysis, and finally loss of

prosthesis fixation which are all stimulated by implant derived wear particles (Anderson, Rodriguez and Chang, 2008; Zhang *et al.*, 2009). Released mediators, such as free radicals, nitric oxide, many proinflammatory cytokines such as Tumor necrosis factor alpha (TNF)-α, Interleukin (IL) 1-β, IL-6, and IL-8, and other cytokines are produced from interaction with wear debris leading to macrophage phagocytosis (Sethi *et al.*, 2003; Kaufman *et al.*, 2008). Dalal observed considerable cytokine production (TNF-α and IL-8) in a variety of cells (human osteoblast, fibroblasts, and macrophages) in response to different metal-based particles(Dalal *et al.*, 2012).

With regard to Co ions and their involvement in the immune response during long term exposure, the immune reactivity to wear debris and ions from MoM implants (Co, Cr and Ni) is driven by stimulated T-cell delayed-type hypersensitivity (Hallab *et al.* 2001; Minang *et al.* 2006; Hegewald *et al.* 2005; Fors *et al.* 2012). Almousa and colleagues have suspected the relationship between high concentrations of serum metal ions and metal hypersensitisation (Almousa *et al.*, 2013). High accumulation of metal ions (Co, Cr and Ni) in the body is related to type IV T-cell mediated hypersensitivity reactions (Amini *et al.*, 2014). Both T cells and macrophages mediate these reactions, and sensitisation to MoM implants can also lead to pro-osteoclastogenetic factors that can change bone homeostasis and contribute to osteolysis (Frigerio *et al.*, 2011). Comparison of metal sensitivity between patients with implants found that 10 -15% sensitivity arose in patients with well-functioning implants vs. 25 – 60% in patients with poor-functioning implants by dermal patch testing (Hallab et al. 2001). Failure of MoM prostheses has been reported as occurring in patients with the metal hypersensitivity (Brown *et al.*, 1977; Smith, Mehta and Statham, 2009).

It seems that metal ions react specifically with lymphocytes in patients with poorly functioning implants and cause T-cell-mediated (type IV) hypersensitivity. It has been reported following MoM replacement that lymphocyte infiltrates (vasculitis with intramural and perivascular lymphocytic infiltration of the postcapillary venules), endothelial swelling, localised bleeding and necrosis are all features used to characterise delayed hypersensitivity (Alsaad and Ghazarian, 2005; Willert, 2005). A particular perivascular lymphocytic reaction, leading to vessel constriction and

necrosis, has been described as a characteristic feature in the adverse reaction to MoM patients (Willert, 2005; Revell, 2014). There have been many studies involving hypersensitivity and MoM articulations, for example, unusual lymphocyte infiltrated has been detected in the soft tissue of patients with hypersensitivity (Boardman, Middleton and Kavanagh, 2006; Pandit *et al.*, 2008) and other studies have also shown the presence of damaging immunologic reactions associated with those articulations (Böhler *et al.*, 2002; Davies, 2005; Willert, 2005; Korovessis *et al.*, 2006; Campbell *et al.*, 2010).

The increase of inflammation from wear debris leads to the production of an acidic environment, which may further encourage metallic corrosion. Low pH clearly accelerates corrosion. Local acidification may develop during acute and chronic inflammation from cells (Rajamäki *et al.*, 2013). Low pH at 5.4 has been found in inflamed tissue and may enhance the corrosion process, increasing the release of further metal ions. This has been confirmed by Posada's studies, where low pH during culture *in vitro* caused significantly higher concentrations of Co and Cr to be released from CoCr metal alloy (Posada *et al.*, 2014).

This finding suggests that macrophage-stimulated osteolysis and aseptic loosening from wear debris would lead to increased local tissue inflammation aggravated by acidic conditions. An overview of the mechanism of action of $CoCl_2$ in 3T3 cells is shown in Figure 4-5, and suggests that the immunological reactivity contributes to long term toxicity of $CoCl_2$.

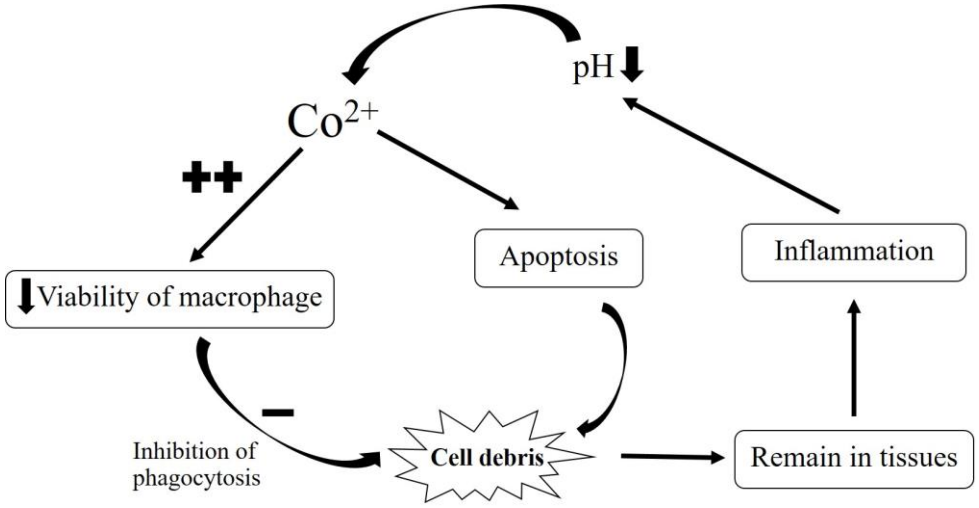

Figure 4-5 The possible mechanism of action of long term $CoCl_2$ toxicity and its effect on 3T3 cells. Co ions induce organ cell death and disturb macrophage viability in the long-term, and inhibit phagocytosis. Hence, the process impairs the clearance ability of the immune system enhancing the deposition of cell debris. Higher deposition of cell debris induces a persistent organ tissue inflammation that additionally promotes lower pH in the extracellular environment. This acidification yields higher corrosion rates that generate more metal ions from the particles around the prosthesis in a positive feedback manner, and this process could ultimately contribute to the acidosis seen in patients with Co poisoning (Cheung *et al.*, 2016).

These discussion points on inflammatory processes indicate the importance of these mechanisms as responses to Co. In acute terms, the main responses to Co are:

1) Co may cause local damage as in cellular toxicity; it has effects on cellular characteristics by causing cytotoxicity, inhibiting proliferation and causing cell death and it is also taken up into cells. Cells in the local tissue area are directly attacked by Co ions due to their persistent release from metallic MoM implants. The corrosion causes persistent hip pain, damage in the local tissue, severe inflammation, and swelling around that implant area which is called "metallosis".
2) Co also induced high protein expression of transporters such as CaMKII, TRPC6 and TRPM7 especially in primary cardiac fibroblass after short-term exposure. The latter two proteins are thought to play an important role in the intracellular uptake of Co. This suggests that Co ions *in vivo* would accumulate in patients' hearts and may thus cause cardiotoxicity.
3) There are not only local effects. The mobile Co ions can be enter the bloodstream and be transported throughout the body casuing non-localised symptoms (systemic effects) such as headaches, nausea, fatigue, vertigo, anxiety, irritability, etc. All of these symptoms seems to be the acute or sudden adverse reactions from metal toxicity.

However, in chronic toxicity additional process must be considered:

1) The slow corrosion of Co from MoM implants over time gradually builds up to the high level of metal ions in the body seen in patients. From our experiments, exposure to a low concentration of Co in chronic toxicity testing demonstrated that Co has no effect on cell viability, but it causes some change in cell morphology over a 4 week-period.
2) Chronic inflammation may be promoted by the action of lymphocytes after long-term Co exposure. These reactions lead to osteolysis and aseptic loosening.
3) The immune reactivity with metallic wear and ions from MoM implants may causes T-cell delayed-type hypersensitivity by the high accumulation of Co in blood.

However, the inflammatory and immune system responses that may develop after long term toxicity due to Co exposure do not occur in all patients. These characteristic adverse reactions to metal ions depend on the physiological response of each individual. Due to this factor, it is very important to consider a revision surgery case by case. Moreover, the experimental design for long term study *in vitro* would be more difficult, and totally different from the long term *in vivo* study. It is impossible to simulate chronic *in vivo* toxicity in *in vitro* experiments because *in vivo* toxicity involves so many interacting systems in the body.

Chapter 5. EFFECTS OF CHRONIC COBALT ADMINISTRATION IN RATS *IN VIVO*.

5.1 Introduction

Initial experiments in chapters 3 and 4 have screened the *in vitro* toxic responses in a cell line commonly used for toxicity testing, the mouse 3T3 fibroblast, and in primary cardiac fibroblasts isolated from adult rat hearts.

To increase the relevance of our data, we were interested to study potential cardiotoxicity *in vivo*. In this experimental work, male Sprague-Dawley rats were given daily injections of 1 mg/kg $CoCl_2$ and control rats were given distilled water for either 7 days or 28 days, before the effects on heart function were monitored.

Clinical echocardiography has been established as a safe, reproducible, and accurate assessment of cardiac anatomy, hemodynamics, and function (Watson *et al.*, 2004). During the last decade, commercially available medical ultrasound systems have made it possible to obtain reliable and accurate images of rat hearts (Litwin *et al.*, 1995; Burrell *et al.*, 1996; Cittadini *et al.*, 1996; Forman *et al.*, 1997). To study the pathophysiological mechanisms of ventricular dysfunction, echocardiography has been used to examine functional and structural cardiac parameters in different models of cardiac disease, and to develop new therapies for treatment of heart failure (Morgan *et al.*, 2004; Martinez *et al.*, 2011; Desrois *et al.*, 2014). Rats are commonly use in cardiovascular research. The rat model has been widely used as an experimental model because of its convenience in handling and housing as well as its lower costs when compared with other larger rodents. Moreover, the knowledge of baseline normal cardiovascular parameters for rats have been been well characterised(Coatney, 2001).

Echocardiography in rats is extensively applied as a method to determine changes in cardiac function during progression of cardiac disease, or with therapeutic interventions for heart disease. For example echocardiography has been used to assess cardiac function following occlusion of the left descending coronary artery in a rat model of myocardial infarction (Yoshiyama *et al.*, 1999). Echocardiography in small laboratory animals is challenging due to technical problems because of the small size of the rat heart relative to the human heart (Brown *et al.*, 2002). In rats the average measurements of cardiac parameters such as left ventricular (LV) wall thickness, end-diastolic and end-systolic diameter (EDD and ESD) and aortic root and left atrial (LA)

diameter are approximately 1/10 of the reported values in humans (Oh, Seward and Tajik, 2006). Assessment of cardiac anatomy and hemodynamics can be consistently carried out on the rat to provide evidence for cardiac dysfunction or disease similar to what is observed in human clinical conditions. Precise echocardiographic diagnosis of an experimental rat model could therefore result in a better understanding of the adverse effects of Co treatment on the heart and determine how it might affect cardiac function.

The dose of Co administered to rats in this study was chosen to give similar blood concentrations as reported in human MoM patients (Langton *et al*., 2008; MHRA, 2012; Tower, 2010). Widely different metal ion concentrations in blood and serum have been reported with metal-on-metal (MoM) implants. But a safe level of 7 ppb (µg/l) or 120 nM of Co in blood was suggested in patients with implants by MHRA. Patients with levels higher than this safe level, should give cause for concern and may have their implants revised. One study investigated the total amounts of Co in blood following the administration by i.p injection of 3 mg/kg of $CoCl_2$ and found it to be 5.02±1.36 µg after 24 h (Afolaranmi, 2011). For the long term study performed in this project, a lower concentration of Co for administration was therefore chosen.

In vivo experiments on rats were carried out

: To assess left ventricular (LV) function using echocardiography at both 7 and 28 days.

: To predict the distribution of soluble metal ions that are released from metal implants in patients, by measuring organ distribution of Co ions in rats after an intra-peritoneal (i.p.) injection of Co at clinically relevant concentrations.

: To understand the mechanism(s) or target protein(s) that may be involved in Co toxicity as previously described *in vitro* (section 2.2.17). Western blotting was also used to this end. The *in vivo* effects of Co on rat heart has been examined by western blotting for the same proteins that were investigated *in vitro*.

5.2 Aims

The aims of this chapter were to treat rats daily with 1 mg/kg Co and:

5.2.1 Observe the animals on a daily basis for signs of any adverse effects and measure body weight daily.

5.2.2 Monitor the cardiac function of rats after Co exposure at two points - 1 and 4 weeks by echocardiography. The following measurements were taken - systolic and diastolic left ventricular (LV) wall measurements including anterior wall(AW) and posterior wall (PW) measurements, LV end systolic dimension (LVESD), LV end diastolic dimension (LVEDD). Fractional shortening (%FS) was calculated from these.

5.2.3 Determine the weight of liver, heart, kidney, spleen, brain, lung and testes at the time of death.

5.2.4 Collect and store blood samples and tissue samples of each of the organs to detect Co levels by ICP-MS, and to carry out Immunoblotting and RNA analysis of these samples to assess expression levels of specific proteins that may be involved in Co toxicity.

5.3 Results

5.3.1 Animal observation: Body weight and organ weight

5.3.1.1 Body weight

Animals were handled daily and weighed daily throughout the treatment period. Animal weight data reflect the behaviour of the animal to a large extent, confirming that they are eating normally. No unusual behaviour was noted in any of the animals used.

In this study, male Sprague-Dawley rats each weighing 200-250 g were used to avoid any bias. Animals were individually identified by ear-punching. This study was divided into two control groups (7 and 28 days) and two treatment groups (7 and 28 days), each with 3 animals for control groups and 6 animals for treatment groups. The data collected show that body weight continuously increased over a 7 day period in both the control and treatment groups (Figure 5-1). By day 7, there were no significant differences in growth rates among the various groups.

The body weight gain was calculated as a percentage of the initial body weight (Figure 5-2). There was a dramatic increase in body weight gain after 7 days. By 28 days, there were significant differences between Co treated rats and control rats.

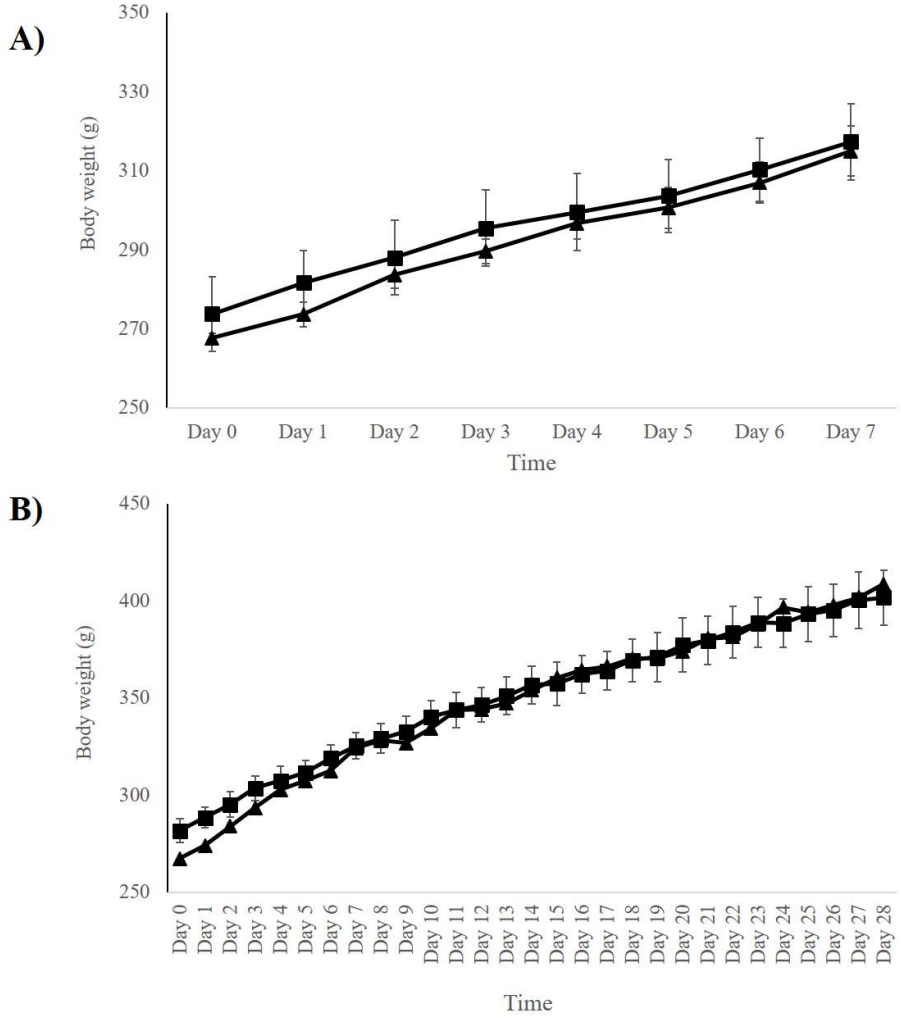

Figure 5-1 The effect of Co treatment on Body weight. Body weight changes in rats resulting from Co treatment for (A) 7 days and (B) 28 days. Male Sprague-Dawley rats each weighing 200-250 g were given daily i.p injections of 1 mg/kg $CoCl_2$ (n=6). Control rats (n=3) were given daily i.p. injections of distilled water. Triangles in panels (A-B) represent the body weight of rats in control groups and square represent the body weight of rats in Co treated groups. No significant differences exist in the results of body weight at both durations of exposure.

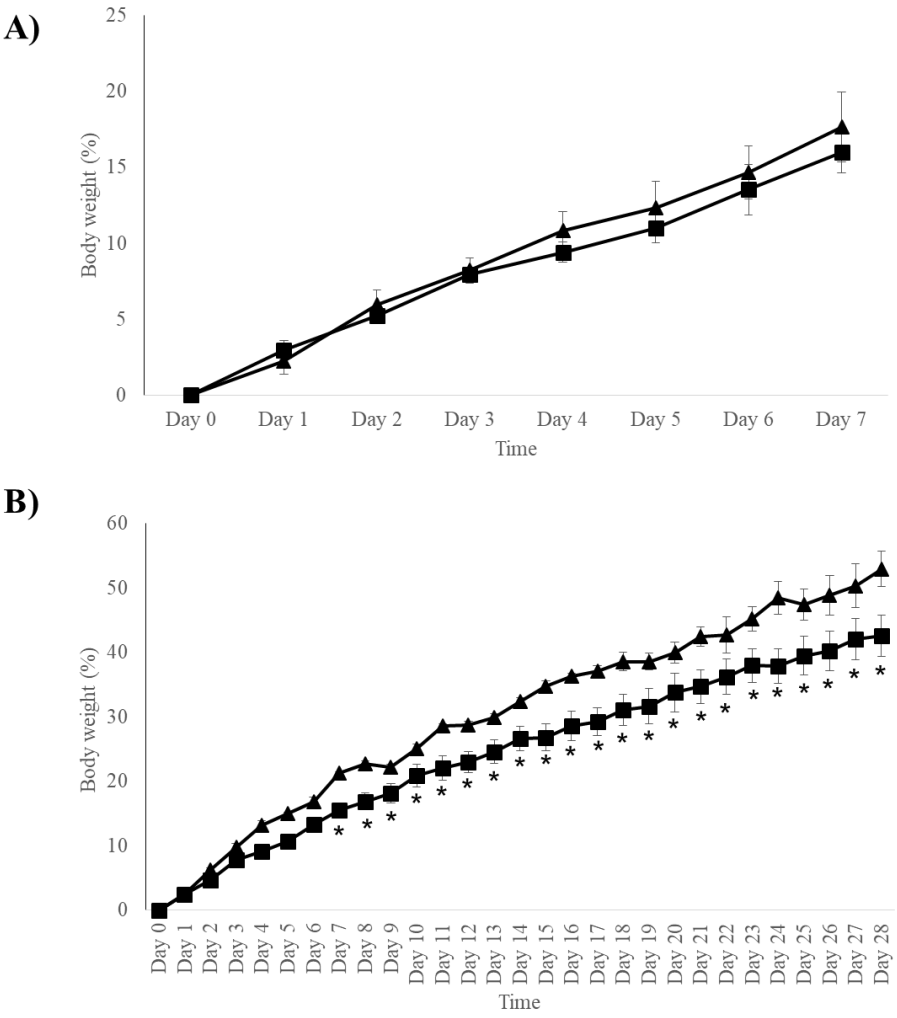

Figure 5-2 The effect of Co treatment on Body weight gain. Rats were given daily i.p. injections of 1 mg/kg $CoCl_2$ for (A) 7 days and (B) 28 days. Triangles in panels (A-B) represent the body weight of rats in control groups (n=3) and squares represent the body weight of rats in Co treated group (n=6). No significant differences exist in the results of body weight gain after 7 days, whereas significantly different body gain weight after 28 days treatment. For 28 days, the control males gained significantly more weight (mean [SEM] per cent) than the Co treated male rats. Data presented as percentage of body weight compared with initial body weight ±SEM, (two-sample t-test, $^{*}p<0.05$ with respect to control).

5.3.1.2 Organ weight

Analysis of organ weight in toxicology studies is an important endpoint for identification of potentially harmful effects of chemicals. Change of organ weight can be the most sensitive indicator of an effect of treatment, as significant differences in organ weight between control and treatment groups might occur in the absence of any morphological changes. Analysis was made very complicated by differences in body weights between groups. Thus, all the data shown for organ weights are the ratio of the organ weight to body weight (to account for differences in body weight). The relationship between organ weight (Heart, Liver, Kidney, Brain, Lung, Spleen and Testis) and body weight has been determined to detect any overt target organ toxicity (Figure 5-3).

No change of any organ weight measured by the organ to body weight ratios was detected (Heart, Liver, Kidney, Brain, Lung, Spleen and Testis) when compared to the control group. The highest organ weight to body weight ratio is liver, which is the heaviest organ that was recorded.

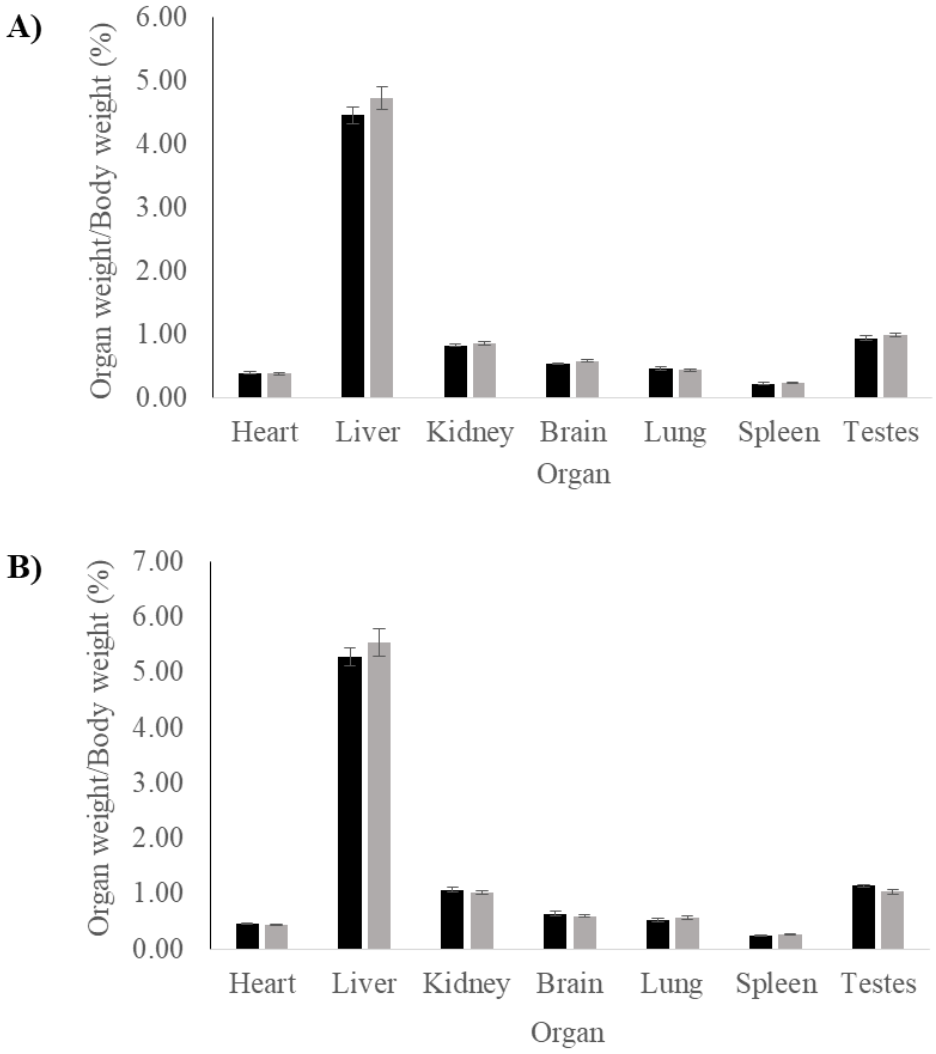

Figure 5-3 The effect of Co treatment on Organ weight: Body weight ratios. The various organ to body weight ratio were unaffected by Co ions after (A) 7 and (B) 28 days. Male Sprague-Dawley rats each weighing 200-250 g were given daily i.p injections of 1 mg/kg $CoCl_2$ (grey, n=6) in distilled water. Control rats (black, n=3) were given a daily i.p injection of distilled water. Data represent ratio ± SEM. All results are not statistically different from their respective controls by two sample t test ($p<0.05$ with a significant difference to control).

5.3.2 Echocardiographic examination.

Figure 5-4 shows the echocardiographic parameters of ventricular performance, which are diastolic and systolic left ventricular (LV) posterior wall measurements (LVPWd and LVPWs), LV end systolic dimension (LVESD), LV end diastolic dimension (LVEDD) and fractional shortening (%FS) from M mode traces. Echocardiography was performed the day the animals were killed (7 and 28 days) and was measured using a short axis view of the heart. Echocardiography showed that the diameter of left ventricular end diastolic / systolic (LVEDD and LVESD) and also the dimension of left ventricular posterior diastolic / systolic (LVPWs/ PVPWd) was similar between control and Co treated animals after 7 and 28 days (see Table 5-1). The exception was the diameter of the left ventricular diastolic dimension (LVEDD), which was reduced when animals were treated with 1 mg/kg $CoCl_2$, by daily i.p injection for 28 days. There was no significant difference in individual left ventricular parameters; LVPWd, LVPWs, LVESD and LVEDD after daily i.p injection of Co over 7 and 28 days. Fractional shortening (%FS) which shows ventricular performance was 64.97 ± 0.91 % and 61.19 ± 2.05 % for control and treated rats, respectively after 7 days. The measurements were 60.29 ± 0.53% and 54.01 ± 0.90% for control and treated rats, respectively after a daily i.p injection for 28 days. Thus, there was a significant reduction in the %FS after the 28 day period treatment of daily i.p injection of 1 mg/kg $CoCl_2$ when compared with control group in the same period but the %FS was not significantly reduced after the 7 day period. From these results, it appears that 1 mg/kg of $CoCl_2$ daily i.p injection for 28 days may cause some compromise in heart function as shown by the percentage fractional shortening. This could indicate compromised filling during diastole, and the potential for increased myocardial stiffness.

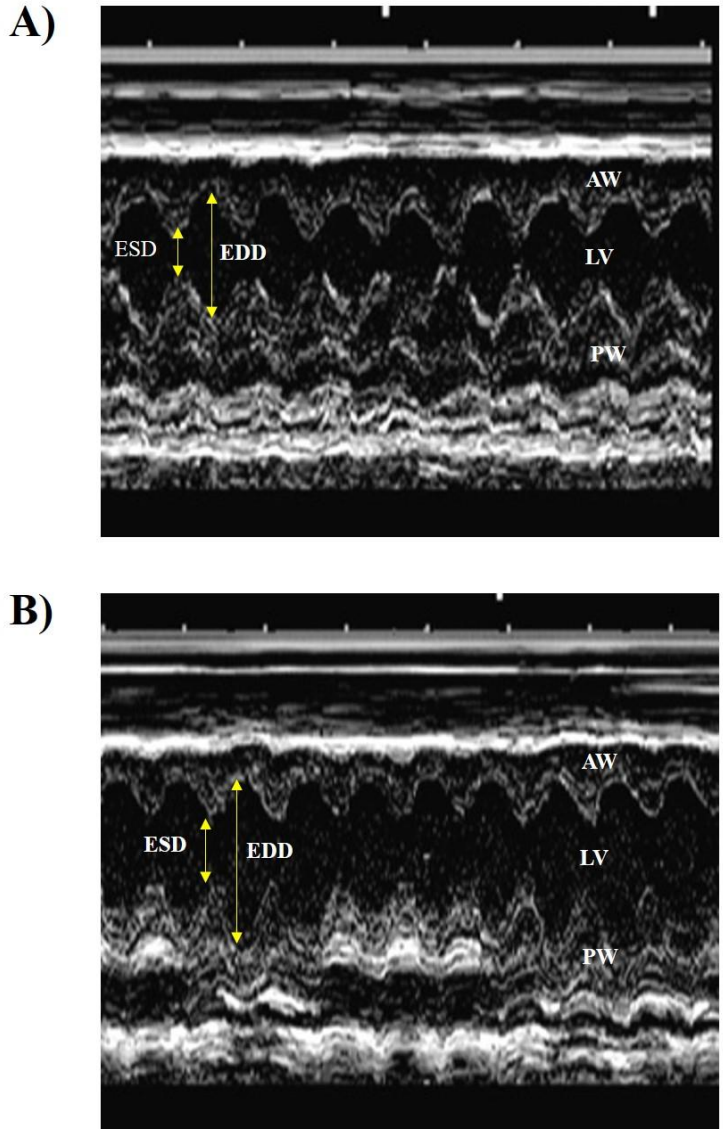

Figure 5-4 An example of the Echocardiogram from rats treated with Co daily for 28 days and control rats. Echocardiogram in the parasternal long-axis view, showing a measurement of the heart's left ventricle. Echocardiography studies were performed in (A) control rats ; (B) Co treated rats; EDD measured from M-mode traces revealed a decrease with Co treated 28 days treatment, (n=6, $p<0.05$). ESD, end-systolic dimension; EDD, end-diastolic dimension; AW, anterior wall; PW, posterior wall; LV, Left ventricle.

Table 5-1 Comparison between control and Co treatment group systolic and diastolic left ventricular (LVPW) posterior wall measurements, LV end systolic dimension (LVESD), LV end diastolic dimension (LVEDD) and fractional shortening (%FS) from M mode traces.

Group	LV end-diastolic diameter (LVEDD;cm)	LV end-systolic diameter (LVESD;cm)	%Fractional shortening	Left Ventricular Posterior wall (LVPW;cm.)	
				Diastolic(d)	Systolic (s)
Control (7 days)	0.56 ± 0.04	0.20 ± 0.02	64.97 ± 0.91	0.19 ± 0.01	0.33 ± 0.01
$CoCl_2$ 1 mg/kg BW (7 days)	0.49 ± 0.02	0.19 ± 0.01	61.19 ± 2.05	0.22 ± 0.01	0.33 ± 0.01
Control (28 days)	0.57 ± 0.01	0.23 ± 0.00	60.29 ± 0.53	0.20 ± 0.01	0.32 ± 0.02
$CoCl_2$ 1 mg/kg BW (28 days)	0.52 ± 0.02	0.24 ± 0.01	54.01 ± 0.90*	0.22 ± 0.01	0.31 ± 0.01

Data represent mean ± SEM. Statistical analysis was carried out using two sample t test. (n = 6, *$p<0.05$ with a significant difference to control). Fractional shortening was significantly reduced in $CoCl_2$-treated rats following 28 days treatment when compared with control animals (54.01±0.90% vs 60.29±0.53%%, n=6, $p<0.05$)

5.3.3 Distribution of Co ions in rats over 7 and 28 days.

Organ and blood distribution of Co ions in untreated and Co treated rats after a daily i.p. injection of 1 mg/kg $CoCl_2$ are shown in Table 5-2 and Figure 5-5. Co was found to enter all the organs of rats and the Co levels in all organs and blood of Co treated rats were significantly different from the controls that had no metal treatment. Significant accumulation of Co in heart, kidney, brain and spleen occurred between 7 and 28 days (ANOVA $p<0.05$; see Table 5-2 and Figure 5-5).

After daily injection of Co over 7 days, levels of Co in organs were: 1,839.86±177.30, 1,536.01±83.95, 307.82±35.74, 185.59±13.92, 176.43±26.52, 68.80±7.25 and 46.85±3.97 ng/g in liver, kidney, heart, spleen, lung, testes and brain, respectively and 99.01±13.83 µg/L in whole blood. After daily injection of Co over 28 days, levels were 2,003.02±178.28, 1,928.02±90.64, 511.14±47.06, 324.44±63.67, 230.51±44.37, 100.48±22.61 and 87.76±10.58 ng/g in kidney, liver, heart, spleen, lung, testes and brain, respectively and 121.00±9.88 µg/L in whole blood.

The two organs that accumulated most Co were liver and kidney (around 1,500-2,000 ng/g); the Co content was more than 4 – 40 times higher than in other organs. Moreover, the concentration of Co ions in whole blood from Co treated rats had significantly increased, and was nearly 100 times more than non-Co treated rats. Significantly higher levels of Co entered heart tissue (307.82±35.74 ng/g and 511.14±47.06 ng/g for 7 and 28 days, respectively) in rats that received Co when compared with untreated rats .In each organ, the Co content was greater after 28 days treatment than at 7 days .From these data, accumulation of Co in heart had significantly increased, and this could cause toxicity to the heart as shown on Table 5-1 where cardiac function is altered by Co treatment of the animals.

Table 5-2 Metal content in each tissue between Co treated and untreated groups after 7 and 28 days i.p. injection. Male Sprague-Dawley rats each weighing approximately 200-250 g were given daily i.p injections of 1 mg/kg $CoCl_2$ (n=6) in distilled water for 7 and 28 days. Control rats (n=6) were given daily i.p injection of distilled water. Co concentration was reported as mean values ±SEM, (one-way ANOVA,$^{*}p<0.05$ with respect to control and $^{\#}p<0.05$ with respect to 7 days injection).

Group	Whole Blood (µg/L)	Heart (ng/g)	Liver (ng/g)	Kidney (ng/g)	Brain (ng/g)	Lung (ng/g)	Spleen (ng/g)	Testes (ng/g)
Control	1.14±0.09	47.62±15.74	92.98±24.37	257.61±30.77	15.48±2.63	23.52±8.14	28.58±6.67	15.38±5.06
$CoCl_2$ 1 mg/kg BW (7 days)	99.01±13.83*	307.82±35.74*	1,839.86±177.30*	1,536.01±83.95*	46.85±3.97*	176.43±26.52*	185.59±13.92*	68.80±7.25*
$CoCl_2$ 1 mg/kg BW (28 days)	121.00±9.88*	511.14±47.06$^{*,\#}$	1,928.02±90.64*	2,003.02±178.28$^{*,\#}$	87.76±10.58$^{*,\#}$	230.51±44.37*	324.44±63.67$^{*,\#}$	100.48±22.61*

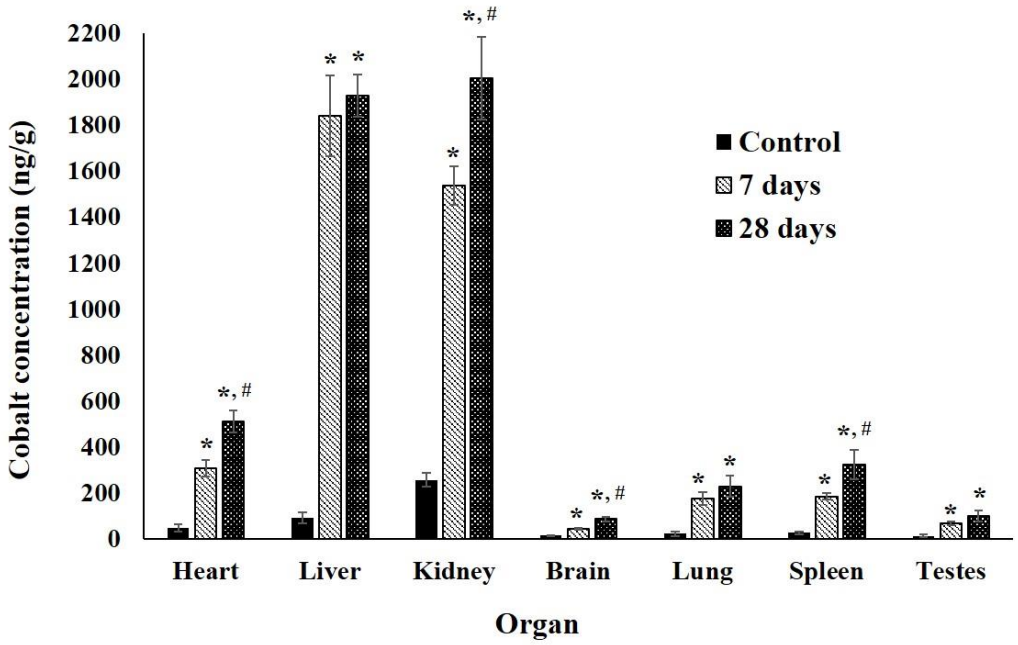

Figure 5-5 Metal content in each tissue between treated and untreated groups after 7 and 28 days daily i.p. injection of Co. Male Sprague-Dawley rats each weighing approximately 200-250 g were given daily i.p injections of 1 mg/kg $CoCl_2$ (n=6) in distilled water for 7 and 28 days. Control rats (n=6) were given daily i.p injection of distilled water. Co concentration was reported as mean values ±SEM, (one-way ANOVA,*$p<0.05$ with respect to control and, $^{\#}p<0.05$ comparing 7 and 28 days.

5.3.4 Immunoblotting of the CaMKII family of proteins in the hearts of Co treated rats.

Samples of homogenate from all the organs were collected and stored at -80°C, in aliquots. The total protein content of each of the homogenates was determined by the Lowry assay, and up to 20 µg total protein was run in the agarose gel. The parameters that were used for immunoblotting in this experiment, were the same as those in chapter 3.

All heart tissue homogenates were probed with specific antibodies (CaMKIIδ, ox-CaMKII and p-CaMKII, DMT1, TRPC6 and TRPM7), as previously described in section 3.3.8. The results are shown as expression of protein of interest compared with the expression of GAPDH as a ratio of the optical densities.

5.3.4.1 Expression of Total-CaMKIIδ, ox-CaMKII and p-CAMKII in control and Co treated rat heart homogenates.

Western blot analysis showed CaMKII (CaMKIIδ, ox-CaMKII and p-CaMKII) expression in heart tissue of both untreated and treated rats. Co treatment of rats resulted in a significantly higher protein level of CaMKIIδ (0.64 ± 0.01 vs. 0.59 ± 0.02, Co-treated vs untreated after 28 days) ($p<0.05$). Whereas after 7 days, the results showed no change in CaMKIIδ level (0.75 ± 0.03 vs. 0.83 ± 0.04, Co-treated vs untreated). p-CaMKII shows two bands therefore the optical density of both molecular weights was taken as the expression of p-CaMKII, with a molecular weight of ~60 kD. Both protein expression levels of ox-CaMKII and p-CaMKII were increased slightly after the 7 day treatment period and there was a decrease in the protein level of ox-CaMKII and p-CaMKII after 28 days treatment.

None of these changes were significant compared with the controls. As shown in Figure 5-6, Figure 5-7 and Table 5-3, there is obvious expression of p-CaMKII in whole heart homogenate which is not observed in cell (CF) preparations.

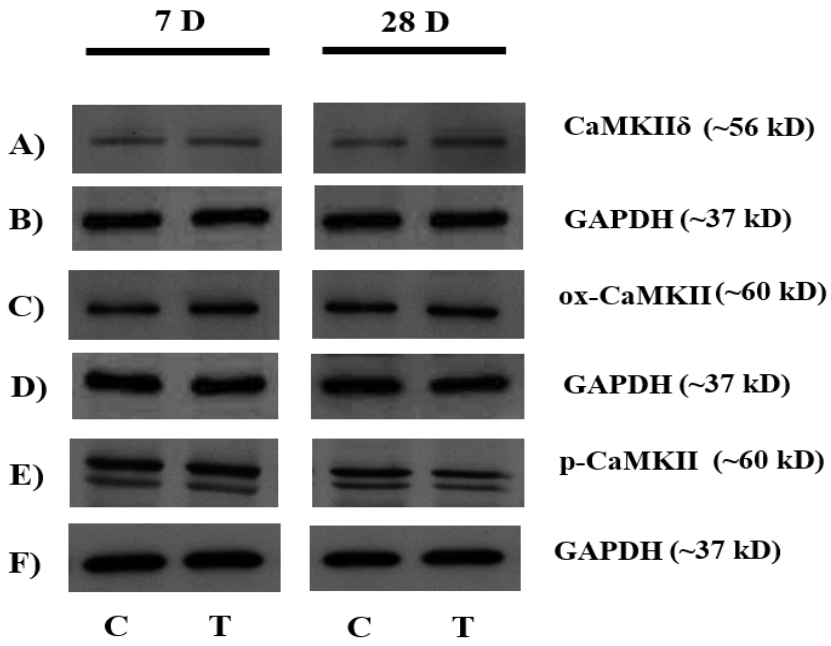

Figure 5-6 Effects of $CoCl_2$ treatment on CaMKIIδ, ox-CaMKII and p-CaMKII expression in rat hearts. Results of expression of **(**A**)** CaMKIIδ, **(**C**)** ox**-** CaMKII, (E) p**-**CaMKII and (B, D and **F**) GAPDH**.** p-CaMKII shows as two bands on the immunoblot**.** Quantification was carried out on the both upper and lower bands, a molecular weight of ~60 kD**.** C **(**control rats**)**, T **(**Co treated rats**).**

Table 5-3 Quantitative analysis of CaMKII family protein expression in rat hearts. Western blot analysis of CaMKIIδ, ox-CaMKII and p-CaMKII in rat hearts (control rats and Co treated rats 1 mg/kg BW, daily i.p injection for 7 and 28 days).

Group	CaMKII Family		
	CaMKIIδ	**ox-CaMKII**	**p-CaMKII**
Control (7 days)	0.83 ± 0.04	0.99 ± 0.10	0.88 ± 0.04
$CoCl_2$ 1 mg/kg BW (7 days)	0.75 ± 0.03	1.04 ± 0.02	0.94 ± 0.06
Control (28 days)	0.59 ± 0.02	0.73 ± 0.06	0.79 ± 0.11
$CoCl_2$ 1 mg/kg BW (28 days)	0.64 ± 0.01*	0.69 ± 0.04	0.69 ± 0.05

Data represent mean ± SEM fold over control and Statistical analysis was carried out using two-sample t-test (n = 3 for control group and n = 6 for treated group, *$p<0.05$ with a significant difference to untreated cells). BW, Body weight; CaMKIIδ, Total-CaMKIIδ; ox-CaMKIIδ, oxidised CaMKII; p-CaMKII, phosphorylated CaMKII, Results are expressed as the ratio of the density values for the protein of interest in relation to the density value for GAPDH, which acted as a loading control.

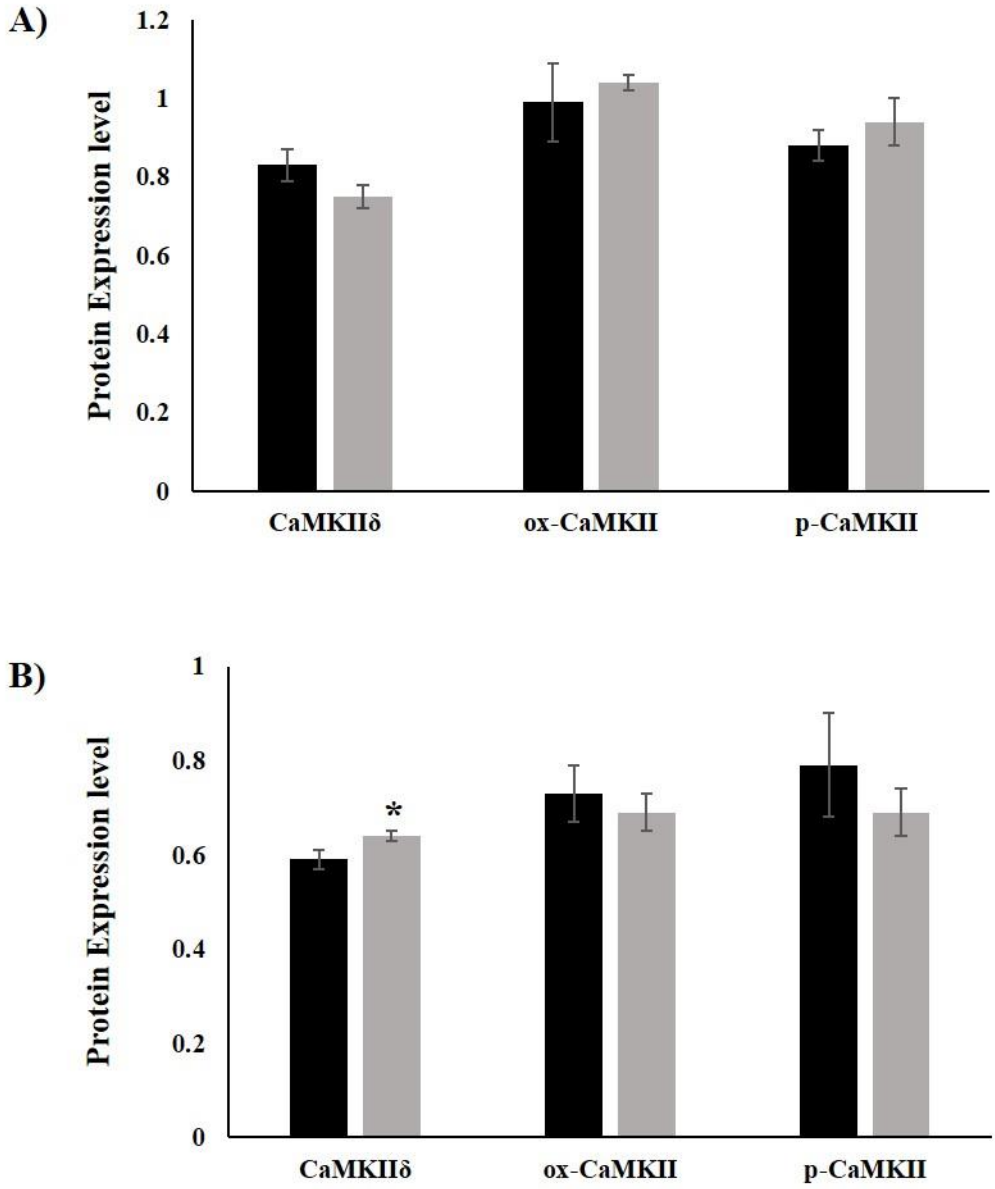

Figure 5-7 Relative expression of CaMKIIδ, oxidised-CaMKII (ox-CaMKII) and phosphorelated-CaMKII (p-CaMKII) in rats' hearts. Histrogram demonstrating the expression of CaMKII (A) 7 days and (B) 28 days after treatment with $CoCl_2$. Control (black) and Co treatment (grey), compared with control groups. (Mean ± SEM) Statistical analysis was carried out using two-sample t-test ($n \geq 3$, **p<0.05*, treatment group vs. control group). Heart lysates were analysed by western blot for CaMKIIδ, ox-CaMKII and p-CaMKII with specific antibody **.**CaMKIIδ means Total-CAMKIIδ, ox-CaMKII means oxidised CaMKII, p-CaMKII means phosphorylated CaMKII**.** The expression is presented as the ratio of the density value for the protein of interest compared with that of GAPDH, loading control.

5.3.4.2 Expression of potential Co transporters in the hearts of Co treated rats.

From the samples collected during the *in vivo* experiment, we investigated the expression of potential Co transporters; DMT1, TRPC6 and TRPM7 expression in whole heart homogenates by western blotting, as shown in Figure 5-8. The results are shown as expression of protein of interest compared with the expression of GAPDH as a ratio of the optical densities. As illustrated in Table 5-4 and Figure 5-9, $CoCl_2$ treatment significantly decreased the expression of DMT1 in the heart homogenates (1.91 ± 0.11 after 7 days of Co treatment compared with 2.67 ± 0.16 in controls) compared with control ($p < 0.05$). Whereas after Co treatment of rats for 28 days, the expression of DMT1 was close to the control group values (1.55 ± 0.09 compared with 1.65 ± 0.22 in controls).

Interestingly, TRP channel, TRPC6 and TRPM7 expression were both significantly increased in the heart samples following $CoCl_2$ treatment by 0.79 ± 0.04 compared with 0.67 ± 0.03 for TRPC6 and 0.99 ± 0.06 compared with 0.74 ± 0.14 for TRPM7, respectively after 28 days treatment. This induction was not evident for either protein after 7 days Co treatment of animals. Expression of both TRP channels, TRPC6 and TRPM7, are therefore altered following 28 days $CoCl_2$ treatment and could possibly be involved in Co uptake. Perhaps, these proteins (in particular the elevated TRP channels) may serve as potential molecular targets for preventing or minimising Co uptake into heart tissue *in vivo*.

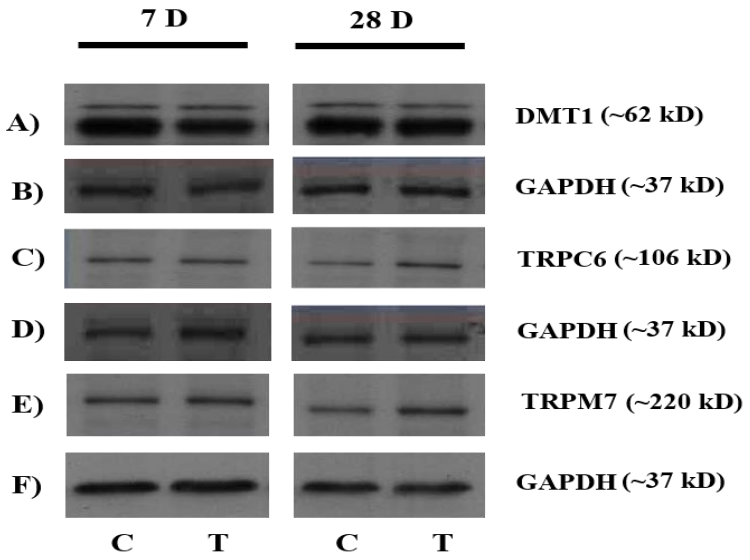

Figure 5-8 Effects of $CoCl_2$ on Co tranporter (DMT1, TRP channels (TRPC6 and TRPM7)) expression after Co-treatment in rats' hearts. Results of expression of (A) DMT1, (C) TRPC6, (E) TRPM7 and (B, D and F) GAPDH. Protein expression was determined by western blotting. Heart lysates were analysed by western blot for transporter with specific antibodies. DMT1 shows as two bands on the immunoblot. Quantification was carried out on the both upper and lower molecular weight band, MW = ~62 kD. Divalent metal transporter (DMT1), TRPC6 means Transient receptor potential/canonical receptor subtype 6; TRPM7 means Transient receptor potential/melastatin receptor subtype7, D means day, C mean control rats, T means Co treated rats.

Table 5-4Quantitative analysis of Co transporter protein expression in rats' hearts. Western blot analysis of DMT1, TRPC6 and TRPM7 in rat hearts (control rats and Co treated rats 1 mg/kg BW, daily i.p injection for 7 and 28 days).

Group	Co Transporter		
	DMT1	**TRPC6**	**TRPM7**
Control (7 days)	2.67 ± 0.16	0.85 ± 0.03	0.68 ± 0.07
$CoCl_2$ 1 mg/kg BW (7 days)	1.91 ± 0.11*	0.88 ± 0.08	0.64 ± 0.02
Control (28 days)	1.65 ± 0.22	0.67 ± 0.03	0.74 ± 0.14
$CoCl_2$ 1 mg/kg BW (28 days)	1.55 ± 0.09	0.79 ± 0.04*	0.99 ± 0.06*

Data represent mean ± SEM. Statistical analysis was carried out using two-sample t-test (n = 3 for control group and n = 6 for treated group, $*p<0.05$ with a significant difference to untreated cells). BW, Body weight; Divalent metal transporter (DMT1); TRPC6, Transient receptor potential/canonical receptor subtype 6; TRPM7, Transient receptor potential/melastatin receptor subtype 7. Results are expressed as the ratio of the density values fot the protein of interest in relation to the density value for GAPDH, which acted as a loading control.

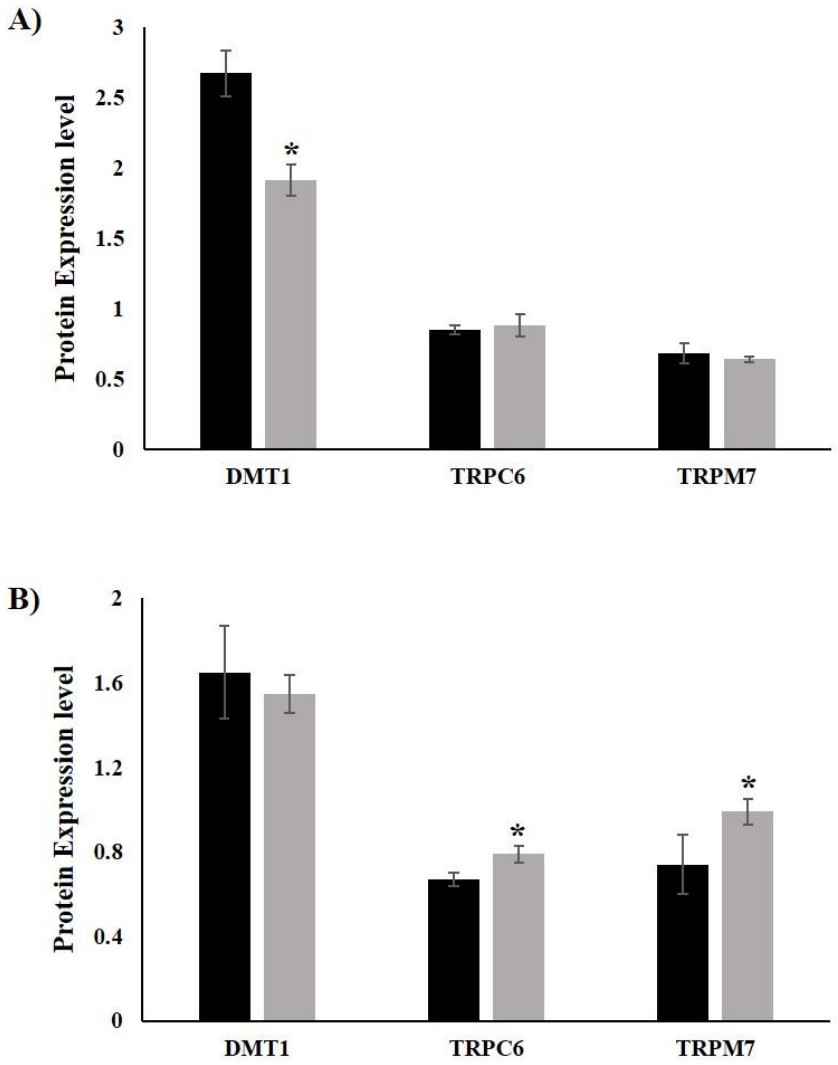

Figure 5-9 Relative expression of DMT1, TRPC6 and TRPM7 in rats' hearts. Western blotting demonstrating the expressions of all protein expression level (DMT1, TRPC6 and TRPM7) for (A) 7 days and (B) 28 days after treatment with $CoCl_2$. Control (black) and Co treatment (grey), compared with control groups. (Mean ± SEM) Statistical analysis was carried out using two-sample t-test ($n \geq 3$, **p<0.05*, treatment group vs. control group). Heart lysates were analysed by western blot for DMT1, TRPC6 and TRPM7 with specific antibodies. Divalent metal transporter (DMT1), TRPC6 means Transient receptor potential/canonical receptor subtype 6; TRPM7 means Transient receptor potential/melastatin receptor subtype7. The expression is presented as the ratio of the density value for the protein of interest compared with that of GAPDH, loading control.

5.3.5 Summary of major findings

In this chapter, *in vivo* experiments on rats were carried out to determine the toxicological effects of $CoCl_2$ by observation (Body weight) , cardiac function (echocardiography) and organ distribution of Co ions. These have been studied compared to the untreated group by sacrificing all the animals on day 7 or day 28. Moreover, western blotting of CaMKII, DMT1 and TRP channels (TRPC6 and TRPM7) in the heart tissue homogenate has been examined to understand the mechanism of toxicity and to identify potential target proteins for future intervention studies. The main findings of this study are:

- No major changes in behaviour were observed between groups.
- No obvious toxicity signs were observed in the Co treatment group (7 and 28 days, daily i.p injections of 1 mg/kg $CoCl_2$) compared to the control group.
- No significant differences in the ratios of each weight of body and organ were observed during study (7 and 28 days, daily i. p injections of 1 mg/ kg) compared with control group.
- Echocardiography showed evidence of altered cardiac function (significant decrease in % FS) in rats following 28 days of $CoCl_2$ treatment. Cumulative Co exposure was associated with echocardiographic changes indicating altered left ventricular diastolic function. This suggests there may be some compromise in contractile function in these animals with impaired relaxation of the heart.
- Significant Co accumulation was observed in all organs studied. The kidney and liver showed the highest Co levels, followed by the heart. Relevant to compromised cardiac function is the significant accumulation of Co observed in the heart.
- Western blot analysis confirmed increased levels of total CaMKIIδ protein in heart lysates after 28 days administration of $CoCl_2$ treatment whereas no change in activation of CaMKII was evident (ox-CaMKII and p-CaMKII).
- In cardiac cells, increased expression of TRPC6 and TRPM7 transport channel proteins is induced by $CoCl_2$ after 28 days administration. These transporters might mediate uptake of Co^{2+} into the heart and thus contribute to compromised heart function.

5.4 Discussion

Based on what was discussed earlier in chapter 4 about the limitations of primary culture, *in vivo* study was chosen to support the study of the long term effects of Co. This is particularly because of limitations with long term treatment of primary cardiac fibroblast cells. To study cardiotoxicity, the toxic effect of a dose of Co (1 mg/kg BW) administered daily by i.p injection to the rat for 7 and 28 days has been investigated. The studies revealed that $CoCl_2$ administration had no effect on body weight, and all rats survived for the period of experiment (7 and 28 days). Some abnormality of heart function was observed after 28 days administration, but all body and organ weights were similar in the control and experimental rats at both exposure times. The dose of Co we used is very low when compared with the lethal dose. A LD_{50} value of 35 mg/kg BW i.p was calculated in rats (Van Liew and Chen, 1972). Several studies have reported rodents receiving a high oral dose of $CoCl_2$ (40 mg/kg, daily for up to 4 months) and showing no severe systemic toxic effects and/or mortality.(Endoh *et al.*, 2000; Rakusan, Cicutti and Kolar, 2001). Similarly, in humans, no mortality and no appreciable toxic effect was observed on thyroid or liver function in patients under anaemia therapy condition (75–100 mg daily for 6 –9 months) (Holly, 1955; Scott and Reilly, 1955).

The evidence presented in this chapter from chronic Co exposure in rats suggests that Co induces alterations in cardiac function and protein expression even at the lower dose used in this study. Haemodynamic changes such as a decrease in left ventricular end diastolic diameter (LVEDD) and resultant changes in fractional shortening were clearly observed at 28 days after Co treatment. Our results are similar to results obtained by Murakoshi and coworkers. They also reported that left ventricular fractional shortening was significantly decreased in the $CoCl_2$ treated group (5 mg/kg BW, i.p twice a day for 3 wks) compared with that in the control group (47.4± 3.3% vs 57.7± 3.6%). The treatment also markedly increased myocardial expression of prepo- endothelin- 1 and natriuretic peptide (ANP) mRNA. These are molecular markers of heart failure (Murakoshi *et al.*, 2000).

Although the fractional shortening calculated from our research is not as much attenuated as that described by Murakoshi et al., it follows a similar trend, thus

confirming that $CoCl_2$ affects cardiac function in rats. The dose we used was much smaller than that used by Murakoshi, that approximates to the Co ion levels detected in patients with MoM implant. Therefore, it might be assumed that 1mg/kg BW for 28 days causes compromised heart function in rats. Signs of systolic cardiac dysfunction include reduced ejection fraction (EF), fractional shortening (FS), and left ventricular end diastolic diameter (LVEDD) (Horowitz *et al.*, 1988; D'Adda *et al.*, 1994).

With reference to the impaired contractile function of the hearts in Co-treated animals, it is likely that Co affects Ca^{2+} handling in the cardiac myocytes. This could be at a number of levels. Reduced contraction and/or relaxation is associated with impaired function at the level of the L-type Ca^{2+}channel affecting Ca^{2+} entry to the cell and/or depressed SR function whereby the ryanodine receptor (RyR) and sarco/endoplasmic reticulum Ca^{2+}ATPase (SERCA2a) and its regulator protein phospholamban (PLB) activity are both altered. Ca^{2+} binding to, and release from, troponin C within the myofilaments is likely to be affected and this will ultimately affect the contractile performance of the heart. Data shown in this study suggest impairment of relaxation following Co treatment therefore it is possible that Co has a greater effect on cytosolic Ca^{2+} removal via SERCA2a and/or the sarcolemmal Na^{+} and Ca^{2+} exchanger (NCX) causing impaired lusitropy (Luo & Anderson., 2013).

In most cardiac diseases the initial sign of dysfunction is impaired relaxation. Higher Co exposure was associated with altered left ventricular diastolic function, as measured by echocardiography(Oh, Seward and Tajik, 2006). Akinrinde and coworker reported that Co treatment of rats (350 mg/kg in drinking water) resulted in attenuation of systolic, diastolic and mean arterial pressures taken after 7 days of administration and also histopathological lesions including myocardial infarction and inflammation, renal tubular necrosis and inflammation (Akinrinde *et al.*, 2016). Rona also studied the extensive myocardial damage in rats treated with high Co exposure (oral dose, 100 mg/kg cobalt sulfate)(Rona, 1971)(see Table 5-5).

Table 5-5 List of Co effects on rat after Co exposure.

Dose	Effect	Author
Higher $CoCl_2$	Altered left ventricular diastolic function	(Oh, Seward and Tajik, 2006)
350 mg/ kg $CoCl_2$ in drinking water	Systolic, diastolic and mean arterial pressures, renal tubular necrosis and inflammation	(Akinrinde *et al.*, 2016).
100 mg/ kg $CoSO_4$ (one time)	Myocardial damage	(Rona, 1971)

In addition, D' Adda and colleagues reported that accumulation of Co in the myocardium might result in increased myocardial stiffness (D'Adda *et al.*, 1994). The curiously individual variance of Co - induced cardiotoxicity has been well recognised by several investigators(Alexander, 1969; Grice *et al.*, 1969, 1970; Wiberg *et al.*, 1969). The potential of Co to be toxic could be affected by various factors including route of administration, pre-existing heart damage, age of animal, length of exposure, nutritional status, and dietary composition (e. g. , low protein and high alcohol concentration) (Alexander, 1969; Wiberg *et al.*, 1969).

Several researchers have attempted to investigate this Co induced pathological variability in humans by using animal models of Co induced cardiomyopathy (Grice *et al.*, 1969, 1970; Mohiuddin *et al.*, 1970; Morin, Têtu and Mercier, 1971). Analysis of the morphological changes in the myocardial lesions induced by Co administration in different species and the effects of various modifying factors in the severity of Co cardiotoxicity have also been investigated. For instance, in a canine model, Co caused cardiomyopathy after a daily intravenous dose of 5 mg/kg $CoSO_4$ in conjunction with a low-protein, low thiamine diet (Unverferth *et al.*, 1984) and administration of Co via chronic exposure up to 6 months resulted in a noticeable decrease in the activity of manganese superoxide dismutase, which is involved in mitochondrial ATP production in rat myocardium (Clyne *et al.*, 2001).

Despite its detrimental effect, $CoCl_2$ has also been identified as having cytoprotective effects. For example, chronic treatment with $CoCl_2$ (75 mg/kg, 3 times/wk for 5 wk) caused significant angiogenesis in rat myocardium (Rakusan, Cicutti and Kolar, 2001). Long- term effects of low- dose $CoCl_2$ (orally, 5 mg/ kg for 4 wk) were also found to

enhance postischemic ventricular function of rats (Endoh *et al.*, 2000). $CoCl_2$ has been observed as cytoprotective not only in the heart but also in other organs including the brain (Bergeron *et al.*, 2000), liver (Kato *et al.*, 2001), and kidneys (Matsumoto *et al.*, 2003).

In vitro, in hepatoma HepG2 cells, $CoCl_2$ has been shown to decrease the number of apoptotic cells as measured by DNA fragmentation after inducing toxicity with tert-butyl hydroperoxide and serum deprivation (Piret *et al.*, 2002). In addition, pretreatment with Co protoporphyrin has been shown to reduce the number of apoptotic myocytes/ endothelial cells in the rat heart 24 h after cold ischemia/ reperfusion (I/R) injury. That resulted in a significant improvement in cardiac graft survival (Katori *et al.*, 2002). Therefore, Co has been proposed as an effective inducer of ischemia-resistant phenotype for some applications eg. organ transplantation or bypass surgeries.

In order to help predict the deposition of Co ions in patients after their release from MoM implants, the organ distribution pattern of Co ions in rats after an intra-peritoneal (i.p.) injection of 1 mg/kg $CoCl_2$ was studied in this thesis.

Following an intraperitoneal injection Co is rapidly taken up by the tissues and, although the majority of the metal may leave the body rapidly, prolonged administration means a small amount is retained for longer periods of time. The distribution of Co in the liver, kidney, heart, brain, spleen, lung, testes and blood of treated rats is presented in the results section (Figure 5-5) Co rapidly reaches a high level in the liver and kidney. There are small increases in the heart and whole blood, while minimum concentrations are found in the brain, spleen, lung and testes on prolonged administration. These results are similar to those found in other studies observing the accumulation of Co after injection (Battaglia *et al.*, 2009; Afolaranmi *et al.*, 2012; Afolaranmi and Grant, 2013). However, a dose of $CoCl_2$, which is more soluble, is excreted primarily via faeces (70-83% of administered dose) in rats, with urinary excretion accounting for the remainder of the dose (Barnaby, Smith and Thompson, 1968; Hollins and McCullough, 1971).

The kidney and liver showed the highest Co levels, followed by heart, spleen, lung, testes and brain, in descending concentration order. The comparison of Co content in each organ between 7 days and 28 days after daily i.p injection showed that there were 4 organs (Heart, Kidney, Brain and Spleen) that had significantly higher Co levels after 28 days when compared with 7 days injection. Co ions appear to be stored and deposited in heart tissue in a time dependent manner, which may be a cause of the cardiotoxicity. There are some studies *in vivo* that measured the deposition of Co in patients with metal implants, and the organ distribution pattern of Cr and Co ions in mice after implantation of CoCr nanoparticles (Afolaranmi *et al.*, 2012). Some studies showed that metal particles can be distributed through the body and have been detected in spleen and liver of patients postmortem indicating that metal released from MoM implants can spread and accumulate in many body organs (Langkamer *et al.*, 1992). Most accumulated in the liver, kidneys, heart and spleen, while minimum concentrations levels are found in the blood serum, brain and pancreas (Kravenskaya and Fedirko, 2011).

From the data on Figure 5-5, it is evident that the Co concentration in the organs is increasing significantly in the heart, brain, spleen and kidney between 7 and 28 days, and has not reached steady state, however this is not the case with blood Co content (Table 5-2). In blood, there is no significant difference between 7 and 28 days Co levels. It is not clear whether a steady state situation has been reached by 28 days, but certainly organ Co uptake could continue beyond 28 days. It would be essential to repeat this experiment using longer exposure times perhaps up to 3 months.

An important point is that the toxicity of Co depends on strong accumulation over a period of time, and Co ions appear to be stored and deposited in heart tissue in the long- term. Here, we report a significant accumulation of Co in the heart - 307.82±35.74 ng/g and 511.14±47.06 ng/g for 7 and 28 days, respectively. Co deposition in the heart tissue and the percentage of fractional shortening (%FS) in Table 5-1 may be correlated, but there are insufficient data to make a definite correlation.

It is important to note that concentrations of Co in the blood circulation of the rats is equivalent to that measured in the blood of patients with MoM implants. In the rats, the level of Co in whole blood was around 100 times more than control, 99.01 ± 13.83 and 121.00 ± 9.88 μg/L, on both 7 and 28 days, respectively. In the MoM patients, levels of Co in serum have been detected that are more than 100-fold that of physiologic levels (0.032-0.29 μg/L) (De Smet *et al.*, 2008). One case study reported that the level of Co in patients with MoM implants was 23 μg/L, and this was reported along with an echocardiogram showing diastolic dysfunction(McLaughlin L. 2010). However, a variety of Co levels in patient blood have been reported in many studies in chapter 1. Wapner and Okazaki reported that rats are a good animal model for investigating the response to orthopaedic implants in patients in terms of metal ion release. (Wapner, Morris and Black, 1986; Okazaki *et al.*, 2004).

There are a wide variety of blood Co levels reported in MoM patients, and a variety of adverse effects from exposure to metal reported, such as hip pain, fatigue, hypothyroidism, hearing or vision loss, cardiac abnormalities and polyneuropathy. In many of these patients the Co concentration in whole blood and serum were reported to be from 398 μg/L to 625 μg/L, and these may represent severe cases of toxic response. All of the symptoms improved after surgical revision, when the blood Co level was significantly decreased returning to within the normal physiological range (Oldenburg, Wegner and Baur, 2009; Rizzetti *et al.*, 2009; Ikeda *et al.*, 2010; Pelclova *et al.*, 2012). Alterations in organ function in response to Co exposure may therefore be reversible. This would be an interesting study to set up with the rat model. It remains to be established how Co^{2+} exerts its cardiotoxic effects and what the cellular mechanism(s) of action may be. Possible mechanisms of cytotoxicity were explored initially using immunoblotting to determine expression of selected proteins in order to gain an insight into an alterations in profile.

The first protein investigated by immunoblotting was expression of CaMKII (Total CaMKIIδ, ox-CaMKII and p-CaMKII). Given the pivotal role that CaMKII plays in cardiac dyfunction during disease, it was expected that CaMKIIδ would be significantly elevated following Co exposure and may affect other toxicologically-related pathways. CaMKII is a major regulator of Ca^{2+} homeostasis and is vital for

cardiac function (Simmerman *et al.*, 1986; Hohenegger and Suko, 1993; Anderson *et al.*, 1994; Hawkins, Xu and Narayanan, 1994).

A key factor contributing to systolic and diastolic dysfunction and ultimately heart failure is abnormal Ca^{2+} handling and altered CaMKII expression and activation (Beuckelmann, Näbauer and Erdmann, 1992; Takahashi *et al.*, 1992; De Tombe, 1998). To see whether this also holds true for Co-induced cardiac effects, expression of CaMKII was compared in normal left ventricular tissue with corresponding tissue from Co treated rats.

Western blotting performed using left ventricular tissue of Co treated rats showed a significant increase in expression of CaMKIIδ at the protein level (0.64 ± 0.01 vs 0.59 ± 0.02 in untreated group). We observed a similar effect with *in vitro* studies on primary cardiac fibroblasts, as previously described in section 3.3.8.1. After increasing exposure to Co concentration (between 0.1-10 µM) at 72 h there was a change in expression of CaMKIIδ. In comparison, activated CaMKII (ox-CaMKII and p-CaMKII) in Co-treated rats did not show any changes of expression when compared with control group.

Much to our pleasure, our data characterised for the first time the CaMKIIδ expression pattern in left ventricular tissue of rat hearts following treatment with $CoCl_2$ injection and correlated these changes with functional changes using echocardiographic measurement. After 28 days administration, there was a significant increase in CaMKIIδ expression combined with significantly increased Co uptake in heart tissue. Both events might have a role in the reduced percentage of fractional shortening. A relationship between increased level and activity of CaMKII along with altered cardiac calcium handling and contractility in reference to the characteristics of heart disease has been reported in many studies (Zhang *et al.*, 2005; Sag *et al.*, 2009; Dybkova *et al.*, 2011; Martin *et al.*, 2014). For the reasons mentioned above, we can assume that CaMKII is possibly a target of $CoCl_2$ and changes in this enzyme expression might be causing problems related with heart induced toxicity as previously reported.

As explained above, CaMKII plays a vital role in cardiac disorders. This is confirmed by the up-regulation of the kinase in human and animal models of cardiac remodelling

and heart failure(Kirchhefer *et al.*, 1999; Kato *et al.*, 2000; Maier and Bers, 2002; Colomer *et al.*, 2003). Increased myocardial CaMKII activity and expression have been found in various animal models (Rude *et al.*, 2005; Dai *et al.*, 2011; Currie and Smith, 1999; Anderson, Brown and Bers, 2011) of cardiac disease.

In animal models, Martin revealed that CaMKIIδ expression (relative to GAPDH) was increased in hypertrophied compared to sham animals (0.41±0.05 vs. 0.27±0.03) along with the phosphorylation status of CaMKII (p-CaMKII), which was significantly increased in MTAB hearts (0.38±0.06 vs. 0.24±0.03, MTAB vs. sham), thus providing evidence that the activity of CaMKIIδ was increased in hypertrophied hearts (Martin *et al.*, 2014). In addition, mice overexpressing cardiac-specific CaMKIIδ also developed significant cardiac chamber enlargement, myocardial dysfunction, and loss of cellular Ca^{2+} homeostasis (Maier *et al.*, 2003).

In human heart, Hoch suggested that the changes in CaMKII isoform expression at both mRNA and protein level in dilated cardiomyopathy may reflect a significant role of this enzyme class in human heart failure (Hoch *et al.*, 1999). In human heart failure, CaMK activity was increased almost 3-fold and was suggested to be compensatory correlating positively with the cardiac index and ejection fraction of patients (Kirchhefer *et al.*, 1999). The suggestion of CaMKII as a possible modulator of cardiac disease encouraged the use of pharmacological tools to target this kinase in the heart, in order to inhibit dysfunctional responses (Zhang, 2004; Couchonnal and Anderson, 2008; Anderson, Brown and Bers, 2011; Maier, 2012). This included the selective inhibition of CaMKII activity, which could be a tool to protect against cardiac remodelling and maintain myocardium function by pharmacological or transgenic approaches (Hempel *et al.*, 2002; Zhang *et al.*, 2005). Khoo reported that CaMKII inhibition can reduce arrhythmias and mortality and improve myocardial function even in mice with severe cardiomyopathy due to overexpression of the Ca^{2+}/CaM activated phosphatase 2B reduce left ventricular dilation and improve myocardial function after surgical myocardial infarction in mice (Khoo *et al.*, 2004). Given these properties, this enzyme has been highlighted as an important target for therapeutic approaches in the future. It is of note that in the potentially toxic environment created following Co

treatment in the present study, CaMKII (an enzyme known to be elevated during cardiac disease) is significantly up-regulated.

In addition to studying CaMKII, western blotting was also used to determine whether transporter mechanisms involving DMT1 and TRP channel proteins may be important as a mode of Co transport into cardiac cells. The involvement of TRP channels such as TRPC6 and TRPM7 in transport of Ca and Na ions is documented, and their contribution to transport of metal ions like Zn, Mg, Mn and Co is well understood (Bouron, Kiselyov and Oberwinkler, 2015). In addition, DMT1 has broad specificity transporting many divalent metal ions including Co (Park, Cherrington and Klaassen, 2002; Forbes and Gros, 2003; Griffin *et al.*, 2005).

Regarding DMT1, it is a widely expressed mammalian iron transporter that is energised by the H^+ electrochemical potential gradient across cells (Gunshin *et al.*, 1997; Mackenzie *et al.*, 2006, 2007). DMT1 is a H^+-coupled metal-ion transporter role that plays essential roles in iron homeostasis. It exhibits reactivity with a broad range of metal ions being a likely route of entry for the toxic heavy metal cadmium, and also Co, manganese, and vanadium (Illing *et al.*, 2012).

Interestingly, DMT1 expression in primary cardiac fibroblasts at 1 and 10 µM $CoCl_2$ doses, 48 h, is reduced, where after 72 h exposure, no changes were evident when compared with untreated cells. In *in vivo* studies, the DMT1 levels are diminished on 7 days exposure but the expression of DMT1 was not affected after 28 days.

As previously presented in Figure 3-21 and described in section 3. 4, DMT1 is regulated by Ndfip1. Howitt demonstrated that Ndfip1- binding to DMT1 is instrumental for ubiquitination and downregulation of DMT1 and identified Nedd4–2 as an ubiquitin ligase for polyubiquitination of DMT1 under metal- induced stress (Howitt *et al.*, 2009). In the same manner, western blot analysis in $Ndfip1^{-/-}$ mice showed an increased level of DMT1 protein and it is of interest to know whether other metal entry pathways were disrupted due to the misregulation of DMT1(Howitt *et al.*, 2009).

As regards the critical role of DMT1 in iron homeostasis, Illing found that DMT1 favors Fe^{2+} over any of its other physiological substrates and that Co^{2+} and Mn^{2+} are also transported with moderately high affinity (Illing *et al.*, 2012). Whether DMT1 serves the physiological absorption or cell-specific transport of Co, Zn, or Va remains to be established using specific cell preparations or rodent models. Co and Fe appear to share a common absorptive pathway in the rat(Schade *et al.*, 1970; Thomson, Valberg and Sinclair, 1971).

The other two protein transporters investigated that might be involved in Co transport were TRPC6 and TRPM7. Several types of TRP channel have recently been described in the heart of different species. They include TRPC6 in human (Kuwahara *et al.*, 2006) and rat (Inoue, Jian and Kawarabayashi, 2009b) cardiac tissue and TRPM7 in human (Du *et al.*, 2010), rat and pig cardiac tissue (Gwanyanya *et al.*, 2004, 2006).

The important role of TRPC channels in cardiac hypertrophy has been extensively studied and it appears that all TRPC isoforms with exception of TRPC2 are involved in cardiac hypertrophy as decribed in section 3.4. In particular, TRPC6 plays an important role in cardiac hypertrophic responses in the mouse model, and is also upregulated in patients with heart failure (Kuwahara *et al.*, 2006).

Similarly, a growing number of studies have demonstrated an altered TRPM7 protein expression in a number of diseases, especially cardiac disease. In the heart, much of our understanding of the role of TRPM7 in cardiac pathophysiology has been obtained from studies involving heart-derived fibroblasts (Runnels, Yue and Clapham, 2002; Pujadas *et al.*, 2010; Yu *et al.*, 2014).

Here, western blot analysis revealed that $CoCl_2$ *in vivo* treatment, increases TRPC6 and TRPM7 protein expression in rat heart. Expression of both TRPC6 and TRPM7 channel proteins was significantly increased in rat left ventricular tissue after 28 days administration of $CoCl_2$. The effects of Co on the upregulation of TRPC6 and TRPM7 occurred in a dose-dependent manner.

Functionally, TRPM7 may also be associated with the defects of cardiac function. TRPM7 channels have already been discovered in isolated human cardiomyocytes

from atrial tissues. Patch-clamp techniques have that the TRPM7 current density in human atrial cardiomyocytes highly depends on the underlying pathology, and is higher in cells from patients with atrial fibrillation and ischemic cardiomyopathy, in particular patients with history of coronary artery disease(Mačianskiene *et al.*, 2017). In addition, sensitivity to divalent cations (Mg^{2+}) was also shown to be enhanced in human atrial cardiomyocytes (Mačianskiene *et al.*, 2012). An overexpression of TRPM7 and its correlation with the severity of injury during myocardial ischemia/reperfusion has been shown in rat hearts (Demir *et al.*, 2014).

Additionally, previous studies reported that oxidative stress, membrane stretch, and shear stress could activate TRPM7(Aarts *et al.*, 2003; Oancea, Wolfe and Clapham, 2006; Numata, Shimizu and Okada, 2007), which may imply a potential role of TRPM7 in myocardial pathological processes. Moreover, another study has also reported that TRPM7 channel gene expression is remarkably increased in human atrial fibroblasts isolated in patients with atrial fibrillation. It is, therefore, believed that TRPM7-mediated Ca^{2+} signals may mediate fibrogenesis in human atrial fibrillation (Du *et al.*, 2010) as previously mentioned earlier regarding TRPM7 and AF patients. However, a change in TRPM7 protein expression and/or in channel modulation due to modified cellular signalling during acute ischemia may also affect the contribution of the channels (Demir *et al.*, 2014).

CaMKIIδ, TRPC6 and TRPM7 proteins all show increased expression in rat heart following increasing periods of animal exposure to Co. These changes in expression correlate with the cardiac dysfunction represented by the reduced fractional shortening, which in turn is associated with the significant accumulation of Co in heart tissue. Collectively, these events may confirm that $CoCl_2$ causes compromised heart function even at low levels of administration. In our study we paid special attention to identifying possible changes in CaMKIIδ, TRPC6 and TRPM7 channels, proteins that are all affected in heart disease and contribute to the pathophysiology of the condition. The similar effects on expression of these proteins following Co exposure to what is observed in heart disease could highlight potential mechanisms of uptake and cytotoxicity induced by Co in the heart. This work certainly highlights novel areas for future lines of research.

Chapter 6. RNA SEQUENCING OF COBALT EFFECTS FOR *IN VITRO* AND *IN VIVO* TREATMENTS

6.1 Introduction

The results from the previous chapters showed that Co ions are toxic and have considerable influence on protein expression. This could have serious implications as it means that patients undergoing adverse reactions after implant surgery and revision surgery may be at higher risk of adverse tissue response and implant failure due to altered gene expression and consequent protein function. Changes in general toxicology-related gene expression in response to CoCr wear debris and Co ion exposure is a concern and should be investigated.

Molecular biology techniques can provide a means for the analysis of DNA, RNA, proteins, and lipids and their expression. The transcriptome is the sum of all of the RNA transcripts expressed by a cell or tissue and transcriptome analysis aims to identify genes differentially expressed under various conditions that might lead to understanding of the genes or pathways involved. RNA Sequencing (RNA-Seq) is a transcriptomic tool seeing increasing use (Finotello *et al.*, 2014). There have been extensive efforts in the identification and characterisation of gene expression profiles and biomarkers involved in heart disease and cardiac disorders (Steenman *et al.*, 2005; Joehanes *et al.*, 2013; Kazmi and Gaunt, 2016).

Quantitative real-time PCR (RT-qPCR) can measure the gene expression levels in RNA isolated from cells and tissues and any change in response to treatments or conditions (Wagner, Kin and Lynch, 2013). Messenger RNAs (mRNA) isolated from the cells or tissues are first converted to complementary DNA (cDNA) to act as templates for the polymerase chain reaction (PCR), which carries out an amplification of a fragment of the targeted transcript of interest. The accumulation of this PCR product or amplicon, is detected and measured in real-time and allows quantification of the target mRNA expression level (Ho-Pun-Cheung *et al.*, 2009).

The first part of this section covers the RNA-Seq transcriptomics data and analysis of the cell lines, 3T3 cells and primary adult cardiac fibroblast (CFs) at 1 and 10 µM Co after 48 h, and heart tissue after after 7 and 28 days treatment of 1 mg/kg Co. This aims to give overviews on the impact Co is having on both *in vitro* and *in vivo* and possible insights on the pathways to help in our understanding of the mechanism(s) that are

responsible for the toxicity of Co exposure. RNA-Seq expression profiles the alterations of gene expression in response to Co to determine if a gene signature can be identified. For example, Co exposure may lead to cardiovascular dysfunction through a calcium-related mechanism, via alteration of a range of channel gene expressions and activities.

A focussed gene expression analysis was carried out on five targeted genes (*Camkiid, Dmt1, Trpc6, Trpm7 and* Transient receptor potential vanilloid 1 (*Trpv1*)) using RT-qPCR. This was intended to continue the investigation conducted on their protein expression in Chapters 3 and 5, and follow on by examining the impact of Co exposure on the expression of these particular genes. Each gene is relevant to the toxicity of Co ions in terms of metal transporter, modulation of ion channel activity, and the regulation of relevant proteins that interact with Co. As with the western blot analysis, *in vivo*, the biological effects and the change in gene expression between treated and untreated rat hearts was compared to their respective controls. *In vitro*, the potentially effective dose (1 and 10 μM Co) from western blotting was chosen to assess the impact of Co exposure on cell line gene expression compared with controls.

CaMKII has a crucial role in cardiovascular activity by regulating Ca^{2+} handling and cardiac contractile function. Potential Co transporters are DMT1, TRPM7, TRPC6 and TRPV1. DMT1 is a member of the proton-coupled metal ion transporter family. Transient receptor potential (TRP) family; TRPM7, TRPC6 and TRPV1, are cation channels and responsible for metal ion transport.

TRPV1, which is the transient receptor potential cation channel subfamily V member 1 (TRPV1), is also known as the capsaicin receptor and the vanilloid receptor 1. It has functional cation-(including calcium) permeable pores (Kedei *et al.*, 2001; Kuzhikandathil *et al.*, 2001; Clapham, 2003). *Trpv1* is also involved in metal ion influx via a non-selective cation channel. All TRP channels (TRPM7, TRPC6 and TRPV1) play roles as modulators of intracellular Ca^{2+} signalling (Gees, Colsoul and Nilius, 2010).

We hypothesise that utilising RNA-Seq and RT-qPCR for the quantitative analysis of specific genes will allow the assessment of the impact of Co exposure on the

transcriptome of cardiac tissue and cell lines and help to elucidate the molecular mechanisms involved in the cellular response.

6.2 Aims

6.2.1 To identify and establish the protocol for extracting RNA from samples collected during in-vivo (heart tissue) and in vitro (3T3 cells and cardiac fibroblasts) studies of the effects of exposure of rat cells and tissues to Co. This RNA should be suitable for molecular applications.

6.2.2 To determine the gene expression level of 5 selected genes (Camkiid, Dmt1, Trpc6, Trpm7 and Trpv1) that are thought to be involved in the effects of Co exposure in-vitro and in-vivo, and may help to understand the mechanism of toxicity of Co in terms of the molecular biology.

6.3 Results

In this section, we describe the quantity and quality of RNA extracted for samples from both *in vitro* experiments on the exposure of 3T3 cells and cardiac fibroblasts to Co in cell culture, and from the treatment of rats *in vivo* with Co and the subsequent isolation of RNA from their heart tissue. Using RNA-Seq we conducted differential gene expression analysis on four samples of rat hearts and on three samples of mouse 3T3 cells and rat cardiac fibroblasts (CF). RNA was extracted using RNeasy Plus Universal Midi Kit (Qiagen, Manchester, UK) for the *in vivo* samples. Heart tissue was collected from four groups; Control and Co-treated animals at two time points (7 days and 28 days). The RNeasy Plus Mini kit (Qiagen, Manchester, UK) was used to extract RNA from six groups of cultured cells for the *in vitro* experiments: - 3T3 cells and CFs from Control and Co treatment at 1 and 10 μM for 72 h.

Each RNA extraction from both the *in vivo* and *in vitro* Co exposure experiments was assessed and checked individually for both the quantity and quality of RNA, then submitted to BGI-Tech (BGI Tech Solutions Co. Ltd, Hong Kong) for RNA-Seq. The concentration and quality was confirmed using a Nanodrop™ 2000c Spectrophotometer (Thermo Scientific, Paisley, UK) via absorbance readings at 260nm and ratios at A260/280nm and A260/230. The integrity of the RNA was confirmed using an Experion™ RNA StdSens Analysis kit (Bio-Rad, Watford, UK). The kit was used as per the manufacturer's instructions. Where possible, MIQE guidelines were followed throughout (As shown in Appendix, Table A4-1 MIQE checklist) (Bustin *et al.*, 2009).

All samples were submitted to BGI-Tech (Hong Kong) for RNA-Seq Quantification analysis on their BGISEQ-500 platform with 20Mb clean reads. Pairwise comparisons were carried out on the data from the *in vivo* Co treatment experiment groups:

(1) Control vs. Co treatment for 7 days

(2) Control vs. Co treatment for 28 days.

In vitro experiment data were compared similarly dependent on the concentration of Co-treatment:

(3) Control, Co treatment 1 μM and Co treatment 10 μM for 3T3 cells

(4) Control, Co treatment 1 μM and Co treatment 10 μM for CFs.

RT-qPCR was used to confirm the expression levels of the *Camkiid, Dmt1, Trpc6, Trpm7,* and *Trpv1* mRNA transcripts to build upon the findings from the Western blotting study as described earlier in Chapter 3 and 5. RT-qPCR for *Camkiid, Dmt1, Trpc6, Trpm7 and Trpv1* was also used to validate the RNA-Seq data to confirm the changes in the genes as targets for the action of Co on cells and tissues in the *in vitro* and *in vivo* models used.

6.3.1 RNA Extraction and Quality control (Nanodrop Analysis and Experion™ RNA StdSens Analysis)

The Nanodrop spectrophotometer (Thermo Fisher Scientific) can assess concentration of RNA and also provide some purity data via A260/280 nm and A260/230 nm readings. The concentration of RNA of the samples varied between 200-1400 ng/µl, which is acceptable by the BGI-Tech requirements of sample quantity of more than 20 ng/µl. All of the ratios indicated high purity with values between 2.0 and 2.2 (Table 6-1).

The Experion™ automated electrophoresis system (Bio-Rad Laboratories) provides an automatic assessment of RNA integrity by providing the RNA quality indicator (RQI) on a scale of 0-10, where degraded, poor quality RNA will have a RQI of 0, while high quality, intact RNA has a RQI of 10 (Denisov *et al*., 2008). The Experion software can provide a virtual gel view, showing the relative levels and integrity of the 28S:18S ribosomal RNAs (Figure 6-1). The RNA samples were of high quality with all RNA samples having an RQI > 9.0). These values are recorded on Table 6-1. All samples passed the criteria for further analysis via RNA-Seq.

Table 6-1 Quantification of RNA from heart, CFs and 3T3 cell samples as determined by absorbance (NanoDrop 2000c spectrophotometer) and RNA Quality Indicator (RQI) number (Experion™ Automated Electrophoresis System).

Sample	Nanodrop 2000c spectrophotometer			Experion™ Automated System
	Concentration (ng/µl)	A260/A280 Ratio	A260/A230 Ratio	RQI
In Vitro				
3T3s Co 0 µM	1120.5	2.08	2.24	9.1
3T3s Co 1 µM	1168.4	2.08	2.15	9.2
3T3s Co 10 µM	1348.4	2.07	2.23	9.6
CFs Co 0 µM	428.1	2.05	2.12	9.8
CFs Co 1 µM	430.9	2.09	2.16	9.8
CFs Co 10 µM	399.8	2.06	2.01	9.8
In vivo				
Control 7 D	303.0	2.05	2.30	9.3
Co treatment 7 D	316.4	2.05	2.22	9.4
Control 28 D	346.0	2.07	2.19	9.5
Co treatment 28 D	253.5	2.05	2.14	9.6

Figure 6-1 Experion™ RNA Std-Sens virtual gel report showing bands for 18S and 28S. L: ladder; 1-9 refer to samples tested: 1 – Control 7 D; 2 – Co treatment 7 D; 3 – Control 28 D; 4 – Co treatment 28 D; 5 –CFs Control; 6 – CFs Co treatment 1 µM; 6 – CFs Co treatment 10 µM; 7 –3T3 cells Control; 8 – 3T3 cells Co treatment 1 µM; and 9 – 3T3 cells Co treatment 10 µM.

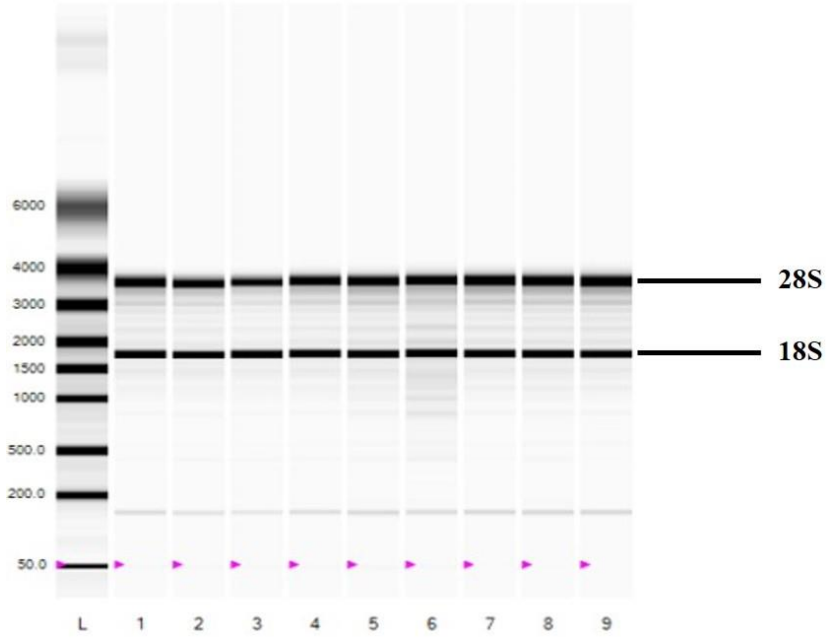

6.3.2 RNA Sequencing (RNA-Seq)

The sequencing data generated was subjected to quality control and filtering into clean reads by BGI-Tech. The alignment of clean reads to the reference genome (*Rattus;* genome version rn6 and *Mus;* genome version mm10*;* University of California Santa Cruz (UCSC)), was used for quality control analysis by BGI-Tech. Both the *in vitro* and *in vivo* studies had the number of total mapped reads at 24.0 to 24.1 million base pairs, accounting for approximately 92% to 97% of total reads (Table 6-2). The percentage of total un-mapped reads was about 3-8% in the libraries. The mapping quality parameter depends on the percentage of mapped reads, which is shown as an indicator of the overall sequencing accuracy and of the presence of contaminating DNA.

Table 6-2 Summary of mapping results.

Sample	Total Reads[1]	Total Mapped Reads[2] (%)	Unique match[3] (%)	Multi-position match[4] (%)	Total unmapped reads (%)
In vitro					
3T3s Co 0 µM	24,068,600	93.47	55.58	37.89	6.52
3T3s Co 1 µM	24,076,554	93.14	59.17	33.97	6.86
3T3s Co 10 µM	24,076,866	92.34	59.99	32.35	7.66
CFs Co 0 µM	24,073,071	96.60	77.39	19.21	3.40
CFs Co 1 µM	24,091,236	96.74	77.60	19.14	3.27
CFs Co 10 µM	24,076,958	96.51	77.28	19.23	3.49
In vivo					
Control 7 D	24,116,170	93.59	63.22	30.37	6.47
Co treatment 7 D	24,117,085	92.89	61.41	31.48	7.11
Control 28 D	24,108,919	93.59	61.46	32.13	6.42
Co treatment 28 D	24,113,838	93.31	61.71	31.60	6.69

1, Total Reads : all reads included in this study
2, Total Mapped Reads: number of reads that are similar in sequence to part of reference
3, Unique match: portion of total mapped reads that have only one mapped site in reference
4, Multi-position match: portion of total mapped reads that have multiple mapped sites in reference.
5, Total unmapped reads: number of reads that have no similar sequences as any part of reference.

6.3.3 RNA Sequencing for in vitro experiment.

6.3.3.1 Pearson correlation heat map in vitro experiment

The correlation between the number of gene expression changes of each of the cell types (3T3 cells and CFs) is represented in terms of their Pearson value as shown in Pearson heatmap correlation coefficient values. The Pearson value is the degree of correlation coefficient that is measured by the linear relationship between two variations (Pearson, 1895).

The Pearson heat map of correlation coefficient values across samples, in comparison to the control group, the Co-treatment at 1 µM and 10 µM, show a coefficient value between 0.992 and 0.981 on 3T3 cells, and 0.997 and 0.993 on CFs, respectively. Moreover, the Co-treatment at 10 µM and control group show more differences with a coefficient value of 0.981 on 3T3 cells, whereas in CFs it shows a coefficient value of 0.993. A seen from the coefficient values, this suggests that there are more changes in gene expression in 3T3 cells than in CFs in response to Co. The Pearson correlation heatmaps also suggest that gene expression responses in the two cell lines act in a dose-dependent manner to Co (Figure 6-2).

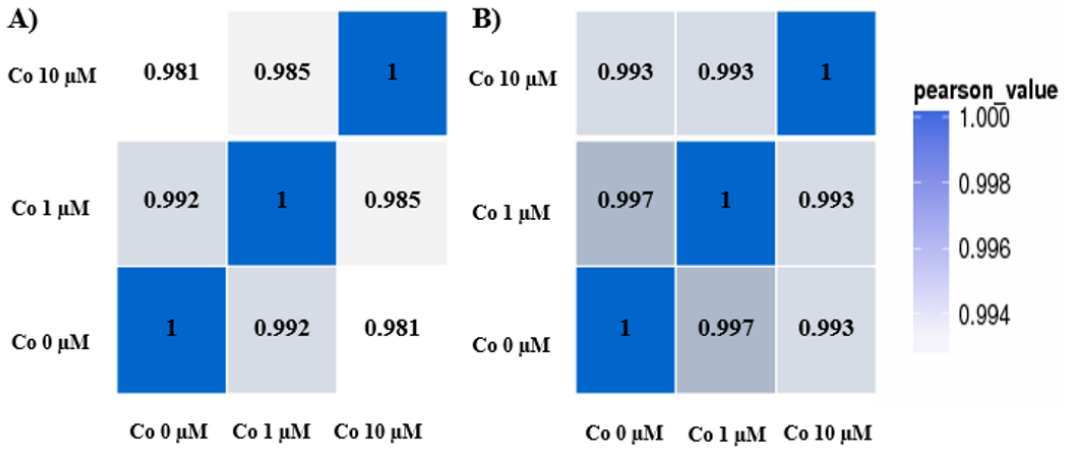

Figure 6-2 Pearson correlation heat map of differentially expressed genes following Co-exposure *in vitro*. (A) 3T3 cells and (B) CFs show the gradient colour barcode for comparisons between Co-treatment (1 and 10 µM) and the control group. In comparison to the control group, the Co-treatment at 1 µM and 10 µM, show a coefficient value between 0.992 and 0.981 on 3T3 cells, and 0.997 and 0.993 on CFs, respectively. Moreover, the Co-treatment at 1 µM and control group show most differences with a coefficient value of 0.981 on 3T3 cells, whereas in CFs it shows a coefficient value of 0.993.

6.3.3.2 Differential Gene Expression in vitro experiment

RNA-Seq was used to gain transcriptomic insights into the molecular mechanisms in each of the cell types in response to Co. Both 3T3 cells and CFs were treated with two concentrations of Co (1 and 10 µM) and then the total RNA extracted to examine the changes of differentially expressed genes (DEGs).

The number of identified expressed genes were counted and the proportion identified and then compared to each gene reference annotation (Figure 6-3). In mouse 3T3 cells, the total number of genes expressed is approximately 14,000 genes or around 57% of genes from the reference transcriptome in 3T3 cells (24,573 genes), whereas rat CFs are approximately 12,000 genes or 70% of reference transcriptome (17,449 genes). (Figure 6-3).

JavaTreeView was used to observe the results of hierarchical clustering of the gene data list (http://jtreeview.sourceforge.net) (Eisen *et al.*, 1998). DEGs analysis of gene expression identified by heatmap clustering comparisons between the control vs. Co 1 µM and control vs. Co 10 µM of 3T3 cells (Figure 6-4, Table 6-3 and Appendix 5) and CFs (Figure 6-5 and Table 6-4) provided an overview of the molecular effects of Co exposure in these cells.

The 3T3 cell heatmap displays four main clusters of gene expression changes between the two treatment concentration responses. These are 4 main clusters, indicated in Table 6-3 and the genes within each of these clusters are listed in Appendix 5.

Cluster 1; C1, This cluster of genes were highly up-regulated following 1 and 10 µM Co treatment in 3T3 cells. Analysis of the KEGG database and GO terms, revealed these genes were involved in the modulation of chemokine and neurothropin signalling pathways - *Nfkbie* (NFKB inhibitor epsilon); and apoptosis process - *Moap1* (Modulator of apoptosis1); cortisol synthesis and hypoxia response - *Kcnk2* (potassium two pore domain channel subfamily K member 2) and immune system; *Nfkbie*

In cluster 2; C2, 1 µM Co treatment induced the down-regulation of this gene cluster, whereas at high concentration, 10 µM, showed up-regulation of the genes in this cluster. The pathways involved, as well as the genes listed include: metabolic pathway

- *Galnt4* (polypeptide N-acetylgalactosaminyltransferase 4) , Signalling pathway; *Apln* (Apelin) and *Egr1* (early growth response 1), cytokine and chemokine; *Ccl6* (chemokine (C-C motif) ligand 6), *HIF-1* (hypoxia inducible factor 1); *Tfrc* (transferrin receptor), *FoxO* (forkhead box O; *Bnip3* (BCL2 interacting protein 3), and *TLR*; *Tlr6* (toll like receptor 6), in addition with the endocytosis; *Tfrc*.

In cluster 3; C3 of 3T3 cells, gene expression altered in response to Co exposure by showing up-regulation at 1 and 10 µM but the higher concentration of Co led to a greater increase in gene expression when compared with the lower dose. The pathways and their genes that responded in what appears to be a linear dose-dependent manner of Co exposure are: metabolic pathways - *A4galt, Hlcs, Gys1, Man1c1, Pfkl, Suox, Man2a1, Dpm3, P4ha2, Galnt13, Hsd17b4, St3gal6, Ugt1a6a* and *Tpi1*; signalling pathway - *HIF-1*; *Egln3, Pdk1* and *Pfkl*; chemokine - *Ccl28, Cxcl1* and *Shc4*; cytokine - *Ccl28* and *Cxcl1*; calcium ion channel - *Erbb3, Calu, Edil3, Vldlr, Ehd3, Masp1, Cdh2, Pcdh19, Pros1, Man1c1, Cd248, Sulf2* and *Pkd2;* and metal ion binding - *Zfp523, Calu, Morc2a, Man2a1, Suox, Edil3, Rnf150, Ehd3, Col3a1, Pfkl, P4ha2, Adamts5, Fbxl19, Lmln, Egln3, Plod2, Pros1, Ppp1r10, Pkd2, Nr3c2, Mblac2, Antxr2, Cp, Vldlr, Trim2, Man1c1, Zfp41, Zfp74, Galnt13, Masp1, Lox, Cdh2, Thap2, Zmat1, Irak4, Pcdh19, Cd248* and *Sulf2.*

The genes in cluster 4 (C4) were significantly down regulated in 3T3 cells at both 1 and 10 µM Co. As with C3, there was a dose-dependent response with the genes having a greater downregulation at 10 µM than at 1 µM. Mapping the gene lists to their GO terms and KEGG pathways, the following Co-affected pathways and their genes were indentified : FoxO - *Gadd45b*; NF-kappaB - *Gadd45b* and ; MAPK - *Ddit3* and *Gadd45b,* in addition to the metabolic pathway; *Dpm3* and *St3gal6,* apoptosis and programme cell death process; *Siva1, Ung, Rps29, Gadd45b, Pim1, Ddit3 and Sdf2l1* that relate to the response to stress, and also pathways in cancer; *Gadd45b, Co14a6* and *Pim1*.

According to our findings, expression of over one hundred genes altered significantly in response to Co exposure in 3T3 cells. Our limited study identified 3T3 transcriptomic signatures and possible pathways that were affected by these two doses

of Co exposure over this time period. Within these expression profiles, linear Co-dose-dependent responses appeared to be present. Co treatment of 3T3 cells impacted on gene expression across a small number of pathways including metabolic pathways; calcium ion binding, metal ion binding, apoptosis and programme cell death, cell signalling pathway, immune system response.

In CFs, overview details of the information on CFs genes are present in Figure 6-5 and Table 6-4; they were spliced into 4 clusters. Cluster 1; C1, this cluster of genes was highly down-regulated following 1 and 10 µM Co treatment in CFs. *LOC100363112* showed a dose-response with the genes having a greater downregulation at 10 µM than at 1 µM Co. The genes in cluster 2 (C2) were more up-regulaed at 10 µM than at 1 µM Co. Cluster 2 genes showed the related pathways involved with the spliceosome - *Tsen34, Gjb4* and *Crnk11*; Cell cycle - *G0s2* and *Gjb4*; interaction with the vascular wall and metabolism by *Slc16a3* and Myocardial infarction was present in *Miat* gene.

Cluster 3 of CFs gene showed downregulation after both 1 and 10 µM Co treatment, when examining the pathways that involved these genes, they are related to the Signalling pathway -*Vcam1* and *Gpc2*; Calcium binding - *Tnnt3*; metabolic pathway - *Hsd3b5* and neuron system - *Gpc2*; Phototransduction - *Slc24a1* and particularly the cardiovascular system, Troponin T binding and cardiac ventricle development - *Vcam1* and *Tnnt3*. Interestingly, in cluster4 , Co exposure showed high potential downregulation of *Moap1* at 1 µM that is related to the apoptosis process, but at 10 µM Co treatment showed upregulation in this gene.

It can be observed that the changes in transcriptomics in terms of enriched pathways showed similar functional categories in both cell types during Co exposure at different concentrations. The more surprising correlation is with the overview of biological changes between 3T3 cells and CFs after the GO terms and KEGG pathways. This shows the common pathways after Co exposure are metabolic pathways, calcium channel activity, apoptosis pathway and cell cycle. The most interesting aspect highlights pathways relating to cardiovascular processes involving cardiac ventricle development, vacular muscle contraction and cardiac enzyme activity.

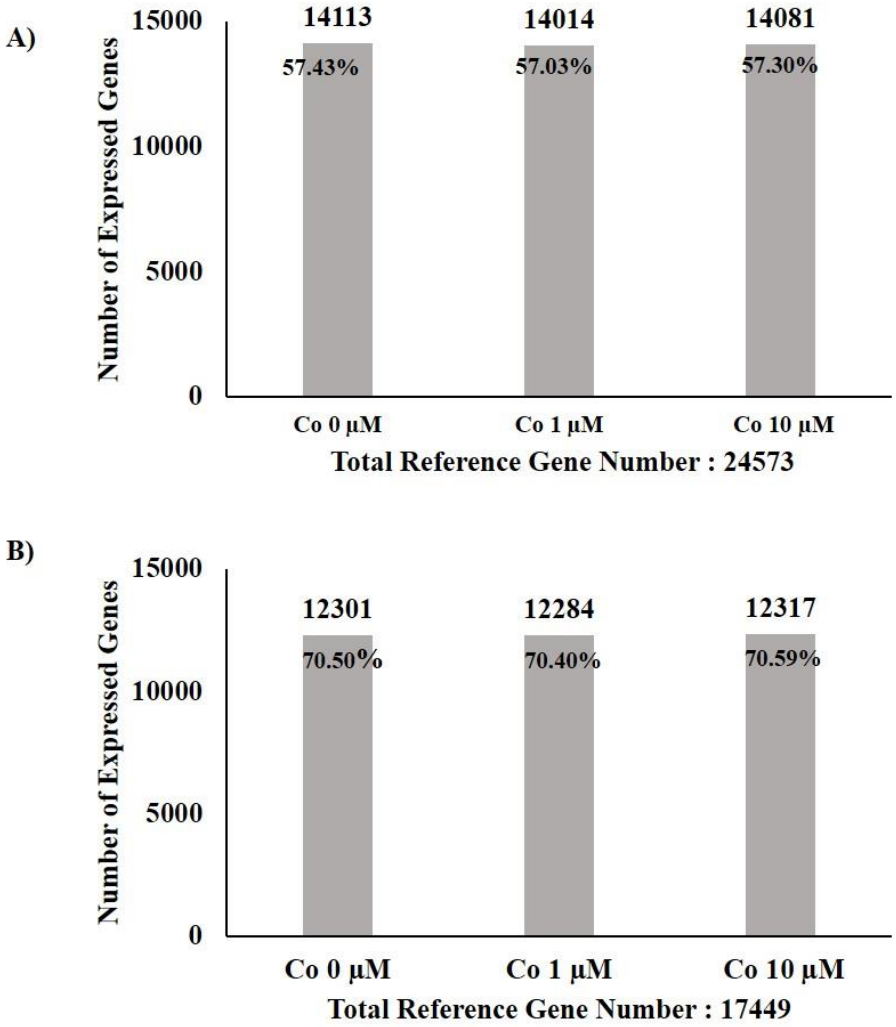

Figure 6-3 Number of expressed gene by 3T3 cells and CFs identified by RNA-Seq. Both (A) 3T3 cells and (B) CFs were treated with concentrations of $CoCl_2$ (1 and 10 µM) for 72 h. 3T3 cell genes are approximately 14,000 genes or around 57%, whereas, CFs are approximately 12,000 genes 70% of genes from the total reference gene. X-axis is sample name .Y-axis is number of identified expressed genes .The number of expressed genes is shown above each bar. The proportion at the top of each bar equals expressed gene number divided by total gene number reported in each gene reference annotation**.**

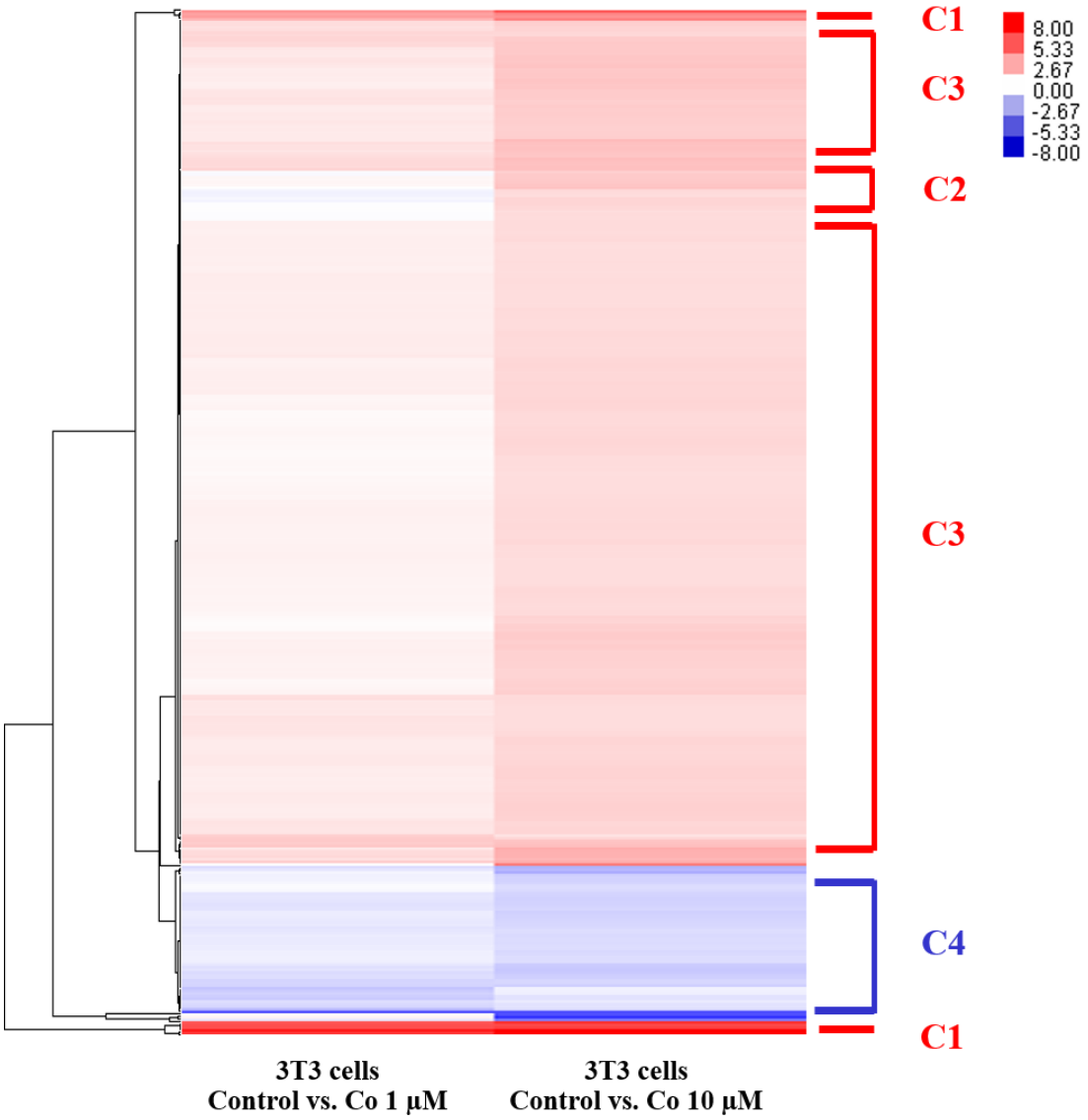

Figure 6-4 Clustering of DEGs in 3T3 cells after Co treatment. The first column (Control vs. Co 1 µM) and the second column (Control vs. Co 10 µM) represent differential DEGs fold change values which are clustered**.** Fold changes of gene expression were normalised with untreated cells. The gradient colour barcode at the right top indicates log2 (FC) value (Red:upregulation of expression; Blue:downregulation of expression). Clusters are indicated in Table 6-3. Abbreviations of selectd gene list are indicated in Appendix 5; C, Cluster.

Table 6-3 List of Pathways (3T3 cells)

Module	Related functions (GO Terms/KEGG)	Module	Related functions (GO Terms/KEGG)
C1 (High upreg in both 1 and 10 µM)	Apoptotic process[G] Neurotrophin signalling pathway[K] Chemokine signalling pathway[K] RNA transport[K] Hormone (steroid, estrogen, cortisol) synthesis[G] Immune system[K] Ras signalling pathway[K] Pathway in cancer (Breast, Gastric, Leukemia)[K] Focal adhesion[K] Globoside biosynthetic process[G]	**C2 (Downreg in 1, upreg in 10 µM)**	Metabolic pathways[K] Chemokine signalling pathway[K] Endocytosis [K] HIF-1 signalling pathway[K] FoxO signalling pathway[K] Ferroptosis[K] Cytokine activity[K] Autophagy[K] / Mitophagy[K] Toll-like receptor signalling pathway[K] Interleukin-1 beta biosynthetic process[G] G-protein coupled receptor internalisation[G]
C3 (Up increased from 1-10µM)	Metabolic pathways[K] HIF-1 signalling pathway[K] Endocytosis [K] Glycolysis / Gluconeogenesis[K] Calcium signalling pathway[K]/Calcium ion binding[G] Pathway in cancer[K] Immune system[K] Protein hydroxylation [G] Focal adhesion[K] Chemokine signalling pathway[K] Cytokine activity[K] Cell adhesion molecules (CAMs)[K] Hormone (steroid, estrogen, cortisol) synthesis[G] Receptor clustering[G]	**C4 (Increased in downreg from 1-10µM)**	MAPK signalling pathway [K] Pathways in cancer [K] Ribosome [K] Metabolic pathways [K] Apoptosis process [K] Regulation of programmed cell death[G] FoxO signalling pathway [K] NF-kappa B signalling pathway [K] Cellular senescence [K] Regulation of myoblast differentiation[G] Positive regulation of molecular function[G] Response to stress[G] Positive regulation of cellular metabolic process[G]

C, Cluster; G, GO terms; K, KEGG

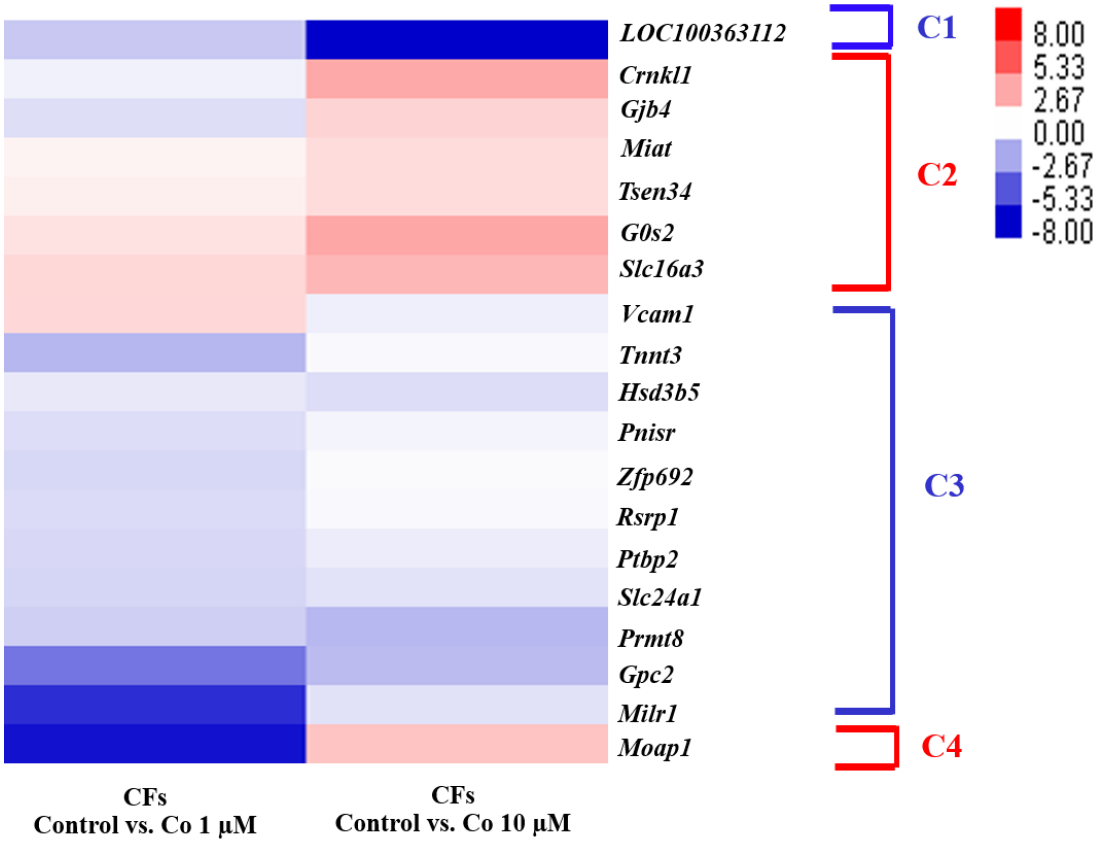

Figure 6-5 Clustering of DEGs in CFs after Co treatment. The first column (Control vs. Co 1 µM) and the second column (Control vs. Co 10 µM) represent differential DEGs fold change values**.** Fold change of gene expression were normalised with untreated cells. The gradient colour barcode at the right top indicates log2 (FC) value (Red:upregulation of expression; Blue:downregulation of expression). Clusters and abbreviations of selected gene list are indicated in Table 6-4; C, Cluster.

Table 6-4 The details of selected gene and pathway enrichment in the clusters of CFs after Co treatment 1 and 10 µM.

Cluster	Genes	1 µM Fold change	10 µM Fold change	Related functions (GO Terms/KEGG)
C1 (High downreg in both 1 and 10 µM)	*LOC100363112*; Aa2-296-like	-1.699134	-8.108524	-
C2 (Upreg in 1 µM , up in 10 µM)	*Crnkl1;* crooked neck-like protein 1	-0.394279	2.646363	Spliceosome[K] Myocardial infarction[K] Cell cycle[G] Cell surface interactions at the vascular wall and Metabolism[K]
	Gjb4; Gap Junction Protein Beta 4	-1	1.351675	
	Miat; myocardial Infarction Associated Transcript	0.343954	1.067745	
	Tsen34; tRNA-splicing endonuclease subunit Sen34	0.462254	1.059249	
	G0s2; G0/G1 switch protein 2	0.859519	2.737709	
	Slc16a3; solute Carrier Family 16, Member 3 (Monocarboxylic Acid Transporter 4)	1.227806	2.211504	

C,Cluster; G, GO terms; K, KEGG

Table 6-4 The details of selected gene and pathway enrichment in the clusters of CFs after Co treatment 1 and 10 µM (cont.).

Cluster	Genes	1 µM Fold change	10 µM Fold change	Related functions (GO Terms/KEGG)
C3 (Downreg in both 1 and 10 µM)	*Vcam1;* Vascular Cell Adhesion Molecule 1	1.186878	-0.453051	IL-4 signalling pathway[K] Cell adhesion molecules (CAMs) [K] NF-kappa B signalling pathway[K] Leukocyte transendothelial migration[K] Calcium-dependent protein binding[G] Troponin T binding[G] Muscle contraction[G] Metabolic pathways[K] Steroid hormone biosynthesis[K] Regulation of ATPase activity[G] Hormone (steroid, aldosterone, cortisol) synthesis[G] Phototransduction[K] Neuron differentiation[G] Smoothened signalling pathway[G] Mast cell degranulation[G]
	Tnnt3; troponin T, fast skeletal muscle	-2.22995	-0.152506	
	Hsd3b5; 3 beta-hydroxysteroid dehydrogenase type 5	-0.681381	-1.016624	
	Pnisr; PNN-interacting serine and arginine-rich protein	-1.032433	-0.299777	
	Zfp692; zinc finger protein 692	-1.215206	-0.118181	
	Rsrp1; arginine/serine-rich protein 1	-1.073773	-0.129554	
	Ptbp; polypyrimidine tract-binding protein 1	-1.172686	-0.554934	
	Slc24a1; solute Carrier Family 4 Member 1	-1.271302	-0.853159	
	Prmt8; protein Arginine Methyltransferase 8	-1.451211	-2.203284	
	Gpc2; glypican-2	-4.33985	-2.091922	
	Milr1; allergin-1	-6.569856	-0.89743	
C4 (High downreg in 1 µM, up in 10 µM)	*Moap1;* modulator of apoptosis 1	-7.434628	1.855391	Apoptotic process[G] Regulation of apoptosis pathway[K]

C,Cluster; G, GO terms; K, KEGG

Differential gene expression (DEG) analysis was carried out to determine the differentially expressed genes between treated (1 and 10 µM Co) and untreated groups after 72 h using the weighted cut-off.

Our study has applied a fold change cutoff and then ranked the statistical significance of all the genes above that fold change threshold by *p-value*. The resulting set of genes has a weighted cut off and considers fold changes by selecting transcripts with fold changes of >2 [$\log_2$FC (Fold change)] ≥ 2 and $p<0.05$ (Dalman *et al.*, 2012; Lazic, 2015). The weighted cut off DEGs of the effect of Co on 3T3 cells and CFs are presented by a histogram Figure 6-6. In the 10 µM up-regulated list (98 genes), only 20% of these genes are present in the 1 µM upregulated gene list (20 genes). Whereas in the 10 µM down-regulated list (58 genes), 40% of genes are also present on the 1 µM downregulated gene list (22 genes).

Whereas in CFs, in the 10 µM up-regulated list (33 genes), 30% of these genes are present in the 1 µM upregulated gene list (10 genes), in the 10 µM down-regulated list (35 genes), 25% of genes are also present on the 1 µM downregulated gene list (9 genes).

Comparison of the fold change between Co 1 µM and Co 10 µM showed that in 3T3 cells 15% of up-regulated genes and 27% of down regulated genes were increased after increasing the Co concentration. In CFs after increasing Co doses, 4 out of 10 in the up-regulated gene list and only 1 out of 9 in the down-regulated gene list showed greater regulation after increasing the Co concentration.

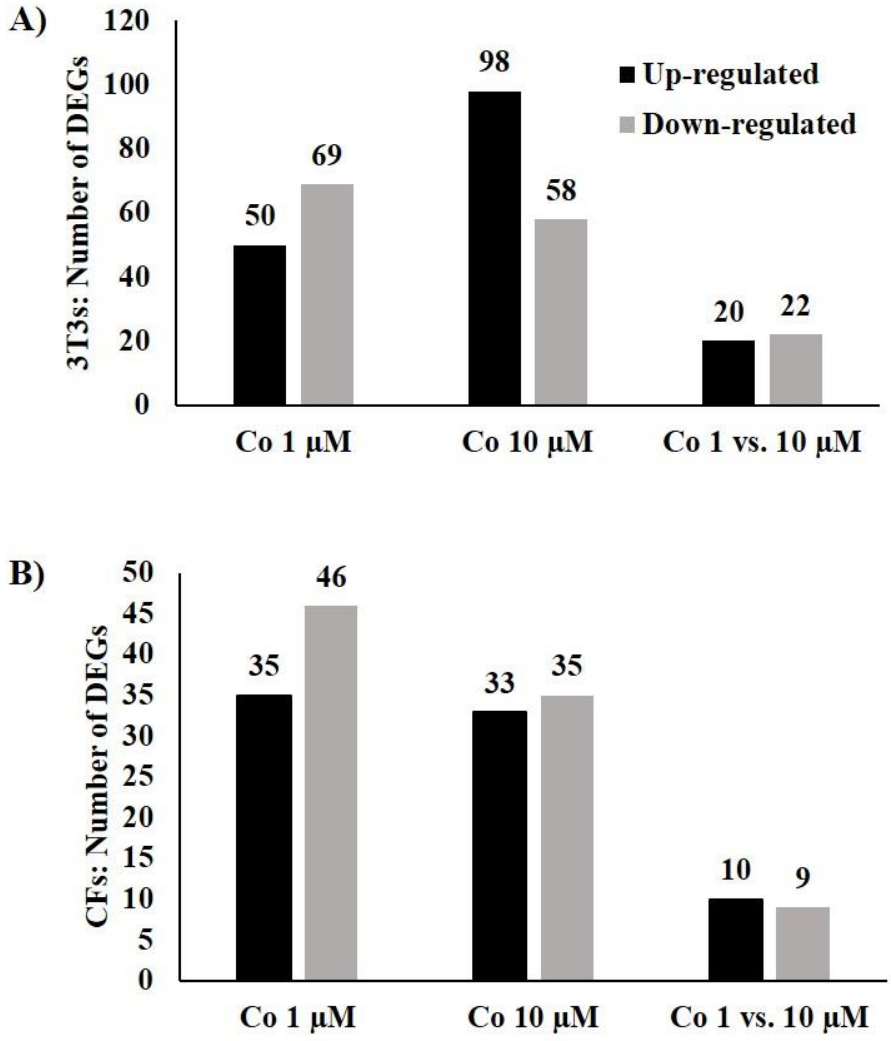

Figure 6-6 Differentially Expressed Genes (DEGs) and the effect of Co *in vitro* on 3T3 cells and CFs. Both (A) 3T3 cells and (B) CFs were treated with concentrations of $CoCl_2$ (1 and 10 µM) for 72 h. The cut-off criteria for DEGs were [log_2FC (Fold change)] ≥ 2 and $p<0.05$. The number of changed genes is shown above each bar.

6.3.3.3 Correlation heat map of 3T3 cells after 1 and 10 µM Co treatment.

For visualisation purposes, heat map correlations between the two concentrations of Co were created by MATLAB software analysis using cutoff DEGs (Figure 6-7). The heat map shows cross-correlation by treatment and similarity of gene-expression profiles of cut-off DEGs (≥ 2.0 and ≤ -2.0 log2 fold change, $p<0.05$) of each pairwise comparison – Control vs. Co 1 µM and Control vs. Co 10 µM.

In 3T3 cells, the heat map that demonstrated the gene expression clustering between the control and Co-treatment groups when the DEG list between the 1 and 10 µM Co treatments were compared, showed that 42 genes were differentially expressed. There were 20 up-regulated DEGs, and 22 down-regulated DEGs observed (List of abbreviations on Table 6-5 and Table 6-6).

GOrilla, Cytoscape, and KEGG mapper were used to conduct pathway enrichment analysis of the all genes between Control vs. Co 1 µM and Control vs. Co 10 µM treatments in GO terms and KEGG pathways. This analysis helps identify pathways that may be affected following Co exposure.

The DEG lists from the treated 3T3 cells are detailed in Table 6-5 and Table 6-6 along with their GO terms and KEGG pathways. The involvement of a number of pathways were identified that related to the changes gene expression in 1) Metabolic pathways (*Acsbg2, Alppl2, Pipox* and *Ugt1a1*), 2) calcium ion channels (*Grin2d, Pcdha8, Syt13* and *Smoc2*), 3) cytokine signalling pathways (*Grk1, Acsbg2* and *Nfkbie*), 4) Endocytosis (*Grk1* and *H2-Q8*), and 5) phototransduction (*Grk1, Rgr* and *Ugt1a1*). Of particular interest, *Nfkbie* is also involved with vascular smooth muscle contraction and the immune system in terms of the T and B cell receptor signalling pathway and Helper T (Th1, Th2 and Th17) cell differentiation; *H2-Q8* is related to cell apoptosis and cell adhesion; and *Acsbg2* involved in fatty metabolism, including fatty acid biosynthesis and degradation.

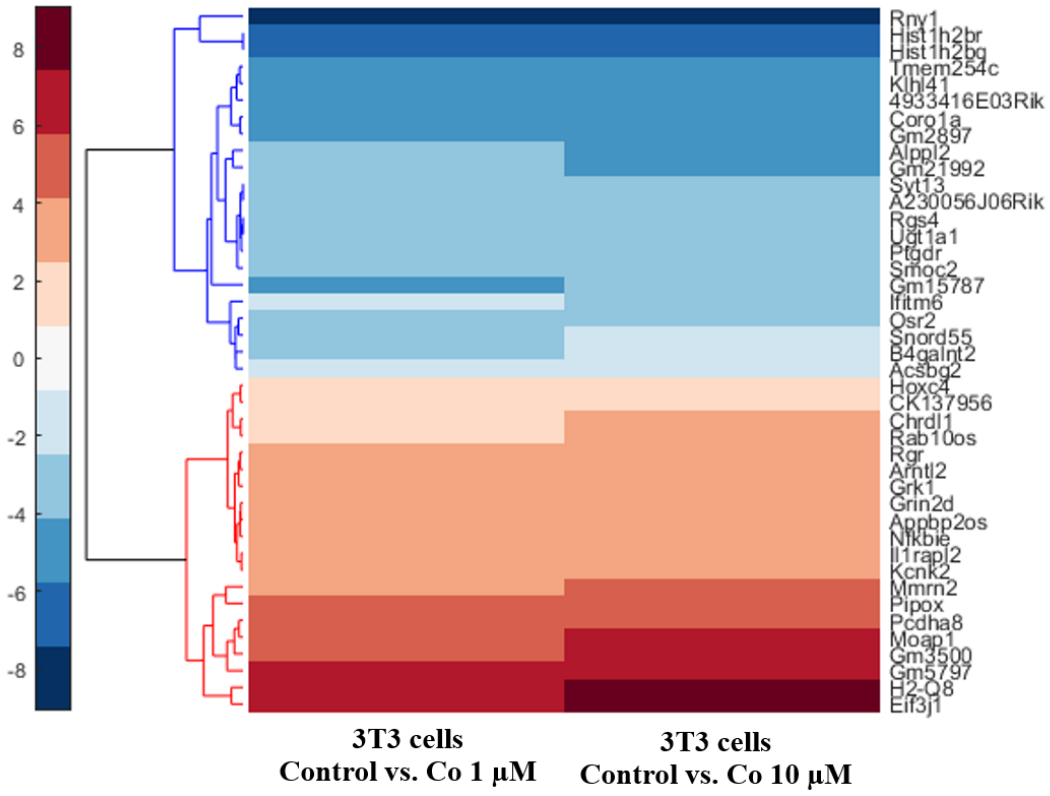

Figure 6-7 Correlation heat map of DEGs in 3T3 cells after 1 and 10 µM Co treatment in 3T3 cells. Heatmap showing differential expression of DEGs between Control vs. Co 1 µM (3T3 1 µM) and Control vs. Co 10 µM (3T3 10 µM) treatments. The first column is 3T3 cells after Co treatment at 1 µM and the second column is 3T3 cells after Co treatment at 10 µM. DEGs (≥ 2.0 and ≤ -2.0 log2 ratio, p<0.05) of each pairwise comparison. Fold changes of gene expression were normalised with untreated cells. x-axis:columns display two concentration treatments clustered by similarities among gene expression profiles; y axis: each row displays the expression strength of a particular gene in the DEGs, clustered by similarities across treatments. Colour key indicates the intensity associated with normalised expression values. Values are colour coded (Red:upregulated expression; Blue:downregulated expression) (Gene symbols as in Table 6-5 and Table 6-6.

Table 6-5 Highly expressed up-regulated genes and relevant enrichment pathways analysis in 3T3 cells treated with Co for 72 h.

Gene name	Description	Representative affected pathway (GO terms/KEGG)	Log2 FC Co 1 µM	Log2 FC Co 10 µM
Eif3j1	Eukaryotic translation initiation factor 3, subunit J1	Eukaryotic translation initiation factor 3 complex[G] RNA transport[K]	6.35755	8.18982
H2-Q8	Histocompatibility 2, Q region locus 8	Cell adhesion molecules (CAMs) [K] Endocytosis[K]/ Phagosome[K] Cellular senescence[K] Antigen processing and presentation [K]	7.17991	7.84549
Gm5797	Predicted gene 5797, Takusan like	Regulate synaptic activity[G]	6.58496	6.12928
Gm3500	Predicted gene 3500, Alpha10-takusan	Regulate synaptic activity[G]	5.20945	6.40939
Moap1	Modulator of apoptosis 1	Apoptosis process[G]	5.20945	6.40939
Pcdha8	Protocadherin alpha-8 precursor	Calcium ion binding[G]	5.49185	5.67242
Pipox	Pipecolic acid oxidase	Metabolic pathways [K] Peroxisome [K]	4.45943	4.52356
Mmrn2	Multimerin-2 precursor	Cell migration[G] Regulation of vascular endothelial growth factor[G] Receptor signalling pathway[K]	3.32193	5.16993
Kcnk2	Potassium channel, subfamily K, member 2	Cortisol synthesis and secretion [K] Gastric acid secretion[G]	2.87447	3.70044
Il1rapl2	Interleukin 1 receptor accessory protein-like	Interleukin-1, Type II, blocking receptor activity[G]	3	3.70044
Nfkbie	Nuclear factor of kappa light polypeptide gene enhancer in B cells inhibitor, epsilon	Immune system[K] Adipocytokine signalling pathway[K]	3.07529	3.42146

Table 6-5 Highly expressed up-regulated genes and relevant enrichment pathways analysis in 3T3 cells treated with Co for 72 h(cont.)

Gene name	Description	Representative affected pathway (GO terms/KEGG)	Log2 FC Co 1 µM	Log2 FC Co 10 µM
Appbp2os	Amyloid beta precursor protein (cytoplasmic tail) binding protein 2, opposite strand	Metabolic pathways[K]	3.23030	3.33298
Grin2d	Glutamate receptor, ionotropic, NMDA2D (epsilon 4)	Calcium signalling pathway[K] cAMP signalling pathway[K] Glutamatergic synapse[G] Long-term potentiation[G] N-methyl-D-aspartate (NMDA) receptor [G]	3.16993	3.16993
Grk1	G protein-coupled receptor kinase 1	Endocytosis[K] Chemokine signalling pathway [K]	3	2.80735
Arntl2	Aryl hydrocarbon receptor nuclear translocator-like protein 2 isoform 1	Circadian rhythm[K] DNA binding transcription factor activity[G]	2.80735	3.11548
Rgr	Retinal G protein coupled receptor	Phototransduction [K] G-protein coupled photoreceptor activity[G] G-protein coupled receptor activity[G]	2.70044	2.90689
Rab10os	Protein RAB10, member RAS oncogene family	Early embrogenesis[G] Neurogenesis [G]	2.13750	2.97575
Chrdl1	Chordin-like protein 1 isoform X8	Cell differentiation [G] Eye and neuron system development[K]	2.16992	2.80735
CK137956	cDNA sequence CK137956	-	2.19265	2.14684
Hoxc4	Homeobox protein Hox-C4	HMG box domain binding[G]	2.35755	2.06609

Genes listed in this table have Fold of change of log2 ratio ≥ 2.0, over control (non-Co treated). *p<0.05* refer to the significance test; FC, Fold change G, GO terms; K, KEGG.

Table 6-6 Highly expressed down-regulated genes and relevant enrichment pathways analysis in 3T3 cells treated with Co for 72 h.

Gene name	Description	Representative affected pathway (GO terms/KEGG)	Log2 FC Co 1 µM	Log2 FC Co 10 µM
Acsbg2	Acyl-CoA synthetase bubblegum family member 2	Metabolic pathways[K] Adipocytokine signalling pathway[K] PPAR signalling pathway [K] Fatty acid biosynthesis[K]	-2.12928	-2.32193
B4galnt2	Beta-1,4 N-acetylgalactosaminyltransferase 2	Acetylgalactosaminyltransferase activity[G] Cell adhesion [K] Lipid glycosylation[G] UDP-N-acetylgalactosamine metabolic process [G]	-2.58496	-2
Snord55	Small Nucleolar RNA, C/D Box 55	Cytoplasmic Ribosomal Proteins [G]	-2.52938	-2.42669
Osr2	Protein odd-skipped-related 2 isoform X1	Cellular quiescence [G] Cell proliferation [G]	-2.72247	-2.72247
Ifitm6	Interferon induced transmembrane protein 6	Cell adhesion [K] Cell differentiation [G]	-2.39689	-3.30378
Gm15787	Predicted gene 15787	-	-5.52356	-2.71621
Smoc2	SPARC-related modular calcium-binding protein 2 precursor	Calcium ion channel [G] Interstitial matrix [G]	-4.08746	-4.08746
Ptgdr	Prostaglandin D2 receptor 2	G-protein coupled receptor activity [G] Calcium-mediated signalling [G] Chemotaxis [G]	-3.90689	-3.90689
Ugt1a1	UDP glucuronosyltransferase 1 family, polypeptide A1	Metabolic pathways[K]	-3.80735	-3.80735
Rgs4	Regulator of G-protein signalling 4 isoform X1	GTPase activator activity [G] G-protein coupled receptor signalling pathway [G]	-3.80735	-3.80735
A230056J06Rik	RIKEN cDNA A230056J06 gene, mCG148433	Grooming activity[K] (grooming behavior through multiple mechanisms)	-3.70044	-3.70044

Table6-6 Highly expressed down-regulated genes and relevant enrichment pathways analysis in 3T3 cells treated with Co for 72 h (cont.)

Gene name	Description	Representative affected pathway (GO terms/KEGG)	Log2 FC Co 1 µM	Log2 FC Co 10 µM
Syt13	Synaptotagmin-13	Calcium ion binding [G] Syntaxin binding [G]	-3.70044	-3.70044
Gm21992	Predicted gene 21992	RNA binding [G] Zinc ion binding [G] Focal ischaemia [K]	-2.93860	-4.52356
Alppl2	Alkaline phosphatase, placental-like 2	Metabolic pathways[K]	-3.24793	-5.24793
Gm2897	Predicted gene 2897, Takusan like	Regulate synaptic activity [G]	-4.70045	-4.70044
Coro1a	Cronin-1A	Actin binding [G] Cytoskeletal protein binding [G] Phagosome [K]	-4.85798	-4.85798
4933416e 03Rik	RIKEN cDNA 4933416e03 gene, mCG113487	-	-5.20945	-5.20945
Klhl41	Kelch-like protein 41	Myofibril assembly[G] Protein ubiquitination[G] Skeletal muscle cell differentiation [G]	-5.45943	-5.45943
Tmem254c	Transmembrane protein 254 isoform 1	Integral component of membrane [G]	-5.64386	-5.64386
Hist1h2bq	Histone cluster 1, H2bq	DNA binding[G]	-6.27612	-7.27612
Hist1h2br	Histone cluster 1 H2br	DNA binding [G]	-6.27612	-7.27612
Rny1	Ribonuclease Y 1	Pro-apoptotic [G] Relevant in coronary artery disease [G]	-9.06340	-9.06340

Genes listed in this table have Fold of change of log2 ratio ≥ 2.0, over control (non-Co treated). *p<0.05* refer to the significance test; FC, Fold change G, GO terms; K, KEGG

6.3.3.4 Correlation heat map of CFs after 1 and 10 µM Co treatment.

Analysis of the RNA –seq data from the CF study was conducted in the same manner as that of the 3T3 cells. DEGs of CFs were filtered by the same criteria as with 3T3 cell genes (≥ 2.0 and ≤ -2.0 log2 ratio, p<0.05) and are plotted in Figure 6-8.

CFs showed the expression of gene clustering between the 1 and 10 µM Co treatment. A number of CF DEGs between the 1 and 10 µM treatment groups were differentially expressed, only 19 genes were differentially expressed, of which 10 were up-regulated genes and 9 down-regulated genes. (List of abbreviation on Table 6-7)

Heat map visualised using MATLAB shows the cross-correlation on CFs, and Figure 6-6 shows the DEGs of each pairwise comparison – Control vs. Co 1 µM and Control vs. Co 10 µM. The higher concentration of Co appears to cause more changes in expression in terms of $\log_2$FC (Fold change).

Based on the analysis of 19 genes in the data set of Co treatment at 1 and 10 µM, these were evaluated using GOrilla, Cytoscape and KEGG mapper as shown in Table 6-7. Involvement of changes and similar functionalities in 1) calcium ion channel (*Calml4, Stx1b, Syt13* and *Syt9*), 2) metal binding eg. zinc etc. (*Adam30, Pcdhb8, Zfp36l3* and *March1*), 3) ubiquitin protein ligase activity (*Ube3d* and *March1*), and 4) smoothened signalling pathways (*Gpc2, Ulk3* and *Lrrc34*) were illustrated. Of interest, *Calml4* is involved in vascular smooth muscle contraction, fluid shear stress and atherosclerosis. *Ugt1a3* is related to the metabolic pathways and drug metabolism, including P450.

Notably, these *in vitro* findings suggested that Co alters calcium channel activity and has impacts on gene expression relevant to metabolic pathways. However, some of the DEGs following Co exposure are involved in other ontology categories such as exocytosis, synapse activity, cytokine activity, the immune system, and the impairment of cardiovascular process.

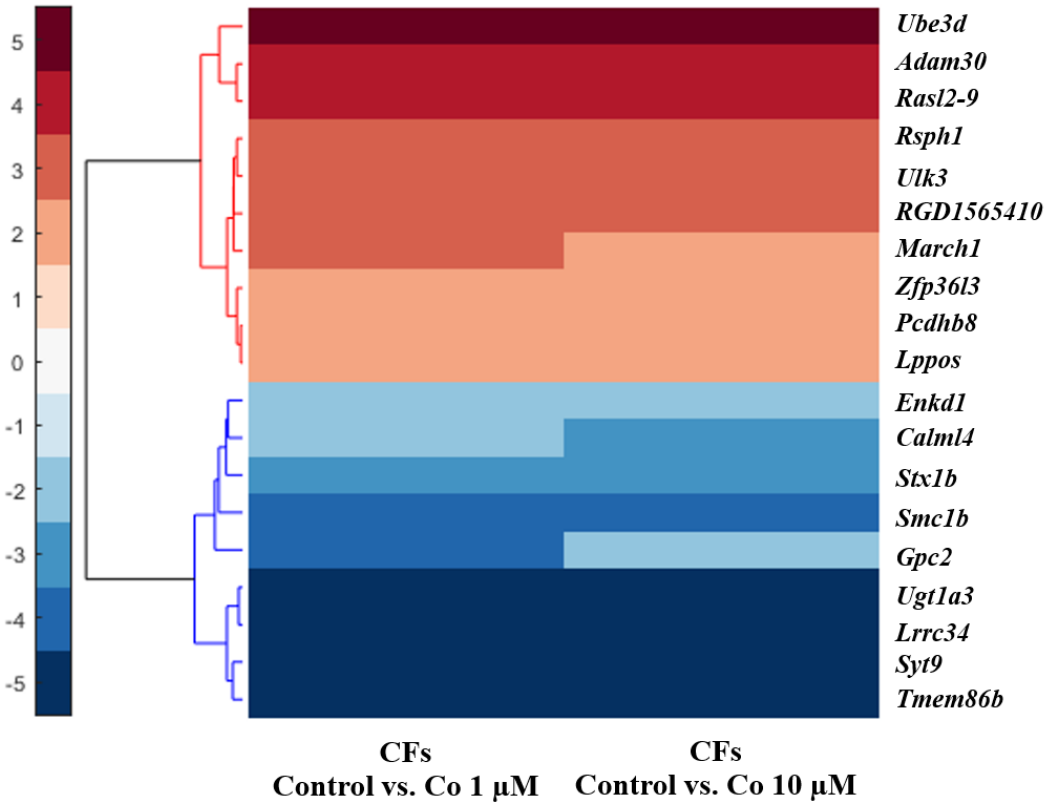

Figure 6-8 Correlation heat map of DEGs in CFs after 1 and 10 µM Co treatment. Heatmap showing differential expression of DEGs between Control vs. Co 1 µM (CFs 1 µM) and Control vs. Co 10 µM (CFs 10 µM) treatments. The first column is CFs after Co treatment at 1 µM and the second column is CFs after Co treatment at 10 µM. DEGs (≥ 2.0 and ≤ -2.0 log2 ratio, $p<0.05$) of each pairwise comparison are shown. Fold change of gene expression were normalised with untreated cells. x-axis:columns display two concentration treatments clustered by similarities among gene expression profiles; y axis: each row displays the expression strength of a particular gene in the DEGs, clustered by similarities across treatments. Colour key indicates the intensity associated with normalised expression values. Values are colour coded (Red:upregulated expression; Blue:downregulated expression) (Gene symbols as in Table 6-7)

Table 6-7 Highly expressed genes and relevant enrichment pathways analysis in CFs.

Gene name	Description	Representative affected pathway (GO terms/KEGG)	**Log2 FC Co 1 µM**	**Log2 FC Co 10 µM**
Lppos	LIM domain containing preferred translocation partner in lipoma, opposite strand	Cell periphery in focal adhesion[G] Cell adhesion and cell motility[K] Cytoskeletal signalling[G]	2.12928	2.15650
Pcdhb8	Protocadherin beta 8 precursor	Calcium ion binding[G] Cell-adhesion protein[G] Metal binding activity[G]	2.06413	2.24101
Zfp36l3	Zinc finger protein 36, C3H type-like 3	Metal binding activity (zinc)[G]	2.39232	2.39232
March1	Membrane Associated Ring-CH-Type Finger 1	Metal binding activity (zinc)[G] MHC protein binding[G] Ubiquitin protein ligase activity[G]	2.89077	2.584962
RGD1565410	Similar lymphocyte antigen 6 complex, locus C1 (Ly6-C antigen)	Lymphocyte cell adhesion[K]	2.75489	2.87447
Ulk3	Serine/threonine-protein kinase ULK3	ATP binding [G] Protein serine/threonine kinase activity [G] Autophagy[K] Smoothened signalling pathway[G]	3.11548	2.66297
Rsph1	Radial spoke head 1 homolog (chlamydomonas)	Condensed nuclear chromosome[G] Axoneme assembly[G] Spermatid development[G]	3.44478	2.80735
Rasl2-9	RAS-like, family 2, locus 9	Cell cycle[K] RNA transport[K] Virus infection[K]	3.85798	4.04439
Adam30	Disintegrin and metalloproteinase domain-containing protein 30 precursor	Metal binding protein [G] Metalloendopeptidase activity [G]	4.16992	4.24793
Ube3d	E3 ubiquitin-protein ligase E3D	Cyclin binding activity[G] Ubiquitin protein ligase activity[G]	5.20945	5

Table 6-7 Highly expressed genes and relevant enrichment pathways analysis in CFs (cont.).

Gene name	Description	Representative affected pathway (GO terms/KEGG)	Log2 FC Co 1 µM	Log2 FC Co 10 µM
Tmem86b	Lysoplasmalogenase	Lipid metabolic process [K] Alkenylglycerophosphocholine/ Alkenylglycerophosphoethanolamine hydrolase activity[G]	-5.52356	-5.52356
Syt9	Synaptotagmin ix	Calcium ion-regulated exocytosis of neurotransmitter[G]	-5.08746	-5.08746
Lrrc34	Leucine-rich repeat-containing protein 34	Cell differentiation[G]	-4.70043	-4.70044
Ugt1a3	UDP glycosyltransferase 1 family, polypeptide A3	Metabolic pathways [K] Drug metabolism[K]	-4.52356	-4.52356
Gpc2	Glypican 2 network	Proteoglycan binding[G] / Smoothened signalling pathway[G]	-4.33985	-2.09192
Smc1b	Structural maintenance of chromosomes 1b	Cell cycle [K] and Condensed nuclear chromosome[G]	-3.58496	-3.58496
Stx1b	Syntaxin 1b	Calcium ion-regulated exocytosis of neurotransmitter[G] Protein domain specific binding (SNARE) [K] Long term potential[K] Positive regulation of excitatory postsynaptic potential[G]	-3.27302	-2.53605
Calml4	Calmodulin-like 4	Signalling pathway (calcium, cAMP, cGMP PKG, phosphatidylinositol) [K] Inflammatory mediator regulation of TRP channels [K] Vascular smooth muscle contraction [K] Fluid shear stress and atherosclerosis [K]	-2.35548	-2.91938
Enkd1	Enkurin Domain Containing 1	Cytoplasmic microtubule and microtubule cytoskeleton compartment[G]	-2.35484	-2.01089

This table includes a list of genes (under weighted cut off, ≥ 2.0 and ≤ -2.0 log2 ratio, *p<0.05*) the highest ranked 19 known genes from a total of more than ten thousand transcripts overexpressed in CFs samples (1 and 10 µM Co treatment) as compared with untreated CFs. FC: Fold change; SNARE: soluble N-ethylmaleimide-sensitive factor attached protein receptor; cAMP: cyclic adenosine monophosphate; cGMP-PKG: cGMP-dependent protein kinase or Protein Kinase G

6.3.3.5 RNA Sequencing for identification of genes of interest associated with Co ions on gene expression of 3T3 cells and CFs after 1 and 10 µM Co treatment.

Chapter 3 conducted western blotting on the lysates of 3T3 and CF cells exposed to Co. That study examined the effects of Co on the expression levels of the following proteins: CaMKIID, DMT1, TRPC6, TRPM7 and TRPV1 as targets for the action of Co in both 3T3 cells and CFs in the *in vitro* models used.

All of the proteins of interest that were selected were shown to be involved as targets of the actions of Co following *in vitro* exposure as described earlier in sections on the western blotting data. To build upon our understanding of the molecular consequences of Co exposure, we continued this focus but this time on the expression of their genes; *Camkiid, Dmt1, Trpc6, Trpm7,* and *Trpv1* to examine their expression changes and to see how they correlate with the western blot data.

From the GO molecular function categories, four of the five genes (*Dmt1, Trpc6, Trpm7,* and *Trpv1*) were enriched in the response to transmembrane transporter activity category; metal ion and cation binding activity (Co, cadmium, nickel, lead and vanadium ion, inorganic cation, cation transmembrane transporter) and calcium ion channel regulatory activity. As discussed in the previous chapters, *Camkiid*, is involved in Ca(2+)/calmodulin-dependent protein kinase subfamily class of enzyme in mammalian cells and is also relevant in cardiovascular disease.

In vitro RNA-Seq studies used 3T3 cells and CFs that were exposed to 1 and 10 µM Co treatment. The expression of the five genes of interest in the treated cells were compared with their expression levels in control cells as shown in Table 6-8. In 3T3 cells exposed to 1 µM Co, *Camkiid* and *Trpm7*, were up-regulated and *Dmt1* and *Trpv1* were observed to be down-regulated. *Trpc6* is absent from the DEG list at this 1 µM Co concentration. At 10 µM Co, all genes of interest, *Camkiid, Dmt1, Trpc6, Trpm7* and *Trpv1,* showed up-regulation of their gene expression.

In CFs, exposed to 1 µM Co, three *Camkiid, Dmt1,* and *Trpv1* were found to be up-regulated while *Trpc6* and *Trpm7*were down-regulated. After 10 µM Co treatment of CFs *Camkiid* continued being upregulated after exposure to Co while *Trpm7* now showed a change in expression direction with a small upregulation at the higher concentration. Both *Dmt1* and *Trpv1* went from an over-regulated expression at 1 µM

to downregulation at 10 µM. Co treatment at both concentrations resulted in *Trpc6* being under expressed, with a slight increase in the downregulation at the higher Co concentration as in Table 6-9.

Table 6-8 RNA-Seq gene expression profiling of 3T3 cells after treatment with 1 and 10 µM Co treatment (Log2 Fold change).

Gene Symbol	Accession	Co 1 µM		Co 10 µM	
		Log2FC	***p-value***	**Log2FC**	***p-value***
Camkiid	BAD90304.1	0.18748*	0.00006	0.19737*	0.00004
Dmt1	EDL04089.1	-0.34565*	0.00368	0.09734*	9.35314E-16
Trpc6	NP_001269015.1	Not on the list	-	1	0.99049
Trpm7	NP_067425.2	0.15703*	0.00075	0.58799*	1.90242E-41
Trpv1	XP_006532643.2	-2	0.23158	0.32193	0.98218

*$p<0.05$, FC, Fold change; *Camkiid*, Calcium/calmodulin–dependent protein kinase II delta; *Dmt1*, Divalent metal transporter; *Trpc6*, Transient receptor potential/canonical receptor subtype 6; *Trpm7*, Transient receptor potential/melastatin receptor subtype7; *Trpv1*, Transient receptor potential/ vanilloid receptor subtype 1. Log_2 Fold change calculated in comparison to the control.

Table 6-9 RNA-Seq gene expression profiling of CFs after treatment with 1 and 10 µM Co treatment (Log2 Fold change).

Gene Symbol	Accession	Co 1 µM		Co 10 µM	
		Log2FC	***p-value***	**Log2FC**	***p-value***
Camkiid	NP_036651.1	0.03045	0.62872	0.07512	0.23237
Dmt1	NP_037305.2	0.01381	0.93501	-0.01394	0.97198
Trpc6	NP_446011.1	-0.13816	0.06310	-0.40490*	2.17E-07
Trpm7	NP_446157.2	-0.09065*	0.02484	0.00349	0.9208
Trpv1	XP_008766104.1	0.22239	0.80197	-0.36257	0.74753

*$p<0.05$, FC, Fold change; *Camkiid*, Calcium/calmodulin–dependent protein kinase II delta; *Dmt1*, Divalent metal transporter; *Trpc6*, Transient receptor potential/canonical receptor subtype 6; *Trpm7*, Transient receptor potential/melastatin receptor subtype7; *Trpv1*, Transient receptor potential/ vanilloid receptor subtype 1. Log_2 Fold change calculated in comparison to the control.

6.3.3.6 Comparison of the in vitro RNA-Seq gene expression data with protein expression determined by Western blotting

It should be noted that a comparison between RNA-Seq data and western blotting data shows important variations in the results. In 3T3 cells, only *Trpc6* and *Trpm7* were compared between RNA-Seq and western blotting data. Both gene and protein expression showed changes in the opposite direction. None of the rest of the genes, *Camkiid, Dmt1* and *Trpv1* were determined by western blotting, so there can be no comparison between the two data sets (as seen in Table 6-10).

Table 6-10 Comparison of 3T3 cells RNA-Seq expression data with protein expression determined by western blotting.

Gene:Protein	**RNA-Seq (Direction vs control)**		**Western blotting (Direction vs control)**	
	Co 1 µM	**Co 10 µM**	**Co 1 µM**	**Co 10 µM**
Camkiid:CaMKIID	UP*	UP*	-	-
Dmt1: DMT1	DOWN*	UP*	-	-
Trpc6: TRPC6	Not on the list	UP	DOWN	DOWN
Trpm7: TRPM7	UP*	UP*	DOWN	DOWN
Trpv1: TRPV1	DOWN	UP	-	-

**p<0.05*, *Camkiid*, Calcium/calmodulin–dependent protein kinase II delta; *Dmt1*, Divalent metal transporter; *Trpc6*, Transient receptor potential/canonical receptor subtype 6; *Trpm7*, Transient receptor potential/melastatin receptor subtype7; *Trpv1*, Transient receptor potential/ vanilloid receptor subtype 1. Log_2 Fold change calculated in comparison to the control.

Table 6-11 shows the comparison of the CFs gene and protein expression levels from the RNA-seq and western blotting data. At 1 µM Co treatment, only *Camkiid* showed significantly increased gene expression from the RNA-Seq data in line with that observed of the respective proteins from the western blotting study. However, in CFs at 10 µM Co treatment, the majority of the gene and protein expressions changes are aligned with the exception of *Trpc6* mRNA expression, which showed opposite (down-regulation) direction to that of its protein.

Table 6-11 Comparison of CFs RNA-Seq expression data with protein expression determined by western blotting.

Gene/Protein	**RNA-Seq (Direction vs control)**		**Western blotting (Direction vs control)**	
	Co 1 µM	**Co 10 µM**	**Co 1 µM**	**Co 10 µM**
Camkiid:CaMKIID	UP	UP	UP*	UP*
Dmt1: DMT1	UP	DOWN	NO CHANGE	DOWN
Trpc6: TRPC6	DOWN	DOWN*	UP*	UP*
Trpm7: TRPM7	DOWN*	UP	UP*	UP*
Trpv1: TRPV1	UP	DOWN	-	-

**p<0.05*, *Camkiid*, Calcium/calmodulin–dependent protein kinase II delta; *Dmt1*, Divalent metal transporter; *Trpc6*, Transient receptor potential/canonical receptor subtype 6; *Trpm7*, Transient receptor potential/melastatin receptor subtype7; *Trpv1*, Transient receptor potential/ vanilloid receptor subtype 1. Log_2 Fold change calculated in comparison to the control.

6.3.4 RNA Sequencing for in vivo experiment.

6.3.4.1 Pearson correlation heat map in vivo experiment

The Pearson heat map of correlation coefficient values across samples are shown in Figure 6-9. In comparison to the control group (7-day), the Co-treatment for 7-day is similar as it shows a coefficient value of 0.998. On the 28-day of exposure, the coefficient value between Co-treatment and control group was 0.996. Values close to 1 represent samples which are very similar. This suggests only a small effect in all treatment groups from Co exposure after 7 and 28 days on gene expression changes.

Values between the two control groups at 7 and 28 days were similar, with a coefficient value of 0.999, so the aging was not a critical factor (comparison at different ages of 21 days). Taken together, these coefficient values all suggest that there are only slightly changes in gene expression after 7 days and 28 days in response to Co treatment.

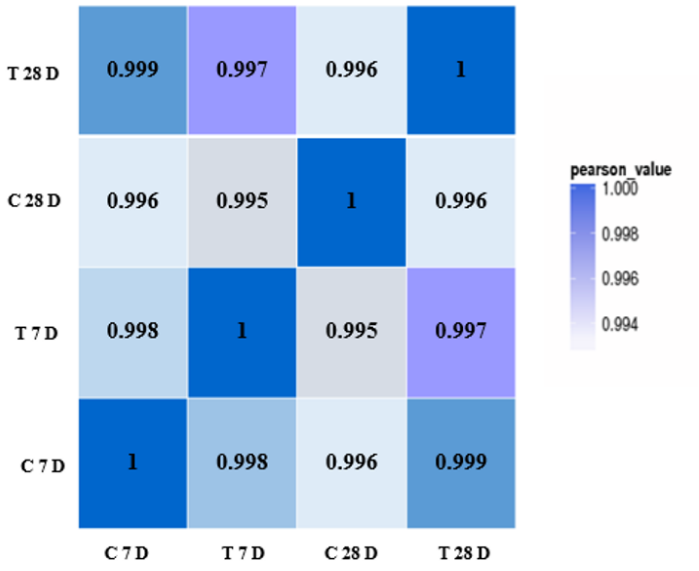

Figure 6-9 Pearson correlation heat map of differentially expressed genes following Co-exposure *in vivo*. Heatmap of correlation coefficient values across samples, shows the gradient colour barcode for comparisons between Co treatment (7 and 28 days) and the control group. Values close to 1 represent samples which are very similar. This suggests only a small effect in all treatment groups from Co exposure after7 and 28 days on gene expression changes.

6.3.4.2 Differential Gene Expression in in vivo experiment

Identification of the number of expressed genes in each group and, subsequently, calculation of its proportion to the total gene number in the database for each sample is shown on Figure 6-10. The total number of genes expressed is approximately 12,000 genes or around 70% of genes from the reference transcriptome (17,407 genes).

DEG analysis of gene expression identified by heatmap clustering comparisons between the control vs. Co 7 days and control vs. Co 28 days of heart samples (Figure 6-11 and Table 6-12) provided an overview of the molecular effects of Co exposure in these cells. The heart RNA heatmap displays four main clusters of gene expression changes between the two treatment exposure time responses. These are 4 main clusters, indicated in Table 6-12.

Cluster 1; C1, showed high significant down-regulation after 7 days Co treatment and reversed to be high up-regulation after 28 days Co exposure but the gene list in this cluster was composed of the microRNAs, for which the function is not known.

The genes in Cluster 2 (C2) showed a high fold change of expression in the heart following 7 and 28 days Co treatment. In this cluster are also *Prm1* and *Hmgn5*, both involved in the DNA binding function, and *Myl4* and *Myl7* involved in cardiac muscle contraction as part of their cardiovascular system action.

The next cluster, C3 showed mainly down-regulation at both exposure times but 7 days exposure show less down regulation compared with 28 days exposure. This group of gene involved in the common pathway, such as cell response stimulus eg. mechanical and abiotic stimulus - *Acta1, Pcp4, Thbs1, Atp1a3, Nppa, Hspa1a* and *Moap1*, signalling pathway(cAMP, cGMP-PKG, PI3K-Akt, p53 and MAPK); *Acta1*, *Thbs1* and *Hspa1a*, hormone system (aldosterone, oestrogen, insulin and thyroid hormone) - *Hspa1a* and *Acta1* and cardiovascular system - *Acta1* and *Nppa*. Moreover, *Acta1* gene is also involved with the regulation of calcium reabsorption.

Lastly in C4, 7 days Co exposure induced up-regulation of genes, similar to 28 days exposure, which also showed up-regulated gene expression and greater up-regulation compared with 7 days exposure. Having KEGG database and GO terms, those genes modulated the cell adhesion molecules- *RT1-Bb* and *RT1-T24-3*, antigen processing

and presentation - *Cited1, RT1-Bb* and *RT1-T24-3*, binding activity (Antigen, peptide, lipid and amide) - *Cited1, Cd1d1, RT1-Bb* and *RT1-T24-3,* immune system - *Cd1d1*, *RT1-Bb* and *RT1-T24-3*, also involved with the neuron system eg. astrocyte and glial cell development and projection - *Mt3* and *Gfap* in addition to endocytosis genes- *RT1-T24-3*.

According to our findings, the expression of more than a hundred genes was altered significantly in response to Co exposure in hearts. Our study identified the possible pathways that respond to Co exposure, which are signalling pathways, binding activity, the immune system and genes related to muscle contraction in cardiovascular disease.

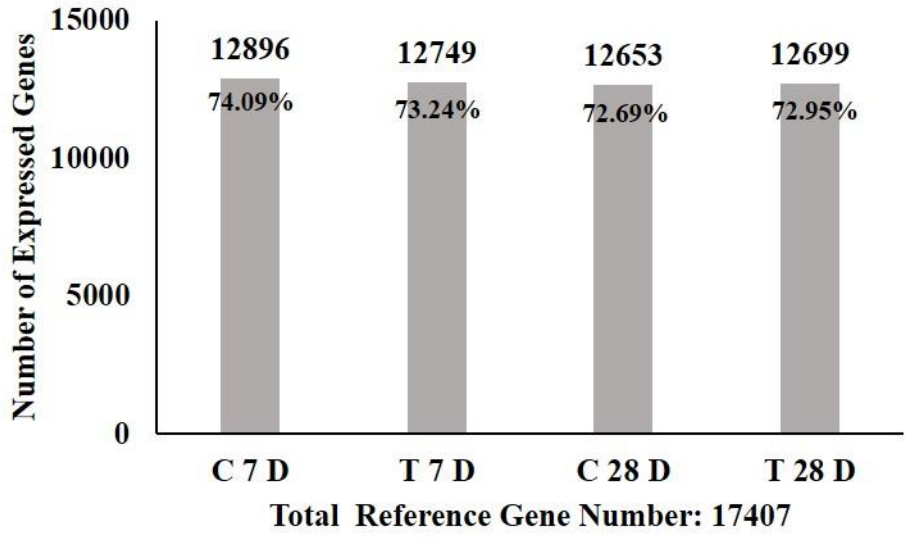

Figure 6-10 Number of identified genes between control and Co-treatment heart RNA after 7 and 28 days. Male Sprague-Dawley rats each weighing approximately 200-250 g were given daily i.p injections of 1 mg/kg $CoCl_2$ in distilled water for 7 and 28 days. Control rats were given daily i.p injection of distilled water**.** There were n=6 rats in each group. There are approximately 12,000 genes or around 74% of genes from the total reference gene. X-axis is sample name. Y-axis is number of identified expressed genes. The number of expressed genes is shown above each bar. The proportion at the top of each bar equals expressed gene number divided by total gene number reported in each gene reference annotation.

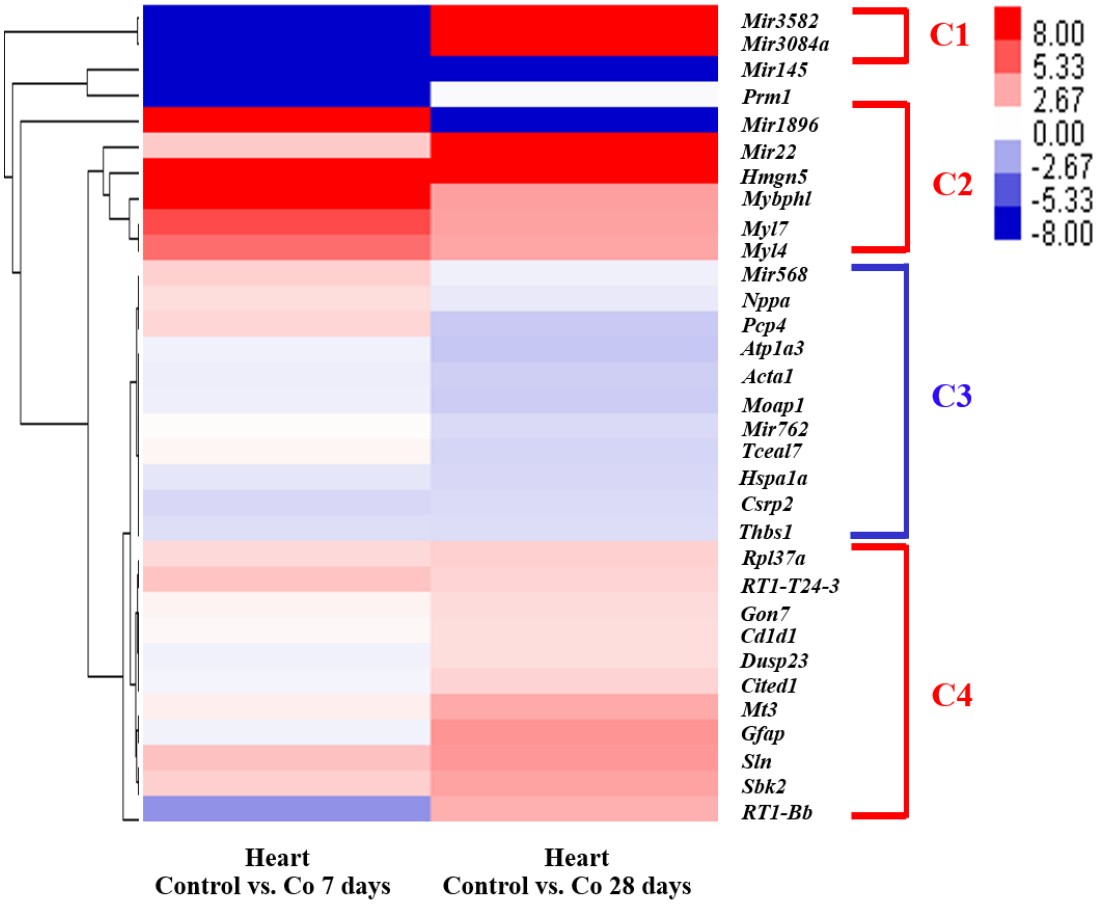

Figure 6-11 The overview clustering of DEG analysis of gene expression profiles in heart after 7 and 28 days Co treatment. The first column (Control vs. Co 7 days) and the second column (Control vs. Co 28 days) represent differentially DEGs fold change values which are clustered**.** Fold change of gene expression were normalised with untreated cells. The gradient colour barcode at the right top indicates log2 (FC) value (Red:upregulation of expression; Blue:downregulation of expression). Clusters and abbreviations of selected gene list are indicated in Table 6-12; C, Cluster.

Table 6-12 The details of selected genes and pathways enriched in the clusters of hearts after Co treatment for 7 and 28 days.

Cluster	Genes	7 days Fold change	28 days Fold change	Related functions (GO Terms/KEGG)
C1 (High downreg at 1, high upreg at 10 μM)	*Mir3582*	-8.72109	8.80413	Micro RNA : Undetermined related function
	Mir3084a	-10.13827	8.22641	
	Mir145	-8.38370	-8.57364	
C2 (High upreg at 1 and 10 μM)	*Prm1*;Protamine 1	-10.33762	-0.10962	DNA binding[G] Chromosome condensation[G] Regulation of transcription, DNA-templated[G] Regulation of actin cytoskeleton[K] Leukocyte transendothelial migration[K] Focal adhesion[K] Cardiac muscle contraction[K] Adrenergic signalling in cardiomyocytes[K] Apelin signalling pathway[K]
	Mir1896	8.66178	-8.78463	
	Mir22	1.65208	8.28540	
	Hmgn5; High Mobility Group Nucleosome Binding Domain 5	8.31288	8.78953	
	Mybphl; Myosin Binding Protein H Like	8.79766	2.99205	
	Myl7; Myosin Light Chain 7	5.66279	2.90527	
	Myl4; Myosin Light Chain 4	4.55751	2.79072	
C3 (Downreg at both 1 and 10 μM)	*Mir568*	1.42268	-0.43347	Cellular response to stimulus[G] Regulation of collecting lymphatic vessel constriction[G] G-protein coupled receptor binding[G] Regulation of cardiac muscle cell membrane potential[G] Cardiac muscle contraction[K] Hormone system(Aldosterone, Oestrogen, Insulin and Thyroid)[K] Carbohydrate digestion and absorption[K] Endocytosis[K] Proteoglycans in cancer[K]
	Nppa; natriuretic peptide a	1.01095	-0.65444	
	Pcp4; purkinje cell protein 4	1.23670	-1.65918	
	Atp1a3; atpase, na+/k+ transporting alpha 3 polypeptide	-0.38504	-1.72334	
	Acta1; actin, alpha 1, skeletal muscle	-0.48791	-1.45092	
	Moap1; modulator of apoptosis 1	-0.44395	-1.55947	
	Mir762	0.06947	-1.10561	
	Tceal7; Transcription Elongation Factor A Like 7	0.272192	-1.272679	

C,Cluster; G, GO terms; K, KEGG

Table 6-12 The details of selected genes and pathways enriched in the clusters of hearts after Co treatment for 7 and 28 days.(cont.)

Cluster	Genes	7 days Fold change	28 days Fold change	Related functions (GO Terms/KEGG)
C3 (Downreg at both 1 and 10 μM)	*Hspa1a*; heat shock 70kd protein 1a	-0.727474	-1.17405	Epstein-Barr virus infection[K] Signalling pathwayK (HIF-1, cAMP, cGMP-PKG, PI3K-Akt, p53 and MAPK)[K] Regulation of calcium reabsorption[K]
	Csrp2; Cysteine And Glycine Rich Protein 2	-1.166039	-1.075474	
	Thbs1; thrombospondin	-0.998811	-1.035962	
C4 (Upreg at both 1 and 10 μM)	*Rpl37a*; Ribosomal Protein L37a	1.143846	1.424382	Astrocyte/Glial cell development and projection[G] Response to interleukin-9[G] Cadmium ion homeostasis[G] Regulation of hydrogen peroxide catabolic process[G] Regulation of oxygen metabolic process[G] Regulation of lysosomal membrane permeability[G] Lipid antigen binding[G] Tight junction[K] Hematopoietic cell lineage[K] Jak-STAT signalling pathway[K]
	RT1-T24-3; RT1 class I, T24, gene 3	1.798874	1.322401	
	Gon7; GON7, KEOPS Complex Subunit Homolog	0.321486	1.074835	
	Cd1d1; cd1d1 molecule	0.193038	1.016573	
	Dusp23; Dual Specificity Phosphatase 23	-0.378978	1.034557	
	Cited1;cbp/p300-interacting transactivator with glu/asp-rich carboxy-terminal domain 1	-0.284258	1.323374	
	Mt3; metallothionein 3	0.485427	2.641157	
	Gfap; glial fibrillary acidic protein	-0.350497	3.313417	
	Sln; Sarcolipin	1.921049	3.203668	
	Sbk2;SH3 Domain Binding Kinase Family Member 2	1.464467	2.884081	
	RT1-Bb;Rano class II histocompatibility antigen, B-1 beta chain	-3.411426	2.471436	

C,Cluster; G, GO terms; K, KEGG

Afterwards, differential gene expression (DEG) analysis was carried out to determine the differential expressed genes between treated (7 and 28 days Co exposure) and untreated groups using the weighted cut-off (≥ 2.0 and ≤ -2.0 log2 ratio, $p<0.05$).

The weighted cut off DEGs of the effect of Co on hearts are presented by a histogram Figure 6-12. In the 28 days up-regulated list (93 genes), only 10% of these genes are present in the 7 days upregulated gene list (9 genes). Whereas no similar genes were found between the 7 and 28 days downregulated gene list. It seems to be that the Co effects at both two endpoints (7 and 28 days) did not differ much in gene expression. So it can predicted that small incremental changes in the effect of Co to heart tissue may produce small or no relative changes in pathways.

However, the comparison of the fold change between 7 and 28 days Co exposure showed that 44% of up-regulated gene in the 28 days gene were increased after increasing the Co concentration.

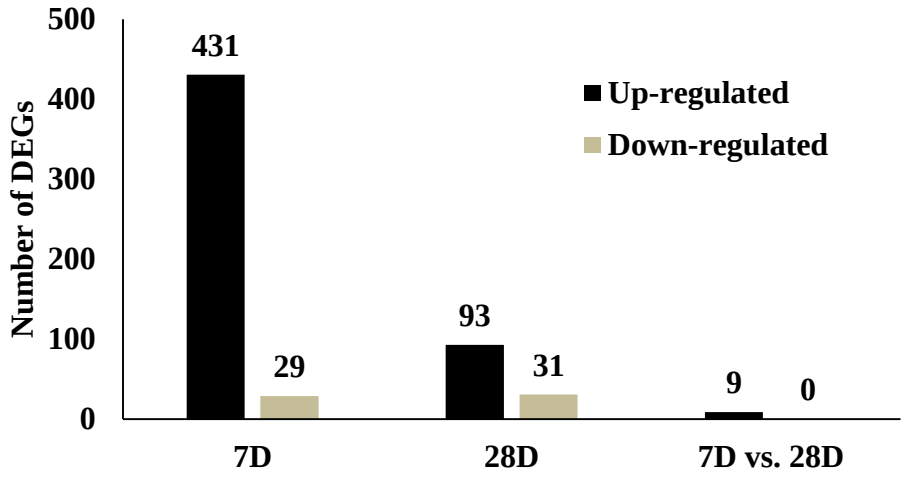

Figure 6-12 DEGs of the effect of Co *in vivo* after 7 and 28 days. Male Sprague-Dawley rats each weighing approximately 200-250 g were given daily i.p injections of 1 mg/kg $CoCl_2$ in distilled water for 7 and 28 days. Control rats were given daily i.p injection of distilled water. Both group n=6. The cut-off criteria for DEGs were [log2FC (Fold change)] ≥ 2 and $p<0.05$. The number of changed genes is shown above each bar.

6.3.4.3 Correlation heat map of heart after 7 and 28 days Co treatment.

For visualisation purposes, heat map correlations between two concentrations of Co were created by MATLAB software analysis using cutoff DEGs (Figure 6-13). Heat map shows cross-correlation by treatment and similarity of gene-expression profiles of cut-off DEGs (≥ 2.0 and ≤ -2.0 log2 fold change, $p<0.05$) for each pairwise comparison – Control vs. Co 7 days and Control vs. Co 28 days.

The expression of DEGs were visualised and plotted using heatmap clustering, Figure 6-13 shows the DEGs of each pairwise comparison – Control vs. Co treatment 7 days and Control vs. Co treatment 28 days. This study identified 9 genes in the comparison data sets between 7 days and 28 days. Along with expression changes, up-and down-regulation was presented between the two exposure times. Upregulated-related genes can be divided into two groups. The first group shows upregulation at 7 days, and down regulation in 28 days (*LOC100134871, Pcdha9, Dnai2,* and *Nrip3*) and *Msln* also shows range in opposite direction. Whereas the second group shows up-regulation after both 7 and 28 days exposure (*Cdca2*, *Myl7, Nek11,* and *Hmgn5*).

Clustering analysis, based on the gene expression patterns, showed similar functionalities using all the software packages (GOrilla, Cytoscape and KEGG mapper). These softwares were used to integrate the enrichment pathways (As shown in Table 6-13). This analysis helps to identify pathways that may be affected following Co exposure.

Cdca2 is a cell-cycle regulator and selectively recruits PP1γ onto mitotic chromatin at anaphase and into subsequent interphase. The reduction of *Cdca2* expression leads to apoptosis in large scale cell death (in interphase/G2 checkpoint), whereas overexpression shows in the dominant negative mutant (Trinkle-Mulcahy *et al.*, 2006). *LOC100134871* is beta globin minor gene. The literature provides evidence that these genes are related to heme/iron ion/oxygen binding and oxygen carrier activity. In preliminary clinical studies, LOC100134871 was used to treat in vascular dementia (VD) (Zhang *et al.*, 2010; Zhang *et al.*, 2012). And in a study of Wu and coworkers, overexpression of LOC100134871 causes insufficient supply of oxygen in a cerebral ischemia reperfusion in *in vivo* study (Wu *et al.*, 2015). *Pcdha9* is a member of

protocadherin alpha 9, related to calcium ion binding and cell-adhesion protein in the maintenance of neuronal connections in the brain. *Dnai2* belongs to the dynein complex of respiratory cilia and sperm flagella so it is not specific to the heart. But in GO terms, the pathway in the heart is related to respiratory electron transport, ATP synthesis and heat production. This gene has also been studied in Huntington's disease. *Nrip3* is nuclear receptor interacting protein 3, one of the members of rat aspartic protease, which is related to aspartic-type endopeptidase activity and is absolutely conserved in heart muscle. *Myl7* is myosin light chain 7, which is associated with Fechtner syndrome, atrial fibrillation (AF) and also related to pathways of calcium ion binding. *Nek11* (NIMA related kinase 11) is located in the S-phase checkpoint, which is related to protein kinase activity that has important roles in the DNA replication (G2/M checkpoint), response to DNA damage by genotoxic stress. *Hmgnb5* (High Mobility Group Nucleosome Binding Domain 5), is a nuclear protein that binds to nucleosomes. It may function as a nucleosome DNA binding and transcriptional activation protein. Some studies found this gene involved with apoptosis via the mitochondria pathway, and the Bcl-2 family activity in prostate cancer (Zhang *et al.*, 2012). It also plays roles in the cell cycle and cell proliferation(Jiang, Zhou and Zhang, 2010).

In conclusion, the overview of Co effects on heart RNA samples shows enrichment highlighted by 1) cell apoptosis (*Hmgnb5* and *Cdca2*), 2) cell metabolism, G2/M checkpoint regulation (*Cdca2* and *Nek11*), 3) calcium ion channel activity and cell adhesion (*Myl7*, *Msln* and *Pcdha9*) 4) binding affinity of the regulator, heme/iron ion/oxygen activity (*LOC100134871*).

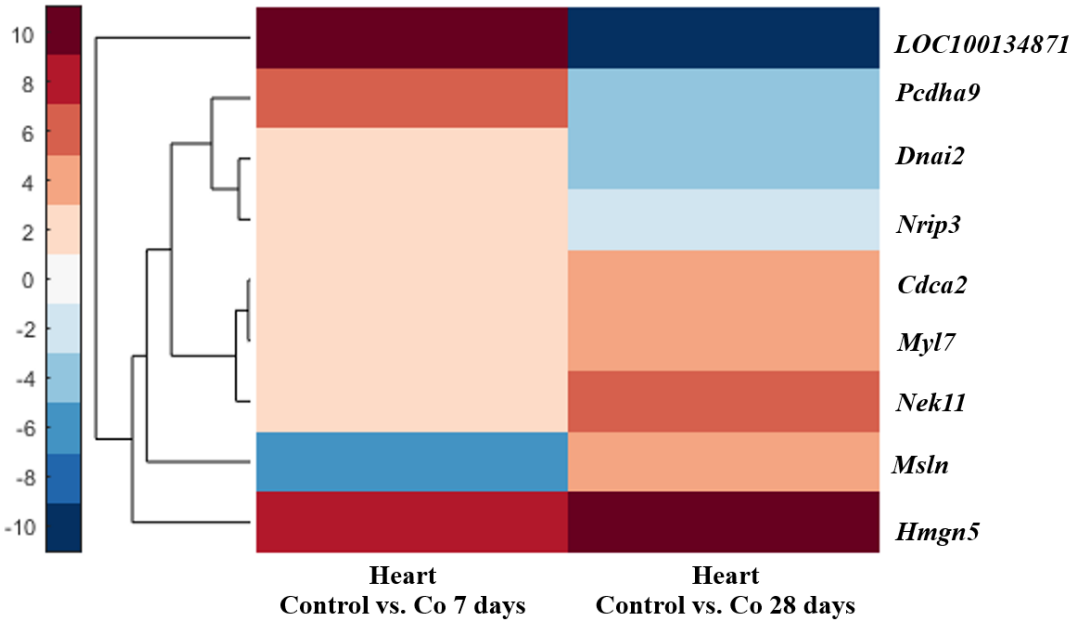

Figure 6-13 Correlation heat map of DEGs in rat hearts after 7 and 28 days Co treatment. Heatmap showing differential expression of DEGs between (Rat7D) Control vs. Co 7 days exposure (Rat7D) and Control vs. Co 28 days exposure (Rat28D). Male Sprague-Dawley rats were given daily i.p injections of 1 mg/kg $CoCl_2$ (n=6). The first column is heart RNA after Co treatment at 7 days and the second column is heart RNA after Co treatment at 28 days. DEGs (≥ 2.0 and ≤ -2.0 log2 ratio, $p<0.05$) of each pairwise comparison. Fold change of gene expression were normalised with untreated cells. x-axis:columns display two timepoint treatments clustered by similarities among gene expression profiles; y axis: each row displays the expression strength of a particular gene in the DEGs, clustered by similarities across treatments. Colour key indicates the intensity associated with normalised expression values. Values are colour coded (Red:upregulated expression; Blue:downregulated expression) (Gene symbols as in Table 6-13).

Table 6-13 Highly expressed genes and relevant enrichment pathway analyses in rat hearts.

Gene name	Description	Representative affected pathway (GO terms/KEGG)	Log2 FC Co 7 days	Log2 FC Co 28 days
LOC100134871	Beta globin minor gene	Binding affinity of the regulator (heme/iron ion and oxygen binding) Oxygen carrier activity	11.08481	-10.08613
Pcdha9	Protocadherin alpha 9	Calcium ion binding	5.78135	-4.64385
Dnai2	Dynein, axonemal, intermediate chain 2	Huntington's disease Respiratory electron transport ATP synthesis Heat production	2.87915	-3.12928
Nrip3	Nuclear receptor interacting protein 3	Aspartic-type peptidase activity Aspartic-type endopeptidase activity	2.03242	-2.35050
Cdca2	Cell division cycle associated 2	Cell apoptosis Cell metabolism / Cell-cycle regulator	2.13327	3.82781
Myl7	Myosin light chain 7	Calcium ion channel and cell adhesion Leukocyte transendothelial migration Focal adhesion Regulation of actin cytoskeleton	2.33869	3.80624
Nek11	NIMA (never in mitosis gene a)-related expressed kinase 11	Cell metabolism Intra-S DNA damage checkpoint	2.80735	5.12928
Msln	Mesothelin	Cell adhesion / Cell protein metabolic process	-6.06609	3.90689
Hmgn5	High mobility group nucleosome binding domain 5	Cell apoptosis Nucleosome DNA binding / RNA binding	8.28077	9.78790

This table includes all genes (under weighted cut off, ≥ 2.0 and ≤ -2.0 log2 ratio, $p<0.05$). The 9 known genes from a total of more than ten thousand transcripts overexpressed in rat hearts (7 days vs. 28 days) as compared with normal rat heart samples.

6.3.4.4 RNA Sequencing for identification of genes of interest associated with gene expression of heart after 7 and 28 days Co treatment.

Similar to the *in vitro* experiments, all of the proteins of interest; CaMKIID, DMT1, TRPC6, TRPM7 and TRPV1 that were selected were shown to be involved as targets of the actions of Co following *in vivo* exposure as described earlier. Heart samples from control and Co treatment group were extracted and then the RNA sequenced to determine the gene expression. Comparisons were carried out as before: 1) Control vs. Co-treatment for 7 days and 2) Control vs. Co-treatment for 28 days.

For comparison of gene expression using RNA-Seq between Co treatment and untreated rats (Table 6-14), the expression of the five genes was measured after 7 days exposure to Co and compared with the control group. Of these 4 genes, *Camkiid, Dmt1*, *Trpc6* and *Trpm7* were up-regulated, *Trpv1* was down-regulated. After 28 days exposure to Co, the five genes: *Camkiid, Dmt1, Trpc6, Trpm7* and *Trpv1* were up-regulated. The up-regulated expression was similar between 7 and 28 days exposure, but for *Trpc6* expression was over 10-fold higher after 28-days compared with 7-days of Co-exposure.

Table 6-14 RNA-Seq gene expression profiling of rat hearts changes (Log2 Fold change) after 7 and 28 days Co administration.

Gene Symbol	Accession	Co 7 days		Co 28 days	
		Log2FC	***p-value***	**Log2FC**	***p-value***
Camkiid	NP_036651.1	0.01473	0.83874	0.00209	0.97823
Dmt1	NP_037305.2	0.17782	0.23454	0.15465	0.32617
Trpc6	NP_446011.1	0.27130	0.60744	2.92057*	0.00126
Trpm7	NP_446157.2	0.09166*	0.02891	0.12940*	1.39E-05
Trpv1	XP_008766104.1	-0.33703	0.77975	1.89309	0.25925

**p<0.05*, FC, Fold change; *Camkiid*, Calcium/calmodulin–dependent protein kinase II delta; *Dmt1*, Divalent metal transporter; *Trpc6*, Transient receptor potential/canonical receptor subtype 6; *Trpm7*, Transient receptor potential/melastatin receptor subtype7; *Trpv1*, Transient receptor potential/ vanilloid receptor subtype 1. Log_2 Fold change calculated in comparison to the control.

6.3.4.5 Comparison of the in vivo RNA-Seq gene expression data with protein expression determined by Western blotting.

Table 6-15 shows the comparison of the heart gene and protein expression levels from the RNA-Seq and western blotting data. At 7 days Co treatment, only *Trpc6* showed significantly increased gene expression from the RNA-Seq data in line with that observed of their respective proteins from the western blotting study. However, with *Camkiid, Trpc6* and *Trpm7* at 28 days Co treatment, the majority of the gene and protein expressions changes are aligned with the exception of *Dmt1* mRNA expression, which showed opposite up-regulation direction to that of its protein.

Table 6-15 Comparison of heart cells RNA-Seq expression data with protein expression determined by western blotting.

Gene/Protein	**RNA-Seq (Direction vs control)**		**Western blotting (Direction vs control)**	
	Co 7 days	**Co 28 days**	**Co 7 days**	**Co 28 days**
Camkiid	UP	UP	DOWN	UP*
Dmt1	UP	UP	DOWN*	DOWN
Trpc6	UP	UP*	UP	UP*
Trpm7	UP*	UP*	DOWN	UP*
Trpv1	DOWN	UP	-	-

**p<0.05, Camkiid*, Calcium/calmodulin–dependent protein kinase II delta; *Dmt1*, Divalent metal transporter; *Trpc6*, Transient receptor potential/canonical receptor subtype 6; *Trpm7*, Transient receptor potential/melastatin receptor subtype7; *Trpv1*, Transient receptor potential/ vanilloid receptor subtype 1. Log_2 Fold change calculated in comparison to the control.

This study confirmed that the RNA-Seq data is associated with western blotting data. This is especilly the case in calcium channel related genes (*Camkiid, Trpc6, Trpm7* and *Trpv1*), which all show up-regulated expression levels compared with the untreated group on both RNA-Seq and western blotting results after 28 days exposure. This combination of findings provides some support for the conceptual premise that the action of Co would be involved with *Camkiid, Trpc6, Trpm7* and *Trpv1* , because the gene expression using RNA-Seq is correlated in a same direction of the protein expression in *in vivo* samples by western blotting.

6.3.5 RT-qPCR for in vitro experiment.

RT-qPCR was also used to validate the RNA-Seq data and also extend the gene expression analysis of the *in vitro* samples by examining the expression profiles in the individual cell samples which made up the pooled RNA samples submitted for RNA-seq. The procedure was carried out for RT-qPCR as recommended by the manufacturer and is detailed in Section 2.2.18.

6.3.5.1 Reference gene determination

The proper selection of a stable reference gene for the purposes of expression normalisation is important in relative gene expression studies using RT-qPCR (Bustin *et al.*, 2009) . To this end, the software, RefFinder, conducts a comprehensive analysis of the candidate reference gene quantification cycle (Ct) values from the control and Co treated cells to examine their variability under these experimental conditions (Jacob *et al.*, 2013).

For the purposes of this study, three candidate reference genes were screened (*B2m, Srp14, and Tbp*) for their stability in the cell lines following Co treatment. RefFinder analysis found that in 3T3 cells exposed to Co, *B2m* had the most stable expression and is the least variant of the three genes between the control and treated 3T3 cells. *Srp14* expression levels are the least stable in 3T3 cells following Co treatment. The 3T3 cells RefFinder results are shown in Figure 6-14. As such *B2m* was used as the reference gene in the 3T3 cells RT-qPCR relative gene expression analysis calculations.

RefFinder analysis found that in CFs exposed to Co, the most stable reference gene is *Srp14* (Figure 6-15), with gene being the least. As a result of these findings, *Srp14* was used as the reference gene in the CFs RT-qPCR relative gene expression analysis calculations.

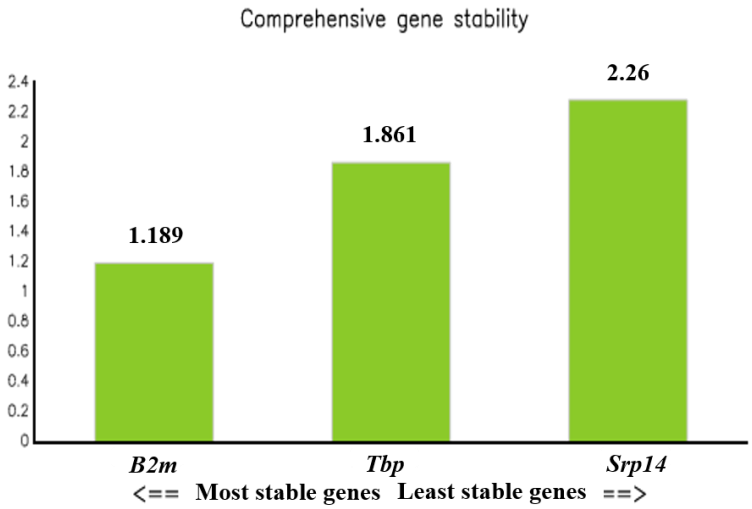

Figure 6-14 RefFinder results. Comprehensive gene stability ranking for the 3 reference genes used in 3T3 cells control and Co-treatment groups. RT-qPCR was carried 3 candidate reference genes (*B2m*, *Tbp* and *Srp14*) using the same RNA 3T3 cell samples from control and Co-treatment groups. Ct values were used to calculate the comprehensive gene stability ranking. "*B2m*" would be the most appropriate reference gene for these samples.

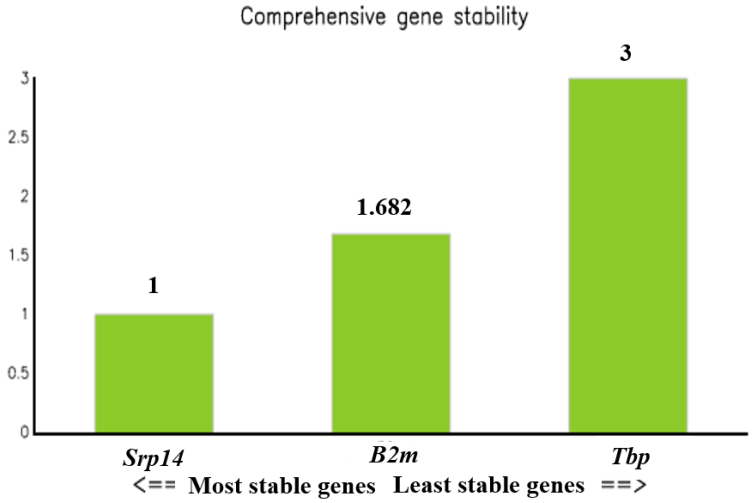

Figure 6-15 RefFinder results. Comprehensive gene stability ranking for the 3 reference genes used in CFs control and Co-treatment groups. RT-qPCR was carried 3 candidate reference genes (*Srp14*, *B2m* and *Tbp*) using the same RNA cardiac fibroblast samples from control and Co-treatment groups. Ct values were used to calculate the comprehensive gene stability ranking. "*Srp14*" would be the most appropriate reference gene for these samples.

6.3.5.2 Relative Gene Expression Analysis (2^-ΔΔC$_T$) of in vitro 3T3 cell line experiment.

The focussed gene expression of 5 selected genes was measured by RT-qPCR using total RNA isolates from control and Co exposure samples of the individual, unpooled 3T3 cells. These samples had undergone RNA-seq as pooled groups and were normalised by their *B2m* expression. The results of this study are shown in Table 6-16. The RT-qPCR results show similarities with the RNA-Seq data from the 3T3 samples across all five of the genes. The RT-qPCR results revealed that *Camkiid* showed a small upregulation in expression following Co treatement as found in the RNA-seq data. The *Trpc6* RT-qPCR assay consistently reported undetermined Cts for the 3T3 cell studies. This lack of detection of *Trpc6* amplicons within the 40 cycles of the RT-qPCR runs suggests *Trpc6* mRNA is either expressed at very low levels in 3T3 cells or not expressed at all. RT-qPCR of *Dmt1*, *Trpm7* and *Trpv1* all revealed expression profiles across the Co treatments similar to that of the RNA-Seq findings, validating the RNA-Seq data.

Table 6-16 Expression of *Camkiid, Dmt1, Trpc6, Trpm7* and *Trpv1* after Co exposure of 3T3 cells using RT-qPCR.

Gene	Co 1 µM		Co 10 µM	
	$2^{-\Delta\Delta Ct}$ (fold change)	Direction vs control	$2^{-\Delta\Delta Ct}$ (fold change)	Direction vs control
Camkiid	1.06 ± 0.02	UP	1.02 ± 0.02	UP
Dmt1	1.06 ± 0.00	DOWN	1.07 ± 0.03	UP
Trpc6	UD	-	UD	-
Trpm7	1.13 ± 0.04	UP	1.47 ± 0.02	UP*
Trpv1	1.60 ± 0.37	DOWN*	2.34 ± 0.31	UP*

**p<0.05*, Ct, cycle threshold; 3T3 cells, 3T3 cell line; Camkiid, Calcium/calmodulin–dependent protein kinase II delta; Dmt1, Divalent metal transporter; Trpc6, Transient receptor potential/canonical receptor subtype 6; Trpm7, Transient receptor potential/melastatin receptor subtype7; Trpv1, Transient receptor potential/ vanilloid receptor subtype 1; B2m, Beta-2-Microglobulin, UD, Undetermined. Log2 ratio calculated in comparison to the control. The $2^{-\Delta\Delta Ct}$ values are differences of log normalised expressions between two different samples (control and Co-treatment) whereby each sample is related to an internal control gene. 3T3 cells normalised with B2m as reference gene.

6.3.5.3 Relative Gene Expression Analysis (2^-ΔΔC_T) of in vitro cardiac fibroblasts experiment.

The gene expression of 5 selected genes was measured by RT-qPCR using total RNA isolates from control and Co exposed in CFs, normalised by their *Srp14* expression as shown in Table 6-17.

With the exception of *Trpv1,* these genes show very small (1.01-1.21) up and down fold changes in expression across the Co concentrations. The small fold changes where also observed with theses genes in RNA-seq data as well. Such small changes in expression in the Co-treated CFs cells compared with the control CFs might be responsible for the lack of consistency with the direction of change of expression beween the RT-qPCR rsults and RNA–Seq results.

While there may appear to be a consensis from both the RT-qPCR and RNA-seq technologies finding very small fold changes for these genes, RT-qPCR can be sensitive to varabilities of factors influencing the fold change calculations, an aspect of the technique which lead to the creation of the MIQE checklist. For example, while this study determined the most appropriate reference gene for each of the cell lines under these experimental conditions, constraints did not permit us to also determine the efficiences of each of the PCR primer pairs used. Pfaffl (2001) found that determination of primer efficiences should also be considered in the calculation of relative gene expression (Pfaffl, 2001).

Table 6-17 Expression of *Camkiid, Dmt1, Trpc6, Trpm7* and *Trpv1* after Co exposure of CFs using RT-qPCR.

Gene	Co 1 µM		Co 10 µM	
	$2^{-\Delta\Delta Ct}$ (fold change)	Direction vs control	$2^{-\Delta\Delta Ct}$ (fold change)	Direction vs control
Camkiid	1.05 ± 0.01	DOWN	1.10± 0.02	UP*
Dmt1	1.05 ± 0.01	UP	1.04 ± 0.02	UP
Trpc6	1.02 ± 0.01	DOWN	1.01 ± 0.02	UP
Trpm7	1.21 ± 0.02	DOWN*	1.02 ± 0.01	UP
Trpv1	1.73 ± 0.35	DOWN*	1.42 ± 0.08	DOWN*

**p<0.05*, Ct, cycle threshold; CFs, cardiac fibroblasts; *Camkiid*, Calcium/calmodulin–dependent protein kinase II delta; *Dmt1*, Divalent metal transporter; *Trpc6*, Transient receptor potential/canonical receptor subtype 6; *Trpm7*, Transient receptor potential/melastatin receptor subtype7; *Trpv1*, Transient receptor potential/ vanilloid receptor subtype 1; *Srp14*; Signal recognition particle 14kDa, Log2 ratio calculated in comparison to the control. The $2^{-\Delta\Delta Ct}$ values are differences of log normalised expressions between two different samples (control and Co treatment) whereby each sample is related to an internal control gene. CFs normalised with *Srp14* as reference gene.

6.3.5.4 Comparison of the Relative Gene Expression (2^-ΔΔC_T) of in vitro cardiac fibroblasts and 3T3 cell line experiments.

Comparison between 3T3 cells and CFs relative gene expression (2^-ΔΔC_T) data are shown in Figure 6-16, both cell types showed similarities in *Camkiid* responses at 10 µM Co treatment. *Dmt1* and *Trpm7*, showed the same trend of gene response by showing up-regulation on both cell types. Of interest, *Trpc6* gene responses showed up-regulation in CFs and absence in 3T3 cells, which were clearly different.

To conclude in our findings, it is clear that *Trpc6* expression responds to Co exposure only in CFs. The difference in response between the two cell types in *Trpc6* expression might affect mechanisms and possible pathways causing the Co toxicity in the CF cells. As previously discussed, TRPC6 is an important protein ion transporter that regulates the calcium ion channel, and is related to cardiovascular disease.

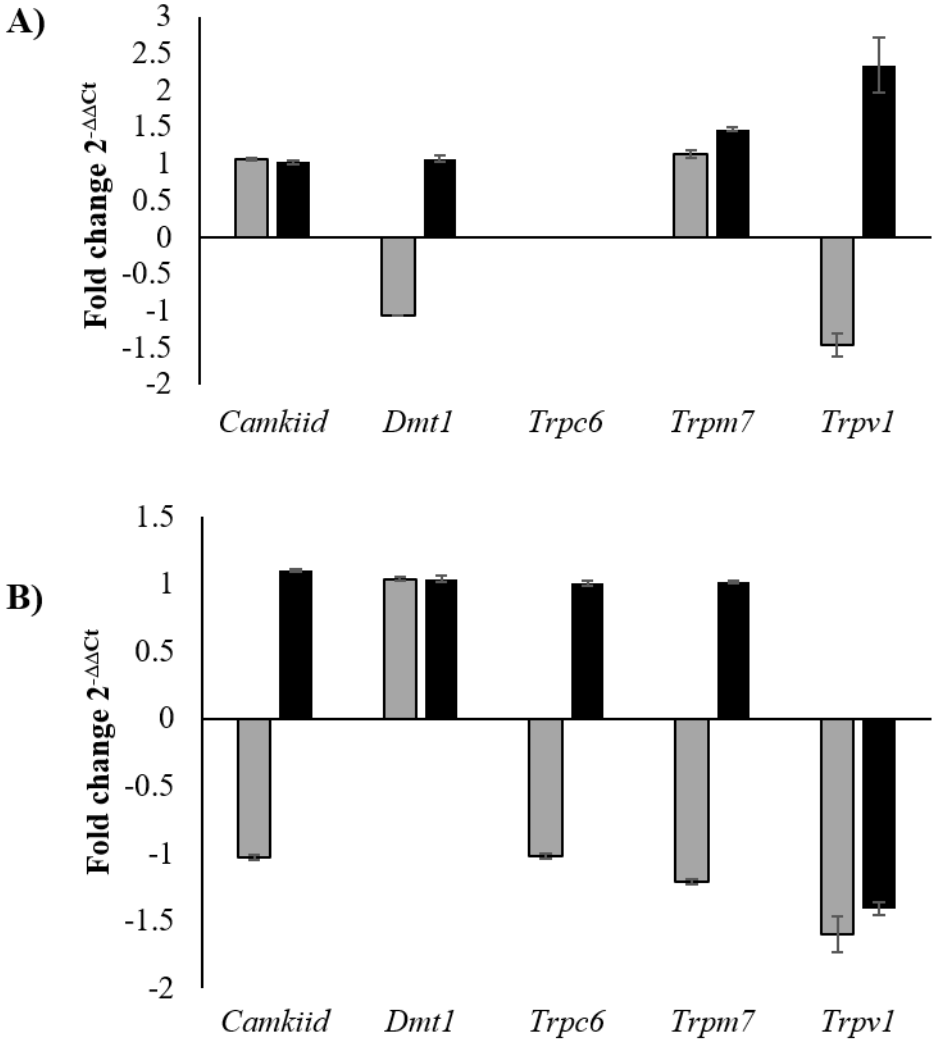

Figure 6-16 Expression of *Camkiid, Dmt1, Trpc6, Trpm7* and *Trpv1* and the effects of Co treatment on 3T3 cells and CFs using RT-qPCR. Real Time PCR was performed in triplicate from two different cDNA reactions. Co treatment on (A) 3T3 cells and (B) CFs at concentrations 1 and 10 µM were compared with untreated cells **(** confirmed hits at gene of interest):*Camkiid, Dmt1, Trpc6, Trpm7* and *Trpv1*, relative gene expression fold changes are determined by $2^{-\Delta\Delta Ct}$. Grey bars show fold change of Co treatment at 1 µM and black showing fold change of Co treatment at 10 µM. 3T3 cells, 3T3 cell line; CFs, cardiac fibroblasts; *Camkiid*, Calcium/calmodulin–dependent protein kinase II delta; *Dmt1*, Divalent metal transporter; *Trpc6*, Transient receptor potential/canonical receptor subtype 6; *Trpm7*, Transient receptor potential/melastatin receptor subtype7; *Trpv1*, Transient receptor potential/ vanilloid receptor subtype 1.

6.3.5.5 Comparison of the Relative Gene Expression (2^-ΔΔCT) and RNA-Seq data of in vitro cardiac fibroblasts and 3T3 cell line experiments.

RT-qPCR was used to validate the RNA-Seq data, at 1 and 10 µM Co treatment. All of the genes, with the exception of *Trpc6*, showed a similar trend of RNA-Seq data in 3T3 cells (Table 6-18). Expression showed an increase in *Camkiid* and *Trpv1*, and a decrease in *Dmt1* and *Trpm7* at 1 µM Co treatment. Also with 10 µM Co treatment, all genes showed increased expression with both RT-qPCR and RNA-Seq. Moreover, in the 3T3 cells *Trpc6* was also absent in RT-qPCR similar to the RNA-Seq data. RT-qPCR therefore confirmed the mRNA expressions.

In CFs after 1 µM Co treatment, two of the genes, *Camkiid* and *Trpv1*, showed totally opposite expression in RNA-Seq data, and at 10 µM Co treatment, two of the genes, *Dmt1* and *Trpc6*, also showed totally opposite expression of their genes (Table 6-19). Typically, RNA-Seq data are generated by summarising the reads over the entire mRNA of each gene, whereas RT-qPCR designs a primer pair over a small piece of mRNA. These differences in the techniques might be causing the different result trends.

Table 6-18 Comparison of 3T3 cells Relative Gene Expression (2^-ΔΔCT) data with gene expression determined by RNA-Seq data.

Gene/Protein	**RT-qPCR (Direction vs control)**		**RNA-Seq (Direction vs control)**	
	Co 1 µM	**Co 10 µM**	**Co 1 µM**	**Co 10 µM**
Camkiid	UP	UP	UP*	UP*
Dmt1	DOWN	UP	DOWN*	UP*
Trpc6	-	-	Not on the list	UP
Trpm7	UP	UP*	UP*	UP*
Trpv1	DOWN*	UP*	DOWN	UP

**p<0.05*, *Camkiid*, Calcium/calmodulin–dependent protein kinase II delta; *Dmt1*, Divalent metal transporter; *Trpc6*, Transient receptor potential/canonical receptor subtype 6; *Trpm7*, Transient receptor potential/melastatin receptor subtype7; *Trpv1*, Transient receptor potential/ vanilloid receptor subtype 1.

Table 6-19 CFs Comparison of CFs Relative Gene Expression (2^-ΔΔCT) data with gene expression determined by RNA-Seq data.

Gene/Protein	RT-qPCR (Direction vs control)		RNA-Seq (Direction vs control)	
	Co 1 µM	**Co 10 µM**	**Co 1 µM**	**Co 10 µM**
Camkiid	DOWN	UP*	UP	UP
Dmt1	UP	UP	UP	DOWN
Trpc6	DOWN	UP	DOWN	DOWN*
Trpm7	DOWN*	UP	DOWN*	UP
Trpv1	DOWN*	DOWN*	UP	DOWN

**p<0.05, *Camkiid*, Calcium/calmodulin–dependent protein kinase II delta; *Dmt1*, Divalent metal transporter; *Trpc6*, Transient receptor potential/canonical receptor subtype 6; *Trpm7*, Transient receptor potential/melastatin receptor subtype7; *Trpv1*, Transient receptor potential/ vanilloid receptor subtype 1.

6.3.5.6 Comparison of the Relative Gene Expression (2^-ΔΔCT) with protein expression determined by Western blotting

As seen in Table 6-20, the comparisons between 2^-ΔΔCT data and western blotting data shows important variations in their results. In 3T3 cells, at 1 and 10 µM Co treatment only *Trpc6* and *Tpm7* were compared between 2^-ΔΔCT and western blotting data. *Tpm7* gene and protein expressions changes showed opposite directions. And RT-qPCR did not determine *Trpc6* gene expression.

Table 6-21 shows the comparison of the CFs gene and protein expression levels from the RT-qPCR and western blotting data. At 1 µM Co treatment, the majority of the genes of interest; *Camkiid, Trpc6* and *Trpm7* showed significantly decreased gene expression from the RT-qPCR data, with the exception of *Dmt1*. However, in CFs at 10 µM Co treatment, the majority of the genes of interest; *Camkiid*, *Trpc6* and *Trpm7* are aligned with both gene and protein expression upregulated. The exception is *Dmt1 gene expression*, which showed up-regulation of the gene but down-regulation of its protein.

Table 6-20 Comparison of 3T3 cells Relative Gene Expression (2^-ΔΔCT) data with protein expression determined by western blotting.

Gene/Protein	RT-qPCR (Direction vs control)		Western blotting (Direction vs control)	
	Co 1 µM	**Co 10 µM**	**Co 1 µM**	**Co 10 µM**
Camkiid	UP*	UP*	-	-
Dmt1	DOWN*	UP*	-	-
Trpc6	-	-	DOWN	DOWN
Trpm7	UP*	UP*	DOWN	DOWN
Trpv1	DOWN*	UP*	-	-

**p<0.05, *Camkiid*, Calcium/calmodulin–dependent protein kinase II delta; *Dmt1*, Divalent metal transporter; *Trpc6*, Transient receptor potential/canonical receptor subtype 6; *Trpm7*, Transient receptor potential/melastatin receptor subtype7; *Trpv1*, Transient receptor potential/ vanilloid receptor subtype 1.

Table 6-21 Comparison of CFs Relative Gene Expression (2^-ΔΔCT) with protein expression determined by western blotting.

Gene/Protein	RT-qPCR (Direction vs control)		Western blotting (Direction vs control)	
	Co 1 µM	**Co 10 µM**	**Co 1 µM**	**Co 10 µM**
Camkiid	DOWN	UP*	UP	UP
Dmt1	UP	UP	NO CHANGE	DOWN
Trpc6	DOWN	UP	UP	UP
Trpm7	DOWN*	UP	UP	UP
Trpv1	DOWN*	DOWN*	-	-

**p<0.05, *Camkiid*, Calcium/calmodulin–dependent protein kinase II delta; *Dmt1*, Divalent metal transporter; *Trpc6*, Transient receptor potential/canonical receptor subtype 6; *Trpm7*, Transient receptor potential/melastatin receptor subtype7; *Trpv1*, Transient receptor potential/ vanilloid receptor subtype 1.

6.3.6 RT-qPCR for in vivo experiment.

6.3.6.1 Reference gene determination

For the purposes of this study, three candidate reference genes were screened (*B2m, Pgk1, and Rpl13a*) for their stability in the cell lines following Co treatment. RefFinder analysis found that in heart exposed to Co, *Pgk1* had the most stable expression and is the least variable of the three genes between the control and untreated rats. *B2m* expression levels are the least stable in hearts following Co treatment. The heart RefFinder results are shown in Figure 6-17. As such *Pgk1* was used as the reference gene in the hearts RT-qPCR relative gene expression analysis calculations.

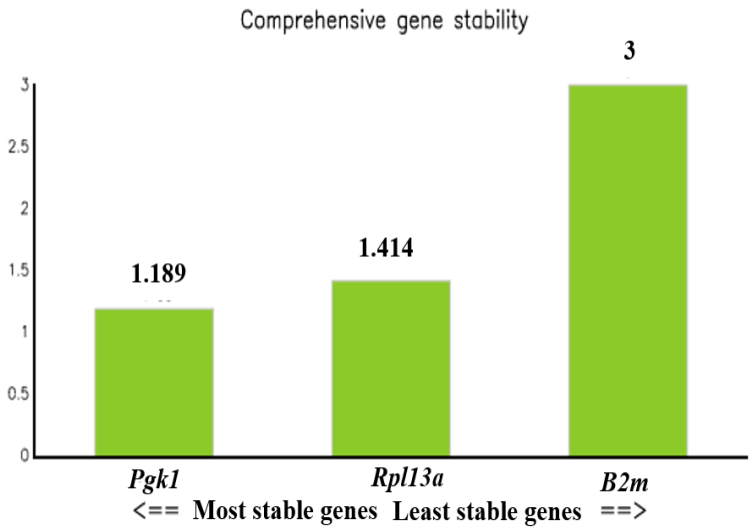

Figure 6-17 RefFinder results. Comprehensive gene stability ranking for the 3 reference genes used in heart control and Co-treatment groups. RT-qPCR was carried out of 3 candidate reference genes (*Pgk1, B2m* and *Rpl13a*) using the same RNA heart samples from control and Co-treatment groups. Ct values were used to calculate the comprehensive gene stability ranking. "*Pgk1*" would be the most appropriate reference gene for these samples.

6.3.6.2 Relative Gene Expression Analysis (2^-ΔΔC$_T$) of in vivo experiment.

The focussed gene expression of the 5 selected genes was measured by RT-qPCR using total RNA isolates from control and Co exposure in the individual samples. Hearts that underwent RNA-seq as pooled groups were normalised by their *pgk1* expression. The results of this study are shown in Table 6-22.

The RT-qPCR results show similarities with the RNA-seq data from the heart samples across all five of the genes. The RT-qPCR results revealed small changes by up-regulation in gene expression after 7 days exposure to Co when compared to untreated groups. One gene, *Trpm7* showed a small decrease in RNA expression. Whereas after 28 days, the fold change of Co-exposure varied between 1.13 - 4.92 fold increase in all the 5 selected genes as seen in Table 6-22 and Figure 6-18. The greatest upregulation was found in the *Trpc6* gene, which was 4.92 fold increased compared with untreated groups.

In summary, the results show that all genes were up-regulated after 28 days exposure to Co, whereas 3 of 5 selected genes: *Dmt1*, *Trpc6* and *Trpv1*, showed up-regulation after 7 days exposure. Thus, there is strong evidence that the hypothesis relating expression of the 5 selected genes with Co exposure is true.

Table 6-22 Expression of *Camkiid, Dmt1, Trpc6, Trpm7* and *Trpv1* after Co exposure to rat hearts *in vivo* using RT-qPCR.

Gene	7 Days		28 Days	
	$2^{-\Delta\Delta Ct}$ (fold change)	Direction vs control	$2^{-\Delta\Delta Ct}$ (fold change)	Direction vs control
Camkiid	1.00 ± 0.01	NO CHANGE	1.46± 0.03	UP*
Dmt1	1.10 ± 0.01	UP	1.79 ± 0.17	UP*
Trpc6	1.20 ± 0.11	UP	4.92 ± 0.20	UP*
Trpm7	1.19 ± 0.01	DOWN*	2.93 ± 0.05	UP*
Trpv1	1.47 ± 0.27	UP*	1.13 ± 0.31	UP

Ct, cycle threshold; *Camkiid*, Calcium/calmodulin–dependent protein kinase II delta; *Dmt1*, Divalent metal transporter; *Trpc6*, Transient receptor potential/canonical receptor subtype 6; *Trpm7*, Transient receptor potential/melastatin receptor subtype7; *Trpv1*, Transient receptor potential/ vanilloid receptor subtype 1; *Rpl13a*, Phosphoglycerate Kinase 1. Log_2 ratio calculated in comparison to the control. The $2^{-\Delta\Delta Ct}$ values are differences of log normalised expressions between two different samples (control and Co treatment) whereby each sample is related to an internal control gene. Rat hearts normalised with *Pgk1* as reference gene.

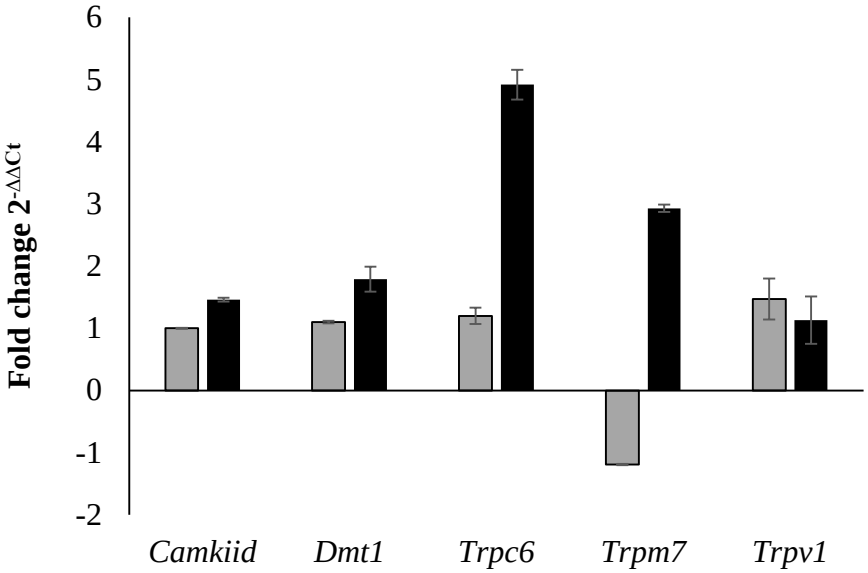

Figure 6-18 Expression of *Camkiid, Dmt1, Trpc6, Trpm7* and *Trpv1* on Co treatment: effects on rat hearts detected by RT-qPCR following exposure to Co *in vivo* for 7 and 28 days. Real Time PCR was performed in triplicate from two different cDNA reactions. Co treatment for 7 and 28 days compared with control) confirmed hits at gene of interest :*Camkiid, Dmt1, Trpc6, Trpm7* and *Trpv1*, relative gene expression fold changes are determined by $2^{-\Delta\Delta Ct}$. Grey bars show fold change of 7-days Co treatment and black showing fold change of 28-days Co treatment; *Camkiid*, Calcium/calmodulin–dependent protein kinase II delta; *Dmt1*, Divalent metal transporter; *Trpc6*, Transient receptor potential/canonical receptor subtype 6; *Trpm7*, Transient receptor potential/melastatin receptor subtype7; *Trpv1*, Transient receptor potential/ vanilloid receptor subtype 1; D, days.

6.3.6.3 Comparison of the Relative Gene Expression (2^-ΔΔCT) and RNA-Seq data of in vivo experiments

RT-qPCR was used to validate the RNA-Seq data. At 7 days of Co treatment, 2 of 5 genes, *Dmt1* and *Trpc6*, showed similar trends in up regulation on both RT-qPCR and RNA-Seq data. Whereas, all of 5 genes showed up regulation expression and presented similar trends between RT-qPCR and RNA-Seq data after 28 days exposure (Table 6-23). It can be concluded that RT-qPCR can be used to validate the RNA-Seq data.

Table 6-23 Comparison of hearts Relative Gene Expression (2^-ΔΔCT) data with gene expression determined by RNA-Seq data.

Gene/Protein	RT-qPCR (Direction vs control)		RNA-Seq (Direction vs control)	
	Co 7 days	Co 28 days	Co 7 days	Co 28 days
Camkiid	NO CHANGE	UP*	UP	UP
Dmt1	UP	UP*	UP	UP
Trpc6	UP	UP*	UP	UP*
Trpm7	DOWN*	UP*	UP*	UP*
Trpv1	UP*	UP	DOWN	UP

**p<0.05, *Camkiid*, Calcium/calmodulin–dependent protein kinase II delta; *Dmt1*, Divalent metal transporter; *Trpc6*, Transient receptor potential/canonical receptor subtype 6; *Trpm7*, Transient receptor potential/melastatin receptor subtype7; *Trpv1*, Transient receptor potential/ vanilloid receptor subtype 1.

6.3.6.4 *Comparison of the Relative Gene Expression (2^-ΔΔCT) with protein expression determined by Western blotting of in vivo experiments.*

As seen in Table 6-24, the comparison between 2^-ΔΔCT data and western data can show important variations in the results. After 7 days exposure to Co both *Trpc6* and *Trpm7* showed similar trends between RT-qPCR and western blotting data. All of genes; *Camkiid*, *Trpc6* and *Trpm7*, with the exception with *Dmt1* showed absolutely up regulation of RT-qPCR and western blotting data after 28 days exposure.

Table 6-24 Comparison of hearts Relative Gene Expression (2^-ΔΔCT) data with protein expression determined by western blotting.

Gene/Protein	RT-qPCR (Direction vs control)		Western blotting (Direction vs control)	
	Co 7 days	Co 28 days	Co 7 days	Co 28 days
Camkiid	NO CHANGE	UP*	DOWN	UP*
Dmt1	UP	UP*	DOWN*	DOWN
Trpc6	UP	UP*	UP	UP*
Trpm7	DOWN*	UP*	DOWN	UP*
Trpv1	UP*	UP	-	-

**p<0.05, *Camkiid*, Calcium/calmodulin–dependent protein kinase II delta; *Dmt1*, Divalent metal transporter; *Trpc6*, Transient receptor potential/canonical receptor subtype 6; *Trpm7*, Transient receptor potential/melastatin receptor subtype7; *Trpv1*, Transient receptor potential/ vanilloid receptor subtype 1.

6.3.7 Summary of major findings

In this chapter, RNA-Seq analysis allowed an overview of the genes and biological pathways affected following Co exposure in *in vitro* and *in vivo* experiments. A focused investigation on the response to Co by a limited number of genes (*Camkiid, Dmt1, Trpc6, Trpm7* and *Trpv1*) involved in calcium handling and ion transport that have an affinity for other metal ions was also conducted using RNA-Seq and RT-qPCR to build upon the earlier protein expression work. The main findings of this study are:

- Analysis of the *in vitro* RNA-seq data found evidence of enrichment of altered gene expression in 3T3 and CF pathways involving:1) metabolic pathway, 2) metal ion binding, 3) calcium ion channel binding and activity 4) cell adhesion, 5) cell apoptosis, and 6) cardiovascular system.
- *In vitro*, RNA-Seq for both 3T3 cells and CFs, showed variation in the mRNA expression levels of the 5 selected genes (*Camkiid, Dmt1, Trpc6, Trpm7* and *Trpv1*) after Co treatment (1 and 10 µM) for 72 h.
- *In vitro*, RT-qPCR in CFs showed increased expression of 4 out of 5 selected genes (*Camkiid, Dmt1, Trpc6,* and *Trpm7*) by $CoCl_2$ at 10 µM. And RT-qPCR in 3T3 cells showed increased expression of 4 out of 5 selected genes (*Camkiid, Dmt1, Trpm7* and *Trpv1*) after being treatment with $CoCl_2$ at 10 µM. Therefore, these channels might mediate transport channel of Co^{2+} into these cells.
- In CFs, an increase in the expression of Trpc6 transport channel protein is induced by $CoCl_2$ at 1 and 10 µM, whereas the *Trpc6* mRNA appears absent in 3T3 cells as assessed by RT-qPCR.
- Using RT-qPCR, all 5 selected genes (*Camkiid, Dmt1, Trpc6, Trpm7* and *Trpv1*) confirmed correlation with Co exposure by showing up-regulation *in vivo* after 28 days, and also *in vitro* in CFs and 3T3 cells after treatment 10 µM $CoCl_2$. However, in CFs, *Trpv1* showed down-regulated expression.
- The *in vivo* RNA-Seq study found Co exposure lead to changes in the gene expression in molecular pathways in cardiac tissue involving: 1) cell metabolism, 2) calcium ion channel binding and activity 3) cell adhesion and 4) cell apoptosis.
- *In vivo*, RNA-Seq showed increased levels of all 5 selected genes (*Camkiid, Dmt1, Trpc6, Trpm7* and *Trpv1*) after 7 and 28 days administration of $CoCl_2$

treatment, with exception of *Trpv1* at 7 days which exhibited a down-regulation of gene expression and no expression of *Camkiid* at 7 days.

- *In vivo* both RNA-Seq and RT-qPCR show similar directions of changes in gene expression, since all 5 selected genes show increased expression levels in heart RNA after 28 days administration of $CoCl_2$ treatment.

6.4 Discussion

RNA sequencing (RNA-Seq) is a technique able to determine the sequence of RNA molecules in cells or tissues. The results from RNA-Seq can be used for transcriptome analysis and gene annotation where the transcriptome is defined as the set of all RNA molecules expressed in a population of cells. RNA-Seq can be used to quantify gene expression (Kukurba and Montgomery, 2016).

More understanding of the dynamic nature of the content of mRNA in samples helps to give a better understanding of differential expression in biological and disease processes. Over the past two decades, RNA-Seq has become a common tool in molecular biology for transcriptome analysis. RT-qPCR allows a smaller scale level of investigation, below that of transcriptome-wide gene expression analysis such as that by RNA-seq and microarrays (Fleige and Pfaffl, 2006).

The accuracy/reliable interpretation of these techniques (RNA-Seq and RT-qPCR) relies on the MIQE guidelines. Where possible, our study (qPCR assay design and reporting) followed the MIQE guideline's to help ensure the reliability of RT-qPCR results (as in Appendix 4)(Bustin *et al.*, 2009). Normalisation of RT-qPCR data is required for quality control of experimental error during the PCR workflow. Data normalisation in real-time RT-PCR, using an appropriate endogenous control is important in gene quantification analysis to enable the measurement of biologically meaningful results (Pfaffl, 2001; Bustin, 2002; Huggett *et al.*, 2005).

This chapter has focused on molecular studies that examine the consequences of the interactions of Co ions with cells and tissues and their impact on gene expression using RNA-Seq and RT-qPCR.

The results from RNA-Seq can generate lists of thousands of genes that show varying levels of altered expression between control and treated samples. The application of cutoff section criteria, for example, relative expression fold change or significance, can filter out genes showing very small, insignificant changes so that the number of genes in the lists drop from many thousands to hundreds or tens of genes to help

identify only the gene ontologies and pathways that have been significantly affected by the treatment under examination.

The overview of the enrichment analysis *in vitro* showed a variety of related pathways such as metabolic pathways, calcium channel activity, apoptosis pathways and cell cycle, including impairment of pathways in the cardiovascular system. And *in vivo*, related cell signalling-pathways (cAMP/cGMP-PKG, Jak-STAT, HIF-1 and p53), cell homeostasis, hormone synthesis, and the regulation of the cardiovascular system were detected.

Such gene expression in both the *in vitro* and *in vivo* study, also suggests a route for the introduction of cardiac issues such as vascular contraction and atherosclerosis. Investigation of the changes in gene expression and their effects on these pathways in patients with implants, might serve as an indicator of biological complications and adverse reactions from Co exposure.

The RNA-Seq findings align with both the findings in this study and others. As covered in the previous chapter, Co ions induced cytotoxicity and inhibit cell proliferation. With regards to apoptosis, Co^{2+} exposure can lead to cellular and tissue damage by acting as a hypoxic mimic. This was supported by work in human pancreatic cancer cell line (PC-2 cells) where $CoCl_2$ (at 100-200 μM, 72h) induced apoptosis and could effectively induce hypoxia that upregulates the expression of *HIF-1α* , which is a marker for the effect of hypoxia conditions on both mRNA and protein levels (Dai *et al.*, 2012). In our study, *HIF-1α* was upregulated in 3T3s by 0.24 fold (p=3.79 x 10-12), 0.13 fold in CFs (p=0.005) following exposure to Co at 10 μM, and 0.15 fold in cardiac tissue (p= 0.072) following exposure to Co at 7 days exposure. HIF-prolyl 4-hydroxylases (HIF-P4Hs; EGLNs) also play an important role in the hypoxia response, regulating the stability of HIF-1α and the inhibition of HIF-P4H-2 (EglN1) can protect against the development of atherosclerosis and may reduce stroke risk (Karuppagounder and Ratan, 2012; Rahtu-Korpela *et al.*, 2016). *EglN1* was upregulated in 3T3s by 1.21 fold (p=8.74 x 10^{-33}) suggesting a Co-linked induction of oxidative cell death, however, no change was observed in the CFs and cardiac tissue at this concentration of Co.

The homeostasis process concerns the ability of the tissue or cells to maintain a balanced internal environment for such parameters as pH balance, temperature, electrolyte levels and also calcium. This links to the enriched pathways for ion channel binding and activity as ion transporters, and the apoptotic process. More details about the calcium channel and metal transporters will be discussed later.

In comparing the western blotting data from Chapters 3 and 5 and the RNA-seq/RT-qPCR data, the correlation between the protein and gene expression levels varied. *In vitro,* when protein and their mRNA transcript expression levels were compared in CFs, there was no direct correlation between changes in gene expression and similar changes in magnitude and direction of protein levels. This is not unexpected as this relationship between mRNAs and their proteins is a complex and dymanic one (Liu, Beyer and Aebersold, 2016). However, *in vivo,* the cardiac tissue exhibited a positive correlation between the gene expression levels of *Camkiid, Trpc6, Trpm7,* and *Trpv1* and their respective protein levels. The findings of this investigation appear to complement those of chapter 5 where both gene and protein expression levels were directly linked only in the *in vivo* experiments after 28 days Co exposure.

The effects of Co exposure on cells and tissues determined by RNA-Seq and RT-qPCR shows the interaction pathway; calcium ion channel binding and activity, cell adhesion and cardiovascular system, are significantly upregulated in both *in vivo* (at 28 days)and *in vitro* (3T3 cells and CFs) following 10μM Co exposure.

CaMKII regulates calcium homeostasis in cells. *In vivo*, western blotting showed that Co caused a significant increase in *Camkii* mRNA after 28 days exposure, but no significant change in expression was observed in cardiac tissue after 7 days Co exposure. Similarly, *in vitro* a range of Co concentrations (0.1, 1 and 10 μM) caused a significant increase in *Camkii* expression in CFs after 72 h Co exposure, but there was no significant effect on *Camkii* expression after 48 h of Co treatment. It is evident that timing or duration of exposure of Co exposure was a significant factor in both the heart *in vivo* and in CFs *in vitro*. CaMKII plays a critical role in heart failure and AF. A correlation has been demonstrated between CaMKII-ERK (extracellular regulated kinase) interaction and impaired gene expression of atrial natriuretic peptide (ANP), a

marker of cardiac hypertrophy in ventricular adult myocytes from Wistar Kyoto (WKY) rats and cardiomyocytes (H9C2 cell) (Cipolletta *et al.*, 2015). Also, CaMKII function is involved as a transducer of stress that is linked to pathological cardiac remodeling *in vivo* (Backs *et al.*, 2009). Inhibition of CaMKII maintains pathological Ca^{2+} signalling in the heart in response to stress (Molkentin *et al.*, 1998; Zhang *et al.*, 2005; McKinsey, 2007; Fielitz *et al.*, 2008).

DMT1 is one of the metal transporters and transports divalent metal cations, including Co into cells (Forbes and Gros, 2003). Increased expression of *Dmt1* mRNA after exposure to Co was also observed resulting in increased metal ion entry using adult female *Xenopus laevis* frogs (Illing *et al.*, 2012), human neurons (Howitt *et al.*, 2009) and increased protein channel expression in the plasma membrane of CHO cells(Picard *et al.*, 2000). Our 3T3 cells *in vitro* study of *Dmt1* gene expression following 10 µM Co exposure found a small increased expression of this gene using RT-qPCR and RNA-Seq. Whereas in CFs, *Dmt1* showed only a low 1 fold increase in RT-qPCR. Our *in vivo* gene expression study data in our experiments showed up-regulation in *Dmt1* genes after 7 and 28 days Co exposure.

The TRP family members investigated were *Trpc6, Trpm7* and *Trpv1*. The activity and expression of these channels can be regulated by metal ions like Co and they transport trace metal ions into the intracellular cytosolic compartment. TRP members are mainly located in the plasma membrane but also in intracellular membranes. Changes in the expression of these channel proteins may contribute to adverse reactions within and outwith tissues or cells (Kuwahara *et al.*, 2006; Nishida and Kurose, 2008a; Watanabe *et al.*, 2008; Du *et al.*, 2010; Eder and Molkentin, 2011; Zhang *et al.*, 2012). Recent studies have confirmed that TRPC6 functions as a Ca^{2+} permeable cation channel and is widely expressed in the heart and other organs. It acts as an important metabolic regulator to further affect calcium metabolism.

The TRP channels, TRPM7 (Monteilh-Zoller *et al.*, 2003; Li, Jiang and Yue, 2006; Topala *et al.*, 2007; Chigurupati *et al.*, 2010; Sun *et al.*, 2010), TRPC6 (Clarson *et al.*, 2003; Venkataraman, 2008; Chigurupati *et al.*, 2010) and TRPV1 (Caterina *et al.*, 1997; Garcia-Martinez *et al.*, 2000; Sathianathan *et al.*, 2003; Ahern, 2005; Woo *et*

al., 2008; White *et al.*, 2011) display a high permeability for Co^{2+} ions, allowing the metal ion to accumulate intracellularly.

In this chapter, we examined *Trpc6* expression in both *in vitro* and *in vivo* experiments following Co exposure. Our study highlighted the importance of the consideration towards the choice of cell line for *in vitro* studies on Co effects. Many studies have reported that *Trpc6* mRNA was detected in cardiac tissues containing cardiomyocyte and cardiac fibroblasts by RT-qPCR (Nishida *et al.*, 2007a; Du *et al.*, 2010). RNA-Seq and RT-qPCR identified *Trpc6* mRNA expression in rat CFs. Co induced changes in *Trpc6* expression in CFs, with 1 µM Co treatment resulting in down-regulated expression, but 10 µM Co treatment leading to an up-regulation. However, RT-qPCR of 3T3 cells, failed to detect *Trpc6* expression at both 1 µM and 10 µM Co, emphasising the need to choose the cell line carefully. In our *in vivo* study, there was a 4-fold increase in expression after 28 day Co-exposure in RT-qPCR, and 10-fold in RNA-Seq results compared with 7 day Co-exposure. Thus, longer exposures cause greater impact of Co effects on the expression of this gene.

The impact of Co on the expression of *Trpc6* has been observed in other studies. Both TRPC6 protein and mRNA expression and *Trpc3* were found to be increased after exposing term human placenta to 200 µM $CoCl_2$ (Clarson *et al.*, 2003). An overexpression of TRPC6 channels and their mRNA was detected in Co-treatment (100µM) in adult brain tumors (Chigurupati *et al.*, 2010) and also *in vitro*, Co treatment on glioblastoma cells results in overexpression of *TRPC6* by RT-qPCR, Western blot, and immunocytochemistry (Venkataraman, 2008). These studies suggest that the *Trpc6* channel expression is sensitive to Co induction. Our *in vivo* study of echocardiography showed a compromise in cardiac function following 28-day Co exposure and at this time after exposure to Co the data show that *Trpc6* is upregulated (western blotting, RNASeq and RT-qPCR). So it could be concluded that increased levels of Co ions have the potential to alter expression of *Trpc6* channels, which could alter calcium regulation in CF cells.

Dysregulation of *TRPC6* expression has been linked to cardiovascular disorders including heart disease (Shi *et al.*, 2013; Yamaguchi *et al.*, 2017). In humans, Co-

induced cardiomyopathy is linked to altered calcium homeostasis (Zadnipryany *et al.*, 2017). It appears that TRPC6 is essential for the development of cardiac hypertrophy (Nishida and Kurose, 2008a; Watanabe *et al.*, 2008; Eder and Molkentin, 2011) in the mouse model and its levels are increased in patients with heart failure (Kuwahara *et al.*, 2006). Overexpression of *Trpc*6 in transgenic mice results in lethal cardiac growth and heart failure (Kuwahara *et al.*, 2006). Moreover, the relationship between CaMKII and TRPC6 may involve a site on the TRPC6 channels that is crucial for CaMKII – mediated positive regulation of these channels, which regulate both homeostatic and activated Ca^{2+} influx (Shi *et al.*, 2013). This positive regulation of Ca^{2+} influx through the TRPC6 and CaMKII interaction, in concert with intracellular and transmembrane Ca^{2+} mobilisation, could thereby tune cardiovascular functions.

A unique genetic variation in *Trpc6* gene expression has been identified, which might link the cardiac response to upregulation of *Trpc6* expression and ultimate development of cardiovascular abnormalities (Malczyk *et al.*, 2017). Evidence supporting the role of *Trpc6* in the pathogenesis of cardiovascular disease indicates that it might serve as a pharmacological target. Further evaluation of the effect such genetic and environmental factors have on TRPC6 is necessary to define the precise role of TRPC6 in the cardiovascular system.

In this study, *Trpm7* expression is largely upregulated after Co exposure both *in vitro* and *in vivo*, especially after 10 µM and, for the *in vivo* experiments, following 28 day Co exposure. This transporter may have an effect on accumulated intracellular Co exposure. These results can be supported by these previous studies. Harteneck (2005) reported that the TRPM7 channel is permeable to the divalent cations (Zn, Ni, Ba, Co, Mg, Mn, St, Cd and Ca) (Harteneck, 2005). TRPM7 conducts Ca^{2+} and allows Co^{2+} to permeate in zebrafish at doses of 10 mM Co (Jansen *et al.*, 2016) and is induced after exposure to 1 mM Co in HEK-293 cells (Monteilh-Zoller *et al.*, 2003).

As reported in different studies, TRPM7 is an important modulator of cardiac fibrosis (Yue *et al.*, 2013; Yu *et al.*, 2014). Both the TRPM7 protein, and mRNA expression level increase significantly in patients with AF due to rheumatic heart disease (Zhang *et al.*, 2012). Highly expressed *Trpm7* levels, which is stimulated by angiotensin II,

were measured and found to mediate proliferation and apoptosis leading to fibrosis of cardiac interstitial tissue (Zhou *et al.*, 2015). Moreover, other factors such as oxidative stress could activate *Trpm7* which may lead to a potential role in myocardial pathological processes (Aarts *et al.*, 2003; Oancea, Wolfe and Clapham, 2006; Numata, Shimizu and Okada, 2007; Gotru *et al.*, 2017).

On the other hand, it has been reported that the down-regulation of *Trpm7* occurs in tissue samples from both left atria and left ventricle in patients with human ischaemic cardiomyopathy (ICM)(Ortega *et al.*, 2016). However, defective Ca^{2+} homeostasis in heart disease can result from alteration of the *Trpm7* gene expression. TRPM7 can modulate the intra-and extra- cellular level of Ca^{2+} and Mg^{2+}, thereby maintenance of stored Ca^{2+} levels and affecting Ca^{2+} homeostasis(Sun *et al.*, 2015; Faouzi *et al.*, 2017).

Trpv1 expression has been affected by Co exposure. This study found 3T3 cell and CF *Trpv1* expression responded differently to Co levels. In 3T3 cells *Trpv1* expression was downregulated at 1 µM Co but was then increased after exposure to 10 µM Co. Whereas in CFs, 1 and 10 µM Co treatment resulted in a downregulation of *Trpv1*. However, *in vivo* data showed increased expression of *Trpv1* after both 7 and 28 days treatment with Co using RT-qPCR. Other studies have found that *Trpv1* expression is controlled by a balance between CaMKII-mediated sensitisation and calcineurin-mediated desensitisation that may come into play in different cells types following Co treatment (Jung and Kim, 2004; Shi *et al.*, 2013). Other regulatory factors may be involved in the differential Co responses observed between the cell/tissues in this study. There is evidence for involvement of *Trpv1* in Co toxicity from the literature. Co exposure in a dose dependent manner inhibits TRPV1 in the HaCaT keratinocyte cell line (Pecze *et al.*, 2013), and also in adult rat sensory dorsal root ganglion (DRG) neurons (Winter, 1987; Sathianathan *et al.*, 2003). Also, TRPV1 receptors expressed by human urothelial cells respond to increasing Co uptake and increase in its expression have been obvserved using RT-qPCR and immunohistochemistry (Charrua *et al.*, 2009).

Trpc6 can act as an important metabolic regulator and its expression is induced in hypoxic conditions in primary human glioma cells (Chigurupati *et al.*, 2010; Li *et al.*,

2015). Through hypoxia induction the expression of *Dmt1* in colorectal cancer (Xue *et al.*, 2016) and in mice (Mastrogiannaki *et al.*, 2009; Shah *et al.*, 2009) is increased, and finally there is significant expression of *Camkii* in myocardial cells under chronic hypoxia conditions (Zhao *et al.*, 2008).

In terms of our RNA-seq data gene set enrichment analysis (GSEA) none of these five genes had changes in expression levels that passed the cut-off criteria that might highlight any significance in their response to Co and a consequential impact on functional pathways. This chapter has examined the interaction of Co ions and their potential to affect gene expression *in vivo* and *in vitro*. Taking all of the results together, Co treatment appears to affect pathways involving 1) metabolic effects 2) calcium ion channel binding and activity 3) cell adhesion and 4) cell apoptosis. It is evident that Co ions exert subtle and possibly complex effects on *Camkiid, Dmt1,* and *Trp* family members (*Trpc6, Trpm7* and *Trpv1*).

It is important to note that this work has demonstrated the value of RNA-Seq analysis of gene expression as a powerful tool to establish mechanisms of toxicity of Co. It also plays an increasingly recognised role in gene profiling of many diseases and abnormal pathologies.

Importantly, more investigations should be conducted by further experiments on the pathways highlighted by the RNA-seq anaysis in order to ascertain the mechanisms behind how these pathways and their genes respond to Co and contribute to cardiac dyfunction. Such research may help pinpoint genes/proteins responsible for the toxic effects of Co, and may enable us to develop new therapeutic strategies to protect MoM implant patients, and others, from Co-induced cardiac toxicity.

Chapter 7. SUMMARY AND FUTURE WORK

7.1 Summary of thesis results.

The main findings of this thesis are outlined below:

Chapter 3: The effect of Co ions on 3T3 cells and cardiac fibroblasts (short-term).

The core objective for this chapter was to investigate the *in vitro* toxicity of $CoCl_2$ and to compare between primary cardiac fibroblasts and the standard 3T3 fibroblast cell line. Both of the cells were exposed to various concentrations of $CoCl_2$ for different times and toxicity was measured using three assays, proliferation by the BrdU Elisa method, and cell staining both for live/dead cells and Phalloidin-FITC for staining of actin filaments to investigate the morphology of cells. Potential mechanisms of toxicity were investigated by initial examination of proteins that may be directly affected by Co (CaMKII) or may be Co transporters (DMT1 and TRP channels (TRPC6 and TRPM7)).

With MTT and CV assays IC_{50} values for $CoCl_2$ were in the range of ~300 µM. Experiments using BrdU incorporation to assess proliferation suggested that CFs were significantly more sensitive to the anti-proliferative effects of $CoCl_2$ at high concentrations as compared to 3T3 fibroblasts with the IC_{50} values in the range of ~ 20 µM in CFs and ~250 µM in 3T3 cells after either 48h or 72h. Greater accumulation of Co into the CFs than 3T3 cells was measured by detecting intracellular metal content using ICP-MS. Live/Dead staining was assessed using CFDA and propidium iodide staining, the ratio of live:dead cells decreased dramatically with increasing $CoCl_2$ (up to 500 µM). Disruption of actin filaments and structure were evident with increasing $CoCl_2$ using Phalloidin-FITC.

Western blotting with specific antibodies (4 selected proteins: CaMKII, DMT1, TRPC6 and TRPM7) was used to examine any differences in the expression of selected proteins following Co treatment and between 3T3 cells and CFs. Based on our findings, CaMKII (both CaMKIIδ and ox-CaMKII), TRPC6 and TRPM7 all showed up-regulation after treatment with $CoCl_2$ in a dose and time dependent manner. Although the fold change in protein expression following each concentration of Co was not large, this could indicate involvement of any or all of these proteins in the toxicity response.

This may be particularly true for the TRPC6 and TRPM7 channels, where protein expression showed up-regulation in CFs and down-regulation on 3T3 cells. These two channels play a vital role in heart disease. Up-regulation of TRPC6 and TRPM7 channels was reported in the progression of cardiac hypertrophy and heart failure (Patel *et al.*, 2010; Yue *et al.*, 2013).

There is only little information available about Co^{2+} entry or accumulation of Co into cardiac cells in the literature, so information provided in this study could highlight evidence for involvement of these proteins both in the transport pathway and mechanism of toxicity in the heart and might also highlight capacity for these proteins to play a vital role for Co accumulation into other organs. The involvement of these channels could help us to understand the specific pathway of Co uptake.

Chapter 4: Long term effect of Co ion treatment on 3T3 cell lines.

This chapter builds upon the *in vitro* study on acute or short term toxicity of $CoCl_2$ on both 3T3 cells and CFs in chapter 3. High concentrations of Co were studied in terms of acute toxicity in chapter 3. In chapter 4 low concentrations of Co were studied to investigate any long term toxicity (28 days Co exposure).

The objective of this chapter was to determine the impact of Co on long term exposure to metal ions *in vitro*. The cell viability of 3T3s after Co exposure was over 80% at all doses and time periods, measured by combined assay (MTT, NR and CV assay). $CoCl_2$ did not affect 3T3 cell viability at low doses over long term exposure. However, some membrane blebs were found and this may represent a sign of cell apoptosis, and abnormality of f-actin distribution in Co- treated cells after 3 wk exposure using Phalloidin-FITC.

Chapter 5: Effects of chronic Co administration in rats *in vivo*.

Virtually nothing is known of the intracellular mechanisms that link Co exposure to its adverse effects on cardiac function *in vivo* and its role in heart failure development. The major objective of this chapter was to correlate findings from defined *in vivo* experimental Co treatments to the current issue of the adverse biologic effects of Co ions, which are released from orthopaedic implants *in vivo*. The current study

investigated the effects of chronic Co exposure where male SD rats were given $CoCl_2$ or distilled water (single i.p. injection of 1mg/kg, daily) for 7 and 28 days and the cardiac function of the rats examined after Co exposure using echocardiography. Various organs and blood samples were collected and stored to detect Co levels by ICP-MS, and then carry out immunoblotting of the selected proteins of interest.

Echocardiography showed evidence of altered cardiac function (significant decrease in %FS) in rats following 28 days of $CoCl_2$ treatment. This provided evidence for some contractile dysfunction in these animals. Furthermore, organs and blood of rats treated with intraperitoneal injection of $CoCl_2$ had significantly higher Co ion levels compared with levels in the organs and blood of control rats without Co treatment on both 7 and 28 days. The kidney and liver showed the highest Co levels, followed by Heart, Spleen, Lung, Testes and Brain, in descending concentration order.

High accumulation of Co in the hearts of treated rats occurred when compared with untreated rats. The Co containing heart tissue correlated with the dysfunctional cardiac function during monitoring when we investigated the cardiac performance using echocardiography. Echocardiography performed on the same animals showed functional changes correlating with compromised cardiac contractility. Our data provides strong evidence that Co accumulates in the heart resulting in cardiac dysfunction.

Western blotting confirmed that Co exposure *in vivo* caused increased levels of total CaMKIIδ protein after 28 days exposure and also higher expression of TRPC6 and TRPM7 transporter channel at the same endpoint. Importantly all of these proteins have been implicated in playing a vital role in promotion of cardiovascular disease. Here we have shown the accumulation of Co^{2+} in each organ, especially in the heart correlates with increased expression of these transporters (TRPC6 and TRPM7).

Chapter 6: RNA Sequencing and gene expression of Co effect *in vitro* and *in vivo*

This chapter aimed to investigate the gene expression at different exposure times and concentrations of Co both *in vitro* (between 3T3 cells and CFs) and *in vivo* and to understand the possible mechanisms that might be involved with adverse reactions,

especially cardiotoxicity after treatment with Co. Literature data on these genes was available to suggest involvement in the development of cardiovascular disease and action as Co ion transporters.

Initially, we overviewed RNA-Seq data and all of the genes that Co affects by the underlying functions of the differentially expressed gene (DEGs). Interactions of DEGs were analysed and then characterised in terms of GO terms and KEGG pathway. Induction of expressed genes by Co exposure revealed particular areas of interest including:1) cell metabolism 2) ion channel activity (calcium and metal ions), 3) apoptosis and in particular 4) cardiovascular process function.

RNA samples were prepared from the *in vivo* experiments extracted from Co-treated heart tissue (in chapter 5) and the *in vitro* experiments, both from 3T3 cells and CFs, treated with Co at 1 and 10 µM for 72 h. The RNA samples from both *in vivo* and *in vitro* Co exposure were quantified and quality controlled using Nanodrop™ Spectrophotometer and Experion™ RNA StdSens Analysis kit before further submitted and analysed with RT-qPCR.

In vitro, RT-qPCR showed high Co exposure (10 µM, 72 h) in CFs caused increased expression levels of 4 genes (*Camkiid, Dmt1, Trpc6,* and *Trpm7*). Whereas the pattern in 3T3 cells was slightly different with increased expression in a slightly different cohort (*Camkiid, Dmt1, Trpm7* and *Trpv1*. Importantly, $CoCl_2$ (1 and 10 µM) induced expression of *Trpc6* transport channel in CFs whereas 3T3 cells did not express this channel as shown by RT-qPCR and RNA-Seq. So this channel might mediate transport of Co^{2+} in cardiac cells, and not 3T3 cells.

Samples of RNA taken from cardiac tissue showed increased levels of the 5 selected genes (*Camkiid, Dmt1, Trpc6, Trpm7* and *Trpv1*) and this was detected after 28 days of Co exposure using RNA-Seq. Similarly RT-qPCR data, also showed up-regulated gene expression of all the same genes following Co exposure for 28 days.

These results suggest that the induction of these 5 selected genes *in vivo* (cardiac cells) and *in vitro* (CFs, 1 and 10 µM, 72 h) following Co exposure might be a persistent response. To conclude, the molecular toxicology seems to suggest that there is some correlation between changes in the selected genes and the proteins of interest following Co exposure across both *in vitro* and *in vivo* experiments. That said, this work has

highlighted the importance of further investigation into not only the genes and proteins of interest but also other candidate genes induced by Co exposure.

7.2 Main findings

The main findings of this thesis are

- $CoCl_2$ causes time- and dose-dependent toxicity in both 3T3 cells and CFs after short-term treatments (48 and 72 h) as assessed by cell morphology and viability tests.
- $CoCl_2$ has a greater effect on cell proliferation and cellular uptake of $CoCl_2$ in CFs than 3T3 cells and this may at least partly explain the difference in toxicity between the two cell types.
- $CoCl_2$ induced an increased level of CaMKIIδ and TRP channel (TRPC6 and TRPM7) protein expression in CFs at high concentrations as compared to 3T3 fibroblast using immunoblotting.
- $CoCl_2$ was slightly or rather non-toxic at low doses over long exposure periods (28 days) for 3T3 cells as determined by viability tests each week. However, cell death due to initiation of apoptosis (blebs formation) was observed after 3 weeks exposure to 5 μM Co.
- The two organs with highest Co content after *in vivo* exposure were liver and kidney (excretory organs), and a significant accumulation was also seen in heart tissue. Cumulative Co exposure was relevant to altered cardiac function (significant decrease in % Fractional shortening: FS) in rats following 28 days of $CoCl_2$ treatment using echocardiography.
- Western blot analysis confirmed increased expression levels of total CaMKIIδ protein, TRPC6 and TRPM7 transport channel proteins in heart lysates after 28 days administration of $CoCl_2$ treatment. These calcium channels might mediate uptake of Co^{2+} into the heart and thus contribute to compromised heart function (%FS).
- The pathways that showed significant alteration following Co treatment in terms of changes in gene expression were 1) transmembrane transporter activity 2) cell metabolism 3) ion channel activity (calcium and metal ions) and 4) apoptosis
- Co exposure in *in vitro* CFs (10 μM, 72 h) cause an increased level in 4 out of 5 selected genes (*Camkiid, Dmt1, Trpc6* and *Trpm7*) using RT-qPCR. *In vitro* analysis

of 3T3 cells after Co exposure (10 μM, 72 h) also induced higher levels of expression in 4 out of 5 selected genes, although not the same cohort of genes entirely (*Camkiid, Dmt1, Trpm7* and *Trpv1*) using RT-qPCR.

- RT-qPCR confirmed the RNA-Seq results in which the expression of *Trpc6* was absent in 3T3 cells. This transporter might mediate the differential uptake of Co^{2+} in CFs and 3T3 cells.
- Similarity in the regulation of gene expression of all 5 selected genes was detected using both RNA-Seq and RT-qPCR with increasing expression levels in heart RNA after 28 days administration of $CoCl_2$ treatment.

7.3 Relevance of findings to patients with Metal on Metal implants.

From the literature it is known that Co toxicity from internal sources through MoM implants causes adverse effects both locally (local inflammation responses, metallosis and tissue lesions) and systemically (respiratory system, endocrine system, nervous system and cardiovascular system). Increasing incidence of toxicity has been continuously reported from normal to severe. In particular, the incidence of heart disease increases after high continuous exposure to metal ions through MoM implants. Fatalities related to cardiac cobaltism after MoM implants have also been reported in some studies At least three case studies of MoM Co cardiac toxicity have been documented where the outcome has been fatal (Gilbert *et al.*, 2013; Zywiel *et al.*, 2013; Martin *et al.*, 2015). Cardiovascular complications (Ischemic heart disease, pulmonary embolism, cerebrovascular accidents, myocardial infarction and heart failure) appear as the leading cause of death(Berstock *et al.*, 2014). Furthermore, it is important to consider the period of exposure, longer exposure time may serve as a surrogate for causing seriously toxicity. Also the age at which implants were received. Younger patients having such surgery are also at risk of Co toxicity from these internal sources.

In the same manner as MoM implants, other composed devices such as partial denture connectors and dental plates constructed from Co-Cr alloy were more toxic than other orthodontic materials (Titanium alloy) by causing an adverse dental tissue reaction, which was assessed by inflammation index (Ebadian *et al.*, 2008; Arafa, 2016). Chrome-cobalt orthodontic materials have been reported to cause systemic allergic contact dermatitis due to sensitivity of these materials (Brendlinger and Tarsitano, 1970; Guimaraens, Gonzalez and Condé-Salazar, 1994; Pigatto, Zerboni and Guzzi, 2008). Given the orthodontic risk (as well as that from hip implants), we hope that our knowledge gained from the current mechanistic study will help us to understand the fundamental basis of toxicity from metal alloys, that is helpful in long term protection.

Since high accumulation of Co causes severe damage in local areas, monitoring in the suspected area might be useful such as analysis of hip and knee joint fluid, to help with early detection and promote early diagnosis and screening. Early diagnosis and

treatment of patients with implants is essential as medications can delay the progression of the disease.

Slow-release of Co causes gradual accumulation of Co in various organs, especially in vital organs such as the heart. The monitoring of cardiac performance would be an alternative screening for patient with implants. Cardiac screening is an early way to diagnose most cardiac abnormalities by having echocardiography in every patient with an implant. Additional cardiac markers, which are released by the damaged heart muscle would be useful in terms of validating the cardiotoxicity.

The underlying mechanism for Co uptake could have important therapeutic implications. Targeting of potential Co uptake channels might help to reduce the Co accumulation into cells and organs. This study has highlighted some potential key targets but further work examining how these are regulated will be essential. Chelating agents are also an effective strategy to reduce circulating toxic metal ions and the complexes can be easily excreted and removed from the body. Effective prevention and therapeutic healthcare will help minimise the risk of developing certain severe conditions and restore health in following toxic metal ion exposure.

In MoM patients, the follow up period by monitoring metal content in blood or serum of patients with an implant should be every 3 or 6 months. However, another screening might be useful for monitoring purposes. The benefits of molecular techniques for screening like genetic testing would be useful (though expensive) to support routine blood-monitoring. Molecular techniques are part of the most effective and alternative healthcare screening. This could be particularly useful for patients most at risk. Although Co blood levels vary from patient to patient, specific gene screening might be useful to identify genetic disorders that can determine the probability of developing disease. The screening process may include other physiological examinations for example, ultrasound of cardiac performance or tests that assess the risk that patients will develop chronic diseases. Genetic testing is likely to be phenomenally expensive to administer to everyone as a part of clinical care, therefore, the choice of high risk patients should be left to the discretion of the doctor. Advanced prognosis and

diagnosis are powerful in determining health care and greatly beneficial to patients by reducing severity of illness, patient suffering and risk of mortality.

From this thesis it can be concluded that $CoCl_2$ causes effects on expression of different Co^{2+} entry channels and it is possible that the high accumulation of Co via these channels leads to development of cardiovascular disease. It may also be speculated from the increase in CaMKII expression following Co treatment, that Co might exert at least part of its toxic effects via upregulation and/or activation of this enzyme. This is a well-established route for cardiac dysfunction in disease (Mollova, Katus and Backs, 2015).

We envisage that molecular screening by RNA-Seq analysis will uncover biomarkers that can be used to detect adverse effects of Co in MoM patients, and indeed to determine their mechanism. To this end, we would strongly encourage obtaining blood samples from MoM patients whose Co levels are over 20 ppb (µg/L) (Langton *et al*., 2013, Tower, 2010, Oldenburg *et al*., 2009) for molecular screening.

7.4 Limitations of these studies and potential future areas of work

Over the course of this study we have tried to mimic the effects of Co that might be seen from MoM implants in terms of both short and long exposure times. In particular, we have directly examined the impact on adult heart and isolated primary cells from adult heart. However, there are many limitations within the studies.

According to the literature, it appears that Co may have more of an impact in female patients than male (Zywiel *et al.*, 2016). However, it is not certain that Co affects this population more because there are only a few cases and it could be attributed to either design of prosthesis or differences in metabolism between male and female. Due to the time and cost limitations, we could not perform a study of sex-dependent effects so only one sex (male rat) was chosen. Choosing males avoids the changes in hormones (estrous cycles) in female rats that can complicate findings in many fields especially in pharmacology and toxicology. And also male rats have a significantly larger body weight that makes investigation easier. Female rats may show the same response to Co toxicity but it would be interesting to study differences between sexes in further research. From this project though, it will be possible to obtain the trend of toxicity, which could be an incentive to a study further aspects of Co toxicity.

In this work, primary cardiac fibroblasts were used as representative heart cells from the adult. A key function of cardiac fibroblasts is extracellular matrix deposition in the heart, providing structural integrity. Although the majority of cells in the heart are cardiac fibroblasts (40-70%) there are other cell types such as cardiomyocytes, which are essential for cardiac contractile function. Cross-talk between cardiac fibroblasts and cardiac myocytes is very important in terms of overall cardiac function (Civitarese *et al.*, 2017). In order to complete the study *in vitro*, it would be interesting to isolate cardiomyocytes and also study the effects of Co on these cells.

There is a wide range of Co concentrations in the blood levels of patients reported in the literature. Because of the individual variation of each patient and variation in the physiological response to different Co ion levels, this makes reference concentrations somewhat difficult to predict for use in *in vivo* and *in vitro* experiments. Because of this, the Co concentration that we chose for long term studies *in vivo* and *in vitro* is

within the lower range of Co blood levels detected in patients. For example *in vivo*, the final Co concentration in blood of treated rats (1 mg/kg BW for 28 days) is 121±9.98 µg/L. *In vitro*, the range of Co between 0-1,200 µg/L was chosen. It was important to choose lower range concentrations to avoid unnecessary early cell death and more importantly in the *in vivo* studies to avoid any unnecessary suffering to the animals.

The limitations derived from choosing this lower range might be that a less toxic effect is induced. However, we still observed significant effects both *in vitro* (western blotting, RNASeq and RT-qPCR) and *in vivo* even although this might not mirror the exact extent of the effect in patients. The approach we have taken, although limited, might reflect better the Co poisoning effects in a person with an average Co level in blood and might also be reflective of early poisoning stages. So this could the context of our thesis that might help detect a biomarker in the future.

Our *in vitro* study suggested MTT assays were more sensitive in detecting the Co inhibition values (IC_{50}). This assesses cell metabolic activity reflecting mitochondrial function and dysfunction in these systems, when compared with another mechanism of action on Co (NR; lysosomal activity). It might be that the defects in metabolism highlight that Co has a bigger impact on mitochondrial function but it cannot be concluded from this work alone that mitochondria are a target of Co toxicity. MTT is not a specific assay that reflects mitochondrial toxicity. We have not checked specifically mitochondria toxicity, for example in terms of mitotoxicity assays the IC_{50} could be lower. The kind of experiment that is conducted on intact mitochondria would be critical to confirm that this may be a target site of Co. Further studies should verify this hypothesis and specify the impact of mitotoxicity in Co effects.

We observed signs of apoptosis on cell staining both under short and long-term exposure in CFs and 3T3s with different Co concentrations. Furthermore, gene expression in RNA-seq indicates that apoptosis could be taking part or be a contributing mechanism in Co toxicity. However, we did not perform any experiment specific for the detection of apoptosis such as LDH assay, caspase assay, Annexin V or TUNEL assay to confirm its appearance. Apoptosis is demonstrated to be involved

in cardiac remodelling (Van Empel *et al.*, 2005), a process which eventually leads to loss of contractility and heart failure in the long-term (Kemp and Conte, 2012). In that regard, histology could have provided relevant information regarding whether myocyte loss and hypertrophy were the events driving the lower %FS detected in Co treated rats. It is therefore recommended to proceed with histological examination of the tissue in future studies so as to help determine changes that could impact upon patients heart function.

The large amount of information given by RNA-Seq makes it difficult to complete analysis**.** We focused on certain ontology pathways reported by KEGG and GO ontology but in that effort we overlooked other information that might be relevant. In this limitation, we might be missing part of the big picture or big point of specific genes that could also be relevant because of the way the RNA-Seq analysis is conducted leading us to concentrate on a few relevant pathways. This could be an opportunity for other researchers to take the results forward. As far as we know, Co causes local and systemic toxicity. In systemic toxicity, effects on respiratory, nervous, endocrine and cardiovascular systems all exist. The list of genes from our RNA-Seq work provide a massive amount of information that could be used for further study to investigate the expression of genes in every system.

Our novel work on the mechanisms of Co toxicity to the heart in rats illustrates the feasibility of using RNA-Seq to determine the mechanisms of Co induced toxicity in MoM patients. We believe that the high cost of this technology will continue to decrease as its use is fully appreciated and that this may provide a screening tool not only for the adverse effects of MoM implants, but also a diagnostic screen for disease, and pathways for therapeutic intervention. Earlier intervention in the progression of Co related cardiac dysfunction could not only improve the quality of life for implant patients and reduce their mortality risk, but in turn could also bring cost benefits to healthcare systems by helping to reduce their future risk of requiring critical care hospital treatment.

PUBLICATIONS

Posters

Laovitthayanggoon, S., Tate, R., Currie, S. and Grant, M. H. 'Cobalt cardiotoxicity - effects on the contractile and non-contractile cells of the heart', Presented at Experimental Biology 2016, San Diego, CA, USA, April 2016

Laovitthayanggoon, S., Grant, M. H., Henderson, C. J., Tate, R. J.., McCluskey, C., MacDonald, M. and Currie, S. '$CoCl_2$ induced cardiotoxicity associated with CoCr alloy orthopaedic implants- an *in vivo* and an *in vitro* study', Presented at the Scottish Cardiovascular Forum 2017, Glasgow, UK, February 2017

Oral presentations

Laovitthayanggoon, S., Grant, M. H., Henderson, C. J., Tate, R. J. and Currie, S. '*Investigating cobalt toxicity in the context of joint replacement patients – cobalt uptake in primary cardiac fibroblasts and in 3T3 cells',* Presented at The *In Vitro* Toxicology Society (IVTS) Annual Congress, Radisson BLU Hotel, Glasgow, UK, November 2016.

Laovitthayanggoon, S., Henderson, C. J., Tate, R. J., Currie, S., McCluskey, C., MacDonald, M. and Grant, M. H. '*In vivo* and *in vitro* toxicity of cobalt in the heart', Presented at The British Toxicology Society Annual Congress, Hilton Liverpool City Centre, Liverpool, UK, April 2017.

References

Aarts, M. *et al.* (2003) ‘A Key Role for TRPM7 Channels in Anoxic Neuronal Death’, *Cell*, 115(7), pp. 863–877.
Accornero, F. *et al.* (2011) ‘Placental Growth Factor Regulates Cardiac Adaptation and Hypertrophy Through a Paracrine MechanismNovelty and Significance’, *Circulation research*, 109(3), pp. 272–280.
ACGIH, T. (2004). BELs: Threshold limit values for chemical substances and physical agents and biological exposure indices. ACGIH, Cincinnati, pp. 168-176.
Adler, C. P., Ringlage, W. P. and Böhm, N. (1981) ‘DNA content and cell number in heart and liver of children. Comparable biochemical, cytophotometric and histological investigations (author’s transl)’, *Pathology, research and practice*, 172(1–2), pp. 25–41.
Afolaranmi, G. A. *et al.* (2008) ‘Release of chromium from orthopaedic arthroplasties.’, *The open orthopaedics journal*, 2, pp. 10–8.
Afolaranmi, G. A. *et al.* (2012) ‘Distribution of metal released from cobalt-chromium alloy orthopaedic wear particles implanted into air pouches in mice’, *J. Biomed. Mater. Res. Part A*, 100A(6), pp. 1529–1538.
Afolaranmi, G. A. and Grant, M. H. (2013) ‘The effect of ascorbic acid on the distribution of soluble Cr and Co ions in the blood and organs of rats’, *Journal of Applied Toxicology*, 33(3), pp. 220–226.
Ahern, G. P. (2005) ‘Extracellular Cations Sensitize and Gate Capsaicin Receptor TRPV1 Modulating Pain Signalling’, *Journal of Neuroscience*, 25(21), pp. 5109–5116.
Akbar, M., Brewer, J. M. and Grant, M. H. (2011) ‘Effect of chromium and cobalt ions on primary human lymphocytes in vitro’, *Journal of immunotoxicology*, 8(2), pp. 140–149.
Akinrinde, A. S. *et al.* (2016) ‘Alterations in blood pressure, antioxidant status and caspase 8 expression in cobalt chloride-induced cardio-renal dysfunction are reversed by Ocimum gratissimum and gallic acid in Wistar rats’, *Journal of Trace Elements in Medicine and Biology*. Elsevier GmbH., 36, pp. 27–37.
Akita, K. *et al.* (2007) ‘Cobalt chloride induces apoptosis and zinc chloride suppresses cobalt-induced apoptosis by Bcl-2 expression in human submandibular gland HSG cells’, *International Journal of Oncology*, 31(4), pp. 923–929.
Alexander, C. S. (1969) ‘Cobalt and the heart’, *Ann. Intern. Med.*, 70, pp. 411–413.
Alexander, C. S. (1972) ' Cobalt-beer cardiomyopathy: A clinical and pathologic study of twenty-eight cases' *The American journal of medicine*, 53(4), pp. 395-417.
Alexandersson, R. (1988) ‘Blood and urinary concentrations as estimators of cobalt exposure’, *Archives of Environmental Health*, 43(4), pp. 5.
Alexandersson, R. and Lidums, V. (1979) ‘Studies on effects of exposure to cobalt IV Concentration of cobalt in blood and urine as indicators of exposure’, *Arbete och Hilsa*, 8, pp. 23.
Al-Kharafi, F. M., Badawy, W. A. and Al-Ajmi, J. R. (1999) ‘Effect of chloride ions on the corrosion and passivation behaviours of cobalt in neutral solutions’, *Indian Journal of Chemical Technology*, 6, pp. 194–201.
Allen, L. A. *et al.* (2014) ‘Missing elements of the history’, *New England Journal of Medicine*, 370(6), pp. 559–566.
Almdal, T. *et al.* (2004) ‘The independent effect of type 2 diabetes mellitus on ischemic heart disease, stroke, and death: a population-based study of 13 000 men and women with 20 years of follow-up’, *Archives of internal medicine,*

164(13), pp. 1422–1426.
Almousa, S. A. *et al.* (2013) 'The natural history of inflammatory pseudotumors in asymptomatic patients after metal-on-metal hip arthroplasty', *Clinical Orthopaedics and Related Research*, 471(12), pp. 3814–3821.
Alsaad, K. O. and Ghazarian, D. (2005) 'My approach to superficial inflammatory dermatoses', *Journal of Clinical Pathology*, 58(12), pp. 1233–1241.
Amini, M. *et al.* (2014) 'Evaluation and management of metal hypersensitivity in total joint arthroplasty: a systematic review', *Journal of long-term effects of medical implants*, 24(1).
Anderson, J. M., Rodriguez, A. and Chang, D. T. (2008) 'Foreign body reaction to biomaterials', *Seminars in Immunology*, 20(2), pp. 86–100.
Anderson, M. E. *et al.* (1994) 'Multifunctional Ca21/Calmodulin-Dependent Protein Kinase Mediates Ca2+-Induced Enhancement of the L-type Ca2+ Current in Rabbit Ventricular Myocytes', *Circular Research*, 75, pp. 854–861.
Anderson, M. E., Brown, J. H. and Bers, D. M. (2011) 'CaMKII in myocardial hypertrophy and heart failure', *Journal of molecular and cellular cardiology*, 51(4), pp. 468–473.
Andrews, R. E. *et al.* (2011) 'Effects of cobalt and chromium ions at clinically equivalent concentrations after metal-on-metal hip replacement on human osteoblasts and osteoclasts: Implications for skeletal health', *Bone*, 49(4), p. 7.
Anissian, L. *et al.* (2002) 'Cobalt ions influence proliferation and function of human osteoblast-like cells', *Acta orthopaedica Scandinavica*, 73(3), pp. 369–374.
Antoniou, J. *et al*. (2008) 'Metal ion levels in the blood of patients after hip resurfacing: a comparison between twenty-eight and thirty-six-millimeter-head metal-on-metal prostheses', JBJS, 90(Supplement_3), pp. 142-148.
AOANJRR. (2017) 'Australian Orthopaedic Association National Joint Replacement Registry (AOANJRR). Hip, Knee & Shoulder Arthroplasty: 2017 Annual Report'. Available at: https://aoanjrr.sahmri.com/documents/10180/397736/Hip%2C%20Knee%20%26%20Shoulder%20Arthroplasty
Arafa, K. A. O. (2016) 'Comparing the effects of titanium alloy and chrome cobalt in removable partial denture connectors on tooth mobility, bone loss and tissue reaction', *Saudi Journal for Dental Research*. The Saudi Journal for Dental Research, 7(2), pp. 112–117.
Athanasou, N. A. (2016). The pathobiology and pathology of aseptic implant failure. *Bone and Joint Research*, *5*(5), pp. 162-168.
ATSDR, (Agency for Toxic Substances and Disease Registry) (1992) ' Toxicological Profile for Cobalt. U.S. Department of Health and Human Services, Public health service, ATSDR, Atlanta, GA.
ATSDR, (Agency for Toxic Substances and Disease Registry) (2004) 'Toxicological Profile for Cobalt. U.S. Department of Health and Human Services, Public Health Service, ATSDR, Atlanta, GA,
Ayala-Fierro, F., Firriolo, J. M. and Carter, D. E. (1999) 'Dispositiion, Toxicity, and Intestinal Absorption of Cobaltous Chloride in Male Fischer 344 Rats', *Journal of Toxicology and Environmental Health, Part A*, 56(8), pp. 571–591.
Ayswarya, A. and Kurian, G. A. (2016) 'Sensitivity of interfibrillar and subsarcolemmal mitochondria to cobalt chloride-induced oxidative stress and hydrogen sulfide treatment', *Indian journal of pharmaceutical sciences*, 78(1),

pp. 151–158.
Bachetti, T. and Morbidelli, L. (2000) ‘Endothelial cells in culture: a model for studying vascular functions’, *Pharmacological research*, 42(1), pp. 9–19.
Backs, J. *et al.* (2009) ‘The isoform of CaM kinase II is required for pathological cardiac hypertrophy and remodeling after pressure overload’, *Proceedings of the National Academy of Sciences*, 106(7), pp. 2342–2347.
Backs, J. *et al.* (2009) ‘The δ isoform of CaM kinase II is required for pathological cardiac hypertrophy and remodeling after pressure overload’, *Proceedings of the National Academy of Sciences*, 106(7), pp. 2342–2347.
Bader, G. D., Betel, D. and Hogue, C. W. V. (2003) ‘BIND: The Biomolecular Interaction Network Database’, *Nucleic Acids Research*, 31(1), pp. 248–250.
Banerjee, I. *et al.* (2007) ‘Determination of cell types and numbers during cardiac development in the neonatal and adult rat and mouse’, *American Journal of Physiology-Heart and Circulatory Physiology*, 293(3), pp. H1883–H1891.
Bank, H. L. (1987) ‘Assessment of islet cell viability using fluorescent dyes’, *Diabetologia*, 30(10), pp. 812–816.
Bank, H. L. (1988) ‘Rapid assessment of islet viability with acridine orange and propidium iodide’, *In vitro cellular & developmental biology*, pp. 266–273.
Barborik, M., & Dusek, J. (1972) 'Cardiomyopathy accompaning industrial cobalt exposure', *British Heart Journal*, 34(1), p. 113.
Barnaby, C. F., Smith, T. and Thompson, B. D. (1968) ‘Dosimetry of the radioisotopes of cobalt’, *Physics in medicine and biology*, 13(3), pp. 421.
Battaglia, V. *et al.* (2009) ‘Cobalt induces oxidative stress in isolated liver mitochondria responsible for permeability transition and intrinsic apoptosis in hepatocyte primary cultures’, *The international journal of biochemistry & cell biology*, 41(3), pp. 586–594.
Bauckman, K. A., Owusu-Boaitey, N. and Mysorekar, I. U. (2015) ‘Selective autophagy: Xenophagy’, *Methods*, 75, pp. 120–127.
Begg, A. C. *et al.* (1985) ‘A method to measure the duration of DNA synthesis and the potential doubling time from a single sample.’, *Cytometry*, 6(6), pp. 620–6.
Beldame, J. *et al.* (2009) 'Cementless cups do not increase osteolysis risk in metal-on-metal total hip arthroplasty', *Orthopaedics & Traumatology: Surgery & Research*, 95(7), pp. 478-490.
Berber, R. *et al.* (2017) ‘Assessing for Cardiotoxicity from Metal-on-Metal Hip Implants with Advanced Multimodality Imaging Techniques’, *The Journal of bone and joint surgery. American volume*, 99(21), pp. 1827–1835.
Bergeron, M. *et al.* (2000) ‘Role of hypoxia - inducible factor - 1 in hypoxia - induced ischemic tolerance in neonatal rat brain’, *Annals of neurology*, 48(3), pp. 285–296.
Bergmann, O. *et al.* (2015) ‘Dynamics of cell generation and turnover in the human heart’, *Cell*, 161(7), pp. 1566–1575.
Berridge, M., Lipp, P. and Bootman, M. (1999) ‘Calcium signalling’, *Current biology*, 9(5), pp. R157–R159.
Berridge, M. V and Tan, A. S. (1993) ‘Characterization of the Cellular Reduction of 3-(4,5-dimethylthiazol-2-yl)-2,5-diphenyltetrazolium bromide (MTT): Subcellular Localization, Substrate Dependence, and Involvement of Mitochondrial Electron Transport in MTT Reduction’, *Archives of Biochemistry and Biophysics*, 303(2).

Berstock, J. R. *et al.* (2014) ‘Mortality after total hip replacement surgery: A systematic review.’, *Bone & joint research*, 3(6), pp. 175–82.

Beuckelmann, D. J., Näbauer, M. and Erdmann, E. (1992) ‘Intracellular calcium handling in isolated ventricular myocytes from patients with terminal heart failure’, *Circulation*, 85(3), pp. 1046–1055.

Beyersmann, D. (2002) ‘Effects of carcinogenic metals on gene expression’, *Toxicology Letters*, 127(1–3), pp. 63–68.

Bhatia, R., Tu, J. and Lee, D. (2006) ‘Outcome of heart failure with preserved ejection fraction in a population-based study’, *New England Journal of Medicine*, 355(3), pp. 260–269.

Biernacka, A. and Frangogiannis, N. G. (2011) 'Aging and cardiac fibrosis', *Aging and disease*, 2(2), p. 158.

Bindea, G. *et al.* (2009) ‘ClueGO: a Cytoscape plug-in to decipher functionally grouped gene ontology and pathway annotation networks’, *Bioinformatics*, 25(8), pp. 1091–1093.

Bisschop, R. *et al.* (2013) ‘High prevalence of pseudotumors in patients with a birmingham hip resurfacing prosthesis’, *Journal of Bone and Joint Surgery - Series A*, 95(17), pp. 1554–1560.

Bisseling, P. *et al.* (2011) 'Metal ion levels in patients with a lumbar metal-on-metal total disc replacement: should we be concerned?', *J Bone Joint Surg B*r, 93(7), pp. 949-954.

Boardman, D. R., Middleton, F. R. and Kavanagh, T. G. (2006) ‘A benign psoas mass following metal-on-metal resurfacing of the hip’, *The Journal of bone and joint surgery. British volume*, 88(3), pp. 402–4.

Böhler, M. *et al.* (2002) ‘Adverse tissue reactions to wear particles from Co-alloy articulations, increased by alumina-blasting particle contamination from cementless Ti-based total hip implants’, *The Journal of Bone and Joint Surgery*, 84(1), pp. 128–136.

Booth, G. L. *et al.* (2006) ‘Relation between age and cardiovascular disease in men and women with diabetes compared with non-diabetic people: a population-based retrospective cohort study’, *The Lancet*, 368(9529), pp. 29–36.

Bouron, A., Kiselyov, K. and Oberwinkler, J. (2015) ‘Permeation , regulation and control of expression of TRP channels by trace metal ions’, *Pflugers Arch - Eur J Physiol*, 467, pp. 1143–1164.

Brendlinger, D. L. and Tarsitano, J. J. (1970) ‘Generalized dermatitis due to sensitivity to a chrome cobalt removable partial denture’, *The Journal of the American Dental Association*, 81(2), pp. 392–394.

Bresson, C. *et al.* (2013) ‘Cobalt chloride speciation, mechanisms of cytotoxicity on human pulmonary cells, and synergistic toxicity with zinc’, *Metallomics*, 5(2), pp. 133–143.

Brown, G. C. *et al.* (1977) ‘Sensitivity to metal as a possible cause of sterile loosening after cobalt-chromium total hip-replacement arthroplasty’, *JBJS*, 59(2), pp. 164–168.

Brown, S. R. *et al.* (2002) ‘Long-term survival of McKee-Farrar total hip prostheses’, *Clinical Orthopaedics and Related Research*, 402, pp. 157–163.

Brune, D. *et al.* (1980) 'Pulmonary deposition following inhalation of chromium-cobalt grinding dust in rats and distribution in other tissues', *European Journal of Oral Sciences*, 88(6), pp. 543-551.

Bucher, J. R. *et al.* (1990) 'Inhalation toxicity studies of cobalt sulfate in F344/N rats and B6C3F1 mice', *Toxicological Sciences*, 15(2), pp. 357-372.
Burrell, L. M. *et al.* (1996) 'Validation of an echocardiographic assessment of cardiac function following moderate size myocardial infarction in the rat', *Clinical and experimental pharmacology and physiology*, 23(6 - 7), pp. 570–572.
Bustin, S. A. (2002) 'Quantification of mRNA using real-time reverse transcription PCR (RT-PCR): Trends and problems', *Journal of Molecular Endocrinology*, 29(1), pp. 23–39.
Bustin, S. A. *et al.* (2009) 'The MIQE guidelines: minimum information for publication of quantitative real-time PCR experiments', *Clinical chemistry*, 55(4), pp. 611-622.
Bustin, S. A. (2010) 'Why the need for qPCR publication guidelines?—The case for MIQE', *Methods*, 50(4), pp. 217-226.
Cade, W. T. (2008) 'Diabetes-related microvascular and macrovascular diseases in the physical therapy setting', *Physical therapy*, 88(11), pp. 1322–1335.
Camelliti, P., Borg, T. K. and Kohl, P. (2005) 'Structural and functional characterisation of cardiac fibroblasts', *Cardiovascular Research*, 65(1), pp. 40–51.
Campbell, P. *et al.* (2010) 'Histological features of pseudotumor-like tissues from metal-on-metal hips', *Clinical Orthopaedics and Related Research*, 468(9), pp. 2321–2327.
Case, C. P. *et al.* (1994) 'Widespread dissemination of metal debris from implants.', *The Journal of bone and joint surgery. British volume*, 76(5), pp. 701–12. Available at: http://www.ncbi.nlm.nih.gov/pubmed/8083255.
Catalani, S. *et al.* (2012) 'Neurotoxicity of cobalt', *Human & experimental toxicology*, *31*(5), pp. 421-437.
Catelas I et al. (2003) 'Size, shape, and composition of wear particles from metal-metal hip simulator testing: effects of alloy and number of loading cycles', *J Biomed Mater Res A*, 67, pp. 312-27
Catelas, I. *et al.* (2005) 'Quantitative analysis of macrophage apoptosis vs. necrosis induced by cobalt and chromium ions in vitro', *Biomaterials*, 26(15), pp. 2441–2453.
Caterina, M. J. *et al.* (1997) 'The capsaicin receptor: A heat-activated ion channel in the pain pathway', *Nature*, 389(6653), pp. 816–824.
Chamberlain III, J. L. (1961) 'Thyroid enlargement probably induced by cobalt: A rerport of 3 cases', *The Journal of pediatrics*, 59(1), pp. 81-86.
Chang, H. Y. *et al.* (2002) 'Diversity, topographic differentiation, and positional memory in human fibroblasts", *Proceedings of the National Academy of Sciences*, 99(20), pp. 12877-12882.
Chang, E. Y. *et al.* (2013) 'Relationship of plasma metal ions and clinical and imaging findings in patients with ASR XL metal-on-metal total hip replacements', *JBJS*, 95(22), pp. 2015–2020.
Charette, R. S., Neuwirth, A. L. and Nelson, C. L. (2017) 'Arthroprosthetic cobaltism associated with cardiomyopathy', *Arthroplasty today*, 3(4), pp. 225–228.
Charrua, A. *et al.* (2009) 'Functional transient receptor potential vanilloid 1 is expressed in human urothelial cells', *The Journal of urology*, 182(6), pp. 2944–2950.
Chen, F. and Shi, X. (2002) 'Intracellular signal transduction of cells in response to

carcinogenic metals', *Critical Reviews in Oncology and Hematology*, 42(1), pp. 105–121.
Cheung, A. C. *et al.* (2016) 'Systemic cobalt toxicity from total hip arthroplasties: review of a rare condition Part 1 - history, mechanism, measurements, and pathophysiology', *The bone & joint journal*, 98–B(1), p. 8.
Chigurupati, S. *et al.* (2010) 'Receptor channel TRPC6 is a key mediator of Notch-driven glioblastoma growth and invasiveness', *Cancer Research*, 70(1), pp. 418–427.
Cipolletta, E. *et al.* (2015) 'Targeting the CaMKII/ERK interaction in the heart prevents cardiac hypertrophy', *PLoS One*, 10(6), pp. e0130477.
Cittadini, A. *et al.* (1996) 'Differential Cardiac Effects of Growth Hormone and Insulin-like Growth Factor1 in the Rat', *Circulation*, 93(4), pp. 800–809.
Civitarese, R. A. *et al.* (2017) 'Role of integrins in mediating cardiac fibroblast - cardiomyocyte cross talk: a dynamic relationship in cardiac biology and pathophysiology', *Basic research in cardiology*, 112(1), pp. 6.
Clapham, D. E. (2003) 'TRP channels as cellular sensors', *Nature*, 426(6966), pp. 517–524.
Clarke, M. T. *et al.* (2003) 'Levels of metal ions after small-and large-diameter metal-on-metal hip arthroplasty', *The Journal of bone and joint surgery*. British volume, 85(6), pp. 913-917.
Clarson, L. H. *et al.* (2003) 'Store-operated Ca2+ entry in first trimester and term human placenta.', *The Journal of physiology*, 550(Pt 2), pp. 515–28.
Cline, M. S. *et al.* (2007) 'Integration of biological networks and gene expression data using Cytoscape', *Nature protocols*, 2(10), pp. 2366.
Clyne, N. *et al.* (2001) 'Chronic cobalt exposure affects antioxidants and ATP production in rat myocardium', *Scandinavian journal of clinical and laboratory investigation*, 61(8), pp. 609–614.
Coatney, R. W. (2001) 'Ultrasound imaging: principles and applications in rodent research.', *ILAR journal / National Research Council, Institute of Laboratory Animal Resources*, 42(3), pp. 233–247.
Colognato, R. *et al.* (2008) 'Comparative genotoxicity of cobalt nanoparticles and ions on human peripheral leukocytes in vitro', *Mutagenesis*, 23(5), pp. 377–382.
Colomer, J. M. *et al.* (2003) 'Pressure Overload Selectively Up-Regulates Ca $^{2+}$ /Calmodulin-Dependent Protein Kinase II *in Vivo*', *Molecular Endocrinology*, 17(2), pp. 183–192.
Corten, K. and MacDonald, S. J. (2010) 'Hip resurfacing data from national joint registries: what do they tell us? What do they not tell us?', *Clinical Orthopaedics and Related Research®*, 468(2), pp. 351–357.
Couchonnal, L. F. and Anderson, M. E. (2008) 'The role of calmodulin kinase II in myocardial physiology and disease.', *Physiology (Bethesda, Md.)*, 23(60), pp. 151–159.
Cullis, P. R. and Verkleij, A. J. (1979) 'Modulation of membrane structure by Ca2+ and dibucaine as detected by 31P NMR', *BBA - Biomembranes*, 552(3), pp. 546–551.
Cunningham, C. C. (1995) 'Actin polymerization and intracellular solvent flow in cell surface blebbing', *Journal of Cell Biology*, 129(6), pp. 1589–1599.
Currie, S. and Smith, G. L. (1999) 'Calcium/calmodulin -dependent protein kinase II activity is increased in sarcoplasmic reticulum from coronary artery ligated

rabbit hearts', *FEBS letters*, 459(2), pp. 244–248.
Czarnek, K., Terpilowska, S. and Siwicki, A. K. (2015) 'Selected aspects of the action of cobalt ions in the human body', *Central European Journal of Immunology*, 40(2), pp. 236–242.
D'Adda, F. *et al.* (1994) 'Cardiac function study in hard metal workers', *Science of the total environment*, *150*(1-3), pp. 179-186.
Dahms, K. *et al.* (2014) 'Cobalt intoxication diagnosed with the help of Dr House', *The Lancet*. Elsevier Ltd, 383(9916), p. 574.
Dai, D.-F. *et al.* (2011) 'Mitochondrial oxidative stress mediates angiotensin II–induced cardiac hypertrophy and Gαq overexpression–induced heart failure', *Circulation research*, pp. CIRCRESAHA. 110.232306.
Dai, Z. J. *et al.* (2012) 'Up-regulation of hypoxia inducible factor-1α by cobalt chloride correlates with proliferation and apoptosis in PC-2 cells', *Journal of Experimental and Clinical Cancer Research*. BioMed Central Ltd, 31(1), p. 28.
Dalal, A. *et al.* (2012) 'Orthopedic implant cobalt - alloy particles produce greater toxicity and inflammatory cytokines than titanium alloy and zirconium alloy-based particles in vitro, in human osteoblasts, fibroblasts, and macrophages', *Journal of Biomedical Materials Research Part A*, 100(8), pp. 2147–2158.
Dalman, M. R. *et al.* (2012) 'Fold change and p-value cutoffs significantly alter microarray interpretations', *BMC Bioinformatics*. BioMed Central Ltd, 13(Suppl 2), pp. S11.
Davda, K. *et al.* (2011) 'An analysis of metal ion levels in the joint fluid of symptomatic patients with metal-on-metal hip replacements', *J Bone Joint Surg Br*, 93(6), pp. 738-745.
Davies, A. P. (2005) 'An Unusual Lymphocytic Perivascular Infiltration in Tissues Around Contemporary Metal-on-Metal Joint Replacements', *The Journal of Bone and Joint Surgery (American)*, 87(1), pp. 18.
Davis, D. L. and Morrison, J. J. (2016) 'Hip Arthroplasty Pseudotumors: Pathogenesis, Imaging, and Clinical Decision Making', *Journal of Clinical Imaging Science*. India: Medknow Publications & Media Pvt Ltd, 6, pp. 17.
Defenderauto.info. (2018). 'Ball And Socket Joint. [online] Available at: http://defenderauto.info/ball-and-socket-joint/) [Accessed 3 Apr. 2018].
Demir, T. *et al.* (2014) 'Evaluation of TRPM (transient receptor potential melastatin) genes expressions in myocardial ischemia and reperfusion', *Molecular biology reports*, 41(5), pp. 2845–2849.
Denisov, V. *et al.* (2008) 'Development and validation of RQI: an RNA quality indicator for the Experion automated electrophoresis system', *Bio-Rad Bulletin, 5761*.
Desrochers, J., Amrein, M. W. and Matyas, J. R. (2013) 'Microscale surface friction of articular cartilage in early osteoarthritis', *Journal of the Mechanical Behavior of Biomedical Materials*. Elsevier, 25, pp. 11–22.
Desrois, M. *et al.* (2014) 'Effect of isoproterenol on myocardial perfusion, function, energy metabolism and nitric oxide pathway in the rat heart-a longitudinal MR study', *NMR in Biomedicine*, 27(5), pp. 529–538.
Desy, N. M. *et al.* (2011) 'Surgical variables influence metal ion levels after hip resurfacing', *Clinical Orthopaedics and Related Research*, 469(6), pp. 1635–1641.
Di, A. and Malik, A. B. (2010) 'TRP channels and the control of vascular function',

Current opinion in pharmacology, 10(2), pp. 127–132.
Dietrich, A. *et al.* (2005) 'Increased vascular smooth muscle contractility in TRPC6−/− mice', *Molecular and cellular biology*, 25(16), pp. 6980–6989.
Doctor, R. B., Zhelev, D. V., and Mandel, L. J. (1997) 'Loss of plasma membrane structural support in ATP-depleted renal epithelia', *American Journal of Physiology-Cell Physiology*, 272(2), C439-C449.
Domingo, J. L., Llobet, J. M., and Bernat, R. (1984) 'A study of the effects of cobalt administered orally to rats', *Archivos de farmacologia y toxicologia*, 10(1), pp. 13-20.
Dong, X. P., Wang, X. and Xu, H. (2010) 'TRP channels of intracellular membranes', *Journal of Neurochemistry*, 113(2), pp. 313–328.
Doppler, S. A. *et al.* (2017) 'Cardiac fibroblasts : more than mechanical support', *Journal of Thoracic Disease*, 9(Suppl 1), pp. 36–51.
Du, J. *et al.* (2010) 'TRPM7-mediated Ca(2+) signals confer fibrogenesis in human Atrial Fibrillation', *Circulation research*, 106(5), pp. 992–1003.
Duckham, J. M., & Lee, H. A. (1976) 'The treatment of refractory anaemia of chronic renal failure with cobalt chloride', *QJM: An International Journal of Medicine*, 45(2), pp. 277-294.
Dunstan, E., *et al.* (2005) 'Metal ion levels after metal-on-metal proximal femoral replacements: a 30-year follow-up', *Bone & Joint Journal*, 87(5), pp. 628-631.
Dybkova, N. *et al.* (2011) 'Overexpression of CaMKIIδc in RyR2 R4496C+/− knock-in mice leads to altered intracellular Ca 2+ handling and increased mortality', *Journal of the American College of Cardiology*, 57(4), pp. 469–479.
Earley, S. (2010) 'Vanilloid and melastatin transient receptor potential channels in vascular smooth muscle', *Microcirculation*, 17(4), pp. 237–249.
Earley, S. and Brayden, J. E. (2010) 'Transient receptor potential channels and vascular function', *Clinical Science*, 119(1), pp. 19–36.
Earlstevens58.files.wordpress.com. (2018). [online] Available at: https://earlstevens58.files.wordpress.com/2012/12/mom-hip-implant-systems.pdf [Accessed 3 Apr. 2018]
Ebadian, B. *et al.* (2008) 'Evaluation of tissue reaction to some denture-base materials: an animal study', *J Contemp Dent Pract*, 9(4), pp. 67–74.
Ebreo, D. *et al* (2011) 'Metal ion levels decrease after revision for metallosis arising from large-diameter metal-on-metal hip arthroplasty',*Acta Orthopædica Belgica*, 77(6), p. 777.
Eden, E. *et al.* (2009) 'GOrilla: A tool for discovery and visualization of enriched GO terms in ranked gene lists', *BMC Bioinformatics*, 10, pp. 1–7.
Eder, P. and Molkentin, J. D. (2011) 'TRPC channels as effectors of cardiac hypertrophy', *Circulation Research*, 108(2), pp. 265–272.
EFSA (2009) 'Scientific Opinion on the use of cobalt compounds as additives in animal nutrition,EFSA Panel on Additives and Products or Substances used in Animal Feed (FEEDAP), European Food Safety Authority (EFSA), Parma, Italy', *EFSA Journal*, 7(12).
EFSA (2012) 'Scientific Opinion on the use of cobalt compounds as additives in animal nutrition,EFSA Panel on Additives and Products or Substances used in Animal Feed (FEEDAP), European Food Safety Authority (EFSA), Parma, Italy', *EFSA Journal*, 7(10).
EGVM (Expert Group on Vitamins and Minerals). (2003) 'Safe upper levels for

vitamins and minerals' London : Food Standards Agency, 2003.
Ehrlich, A., Kucenic, M., and Belsito, D. V. (2001) 'Role of body piercing in the induction of metal allergies', *American Journal of Contact Dermatiti*s, 12(3), pp. 151-155.
Ehrnstorfer, I. A. *et al.* (2014) 'Crystal structure of a SLC11 (NRAMP) transporter reveals the basis for transition-metal ion transport', *Nature structural & molecular biology*, 21(11), pp. 990–996.
Eisen, M. B. *et al.* (1998) 'Cluster analysis and display of genome-wide expression patterns', *Proc Natl Acad Sci USA*, 95(25), pp. 14863–14868.
Van Empel, V. P. M. *et al.* (2005) 'Myocyte apoptosis in heart failure', *Cardiovascular Research*, 67(1), pp. 21–29.
Endoh, H. *et al.* (2000) 'Improved cardiac contractile functions in hypoxia-reoxygenation in rats treated with low concentration Co 2+', *American Journal of Physiology-Heart and Circulatory Physiology*, 279(6), pp. H2713–H2719.
Erickson, J. R. (2014) 'Mechanisms of CaMKII activation in the heart', *Frontiers in Pharmacology*, 5, pp. 1–5.
Evans, E. J. (1994) 'Cell damage in vitro following direct contact with fine particles of titanium, titanium alloy and cobalt-chrome-molybdenum alloy', *Biomaterials*, 15(9), pp. 713–717.
Evans, E. J. and Thomas, I. T. (1986) 'The in vitro toxicity of cobalt-chrome-molybdenum alloy and its constituent metals', *Biomaterials*, 7(1), pp. 25–29.
Fackler, O. T. and Grosse, R. (2008) 'Cell motility through plasma membrane blebbing', *The Journal of Cell Biology*, 181(6), pp. 879–884.
Faouzi, M. *et al.* (2017) 'The TRPM7 channel kinase regulates store-operated calcium entry', *The Journal of physiology*, 595(10), pp. 3165–3180.
Fautz, R., Husein, B. and Hechenberger, C. (1991) 'Application of the neutral red assay (NR assay) to monolayer cultures of primary hepatocytes: rapid colorimetric viability determination for the unscheduled DNA synthesis test (UDS)', *Mutation Research/Environmental Mutagenesis and Related Subjects*, 253(2), pp. 173-179.
Feoktistova, M., Geserick, P. and Leverkus, M. (2016) 'Crystal violet assay for determining viability of cultured cells', *Cold Spring Harbor Protocols*, 2016(4), pp. pdb. prot087379.
Fielitz, J. *et al.* (2008) 'Requirement of protein kinase D1 for pathological cardiac remodeling', *Proceedings of the National Academy of Sciences*, 105(8), pp. 3059–3063.
Finley, B. L., Monnot, A. D., Paustenbach, D. J., & Gaffney, S. H. (2012). Derivation of a chronic oral reference dose for cobalt. *Regulatory Toxicology and Pharmacology*, 64(3), pp. 491-503.
Finotello, F. *et al.* (2014) 'Reducing bias in RNA sequencing data: a novel approach to compute counts', *BMC Bioinformatics*, 15(1), pp. S7.
Fleig, A. *et al.* (2014) 'Mammalian Transient Receptor Potential (TRP) Cation Channels', *Handbook of experimental pharmacology*, 222(April 2014), pp. 521–546.
Fleige, S. and Pfaffl, M. W. (2006) 'RNA integrity and the effect on the real-time qRT-PCR performance', *Molecular aspects of medicine*, 27(2–3), pp. 126–139.
Fleming, M. D. *et al.* (1998) 'Nramp2 is mutated in the anemic Belgrade (b) rat: Evidence of a role for Nramp2 in endosomal iron transport', *Proceedings of*

the National Academy of Sciences, 95(February), pp. 1148–1153.
Fleury, C. *et al.* (2006) 'Effect of cobalt and chromium ions on human MG-63 osteoblasts in vitro: morphology, cytotoxicity, and oxidative stress', *Biomaterials*, 27(18), pp. 3351–3360.
Foot, N. J. *et al.* (2008) 'Regulation of the divalent metal ion transporter DMT1 and iron homeostasis by a ubiquitin-dependent mechanism involving Ndfips and Regulation of the divalent metal ion transporter DMT1 and iron homeostasis by a ubiquitin-dependent mechanism involving Ndfi', *Blood*, 112(10), pp. 4268–4275.
Foot, N. J. *et al.* (2016) 'Ndfip2 is a potential regulator of the iron transporter DMT1 in the liver', *Scientific Reports*. Nature Publishing Group, 6, pp. 24045.
Forbes, J. R. and Gros, P. (2003) 'Iron, manganese, and cobalt transport by Nramp1 (Slc11a1) and Nramp2 (Slc11a2) expressed at the plasma membrane', *Blood*, 102(5), pp. 1884–1892.
Forman, D. E. *et al.* (1997) 'Cardiac morphology and function in senescent rats: gender-related differences', *Journal of the American College of Cardiology*, 30(7), pp. 1872–1877.
Fors, R. *et al.* (2012) 'Nickel allergy in relation to piercing and orthodontic appliances - A population study', *Contact Dermatitis*, 67(6), pp. 342–350.
Fox, K. A. *et al.* (2016) 'Fatal cobalt toxicity after total hip arthroplasty revision for fractured ceramic components', *Clinical toxicology*, 54(9), pp. 874–877.
Frigerio, E. *et al.* (2011) 'Metal sensitivity in patients with orthopaedic implants: A prospective study', *Contact Dermatitis*, 64(5), pp. 273–279.
Fritzsche, J., Borisch, C. and Schaefer, C. (2012) 'Case Report: High Chromium and Cobalt Levels in a Pregnant Patient with Bilateral Metal-on-Metal Hip Arthroplasties', *Clinical Orthopaedics and Related Research®*, 470(8), pp. 7.
Friesenbichler, J. *et al*. (2012) 'Serum metal ion levels after rotating-hinge knee arthroplasty: comparison between a standard device and a megaprosthesis', *International orthopaedics*, 36(3), 539-544.
Garcia-Martinez, C. *et al.* (2000) 'Identification of an aspartic residue in the P-loop of the vanilloid receptor that modulates pore properties', *Journal of Biological Chemistry*, 275(42), pp. 32552–32558.
Garcia-Rivas, G. *et al.* (2017) 'A systematic review of genetic mutations in pulmonary arterial hypertension', *BMC Medical Genetics*, 18(1), pp. 1–10.
Gees, M., Colsoul, B. and Nilius, B. (2010) 'The role of transient receptor potential cation channels in Ca2+ signalling', *Cold Spring Harb Perspect Biol*, 2(10), pp. a003962.
Germain, M. A. *et al*. (2003) 'Comparison of the cytotoxicity of clinically relevant cobalt–chromium and alumina ceramic wear particles in vitro',*Biomaterials*, 24(3), pp. 469-479.
Gennart, J. P., & Lauwerys, R. (1990) 'Ventilatory function of workers exposed to cobalt and diamond containing dust', *International archives of occupational and environmental health*, 62(4), pp. 333-336.
Giampreti, A., Lonati, D. and Locatelli, C. A. (2014) 'Chelation in suspected prosthetic hip-associated cobalt toxicity', *Canadian Journal of Cardiology*, 30(4), p. 465. e13.
Gibon, J. *et al.* (2011) 'The over-expression of TRPC6 channels in HEK-293 cells favours the intracellular accumulation of zinc', *Biochimica et Biophysica Acta*

- *Biomembranes*. Elsevier B.V., 1808(12), pp. 2807–2818.
Gilbert, C. J. *et al.* (2013) 'Hip pain and heart failure: The missing link', *Canadian Journal of Cardiology*. Canadian Cardiovascular Society, 29(5), pp. 639.e1-639.e2.
Gill, H. S. *et al.* (2012) 'Molecular and immune toxicity of CoCr nanoparticles in MoM hip arthroplasty', *Trends in Molecular Medicine*, 18(3), pp. 2.
Gillam, M. H. *et al.* (2017) 'Heart failure after conventional metal-on-metal hip replacements:A retrospective cohort study',*Acta orthopaedica*, 88(1), pp. 2–9.
Gillies, R. J., Didier, N. and Denton, M. (1986) 'Determination of cell number in monolayer cultures', *Analytical Biochemistry*, 159(1). pp.109-113
Glyn-Jones, S. *et al.* (2009) 'Risk factors for inflammatory pseudotumour formation following hip resurfacing', *Journal of Bone and Joint Surgery - British Volume*, 91–B(12), pp. 1566–1574.
Goh, C. L., Kwok, S. F., and Gan, S. L. (1986) 'Cobalt and nickel content of Asian cements', *Contact dermatitis*, 15(3), pp. 169-172.
Gomez, P. F. and Morcuende, J. A. (2005) 'A historical and economic perspective on Sir John Charnley, Chas F. Thackray Limited, and the early arthroplasty industry', *The Iowa orthopaedic journal*, 25, p. 30.
Goode, A. E. *et al.* (2012) 'Chemical speciation of nanoparticles surrounding metal-on-metal hips', *Chemical Communications*, 48(67), pp. 8335.
Gotru, S. K. *et al.* (2017) 'TRPM7 (Transient Receptor Potential Melastatin-Like 7 Channel) Kinase Controls Calcium Responses in Arterial Thrombosis and Stroke in Mice', *Arteriosclerosis, thrombosis, and vascular biology*, p. ATVBAHA. 117.310391.
Greenberg, D. M., Copp, D. H. and Cuthbertson, E. M. (1943) 'Studies in mineral metabolism with the aid of artificial radioactive isotopes. 7. The distribution and execration, particularly by way of the bile, of iron, cobalt, and manganese', *Journal of Biological Chemistry*, 147, pp. 749–756.
Gregus, Z. and Klaassen, C. D. (1986) 'Disposition of metals in rats: A comparative study of fecal, urinary, and biliary excretion and tissue distribution of eighteen metals', *Toxicology and Applied Pharmacology*, 85(1), pp. 15.
Grice, H. C. *et al.* (1969) 'The pathology of experimentally induced cobalt cardiomyopathies. A comparison with beer drinkers' cardiomyopathy', *Clinical toxicology*, 2(3), pp. 273–287.
Grice, H. C. *et al.* (1970) 'Experimental cobalt cardiomyopathy: correlation between electrocardiography and pathology', *Cardiovascular Research*, 4(4), pp. 452–456.
Griffin, K. P. *et al.* (2005) 'Differential expression of divalent metal transporter DMT1 (Slc11a2) in the spermatogenic epithelium of the developing and adult rat testis', *American Journal of Physiology-Cell Physiology*, 288(1), pp. C176–C184.
Gross, R. T., Kriss, J. P., & Spaet, T. H. (1955) 'The hematopoietic and goitrogenic effects of cobaltous chloride in patients with sickle cell anemia', *Pediatrics*, 15(3), pp. 284-371.
Guimaraens, D., Gonzalez, M. A. and Condé - Salazar, L. (1994) 'Systemic contact dermatitis from dental crowns', *Contact Dermatitis*, 30(2), pp. 124–125.
Gunshin, H. *et al.* (1997) 'Cloning and characterization of a mammalian proton-coupled metal-ion transporter', *Nature*, 388(6641), pp. 482–488.

Guskov, A. and Eshaghi, S. (2012) ‘The Mechanisms of Mg 2+ and Co 2+ Transport by the CorA Family of Divalent Cation Transporters’, *Current Topics in Membranes*, 69(February 2015), pp. 393–414.

Gwanyanya, A. *et al.* (2004) ‘Magnesium-inhibited, TRPM6/7-like channel in cardiac myocytes: permeation of divalent cations and pH-mediated regulation’, *The Journal of Physiology*, 559(3), pp. 761–776.

Gwanyanya, A. *et al.* (2006) ‘ATP- and PIP2-dependence of the magnesium-inhibited, TRPM7-like cation channel in cardiac myocytes’, *Am J Physiol Cell Physiol*, pp. 627–635.

Haddad, F. S. *et al.* (2011) ‘Metal-on-metal bearings: THE EVIDENCE SO FAR’, *The Bone & Joint Journal*, 93–B(5), pp. 572–579.

Hallab, N. J. *et al* (2005) 'Lymphocyte responses in patients with total hip arthroplasty', J*ournal of Orthopaedic Research*, 23(2), pp. 384-391.

Hallab, N. J., *et al* (2005) 'Effects of soluble metals on human peri-implant cells', *Journal of biomedical materials research Part A*, 74(1), pp. 124-140.

Hallab, N. J. and Jacobs, J. J. (2009) 'Biologic effects of implant debris', *Bulletin of the NYU hospital for joint diseases*, 67(2), p. 182.

Hallab, N. J., Merritt, K. and Jacobs, J. J. (2001) ‘Metal sensitivity in patients with orthopaedic implants.’, *The Journal of bone and joint surgery. American volume*, 83–A(3), pp. 428–36.

Hart, A. J. *et al.* (2009) ‘The painful metal-on-metal hip resurfacing’, *The Journal of bone and joint surgery*, 91(6), p. 7.

Hart, A. J. *et al.* (2011) ‘Sensitivity and specificity of blood cobalt and chromium metal ions for predicting failure of metal-on-metal hip replacement’, *The Journal of bone and joint surgery*, 93(10), p. 6.

Harteneck, C. (2005) ‘Function and pharmacology of TRPM cation channels’, *Naunyn-Schmiedeberg’s Archives of Pharmacology*, 371(4), pp. 307–314.

Hartmann, A. *et al.* (2013) ‘Metal ion concentrations in body fluids after implantation of hip replacements with metal-on-metal bearing–systematic review of clinical and epidemiological studies’, *PLoS One*, 8(8), p. e70359.

Haugland, R. P. (2005) *The handbook: a guide to fluorescent probes and labeling technologies*. Molecular probes.

Hawkins, C., Xu, A. and Narayanan, N. (1994) ‘Sarcoplasmic reticulum calcium pump in cardiac and slow twitch skeletal muscle but not fast twitch skeletal muscle undergoes phosphorylation by endogenous and exogenous Ca2+/calmodulin-dependent protein kinase. Characterization of optimal conditions for calcium pump phosphorylation', *Journal of Biological Chemistry*, 269(49), pp. 31198–31206.

Hegewald, J. *et al.* (2005) ‘A multifactorial analysis of concurrent patch-test reactions to nickel, cobalt, and chromate’, *Allergy: European Journal of Allergy and Clinical Immunology*, 60(3), pp. 372–378.

Hempel, P. *et al.* (2002) ‘Hypertrophic phenotype of cardiac calcium/calmodulin-dependent protein kinase II is reversed by angiotensin converting enzyme inhibition’, *Basic research in cardiology*, 97(7).

Higuchi, H. *et al.* (1996) ‘Ca2+/Calmodulin -Dependent Transcriptional Activation of Neuropeptide Y Gene Induced by Membrane Depolarization: Determination of Ca2+-and Cyclic AMP/Phorbol 12-Myristate 13-Acetate-Responsive Elements’, *Journal of neurochemistry*, 66(5), pp. 1802–1809.

Hoch, B. *et al.* (1999) 'Identification and expression of δ-isoforms of the multifunctional Ca2+/calmodulin -dependent protein kinase in failing and nonfailing human myocardium', *Circulation research*, 84(6), pp. 713–721.
Hoelz, A., Nairn, A. C. and Kuriyan, J. (2003) 'Crystal Structure of a Tetradecameric Assembly of the Association Domain of Ca2+ / Calmodulin-Dependent Kinase II', *Molecular Cell*, 11, pp. 1241–1251.
Hohenegger, M. and Suko, J. (1993) 'Phosphorylation of the purified cardiac ryanodine receptor by exogenous and endogenous protein kinases', *Biochemical Journal*, 296(2), pp. 303–308.
Hokin, B. *et al.* (2004) 'Comparison of the dietary cobalt intake in three different Australian diets', *Asia Pacific Journal of Clinical Nutrition*, 13(3), p. 3.
Hollins, J. G. and McCullough, R. S. (1971) 'Radiation dosimetry of internal contamination by inorganic compounds of cobalt: an analysis of cobalt metabolism in rats', *Health physics*, 21(2), pp. 233–246.
Holly, R. G. (1955) 'Studies on iron and cobalt metabolism', *Journal of the American Medical Association*, 158(15), pp. 1349–1352.
Ho-Pun-Cheung, A. *et al.* (2009) 'Reverse transcription-quantitative polymerase chain reaction: Description of a RIN-based algorithm for accurate data normalization', *BMC Molecular Biology*, 10, pp. 1–10.
Horowitz, S. F. *et al.* (1988) 'Evaluation of right and left ventricular function in hard metal workers', *British Journal of Industrial Medicine*, 45(11), pp. 742–746.
Horton, J. S., Buckley, C. L. and Stokes, A. J. (2013) 'Successful TRPV1 antagonist treatment for cardiac hypertrophy and heart failure in mice.', *Channels (Austin, Tex.)*, 7(1), pp. 17–22.
Howitt, J. *et al.* (2009) 'Divalent metal transporter 1 (DMT1) regulation by Ndfip1 prevents metal toxicity in human neurons', *PNAS*, 106(36), pp. 15489–15494.
Huang, D. W., Sherman, B. T. and Lempicki, R. A. (2008) 'Systematic and integrative analysis of large gene lists using DAVID bioinformatics resources', *Nature protocols*, 4(1), p. 44.
Hudmon, A. and Schulman, H. (2002) 'Neuronal Ca2+/calmodulin-dependent protein kinase II: the role of structure and autoregulation in cellular function', *Annual review of biochemistry*, 71(1), pp. 473–510.
Huggett, J. *et al.* (2005) 'Real-time RT-PCR normalisation; strategies and considerations', *Genes and Immunity*, 6(4), pp. 279–284.
Hughes, M. N. (1981) *The inorganic chemistry of biological processes / [by] M. N. Hughes*.
Huk, O. L. *et al* (2004) 'Induction of apoptosis and necrosis by metal ions in vitro', The *Journal of arthroplasty*, 19(8), pp. 84-87.
Hyslop, D. J. S., *et al*. (2010) 'Electrochemical synthesis of a biomedically important Co–Cr alloy', *Acta Materialia*, 58(8), pp. 3124-3130.
Ikarashi, Y. *et al*. (1992) 'Differences of draining lymph node cell proliferation among mice, rats and guinea pigs following exposure to metal allergens', *Toxicology*, 76(3), pp. 283-292.
Ikeda, T. *et al.* (2010) 'Polyneuropathy caused by cobalt-chromium metallosis after total hip replacement', *Muscle & nerve*, 42(1), pp. 140–143.
Illing, A. C. *et al.* (2012) 'Substrate profile and metal-ion selectivity of human divalent metal-ion transporter-1', *Journal of Biological Chemistry*, 287(36), pp. 30485–30496.

Inoue, R. *et al.* (2006) ‘Transient receptor potential channels in cardiovascular function and disease’, *Circulation Research*, 99(2), pp. 119–131.
Inoue, R., Jian, Z. and Kawarabayashi, Y. (2009a) ‘Mechanosensitive TRP channels in cardiovascular pathophysiology’, *Pharmacology & therapeutics*, 123(3), pp. 371–385.
Inoue, R., Jian, Z. and Kawarabayashi, Y. (2009b) ‘Mechanosensitive TRP channels in cardiovascular pathophysiology’, *Pharmacology and Therapeutics*. Elsevier Inc., 123(3), pp. 371–385.
IOM, (Institute of Medicine) (1998) 'Dietary Reference Intakes for Thiamin, Riboflavin, Niacin, Vitamin B6, Folate, Vitamin B12, Pantothenic Acid, Biotin, and Choline' *National Academy Press*, Washington, DC.
Jacob, F. *et al.* (2013) ‘Careful Selection of Reference Genes Is Required for Reliable Performance of RT-qPCR in Human Normal and Cancer Cell Lines’, *PLoS ONE*, 8(3).
Jacobs, J. J. *et al.* (2001) ‘Metal sensitivity in patients with orthopaedic implants’, *Journal of Bone and Joint Surgery*, 83(3), pp. 428–436.
Jacobziner, H., & Raybin, H. W. (1961) 'Accidental cobalt poisoning', *Archives of pediatrics*, 78(5), pp. 200-200.
Jansen, C. *et al.* (2016) ‘The coiled-coil domain of zebrafish TRPM7 regulates Mg·nucleotide sensitivity’, *Scientific Reports*. Nature Publishing Group, 6(August), pp. 1–13.
Jantzen, C. *et al.* (2013) ‘Chromium and cobalt ion concentrations in blood and serum following various types of metal-on-metal hip arthroplasties: A literature overview’, *Acta orthopaedica*, 84(3), p. 8.
Jarvis, J. Q. *et al*. (1992) 'Cobalt cardiomyopathy. A report of two cases from mineral assay laboratories and a review of the literature', *Journal of occupational medicine.: official publication of the Industrial Medical Associatio*n, 34(6), pp. 620-626.
Jelkmann, W. (2012). The disparate roles of cobalt in erythropoiesis, and doping relevance. *Open Journal of Hematology*, 3(1).
Jiang, N., Zhou, L. Q. and Zhang, X. Y. (2010) ‘Downregulation of the nucleosome-binding protein 1 (NSBP1) gene can inhibit the in vitro and in vivo proliferation of prostate cancer cells’, *Asian Journal of Andrology*. Nature Publishing Group, 12(5), pp. 709–717.
Jiang, Y. *et al.* (2011) ‘A systematic review of modern metal-on-metal total hip resurfacing vs standard total hip arthroplasty in active young patients’, *The Journal of arthroplasty*, 26(3), pp. 419–426.
Jin, L. *et al.* (2014) ‘Pathway-based analysis tools for complex diseases: A Review’, *Genomics, Proteomics and Bioinformatics*. Beijing Institute of Genomics, Chinese Academy of Sciences and Genetics Society of China, 12(5), pp. 210–220.
Joehanes, R. *et al.* (2013) ‘Gene expression signatures of coronary heart disease’, *Arteriosclerosis, Thrombosis, and Vascular Biology*, 33(6), pp. 1418–1426.
Jordan, C. *et al*. (1990) 'Memory deficits in workers suffering from hard metal disease', *Toxicology letters*, 54(2-3), pp. 241-243.
Jung, J. *et al.* (2004) ‘Phosphorylation of Vanilloid Receptor 1 by Ca 2+/Calmodulin-dependent Kinase II Regulates Its Vanilloid Binding’, *Journal of Biological Chemistry*, 279(8), pp. 7048–7054.

Jung, J.-Y. and Kim, W.-J. (2004) ‘Involvement of mitochondrial- and Fas-mediated dual mechanism in CoCl 2-induced apoptosis of rat PC12 cells’, *Neuroscience Letter*, 371(2), p. 6.

Kanehisa, M. and Goto, S. (2000) ‘KEGG: kyoto encyclopedia of genes and genomes’, *Nucleic acids research*, 28(1), pp. 27–30.

Karovic, O. *et al.* (2007) ‘Toxic effects of cobalt in primary cultures of mouse astrocytes: similarities with hypoxia and role of HIF-1α’, *Biochemical pharmacology*, 73(5), pp. 694–708.

Karuppagounder, S. S. and Ratan, R. R. (2012) ‘Hypoxia-inducible factor prolyl hydroxylase inhibition: Robust new target or another big bust for stroke therapeutics’, *Journal of Cerebral Blood Flow and Metabolism*. Nature Publishing Group, 32(7), pp. 1347–1361.

Kato, H. *et al.* (2001) ‘Heme Oxygenase-1 Overexpression Protects Rat Livers from Ischemia/Reperfusion Injury with Extended Cold Preservation’, *American Journal of Transplantation*, 1(2), pp. 121–128.

Kato, T. *et al.* (2000) ‘Calmodulin Kinases II and IV and Calcineurin Are Involved in Leukemia Inhibitory Factor–Induced Cardiac Hypertrophy in Rats’, *Circulation Research*, 87(10), pp. 937–945.

Katori, M. *et al.* (2002) ‘Heme oxygenase-1 overexpression protects rat hearts from cold ischemia/reperfusion injury via an antiapoptotic pathway1', *Transplantation*, 73(2), pp. 287–292.

Kaufman, A. M. *et al.* (2008) ‘Human macrophage response to UHMWPE, TiAlV, CoCr, and alumina particles: analysis of multiple cytokines using protein arrays’, *Journal of biomedical materials research Part A*, 84(2), pp. 464–474.

Kazmi, N. and Gaunt, T. R. (2016) ‘Diagnosis of coronary heart diseases using gene expression profiling; Stable coronary artery disease, cardiac ischemia with and without myocardial necrosis’, *PLoS ONE*, 11(3), pp. 1–16.

Kedei, N. *et al.* (2001) ‘Analysis of the native quaternary structure of vanilloid receptor 1’, *Journal of Biological Chemistry*, 276(30), pp. 28613–28619.

Kemp, C. D. and Conte, J. V. (2012) ‘The pathophysiology of heart failure’, *Cardiovascular Pathology*. Elsevier Inc., 21(5), pp. 365–371.

Kerfoot, E.J., Fredrick, W.G. and Domier, E. (1975) 'Cobalt metal inhalation studies on miniature swine', *Am. Industrial Hygiene Association* 36, pp. 17-25

Kesteloot, H., *et al.* (1968). An enquiry into the role of cobalt in the heart disease of chronic beer drinkers. Circulation, 37(5), pp. 854-864.

Khan, A. H. *et al.* (2015) ‘Unusual case of congestive heart failure: cardiac magnetic resonance imaging and histopathologic findings in cobalt cardiomyopathy’, *Circulation: Cardiovascular Imaging*, 8(6), p. e003352.

Khoo, M. S. *et al.* (2004) ‘1001-23 Calmodulin kinase inhibition improves survival in calcineurin transgenic mice’, *Journal of the American College of Cardiology*, 43(5, Supplement 1), p. A6.

Khoo, M. S. *et al.* (2004) ‘1041-92 Calmodulin kinase inhibition improves cardiac function after myocardial infarction’, *Journal of the American College of Cardiology*, 43(5, Supplement 1), p. A255.

Kiec-Swierczynska, M. (1990) 'Allergy to chromate, cobalt and nickel in Lódź 1977–1988',*Contact dermatitis*, 22(4), pp. 229-231.

Kim, B. J. *et al.* (2009) ‘Identification of TRPM7 channels in human intestinal interstitial cells of Cajal’, *World Journal of Gastroenterology*, 15(46), pp.

5799–5804.
Kim, H.-J. *et al.* (2003) ‘Cobalt chloride-induced apoptosis and extracellular signal-regulated protein kinase activation in human cervical cancer HeLa cells’, *J Biochem Mol Biol*, 36(5), pp. 468–474.
Kim, J. H., Gibb, H. J., Howe, P. D., and World Health Organization. (2006) 'Cobalt and inorganic cobalt compounds'
Kirchhefer, U. *et al.* (1999) ‘Activity of cAMP-dependent protein kinase and Ca2+/calmodulin-dependent protein kinase in failing and nonfailing human hearts’, *Cardiovascular Research*, 42(1), pp. 254–261.
Korovessis, P. *et al.* (2006) ‘Metallosis After Contemporary Metal-on-Metal Total Hip Arthroplasty’, *The Journal of Bone & Joint Surgery*, 88(6), pp. 1183–1191.
Kostensalo, I. *et al.* (2013) ‘Effect of femoral head size on risk of revision for dislocation after total hip arthroplasty’, *Acta Orthopaedica*, 84(4), pp. 342–347.
Kotsovilis, S., Karoussis, I. K. and Fourmousis, I. (2006) ‘A comprehensive and critical review of dental implant placement in diabetic animals and patients’, *Clinical Oral Implants Research*, 17(5), pp. 587–599.
Kravenskaya, Y. V and Fedirko, N. V (2011) ‘Mechanisms underlying interaction of zinc, lead, and cobalt with nonspecific permeability pores in the mitochondrial membranes’, *Neurophysiology*, 43(3), p. 10..
Kriss, J. P., Carnes, W. H., & Gross, R. T. (1955) 'Cobalt and Thyroid Function', *Journal of the American Medical Association*, 159(7), pp. 708-708.
Kukurba, K. R. and Montgomery, S. B. (2016) ‘RNA Sequencing and Analysis’, *Cold Spring Harbor Protocol*, 2015(11), pp. 951–969.
Kurz, T., Terman, A. and Brunk, U. T. (2007) ‘Autophagy, ageing and apoptosis: The role of oxidative stress and lysosomal iron’, *Archives of Biochemistry and Biophysics*, 462(2), pp. 220–230.
Kuwahara, K. *et al.* (2006) ‘TRPC6 fulfills a calcineurin signalling circuit during pathologic cardiac remodeling’, *Journal of Clinical Investigation*, 116(12), pp. 3114–3126.
Kuzhikandathil, E. V *et al.* (2001) ‘Functional analysis of capsaicin receptor (vanilloid receptor subtype 1) multimerization and agonist responsiveness using a dominant negative mutation’, *Journal of Neuroscience*, 21(22), pp. 8697–8706.
Kwon, Y. M. et al. (2011) '"Asymptomatic" pseudotumors after metal-on-metal hip resurfacing arthroplasty: prevalence and metal ion study', *The Journal of arthroplasty*, 26(4), pp. 511-518.
Langkamer, V. G. *et al.* (1992) ‘Systemic distribution of wear debris after hip replacement. A cause for concern?’, *The Journal of bone and joint surgery*, 74(6), p. 9.
Langton, D. J. *et al.* (2008) ‘The effect of component size and orientation on the concentrations of metal ions after resurfacing arthroplasty of the hip’, *The Journal of bone and joint surgery*, 90(9), p. 9.
Langton, D. J., *et al*. (2012) 'Taper junction failure in large-diameter metal-on-metal bearings.' *Bone and Joint Research* 1.4: pp. 56-63.
Langton, D. J. *et al.* (2013) ‘The clinical implications of elevated blood metal ion concentrations in asymptomatic patients with MoM hip resurfacings: a cohort study’, *BMJ open*, 3(3), p. e001541.

Lavigne, M. *et al*. (2011) 'Comparison of whole-blood metal ion levels in four types of metal-on-metal large-diameter femoral head total hip arthroplasty: the potential influence of the adapter sleeve', *JBJS*, 93(Supplement_2), pp. 128-136.

Lawan, A. *et al.* (2011) 'Deletion of the dual specific phosphatase-4 (DUSP-4) gene reveals an essential non-redundant role for MAP kinase phosphatase-2 (MKP-2) in proliferation and cell survival', *Journal of Biological Chemistry*, 286(15), pp. 12933-12943.

Lazic, S. E. (2015) 'Ranking, selecting, and prioritising genes with desirability functions', *PeerJ*, 3, p. e1444.

Learmonth, I. D., Young, C., and Rorabeck, C. (2007) ' The operation of the century: total hip replacement', *The Lancet*, 370(9597), pp.1508-1519.

Letourneau, E. G. *et al*. (1972)'The metabolism of cobalt by the normal human male: whole body retention and radiation dosimetry',*Health physics*, 22(5), pp. 451-459.

Lee, J. H. *et al.* (2013) 'CoCl2 induces apoptosis through the mitochondria- and death receptor-mediated pathway in the mouse embryonic stem cells', *Molecular and Cellular Biochemistry*, 379(1–2), pp. 133–140.

Lee, J. K. and Choi, S. M. (2003) 'Synthesis and surface derivatization of processible Co nanoparticles', *Bulletin of the Korean Chemical Society*, 24(1), pp. 32–36.

Leonard, S. *et al*. (1998) 'Cobalt-mediated generation of reactive oxygen species and its possible mechanism', *Journal of inorganic biochemistry*, 70(3-4), pp. 239-244.

Letourneau, E. G. *et al.* (1972) 'The metabolism of cobalt by the normal human male: whole body retention and radiation dosimetry', *Health physics*, 22(5), p. 9.

Li, H.-L. *et al.* (2008) 'Curcumin prevents and reverses murine cardiac hypertrophy', *The Journal of clinical investigation 2008*, 118(3), pp. 879–893.

Li, M., Jiang, J. and Yue, L. (2006) 'Functional Characterization of Homo- and Heteromeric Channel Kinases TRPM6 and TRPM7', *J Gen Physiol*, 127(5), pp. 525–537.

Li, S. *et al.* (2015) 'Crucial role of TRPC6 in maintaining the stability of HIF-1 in glioma cells under hypoxia', *Journal of Cell Science*, 128(17), pp. 3317–3329.

Li, W. *et al.* (2011) 'The multifunctional Ca2+/calmodulin-dependent kinase II δ (CaMKIIδ) controls neointima formation after carotid ligation and vascular smooth muscle cell proliferation through cell cycle regulation by p21', *Journal of Biological Chemistry*, 286(10), pp. 7990–7999.

Liao, Y. *et al.* (2013) 'CoCrMo Metal-on-Metal Hip Replacements', *Physical Chemistry Chemical Physics*, 15(3), pp. 1–26.

Van Liew, H. D. and Chen, P. Y. (1972) 'Cardiorespiratory during histotoxic functions hypoxia caused by cobalt', *Journal of applied physiology (Bethesda, Md. : 1985)*, 32(3), pp. 315–319.

Link, G., Pinson, A. and Hershko, C. (1985) 'Heart cells in culture: a model of myocardial iron overload and chelation', *J Lab Clin Med*, 106(2), pp. 147–153.

Licht, A., Oliver, M., & Rachmilewitz, E. A. (1972) 'Optic atrophy following treatment with cobalt chloride in a patient with pancytopenia and hypercellular marrow', *Israel journal of medical sciences*, 8(1), pp. 61-66.

Little, J. A., & Sunico, R. (1958) 'Cobalt-induced goiter with cardiomegaly and congestive failure', *The Journal of pediatrics*, 52(3), pp. 284-288.

Litwin, S. E. *et al.* (1995) 'Serial echocardiographic-Doppler assessment of left ventricular geometry and function in rats with pressure-overload hypertrophy', *Circulation*, 91(10), pp. 2642–2654.
Liu, F. C. *et al* (2011) 'Co and Cr accumulation in hair after metal-on-metal hip resurfacing arthroplasty', *ANZ journal of surgery*, 81(6), pp. 436-439.
Liu, Y., Beyer, A. and Aebersold, R. (2016) 'On the Dependency of Cellular Protein Levels on mRNA Abundance', *Cell*. Elsevier Inc., 165(3), pp. 535–550.
Livak, K. J. and Schmittgen, T. D. (2001) 'Analysis of relative gene expression data using real-time quantitative PCR and the 2-ΔΔCT method', *Methods*, 25(4), pp. 402–408.
Long, X. *et al.* (1997) 'p53 and the hypoxia-induced apoptosis of cultured neonatal rat cardiac myocytes', *Journal of Clinical Investigation*, 99(11), pp. 2635–2643.
Lohmann, C. H. et al. (2000) 'Pulsed electromagnetic field stimulation of MG63 osteoblast-like cells affects differentiation and local factor production', *Journal of Orthopaedic Research*, 18(4), pp. 637-646.
Lucarelli, M. *et al*. (2004). Modulation of Defense Cell Functions by Nano-particles in vivo. K.E.M. 254–256, pp. 907–910.
Luo, L. *et al.* (2005) 'Effect of cobalt and chromium ions on MMP-1, TIMP-1, and TNF- α gene expression in human U937 macrophages: A role for tyrosine kinases', *Biomaterials*, 26(28), p. 7.
Luo, M., & Anderson, M. E. (2013) 'Mechanisms of altered Ca2+ handling in heart failure', *Circulation research*, 113(6), pp 690-708.
Mabilleau, G. *et al.* (2008) 'Metal-on-metal hip resurfacing arthroplasty: A review of periprosthetic biological reactions', *Acta Orthopaedica*, 79(6), pp. 734–747.
MacGurn, J. A., Hsu, P.C. and Emr, S. D. (2012) 'Ubiquitin and membrane protein turnover: from cradle to grave', *Annual review of biochemistry*, 81, pp.231–259.
Machado, C., Appelbe, A. and Wood, R. (2012) 'Arthroprosthetic Cobaltism and Cardiomyopathy', *Heart, Lung and Circulation*, 21(11), pp. 759–760.
Mačianskiene, R. *et al.* (2012) 'Characterization of Mg2+-regulated TRPM7-like current in human atrial myocytes', *Journal of Biomedical Science*. Journal of Biomedical Science, 19(1), p. 75.
Mačianskiene, R. *et al.* (2017) 'Modulation of human cardiac trpm7 current by extracellular acidic ph depends upon extracellular concentrations of divalent cations', *PLoS ONE*, 12(1), pp. 1–19.
Mackenzie, B. *et al.* (2006) 'Divalent metal-ion transporter DMT1 mediates both H+-coupled Fe2+ transport and uncoupled fluxes', *Pflügers Archiv*, 451(4), pp. 544–558.
Mackenzie, B. *et al.* (2007) 'Functional properties of multiple isoforms of human divalent metal-ion transporter 1 (DMT1)', *Biochemical journal*, 403(1), pp. 59–69.
MacPherson, G. J. and Breusch, S. J. (2011) 'Metal-on-metal hip resurfacing: A critical review', *Archives of Orthopaedic and Trauma Surgery*, 131(1), pp. 101–110.
Mahey, S. *et al.* (2016) 'Effect of cobalt (II) chloride hexahydrate on some human cancer cell lines', *SpringerPlus*, 5(1), p. 930.
Mahomed, N. N. *et al.* (2003) 'Rates and outcomes of primary and revision total hip replacement in the United States Medicare population', *J Bone Joint Surg Am*,

85–A(1), pp. 27–32.
Maier, L. S. *et al.* (2003) 'Transgenic CaMKIIδC overexpression uniquely alters cardiac myocyte Ca2+ handling', *Circulation research*, 92(8), pp. 904–911.
Maier, L. S. (2012) 'Ca2+/calmodulin-dependent protein kinase II (CaMKII) in the heart', in *Calcium Signalling*. Springer, pp. 685–702.
Maier, L. S. and Bers, D. M. (2002) 'Calcium, Calmodulin, and Calcium-Calmodulin Kinase II: Heartbeat to Heartbeat and Beyond', *Journal of Molecular and Cellular Cardiology*, 34(8), pp. 919–939.
Malchau, H. *et al.* (2002) 'The Swedish total hip replacement register', *JBJS*, 84(suppl_2), S2-S20.
Malczyk, M. *et al.* (2017) 'The role of transient receptor potential channel 6 channels in the pulmonary vasculature', *Frontiers in Immunology*, 8(JUN), pp. 1–11.
Manifold, I. H., Platts, M. M., & Kennedy, A. (1978) 'Cobalt cardiomyopathy in a patient on maintenance haemodialysis' *British Medical Journal*, 2(6152), p. 1609.
Mao, X., Wong, A. A. and Crawford, R. W. (2011) 'Cobalt toxicity--an emerging clinical problem in patients with metal-on-metal hip prostheses?', *Medical journal of Australia Mao*, 194(12), pp. 649–651.
Martin, J. R. *et al.* (2015) 'Cardiac cobaltism: A rare complication after bilateral metal-on-metal total hip arthroplasty', *Arthroplasty Today*. Elsevier Inc, 1(4), pp. 99–102.
Martin, T. P. *et al.* (2014) 'Adult cardiac fibroblast proliferation is modulated by calcium/calmodulin-dependent protein kinase II in normal and hypertrophied hearts', *Pflügers Archiv - European Journal of Physiology*, 466(2), pp. 319–330.
Martinez, M. M., Reif, R. D. and Pappas, D. (2010) 'Detection of apoptosis: A review of conventional and novel techniques', *Analytical Methods*, 2(8), p. 996.
Martinez, P. F. *et al.* (2011) 'Echocardiographic detection of congestive heart failure in postinfarction rats', *Journal of applied physiology (Bethesda, Md. : 1985)*, 111(2), pp. 543–551.
Martini, F. H., Nath, J. L., & Bartholomew, E. F. (2015). Fundamentals of Anatomy and Physiology. 2001. *Pentice Hall: New Jersey*, 538-557.
Mastrogiannaki, M. *et al.* (2009) 'HIF-2α, but not HIF-1α, promotes iron absorption in mice', *The Journal of Clinical Investigation*. American Society for Clinical Investigation, 119(5), pp. 1159–1166.
Matsumoto, M. *et al.* (2003) 'Induction of renoprotective gene expression by cobalt ameliorates ischemic injury of the kidney in rats', *Journal of the American Society of Nephrology*, 14(7), pp. 1825–1832.
Mayo Clinic. (2018). Hip resurfacing. [online] Available at: https://www.mayoclinic.org/hip-resurfacing/img-20008999 [Accessed 3 Apr. 2018].
McKinsey, T. A. (2007) 'Derepression of pathological cardiac genes by members of the CaM kinase superfamily', *Cardiovascular Research*, 73(4), pp. 667–677.
McLaughlin L., J. and C. (2010) 'Cobalt Toxicity in Two Hip Replacement Patients ', *State of Alaska Epidemiology Bulletin*, 14.
McMinn, D. J. W. *et al.* (2011) 'Indications and results of hip resurfacing', *International Orthopaedics*, 35(2), pp. 231–237.
Mcminncentre.co.uk. (2018). Metal Ions Questions and Answers – Hip Resurfacing

Derek McMinn, Birmingham. [online] Available at: http://www.mcminncentre.co.uk/metal-ions-questions-answers.html [Accessed 3 Apr. 2018].
Meecham, H. M. and Humphrey, P. (1991) 'Industrial exposure to cobalt causing optic atrophy and nerve deafness: a case report', *Journal of neurology, neurosurgery, and psychiatry*, 54(4), p. 374.
Merritt, K. and Brown, S. A. (1996) 'Distribution of cobalt chromium wear and corrosion products and biologic reactions', *Clinical Orthopaedics and Related Research®*, 329, pp. S233–S243.
Metikoš-Huković, M. and Babić, R. (2007) 'Passivation and corrosion behaviours of cobalt and cobalt-chromium-molybdenum alloy', *Corrosion Science*, 49(9), pp. 3570–3579.
MHRA, (Medicines & Healthcare products Regulatory Agency) (2010) 'Medical Device Alert MDA/2010/001', MDA/20/201(January), pp. 1–7.
MHRA, (Medicines & Healthcare products Regulatory Agency) (2012) 'Medical Device Alert Ref. MDA/2012/036 Issued: 25 June 2012'. Available at: https://assets.publishing.service.gov.uk/media/5485abf6ed915d4c10000273/con155767.pdf.
Michelangeli, F., Ogunbayo, O. A. and Wootton, L. L. (2005) 'A plethora of interacting organellar Ca2+ stores', *Current opinion in cell biology*, 17(2), pp. 135–140.
Mills, J. C., Stone, N. L. and Pittman, R. N. (1999) 'Extranuclear Apoptosis', *The Journal of Cell Biology*, 146(4), pp. 703–708.
Minang, J. T. *et al.* (2006) 'Nickel, cobalt, chromium, palladium and gold induce a mixed Th1- and Th2-type cytokine response in vitro in subjects with contact allergy to the respective metals', *Clinical and Experimental Immunology*, 146(3), pp. 417–426.
Mohiuddin, S. M. *et al.* (1970) 'Experimental cobalt cardiomyopathy', *The American heart journal Mohiuddin*, 80(4).
Molkentin, J. D. *et al.* (1998) 'A Calcineurin-Dependent Transcriptional Pathway for Cardiac Hypertrophy', *Cell*, 93(2), pp. 215–228.
Mollova, M. Y., Katus, H. A. and Backs, J. (2015) 'Regulation of CaMKII signalling in cardiovascular disease', *Frontiers in Pharmacology*, 6(Aug), pp. 1–8.
Moniz, S., Hodgkinson, S. and Yates, P. (2017) 'Cardiac transplant due to metal toxicity associated with hip arthroplasty', *Arthroplasty Today*. Elsevier Inc, 3(3), pp. 151–153.
Monteilh-Zoller, M. K. *et al.* (2003) 'TRPM7 Provides an Ion Channel Mechanism for Cellular Entry of Trace Metal Ions', *The Journal of General Physiology*, 121(1), pp. 49–60.
Morgan, A. J. *et al.* (2011) 'Molecular mechanisms of endolysosomal Ca2+ signalling in health and disease', *Biochemical Journal*, 439(3), pp. 349–378.
Morgan, C. D. *et al.* (1991) ' An improved colorimetric assay for tumor-necrosis-factor using WEHI 164 cells cultured on novel microtiter plates', *J. Immunol. Methods*, 145(1–2).
Morgan, E. E. *et al.* (2004) 'Validation of echocardiographic methods for assessing left ventricular dysfunction in rats with myocardial infarction', *Am J Physiol Heart Circ Physiol*, 287(5), pp. H2049-53..
Morin, Y. and Daniel, P. (1967) 'Quebec beer-drinkers' cardiomyopathy: etiological

considerations', *Canadian Medical Association journal*, 97(15), pp. 926–928.
Morin, Y., Têtu, A. and Mercier, G. (1971) 'Cobalt cardiomyopathy: Clinical aspects', *British heart journal*, 33, pp. 175–178.
Morvai, V. *et al.* (1993) 'The effects of simultaneous alcohol and cobalt chloride administration on the cardiovascular system of rats', *Acta Physiologica Hungarica*, 81(3), pp. 253-261.
Mosier, B. A. *et al.* (2016) 'Progressive cardiomyopathy in a patient with elevated cobalt ion levels and bilateral metal-on-metal hip arthroplasties', *American journal of orthopedics (Belle Mead, NJ)*, 45(3), pp. E132-5.
Mosmann, T. (1983) 'Rapid colorimetric assay for cellular growth and survival: Application to proliferation and cytotoxicity assays', *Journal of Immunological Methods*, 65(1–2).
Mucklow, E.S. *et al*. (1990) 'Cobalt poisoning in a 6-year old', *Lancet*, 335, p. 981
Munro, J. T. *et al.* (2014) 'High complication rate after revision of large-head metal-on-metal total hip arthroplasty', *Clinical Orthopaedics and Related Research*, 472(2), pp. 523–528.
Murakoshi, N. *et al.* (2000) 'Impairment of cardiac energy metabolism in vivo causes hemodynamic abnormality and increases cardiac expression of preproendothelin-1 mRNA', *J Cardiovasc Pharmacol*, pp. S128-31.
Murdock, H. R. (1959) 'Studies on the pharmacology of cobalt chloride', *Journal of Pharmaceutical Sciences*, 48(3), pp. 140-142.
Mwanjewe, J. and Grover, A. K. (2004) 'Role of transient receptor potential canonical 6 (TRPC6) in non-transferrin-bound iron uptake in neuronal phenotype PC12 cells.', *The Biochemical journal*, 378(Pt 3), pp. 975–82.
Nadler, M. J. S. *et al.* (2001) 'LTRPC7 is a Mg-ATP-regulated divalent cation channel required for cell viability', *Nature*, 411(6837), p. 590.
Nag, A. C. (1980) 'Study of non-muscle cells of the adult mammalian heart: a fine structural analysis and distribution', *Cytobios*, 28(109), pp. 41–61.
Naito, A. T. *et al.* (2010) 'Promotion of CHIP-mediated p53 degradation protects the heart from ischemic injury', *Circulation research*, 106(11), pp. 1692–1702.
Nandedkar, A. K., Basu, P. K., & Friedberg, F. (1973). Co++ binding by plasma proteins. *Bioinorganic Chemistry*, 2(2), pp. 149-157.
Navarro-Zarza, J. E. et al. (2012) 'Clinical anatomy of the pelvis and hip' *Reumatologia clinica*, 8, pp. 33-38.
Nemery, B et al. (1992) ' Survey of cobalt exposure ans respiratory health in diamond polishers", *American Review of Respiratory Diease*, 145, pp. 610-616.
Nghiem, P. *et al.* (1994) 'Interleukin-2 transcriptional block by multifunctional Ca2+/calmodulin kinase', *Nature*, 371(6495), p. 347.
NHS Choices (2012) *Metal hip patients 'need annual checks', February 29 2012*. Available at: https://www.nhs.uk/news/medical-practice/metal-hip-patients-need-annual-checks/ (Accessed: 14 November 2017).
Nielsen, N. H. *et al.* (2000) 'Repeated exposures to cobalt or chromate on the hands of patients with hand eczema and contact allergy to that metal', C*ontact Dermatitis*, 43(4), pp. 212-215.
Nikolova-Krstevski, V. *et al.* (2013) 'Transient Receptor Potential Channel 6 (TRPC6) Is An Important Mediator Of Mechanical Stretch Responses In The Atrial Endocardial Endothelium'. *Am Heart Assoc*.
Nilius, B. and Owsianik, G. (2011) 'The transient receptor potential family of ion

channels', *Genome Biology*, 12(218).
NIOSH (2001) 'Metal Working Fluids Recommendation for Chronic Inhalation Studies' *Cincinnati OH USA* 45226
Nishida, M. *et al.* (2007a) 'Gα12/13-mediated up-regulation of TRPC6 negatively regulates endothelin-1-induced cardiac myofibroblast formation and collagen synthesis through nuclear factor of activated T cells activation', *Journal of Biological Chemistry*, 282(32), pp. 23117–23128.
Nishida, M. and Kurose, H. (2008a) 'Roles of TRP channels in the development of cardiac hypertrophy', *Naunyn-Schmiedeberg's Archives of Pharmacology*, 378(4), pp. 395–406.
NJR, N. J. R. (2017) 'NJR 14th Annual Report', *National Joint Registry 14th Annual Report*, 1821(December 2016).
Numata, T., Shimizu, T. and Okada, Y. (2007) 'TRPM7 is a stretch- and swelling-activated cation channel involved in volume regulation in human epithelial cells', *American Journal of Physiology - Cell Physiology*, 292(1), pp. C460–C467.
Oancea, E., Wolfe, J. T. and Clapham, D. E. (2006) 'Functional TRPM7 channels accumulate at the plasma membrane in response to fluid flow', *Circulation research*, 98(2), pp. 245–253.
Oh, J. K., Seward, J. B. and Tajik, A. J. (2006) *The echo manual*. Lippincott Williams & Wilkins.
Okazaki, Y. *et al.* (2004) 'Comparison of metal concentrations in rat tibia tissues with various metallic implants', *Biomaterials*, 25(28), pp. 5913–5920.
Oldenburg, M., Wegner, R. and Baur, X. (2009) 'Severe cobalt intoxication due to prosthesis wear in repeated total hip arthroplasty', *J Arthroplasty*, 24(5), p. 825 e15-20.
Oliveira, A. L. *et al*. (2015) 'Assessment of total hip arthroplasty as a predisposing factor for ischiofemoral impingement', *Skeletal radiology*, 44(12), pp. 1755-1760.
Ortega, A. *et al.* (2016) '*TRPM7* is down-regulated in both left atria and left ventricle of ischaemic cardiomyopathy patients and highly related to changes in ventricular function', *ESC Heart Failure*, 3(3), pp. 220–224.
Ortega, R. *et al.* (2014) 'Low-solubility particles and a Trojan-horse type mechanism of toxicity: the case of cobalt oxide on human lung cells', *Particle and Fibre Toxicology*, 11(1), p. 14.
Pandit, H. *et al.* (2008) 'Pseudotumours associated with metal-on-metal hip resurfacings', *Bone & Joint Journal*, 90(7), pp. 847–851.
Park, J. D., Cherrington, N. J. and Klaassen, C. D. (2002) 'Intestinal absorption of cadmium is associated with divalent metal transporter 1 in rats', *Toxicological Sciences*, 68(2), pp. 288–294.
De Pasquale, D. *et al.* (2014) 'Metal-on-metal hip prostheses: Correlation between debris in the synovial fluid and levels of cobalt and chromium ions in the bloodstream', *International Orthopaedics*, 38(3), pp. 469–475.
Patel, A. *et al.* (2010) 'Canonical TRP channels and mechanotransduction: From physiology to disease states', *Pflugers Archiv European Journal of Physiology*, 460(3), pp. 571–581.
Patrick, G., Batchelor, A. L. and Stirling, C. (1989) 'An interspecies comparison of the lung clearance of inhaled monodisperse cobalt oxide particles—Part VI:

Lung clearance of inhaled cobalt oxide particles in SPF fischer rats', *Journal of Aerosol Science*, 20(2).

Pearson, K. (1895) 'Note on regression and inheritance in the case of two parents', *Proceedings of the Royal Society of London*, 58, pp. 240–242.

Pecze, L. *et al.* (2013) 'Divalent heavy metal cations block the TRPV1 Ca2+channel', *Biological Trace Element Research*, 151(3), pp. 451–461.

Pedersen, a B. *et al.* (2010) 'Risk of revision of a total hip replacement in patients with diabetes mellitus: a population-based follow up study.', *The Journal of bone and joint surgery. British volume*, 92(7), pp. 929–34.

Pelclova, D. *et al.* (2012) 'Severe cobalt intoxication following hip replacement revision: Clinical features and outcome', *Clinical toxicology*, 50(4), pp. 262–265.

Penny, J. Ø. *et al.* (2013) 'Metal ion levels and lymphocyte counts: ASR hip resurfacing prosthesis vs. standard THA: 2–year results from a randomized stud', *Acta orthopaedica*, 84(2), pp. 130-137.

Pennstatehershey.adam.com. (2018) 'Hip joint replacement - series - Penn State Hershey Medical Center. [online] Available at: http://pennstatehershey.adam.com/content.aspx?productId=113&pid=3&gid=100006 [Accessed 3 Apr. 2018].

Perconti, S. *et al.* (2012) 'Distinctive gene expression profiles in Balb/3T3 cells exposed to low dose cobalt nanoparticles, microparticles and ions: potential nanotoxicological relevance', *Journal of biological regulators and homeostatic agents*, 27(2), pp. 443–454.

Peters, K. *et al.* (2001) 'Induction of apoptosis in human microvascular endothelial cells by divalent cobalt ions. Evidence for integrin-mediated signalling via the cytoskeleton', *Journal of Materials Science: Materials in Medicine*, 12(10–12), pp. 955–958.

Pfaffl, M. W. (2001) 'A new mathematical model for relative quantification in real-time RT-PCR', *Nucleic Acids Research*, 29(9), p. 45e–45.

Picard, V. *et al.* (2000) 'Nramp 2 (DCT1/DMT1) expressed at the plasma membrane transports iron and other divalent cations into a calcein-accessible cytoplasmic pool', *Journal of Biological Chemistry*, 275(46), pp. 35738–35745.

Pigatto, P. D., Zerboni, R. and Guzzi, G. (2008) 'Local and systemic allergic contact dermatitis due to dental alloys', *Journal of the European Academy of Dermatology and Venereology*, 22(1), pp. 124–126.

Piret, J. *et al.* (2002) 'CoCl2, a Chemical Inducer of Hypoxia - Inducible Factor - 1, and Hypoxia Reduce Apoptotic Cell Death in Hepatoma Cell Line HepG2', *Annals of the New York Academy of Sciences*, 973(1), pp. 443–447.

Pollock, C., *et al.* (2008). Pure red cell aplasia induced by erythropoiesis-stimulating agents. *Clinical Journal of the American Society of Nephrology*, 3(1), pp. 193-199.

Posada, O. M. *et al.* (2014) 'CoCr wear particles generated from CoCr alloy metal-on-metal hip replacements, and cobalt ions stimulate apoptosis and expression of general toxicology-related genes in monocyte-like U937 cells', *Toxicology and Applied Pharmacology*, 281(1), pp. 125–135.

Posada, O. M. *et al.* (2015) 'In vitro analyses of the toxicity, immunological, and gene expression effects of cobalt-chromium alloy wear debris and Co ions derived from metal-on-metal hip implants', *Lubricants*, 3(3), pp. 539–568.

Prentice, J. R. *et al.* (2013) ‘Metal-on-Metal Hip Prostheses and Systemic Health: A Cross-Sectional Association Study 8 Years after Implantation’, *PLoS ONE*, 8(6), pp. 1–9.

Prescott, E. *et al.* (1992) 'Effect of occupational exposure to cobalt blue dyes on the thyroid volume and function of female plate painters', *Scandinavian journal of work, environment & health*, pp. 01-104.

Pujadas, S. *et al.* (2010) ‘Correlation between myocardial fibrosis and the occurrence of atrial fibrillation in hypertrophic cardiomyopathy: a cardiac magnetic resonance imaging study’, *European journal of radiology*, 75(2), pp. e88–e91.

Raghunathan, V. K. *et al.* (2007) ‘Involvement of reduced glutathione and glutathione reductase in the chronic toxicity of hexavalent chromium to monocytes in vitro’, *Toxicology*, 231(2), pp. 105–106.

Rahtu-Korpela, L. *et al.* (2016) ‘Hypoxia-Inducible Factor Prolyl 4-Hydroxylase-2 Inhibition Protects Against Development of Atherosclerosis’, *Arteriosclerosis, Thrombosis, and Vascular Biology*, 36(4), pp. 608–617.

Raffn, E. *et al.* (1988) 'Health effects due to occupational exposure to cobalt blue dye among plate painters in a porcelain factory in Denmark', *Scandinavian journal of work, environment & health*, pp. 378-384.

Raine, A. E. G. (1988). Hypertension, blood viscosity, and cardiovascular morbidity in renal failure: implications of erythropoietin therapy. *The Lancet*, 331(8577), pp. 97-100.

Rajamäki, K. *et al.* (2013) ‘Extracellular acidosis is a novel danger signal alerting innate immunity via the NLRP3 inflammasome’, *Journal of Biological Chemistry*, 288(19), pp. 13410–13419.

Rakusan, K., Cicutti, N. and Kolar, F. (2001) ‘Cardiac function, microvascular structure, and capillary hematocrit in hearts of polycythemic rats’, *American Journal of Physiology-Heart and Circulatory Physiology*, 281(6), pp. H2425–H2431.

Ramirez, M. T. *et al.* (1997) ‘The nuclear δB isoform of Ca2+/calmodulin-dependent protein kinase II regulates atrial natriuretic factor gene expression in ventricular myocytes’, *Journal of Biological Chemistry*, 272(49), pp. 31203–31208.

Ramsey, I. S., Delling, M. and Clapham, D. E. (2006) ‘An introduction to TRP channels’, *Annu. Rev. Physiol.*, 68, pp. 619–647.

Randelli, F. *et al.* (2013) ‘Radiographically undetectable periprosthetic osteolysis with ASR implants: the implication of blood metal ions’, *The Journal of arthroplasty*, 28(8), pp. 1259–1264.

Randhawa, P. K. and Jaggi, A. S. (2017) ‘TRPV1 channels in cardiovascular system: A double edged sword?’, *International journal of cardiology*, 228, pp. 103–113.

Rao, A.J. *et al.* (2012) 'Revision joint replacement wear particles, and macrophage polarization', *Acta Biomaterialia*, 8, pp. 2815-2823.

Revell, P. A. (2014) ‘10 - Biological causes of prosthetic joint failure*’, in *Joint Replacement Technology (Second Edition)*. Woodhead Publishing, pp. 298–369.

Rizzetti, M. C. *et al.* (2009) ‘Loss of sight and sound. Could it be the hip?’, *Lancet*, 373(9668:1052).

Rodriguez, J. A. and Rathod, P. A. (2012) ‘Large diameter heads’, *The Journal of Bone*

and Joint Surgery. British volume, 94–B(11_Supple_A), pp. 52–54.
Romani, A. M. and Scarpa, A. (2000) 'Regulation of cellular magnesium', *Front Biosci*, 5(720–734), pp. 750–751.
Romano, P. *et al.* (2009) 'Cell Line Data Base: structure and recent improvements towards molecular authentication of human cell lines', *Nucleic Acids Res.*, 37.
Romesburg, J. W., Wasserman, P. L. and Schoppe, C. H. (2010) 'Metallosis and Metal-Induced Synovitis Following Total Knee Arthroplasty: Review of Radiographic and CT Findings', *Journal of Radiology Case Reports*, 4(9), pp. 7–17.
Rona, G. (1971) 'Experimental aspects of cobalt cardiomyopathy', *Heart*, 33, pp. 171–174.
Rothacker, D. L. *et al.* (1988) 'Effects of variation of necropsy time and fasting on liver weights and liver components in rats', *Toxicologic pathology*, 16(1), pp. 22–26.
Rowell, J., Koitabashi, N. and Kass, D. A. (2010) 'TRP-ing up heart and vessels: canonical transient receptor potential channels and cardiovascular disease', *Journal of cardiovascular translational research*, 3(5), pp. 516–524.
Rude, M. K. *et al.* (2005) 'Aldosterone stimulates matrix metalloproteinases and reactive oxygen species in adult rat ventricular cardiomyocytes', *Hypertension*, 46(3), pp. 555–561.
Runnels, L. W., Yue, L. and Clapham, D. E. (2002) 'The TRPM7 channel is inactivated by PIP2 hydrolysis', *Nature cell biology*, 4(5), pp. 329–336.
Sag, C. M. *et al.* (2009) 'CaMKII contributes to cardiac arrhythmogenesis in heart failure', *Circulation: Heart Failure*, p. CIRCHEARTFAILURE. 109.865279.
Sajjad, A. *et al.* (2014) 'Lysine methyltransferase Smyd2 suppresses p53-dependent cardiomyocyte apoptosis', *Biochimica et Biophysica Acta (BBA)-Molecular Cell Research*, 1843(11), pp. 2556–2562.
Samar, H. Y. *et al.* (2015) 'Novel Use of Cardiac Magnetic Resonance Imaging for the Diagnosis of Cobalt Cardiomyopathy', *JACC. Cardiovascular imaging*, 8(10), p. 1231.
Sampson, B. and Hart, A. (2012) 'Clinical usefulness of blood metal measurements to assess the failure of metal-on-metal hip implants', *Annals of clinical biochemistry*, 49(2), pp. 118-131.
Sargeant, A. and Goswami, T. (2007) 'Hip implants–paper VI–ion concentrations', *Materials & Design*, 28(1), pp. 155–171.
Sathianathan, V. *et al.* (2003) 'Insulin induces cobalt uptake in a subpopulation of rat cultured primary sensory neurons', *European Journal of Neuroscience*, 18(9), pp. 2477–2486.
Saucerman, J. J. and Bers, D. M. (2008) 'Calmodulin mediates differential sensitivity of CaMKII and calcineurin to local Ca2+ in cardiac myocytes.', *Biophysical journal*. Elsevier, 95(10), pp. 4597–612.
Schade, S. G. *et al.* (1970) 'Interrelationship of cobalt and iron absorption', *The Journal of laboratory and clinical medicine*, 75(3), pp. 435–441.
Schulman, H. (2004) 'Activity-Dependent Regulation of Calcium/Calmodulin-Dependent Protein Kinase II Localization', *Journal of Neuroscience*, 24(39), pp. 8399–8403.
Scott, J. A. *et al.* (2013) 'The multifunctional Ca2+/calmodulin-dependent kinase IIδ (CaMKIIδ) regulates arteriogenesis in a mouse model of flow-mediated

remodeling', *PloS one*, 8(8), p. e71550.
Scott, K. G. and Reilly, W. A. (1955) 'Cobaltous chloride and iodine metabolism of normal and tumor-bearing rats', *Journal of the American Medical Association*, 158(15), pp. 1355–1357.
Sedrakyan, A. *et al.* (2014) 'Survivorship of hip and knee implants in pediatric and young adult populations: Analysis of registry and published data', *Journal of Bone and Joint Surgery - American Volume*, 96, pp. 73–78.
Seo, K. *et al.* (2014) 'Combined TRPC3 and TRPC6 blockade by selective small-molecule or genetic deletion inhibits pathological cardiac hypertrophy', *Proceedings of the National Academy of Sciences*, 111(4), pp. 1551–1556.
Sethi, R. K. *et al.* (2003) 'Macrophage response to cross-linked and conventional UHMWPE', *Biomaterials*, 24(15), pp. 2561–2573.
Shah, Y. M. *et al.* (2009) 'Intestinal Hypoxia Inducible Transcription Factors are Essential for Iron Absorption Following Iron Deficiency', *Cell metabolism*, 9(2), pp. 152–164.
Shawki, A. *et al.* (2015) 'Intestinal DMT1 is critical for iron absorption in the mouse but is not required for the absorption of copper or manganese', *American Journal of Physiology-Gastrointestinal and Liver Physiology*, 309(8), pp. G635–G647.
Shi, J. *et al.* (2013) 'Molecular determinants for cardiovascular TRPC6 channel regulation by Ca2+/calmodulin-dependent kinase II', *Journal of Physiology*, 591(11), pp. 2851–2866.
Shukla, R. *et al.* (2005) 'Biocompatibility of gold nanoparticles and their endocytotic fate inside the cellular compartment: a microscopic overview', *Langmuir*, 21(23), pp. 10644-10654.
Sidaginamale, R. P. *et al.* (2013) 'Blood metal ion testing is an effectivescreening tool to identify poorly performing metal-on-metal bearingsurfaces.', *Bone & joint research*, 2(5), pp. 84–95.
Sieber, H. P., Rieker, C. B., & Köttig, P. (1999) 'Analysis of 118 second-generation metal-on-metal retrieved hip implants', *J Bone Joint Surg Br*, 81(1), pp. 46-50.
Simesen, M. (1939) 'The fate of cobalt alter oral admmigtration of metalliccobalt and subcutaneous injection of carbonatotetraminecobalt chloride, with remarks on the Quantitative estimation of cobalt in organic materials', *Archives Internationales de Pharmacodynamie et de Thérapie*, 62, pp. 347–356.
Simmerman, H. K. *et al.* (1986) 'Sequence analysis of phospholamban. Identification of phosphorylation sites and two major structural domains', *Journal of Biological Chemistry*, 261(28), pp. 13333–13341.
Simonsen, L. O., Harbak, H. and Bennekou, P. (2012) 'Cobalt metabolism and toxicology--a brief update', *Sci Total Environ*, 432, pp. 210–215.
Singer, H. A. (2012) 'Ca2+/calmodulin-dependent protein kinase II function in vascular remodelling', *The Journal of physiology*, 590(6), pp. 1349–1356.
Siqueira, J. T. *et al.* (2003) 'Bone formation around titanium implants in the rat tibia: role of insulin', *Implant dentistry*, 12(3), pp. 242–251.
Skalli, O. *et al.* (1986) 'A monoclonal antibody against alpha-smooth muscle actin: a new probe for smooth muscle differentiation', *The Journal of Cell Biology*, 103(6), pp. 2787–2796.
De Smet, K. *et al.* (2008) 'Metal Ion Measurement as a Diagnostic Tool to Identify Problems with Metal-on-Metal Hip Resurfacing', *J. Bone Joint Surg.-Am. Vol.*,

90A.
Smith, A. J. *et al.* (2012) 'Failure rates of metal-on-metal hip resurfacings: analysis of data from the National Joint Registry for England and Wales', *The Lancet*, 380(9855), pp. 1759-1766.
Smith, E., Mehta, A. J. and Statham, B. N. (2009) 'Metal sensitivity to Elektra™ prostheses–two cases from a metal on metal implant for hand joint replacement', *Contact Dermatitis*, 60(5), p. 298.
Smith, T., Edmonds, C. J. and Barnaby, C. F. (1972) 'Absorption and retention of cobalt in man by whole-body counting', *Health physics*, 22(4), p. 9.
Snider, P. *et al.* (2009) 'Origin of cardiac fibroblasts and the role of periostin', *Circulation research*, 105(10), pp. 934-947.
Soboloff, J. *et al.* (2005) 'Role of endogenous TRPC6 channels in Ca2+ signal generation in A7r5 smooth muscle cells', *Journal of Biological Chemistry*, 280(48), pp. 39786–39794.
Souders, C. A., Bowers, S. L. K. and Baudino, T. A. (2009) 'Cardiac fibroblast', *Circulation research*, 105(12), pp. 1164–1176.
Speijers, G. J. A. et al. (1982) 'Acute oral toxicity of inorganic cobalt compounds in rats' , *Food and Chemical Toxicology*, 20(3), pp. 311-314.
Steenman, M. *et al.* (2005) 'Distinct molecular portraits of human failing hearts identified by dedicated cDNA microarrays', *European Journal of Heart Failure*, 7(2), pp. 157–165.
Steens, W., Von Foerster, G., and Katzer, A. (2006) 'Severe cobalt poisoning with loss of sight after ceramic-metal pairing in a hip—a case report', *Acta orthopaedic*a, 77(5), pp. 830-832.
Subramanian, A. *et al.* (2005) 'Gene set enrichment analysis: A knowledge-based approach for interpreting genome-wide expression profiles', *Proceedings of the National Academy of Sciences*, 102(43), pp. 15545–15550.
Sun, Y. *et al.* (2015) 'TRPM7 and its role in neurodegenerative diseases', *Channels*, 9(5), pp. 253–261.
Sun, Y. hua *et al.* (2010) 'Calcium-sensing receptor activation contributed to apoptosis stimulates TRPC6 channel in rat neonatal ventricular myocytes', *Biochemical and Biophysical Research Communications*. Elsevier Inc., 394(4), pp. 955–961.
Swennen, B. *et al.* (1993) 'Epidemiological survey of workers exposed to cobalt oxides, cobalt salts, and cobalt metal', O*ccupational and Environmental Medicine*, 50(9), pp. 835-842.
Swiontkowski, M. F. *et al.* (2001) 'Cutaneous metal sensitivity in patients with orthopaedic injuries', *Journal of orthopaedic trauma*, 15(2), pp. 86-89.
Swynghedauw, B. (1999) 'Molecular Mechanisms of Myocardial Remodeling', *Physiol Rev*, 79(1), pp. 215–262.
Tait, S. W. G., Ichim, G. and Green, D. R. (2014) 'Die another way – non-apoptotic mechanisms of cell death', *Journal of Cell Science*, 127(10), pp. 2135–2144.
Takahashi, T. *et al.* (1992) 'Expression of dihydropyridine receptor (Ca2+ channel) and calsequestrin genes in the myocardium of patients with end-stage heart failure', *Journal of Clinical Investigation*, 90(3), p. 927.
Tarzia, V. et al (2007) 'Extended (31 years) durability of a Starr-Edwards Prothesis in Mitral Positioin', *Interactive CardioVasc Thorac Surg*, 6, pp. 570-571.
Tasdemir, E. *et al.* (2008) 'Methods for assessing autophagy and autophagic cell

death', *Autophagosome and Phagosome*, pp. 29–76.
Taylor, A., & Marks, V. (1978) 'Cobalt: a review' *Journal of human nutrition*, 32(3), pp. 165-177.
Tewari, R. K. *et al*, (2002) 'Modulation of oxidative stress responsive enzymes by excess cobalt', *Plant Science*, 162(3), pp. 381-388.
Thomas, R. G. *et al.* (1976) 'Comparative Metabolism of Radionuclides in Mammals-X. Retention of Tracer-level Cobalt in the Mouse, Rat, Monkey and Dog', *Health physics*, 31(4), pp. 323-333.
Thomson, A. B. R., Valberg, L. S. and Sinclair, D. G. (1971) 'Competitive nature of the intestinal transport mechanism for cobalt and iron in the rat', *Journal of Clinical Investigation*, 50(11), p. 2384.
Tkaczyk, C. *et al.* (2010) 'Effect of chromium and cobalt ions on the expression of antioxidant enzymes in human U937 macrophage - like cells', *Journal of Biomedical Materials Research Part A*, 94(2), pp. 419-425.
De Tombe, P. P. (1998) 'Altered contractile function in heart failure', *Cardiovascular Research*, 37(2), pp. 367–380.
Topala, C. N. *et al.* (2007) 'Molecular determinants of permeation through the cation channel TRPM6', *Cell Calcium*, 41(6), pp. 513–523.
Tower, S. S. (2010) 'Arthroprosthetic cobaltism: Neurological and cardiac manifestations in two patients with metal-on-metal arthroplasty: A case report', *JBJS The Journal of Bone & Joint Surgery*, 92(17), pp. 2847–2851.
Tower, S. S. (2012) 'Arthroprosthetic cobaltism associated with metal on metal hip implants', *Bmj*, 344, p. e430.
Trindade, T., O'Brien, P. and Pickett, N. L. (2001) 'Nanocrystalline semiconductors: synthesis, properties, and perspectives', *Chemistry of Material*s, 13(11), pp. 3843-3858.
Trinkle-Mulcahy, L. *et al.* (2006) 'Repo-Man recruits PP1Ɣ to chromatin and is essential for cell viability', *Journal of Cell Biology*, 172(5), pp. 679–692.
Tsujimoto, Y. (1998) 'Role of Bcl-2 family proteins in apoptosis: apoptosomes or mitochondria?', *Genes Cells*, pp. 697–707.
Tsushima, R. G. *et al.* (1999) 'Modulation of Iron Uptake in Heart by L-Type Ca2+ Channel Modifiers Possible Implications in Iron Overload', *Circulation research*, 84(11), pp. 1302–1309.
Tvermoes, B. E., *et al.* (2015). Review of cobalt toxicokinetics following oral dosing: Implications for health risk assessments and metal-on-metal hip implant patients. *Critical reviews in toxicology*, 45(5), pp. 367-387.
Underwood, E. (2012) *Trace elements in human and animal nutrition*. Elsevier.
Unverferth, D. V *et al.* (1984) 'The evolution of β-adrenergic dysfunction during the induction of canine cobalt cardiomyopathy', *Cardiovascular Research*, 18(1), pp. 44–50.
Urban, R. M. *et al.* (2000) 'Dissemination of wear particles to the liver, spleen, and abdominal lymph nodes of patients with hip or knee replacement', *JBJS*, 82(4), p. 457.
Valko, M. *et al*. (2006) 'Free radicals, metals and antioxidants in oxidative stress-induced cancer', *Chemico-biological interactions*, 160(1), pp. 1-40.
Venkatachalam, K. and Montell, C. (2007) 'TRP channels', *Annu. Rev. Biochem.*, 76, pp. 387–417.
Venkataraman, R. (2008) 'Role of Transient Receptor Potential Canonical-6 (Trpc6)

Channel in Metastasis of Glioblastoma Multiforme', 6.
Vennekens, R. (2011) 'Emerging concepts for the role of TRP channels in the cardiovascular system', *The Journal of physiology*, 589(7), pp. 1527–1534.
Volpe, P. and Vezu, L. (1993) 'Intracellular magnesium and inositol 1, 4, 5-trisphosphate receptor: molecular mechanisms of interaction, physiology and pharmacology', *Magnesium research*, 6(3), pp. 267–274.
Wagner, G. P., Kin, K. and Lynch, V. J. (2013)'A model based criterion for gene expression calls using RNA-seq data',*Theory in Biosciences*, 132(3), pp. 159–164.
Walker, N. I. *et al.* (1988) 'Patterns of cell death', *Methods and achievements in experimental pathology*, 13, pp. 18–54.
Wang, J. Y. *et al.* (1996) 'Titanium, chromium and cobalt ions modulate the release of bone-associated cytokines by human monocytes/macrophages *in vitro*', *Biomaterials*, 17(23), p. 8.
Wapner, K. L., Morris, D. M. and Black, J. (1986) 'Release of corrosion products by F - 75 cobalt base alloy in the rat. II: Morbidity apparently associated with chromium release in vivo: A 120 - day rat study', *Journal of Biomedical Materials Research*, 20(2), pp. 219–233.
Washburn, T. C., & Kaplan, E. (1964) 'Cobalt therapy and goiter', *Clinical pediatric*s, 3(2), pp. 89-92.
Watanabe, H. *et al.* (2008) 'TRP channel and cardiovascular disease', *Pharmacology and Therapeutics*, 118(3), pp. 337–351.
Watson, L. E. *et al.* (2004) 'Baseline Echocardiographic Values for Adult Male Rats', *Journal of the American Society of Echocardiography*, 17(2), pp. 161–167.
Van der Weegen, W. *et al.* (2014) 'Treatment of pseudotumors after metal-on-metal hip resurfacing based on magnetic resonance imaging, metal ion levels and symptoms', *Journal of Arthroplasty*. Elsevier Inc., 29(2), pp. 416–421.
White, J. P. M. *et al.* (2011) 'Xenon reduces activation of transient receptor potential vanilloid type 1 (TRPV1) in rat dorsal root ganglion cells and in human TRPV1-expressing HEK293 cells', *Life Sciences*. Elsevier Inc., 88(3–4), pp. 141–149.
Wiberg, G. S. *et al.* (1969) 'Factors affecting the cardiotoxic potential of cobalt', *Clinical toxicology*, 2(3), pp. 257–271.
Willert, H.G. (2005) 'Metal-on-Metal Bearings and Hypersensitivity in Patients with Artificial Hip Joints;A Clinical and Histomorphological Study', *The Journal of Bone and Joint Surgery (American)*, 87(1), pp. 28-36.
Winter, J. (1987) 'Characterization of capsaicin-sensitive neurones in adult rat dorsal root ganglion cultures', *Neuroscience letters*, 80(2), pp. 134–140.
Witkiewicz-Kucharczyk, A. and Bal, W. (2006) 'Damage of zinc fingers in DNA repair proteins, a novel molecular mechanism in carcinogenesis', *Toxicology Letters*, 162(1), pp. 29–42.
Wlodkowic, D. *et al.* (2011) 'Apoptosis goes on a chip: Advances in the microfluidic analysis of programmed cell death', *Analytical Chemistry*, 83(17), pp. 6439–6446.
Wolff, N. A. *et al.* (2014) 'Evidence for mitochondrial localization of divalent metal transporter 1 (DMT1)', *The FASEB Journal*, 28(5), pp. 2134–2145.
Woo, D. H. *et al.* (2008) 'Direct activation of Transient Receptor Potential Vanilloid', *Molecular Pain*, 15, pp. 1–15.

Wretenberg, P. (2008) ‘Good function but very high concentrations of cobalt and chromium ions in blood 37 years after metal-on-metal total hip arthroplasy’, *Medical devices (Auckland, N.Z.)*, 1, p. 2.

Wu, L. *et al.* (2015) ‘Global gene expression profile of the hippocampus in a rat model of vascular dementia’, *Tohoku Journal of Experimental Medicine*, 237(1), pp. 57–67.

Xia, Z. *et al.* (2011) ‘Characterization of metal-wear nanoparticles in pseudotumor following metal-on-metal hip resurfacing’, *Nanomedicine: Nanotechnology, Biology, and Medicine*. Elsevier Inc., 7(6), pp. 674–681.

Xue, X. *et al.* (2016) ‘Iron uptake via DMT1 integrates cell cycle with JAK-STAT3 signalling to promote colorectal tumorigenesis’, *Cell metabolism*, 24(3), pp. 447–461.

Yamagata, N., Murata, S. and Torii, T. (1962) ‘The cobalt content of human body’, *Journal of radiation research*, 3(1), pp. 4–8.

Yamaguchi, Y. *et al.* (2017) ‘Role of TRPC3 and TRPC6 channels in the myocardial response to stretch: Linking physiology and pathophysiology’, *Progress in Biophysics and Molecular Biology*. Elsevier Ltd, 130, pp. 264–272.

Yanatori, I. *et al.* (2015) ‘Inhibition of iron uptake by ferristatin II is exerted through internalization of DMT1 at the plasma membrane’, *Cell biology international*, 39(4), pp. 427–434.

Yang, J. and Black, J. (1994) ‘Competitive binding of chromium, cobalt and nickel to serum proteins’, *Biomaterials*, 15(4), pp. 262–268.

Yang, S.-J. *et al.* (2004) ‘Cobalt chloride-induced apoptosis and extracellular signal-regulated protein kinase 1/2 activation in rat C6 glioma cells’, *Journal of biochemistry and molecular biology*, 37(4), pp. 480–486.

Yao, K. *et al.* (2008) ‘Epigallocatechin gallate protects against oxidative stress-induced mitochondria-dependent apoptosis in human lens epithelial cells’, *Molecular Vision*. Molecular Vision, 14, pp. 217–223.

Ye, J. *et al.* (2012) ‘Primer-BLAST: a tool to design target-specific primers for polymerase chain reaction’, *BMC bioinformatics*, 13(1), p. 134.

Yoshida, K. *et al.* (1995) ‘Light - induced CREB phosphorylation and gene expression in rat retinal cells’, *Journal of neurochemistry*, 65(4), pp. 1499–1504.

Yoshiyama, M. *et al.* (1999) ‘Effects of candesartan and cilazapril on rats with myocardial infarction assessed by echocardiography’, *Hypertension*, 33(4), pp. 961–968.

Yousif, M. H. M. *et al.* (2008) ‘Role of Ca2+/calmodulin - dependent protein kinase II in development of vascular dysfunction in diabetic rats with hypertension’, *Cell biochemistry and function*, 26(2), pp. 256–263.

Yu, Y. *et al.* (2009) ‘A functional single-nucleotide polymorphism in the TRPC6 gene promoter associated with idiopathic pulmonary arterial hypertension’, *Circulation*, 119(17), pp. 2313–2322.

Yu, Y. *et al.* (2014) ‘TRPM7 is involved in angiotensin II induced cardiac fibrosis development by mediating calcium and magnesium influx’, *Cell Calcium*, 55(5), pp. 252–260.

Yue, R. *et al.* (2012) ‘Lycopene Protects against Hypoxia/Reoxygenation-Induced Apoptosis by Preventing Mitochondrial Dysfunction in Primary Neonatal Mouse Cardiomyocytes’, *PLoS ONE*, 7(11), p. e50778.

Yue, Z. *et al.* (2013) ‘Transient receptor potential (TRP) channels and cardiac

fibrosis.', *Current topics in medicinal chemistry*, 13(3), pp. 270–82.
Zadnipryany, I. *et al.* (2017) 'Experimental review of cobalt induced cardiomyopathy', *Russian Open Medical Journal*, 6(1), p. e0103.
Zak, R. (1974) 'Development and proliferative capacity of cardiac muscle cells', *Circ. Res.;(United States)*, 35, Suppl, pp. 17–26.
Zampese, E. and Pizzo, P. (2012) 'Intracellular organelles in the saga of Ca2+ homeostasis: different molecules for different purposes?', *Cellular and Molecular Life Sciences*, 69(7), pp. 1077–1104.
Zhang, B., Kirov, S. and Snoddy, J. (2005) 'WebGestalt: an integrated system for exploring gene sets in various biological contexts', *Nucleic acids research*, 33(suppl_2), pp. W741–W748.
Zhang, K. *et al.* (2009) 'Circulating blood monocytes traffic to and participate in the periprosthetic tissue inflammation', *Inflammation research*, 58(12), pp. 837–844.
Zhang, P., Su, J. and Mende, U. (2012) 'Cross talk between cardiac myocytes and fibroblasts : from multiscale investigative approaches to mechanisms and functional consequences', *Am J Physiol Heart Circ Physiol*, 303.
Zhang, R. *et al.* (2005) 'Calmodulin kinase II inhibition protects against structural heart disease', *Nature medicine*, 11(4), pp. 409–417.
Zhang, T. *et al.* (2003) 'The δC isoform of CaMKII is activated in cardiac hypertrophy and induces dilated cardiomyopathy and heart failure', *Circulation research*, 92(8), pp. 912–919.
Zhang, T. (2004) 'Cardiomyocyte Calcium and Calcium/Calmodulin-dependent Protein Kinase II: Friends or Foes?', *Recent Progress in Hormone Research*, 59(1), pp. 141–168.
Zhang, T. *et al.* (2010) 'Hyperbaric oxygen therapy improves neurogenesis and brain blood supply in piriform cortex in rats with vascular dementia', *Brain injury*, 24(11), pp. 1350–1357.
Zhang, T. and Brown, J. H. (2004) 'Role of Ca2+/calmodulin-dependent protein kinase II in cardiac hypertrophy and heart failure', *Cardiovascular Research*, 63(3), pp. 476–486.
Zhang, X.-Y. *et al.* (2012) 'Small interfering RNA targeting HMGN5 induces apoptosis via modulation of a mitochondrial pathway and Bcl-2 family proteins in prostate cancer cells', *Asian Journal of Andrology*, 14(3), pp. 487–492.
Zhang, Y.-H. *et al.* (2012) 'Evidence for functional expression of TRPM7 channels in human atrial myocytes', *Basic Research in Cardiology*, 107(5), p. 282.
Zhao, P. J. *et al.* (2008) 'Effects of chronic hypoxia on the expression of calmodulin and calcicum/calmodulin-dependent protein kinase II and the calcium activity in myocardial cells in young rats', *Zhongguo dang dai er ke za zhi= Chinese journal of contemporary pediatrics*, 10(3), pp. 381–385.
Zhou, Y. *et al.* (2015) 'Effects of angiotensin II on transient receptor potential melastatin 7 channel function in cardiac fibroblasts.', *Experimental and therapeutic medicine*, 9(5), pp. 2008–2012.
Zijlstra, W. P. *et al.* (2017) 'Effect of femoral head size and surgical approach on risk of revision for dislocation after total hip arthroplasty: An analysis of 166,231 procedures in the Dutch Arthroplasty Register (LROI)', *Acta Orthopaedica*, 88(4), pp. 395–401.
Zou, W. *et al.* (2001) 'Cobalt chloride induces PC12 cells apoptosis through reactive

oxygen species and accompanied by AP-1 activation', *Journal of Neuroscience Research*, 64(6), pp. 646–653.
Zywiel, M. G. *et al.* (2013) 'Fatal cardiomyopathy after revision total hip replacement for fracture of a ceramic liner', *Bone Joint J.*, 95B(1), pp. 31–37.
Zywiel, M. G. *et al.* (2016) 'Systemic cobalt toxicity from total hip arthroplasties', *Bone and Joint Journal*, 98B(1), pp. 14–20.

Appendices

A1 Appendix 1 : Buffers and Solutions used

Versene [ethylenediaminetetraacetate (EDTA) solution] at 0.02% (w/v): pH 7.2

The solution was prepared by dissolving the following compounds in 500 ml of distilled water.

NaCl	(4.00 g / 500 ml Distilled water)
KCl	(0.10 g / 500 ml Distilled water)
Na_2HPO_4 (anhydrous)	(0.5835 g / 500 ml Distilled water)
KH_2PO_4	(0.10 g / 500 ml Distilled water)
EDTA	(0.10 g / 500 ml Distilled water)
Phenol red 0.5% (w/v)	(1.5 ml / 500 ml Distilled water)

The solution was made up and sterilized by autoclaving at 15 lb pressure 120°C for 15 min and stored at room temperature. This was then aliquoted into universals (20 ml) and stored at room temperature or 4°C. For checking contamination, 2-3 ml was added to SAB and BHI for at least 72 h at 37°C. If there is contamination, the solutions go cloudy.

Tris buffered saline (TBS) solution for trypsin stock: pH 7.7

The solution was prepared by dissolving the following compounds in 500 ml of distilled water.

NaCl	(4.00 g / 500 ml Distilled water)
D-Glucose	(0.50 g / 500 ml Distilled water)
Na_2PO_4	(0.05 g / 500 ml Distilled water)
Tris	(1.50 g / 500 ml Distilled water)
KCl	(0.19 ml / 500 ml Distilled water)

Phenol red 0.5% (w/v) (1.50 ml / 500 ml Distilled water)

The solution was made up and sterilized by autoclaving at 15 lb pressure 120°C for 15 min and stored at room temperature. This was then aliquoted into universals (20 ml) and stored at room temperature or 4°C. For checking contamination, this was added to SAB and BHI at least 72 h at 37°C.

Trypsin-versene solution (0.05%)

Trypsin-versene solution was made by diluting the trypsin (0.25%) in Tris buffered saline (TBS) 5-fold by adding 20 ml of sterile trypsin solution 2.5% (w/v) to 80 ml of TBS. The solution was then aliquoted into universals (20 ml) and stored at -20°C.

Propidium iodide (PI)

A Stock solution of propidium iodide (PI, 1 mg/ml) in PBS pH 7.4 was diluted to 20 µg/ml by mixing 0.4 ml of PI with 19.6 ml PBS pH7.4 and stored at 4°C.

Carboxyfluorescein diacetate (CFDA)

A Stock solution of Carboxyfluorescein diacetate (CFDA) in DMSO (2.5 mM) was diluted at a ratio of 1:100 by PBS pH 6.75 and stored at -20°C.

Phalloidin-FITC

A stock solution of Phalloidin-FITC was prepared by dissolving Phalloidin-FITC (0.1mg) in 1 ml methanol by carefully injecting methanol directly into the vial of Phalloidin in the fume hood without opening the lid. After that 4 ml of 1% BSA in PBS (1/50 dilution (w/v) 0.1 mg/5 ml) was added, and this was aliquoted into eppendorffs and keep at -20°C in the dark. Prior to use, the stock solutions of Phalloidin-FITC were diluted with PBS at a ratio of 1:10.

4',6-diamidino-2-phenylindole (DAPI)

A stock solution of 4',6-diamidino-2-phenylindole (DAPI) was prepared by dissolving 5 mg of DAPI in 1 ml PBS pH 7.4, and diluted it again to 50 µg/ml in PBS, aliquoted into Eppendorf tubes and kept at -20°C in the dark. Prior to use, the stock solutions of DAPI (50 µg/ml) were diluted with PBS at a ratio of 1:500. The final concentration used for DAPI was 0.6 nM.

Table A1-1 A comparison of units of concentration of $CoCl_2.6H_2O$ (M.W. 237.93).

Unit	Concentration									
µM	0	1	5	10	25	50	100	250	500	1000
mg/L or ppm	0	0.24	1.18	2.38	5.94	11.8	23.79	59.48	118.95	237.93

A2 Appendix 2 (See Chapter3, p. 105 and 130)

Table A2-1 The IC_{50} value of $CoCl_2$ on the 3T3 cell line and cardiac fibroblast cells by the combined assay.

TIME	IC_{50} of Cobalt (II) Chloride (µM)					
	24 h		48 h		72 h	
	3T3s	CFs	3T3s	CFs	3T3s	CFs
MTT	>1000	>1000	370.89±14.67$^{*,\wedge}$	384.54±6.78$^{*,\wedge}$	348.53±4.76$^{*,\wedge}$	400.27±22.83$^{*,\wedge}$
NR	>1000	>1000	741.18±8.97$^{*,\#}$	768.40±10.87$^{*,\#}$	703.76±15.56$^{*,\#}$	710.73±29.05$^{*,\#}$
CV	>1000	>1000	376.95±6.78$^{*,\wedge}$	387.43±5.46$^{*,\wedge}$	309.66±6.95$^{*,\wedge}$	337.55±14.54$^{*,\wedge}$

Data represent mean ± SEM and Statistical analysis was carried out using one-way-ANOVA with post hoc Dunnett's comparison (n = 3, $^{*}p<0.05$ with a significant difference to control, $^{\#}p<0.05$ with a significant difference to MTT assay, $\wedge p<0.05$ with a significant difference to NR assay. h, hours; SEP, separate assays; COMB, combined assay. There were no significant differences between the 3T3 cells and CFs for each respective time point (using two-sample t-test).

A3 Appendix 3 (See Chapter 3, p.110, 114 and 115)

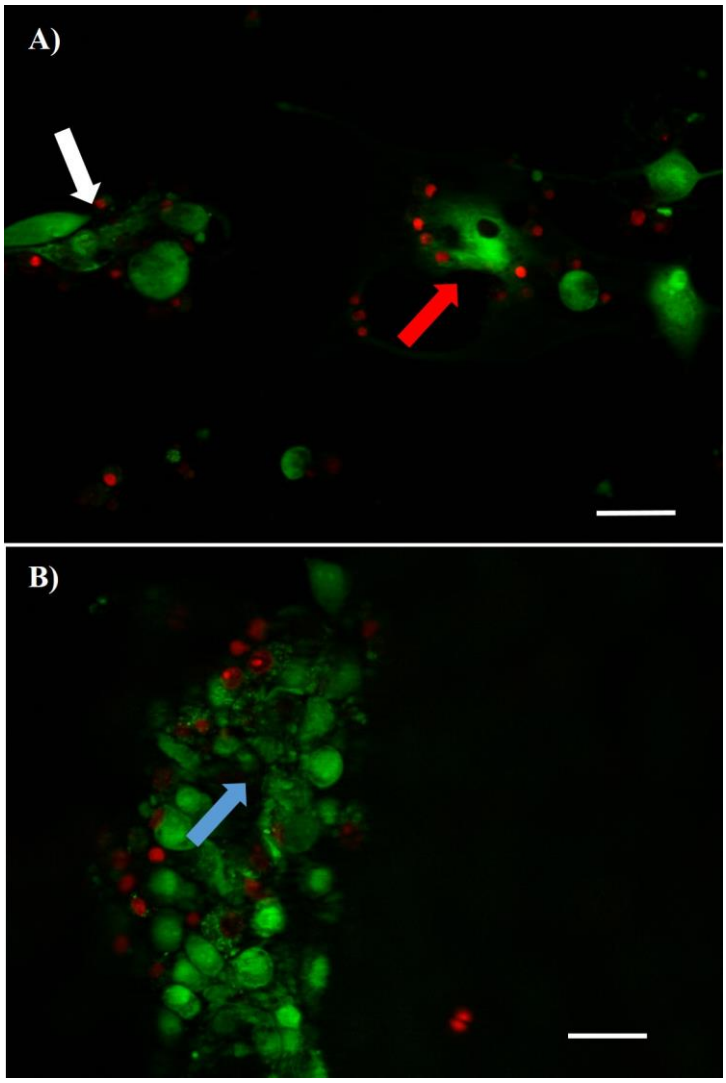

Figure A3-1 Magnified views from Figure 3-10, showing viability of the 3T3 cell line. Live and dead cells simultaneously stained with carboxyfluorescein diacetate (CFDA) and with propidium iodide (PI). CFDA staining of live cells (green) and PI staining of nucleus in dead cells (red) (Bar= 100 µM). A) Red arrows indicate vacuoles occurring in cell. White arrows show cell debris. B) Blue arrows indicate broken nuclei. The Images were obtained using 20X objective lens.

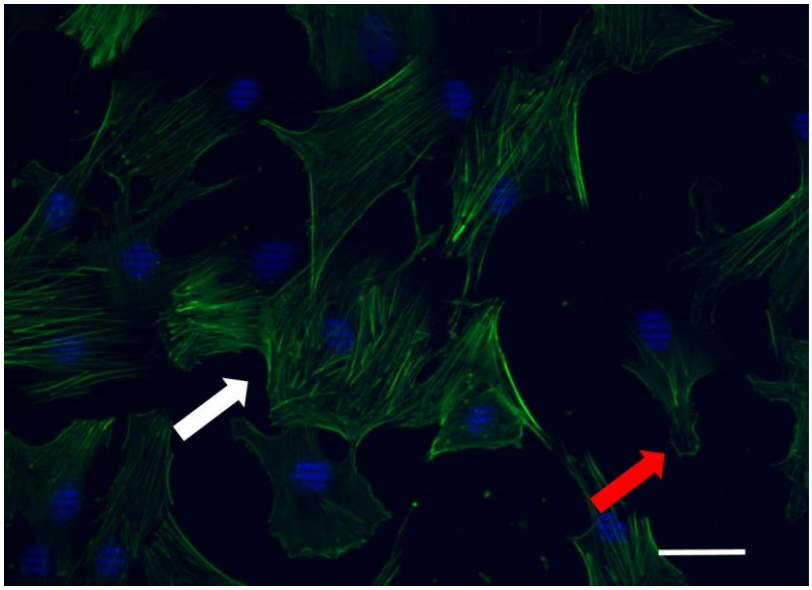

Figure A3-2 Magnified views from Figure 3-12, staining of F-actin filaments of cardiac fibroblasts (CFs). Changes in the actin cytoskeleton were verified by Phalloidin-FITC staining of actin fibres (green) and DAPI staining of the nucleus in cells (blue). (Bar= 100 µM). Red arrows show blebbed cells. White arrows show broken cytoskeleton in cells. Images were obtained using a 20X objective lens.

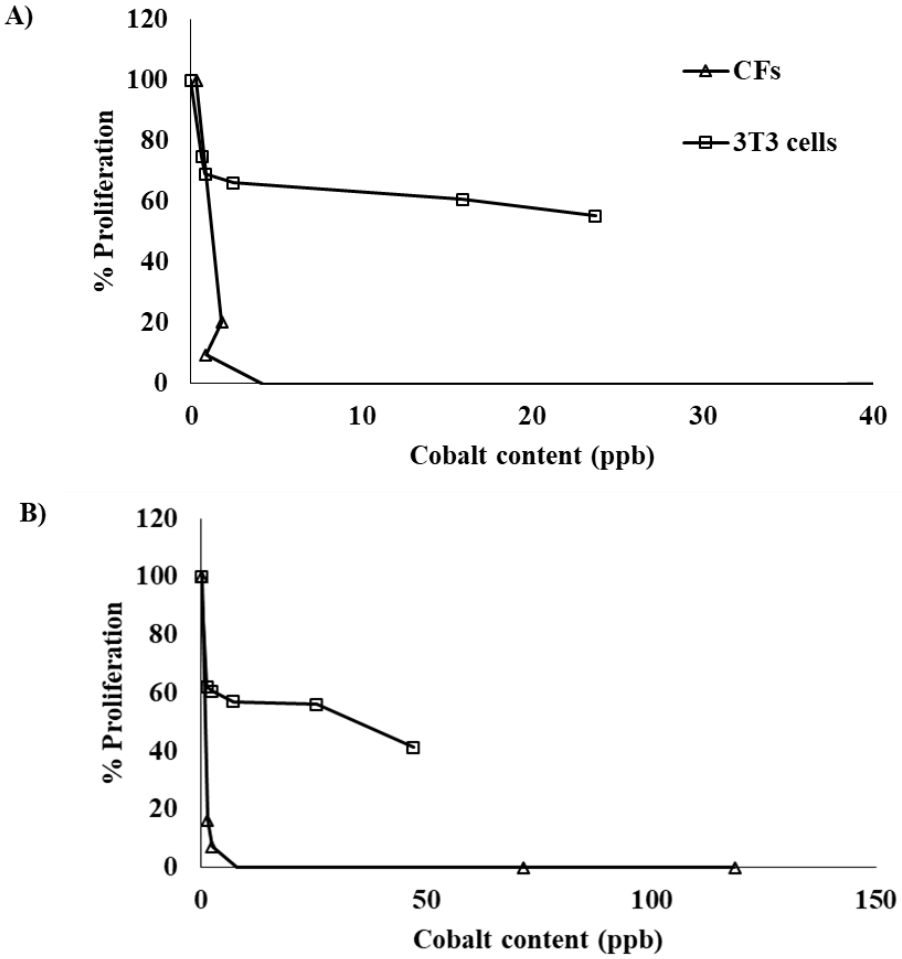

Figure A3-3 Cellular cobalt uptake versus cell proliferation. CFs and 3T3 cells were treated with the various concentration of $CoCl_2$ after incubation for (A) 48 h and (B) 72 h. Total intracellular uptake was measured by ICP-MS and the BrdU assay measured cell proliferation. Results reveal a dissimilar gradient between the two cell types. Increasing the time of exposure from 48 to 72 h results in a similar pattern of the effect on proliferation versus cobalt content.

A4 Appendix 4 : RNA Sequencing (See Chapter 6, p. 200)

Table A4-1 MIQE checklist for authors, reviewers and editors. All essential information (E) must be submitted with the manuscript. Desirable information (D) should be submitted if possible. If using primers obtained from RTPrimerDB, information on qPCR target, oligonucleotides, protocols and validation is available from that source.

The MIQE Checklist for qPCR[a]		
Item to check	**Important**	**Checklist**
Experimental design		
Definition of experimental and control groups	E	✓
Number within each group	E	✓
Assay carry out by core lab or investigator's lab?	D	✓
Acknowledgement of authors' contributions	D	-
Sample		
Description	E	✓
Volume/mass of sample processed	D	✓
Microdissection or macrodissection	E	N/A
Processing procedure	E	✓
If frozen, how and how quickly?	E	✓
If fixed, with what and how quickly?	E	N/A
Sample storage conditions and duration (especially for FFPE samples)	E	✓
Nucleic acid extraction		
Procedure and/or instrumentation	E	✓
Name of kit and details of any modifications	E	✓
Source of additional reagents used	D	✓
Details of DNase or RNase treatment	E	✓
Contamination assessment (DNA or RNA)	E	✓
Nucleic acid quantification	E	✓
Instrument and method	E	✓
Purity(A_{260}/A_{280})	D	✓
Yield	D	✓
RNA integrity method/instrument	E	✓
RIN/RQI or C_q of 3' and 5' transcripts	E	✓
Electrophoresis traces	D	✓
Inhibition testing (C_q dilutions, spike or other)	E	-
Reverse Transcription		
Complete reaction conditions	E	✓
Amount of RNA and reaction volume	E	✓
Priming oligonucleotide (if using GSP) and concentration	E	✓
Priming transcriptase and concentration	E	✓
Temperature and time	E	✓
Manufacturer of reagents and catalogue numbers	D	✓
C_qs with and without RT	D*	✓
Storage conditions od cDNA	D	✓
qPCR Target Information		
If multiplex, efficiency and LOD of each assay	E	N/A
Sequence accession number	E	✓
Location of amplicon	D	-
Amplicon length	E	✓
In silico specificity screen (BLAST, etc)	E	✓
Pseudogenes, retropseudogenes or other homologs?	D	-
Sequence alignment	D	✓

Table A4-1 MIQE checklist for authors, reviewers and editors(cont.).

The MIQE Checklist for qPCR[a] (cont.)		
Item to check	**Important**	**Checklist**
qPCR Target Information (cont.)		
Secondary structure analysis of amplicon	D	-
Location of each primer by exon or intron (If applicable)	E	-
What splice variants are targeted?	E	-
qPCR Oligonucleotides		
Primer sequences	E	✓
RTPrimerDB Identification Number	D	-
dProbe sequences	D**	-
Location and identify of any modifications	E	N/A
Manufacturer of oligonucleotides	D	✓
Purification method	D	-
qPCR Protocol		
Complete reaction conditions	E	✓
Reaction volume and amount of cDNA/DNA	E	✓
Primer, (probe), Mg^{++} and dNTP concentrations	E	✓
Polymerase identity and concentration	E	✓
Buffer/kit identity and manufacturer	E	✓
Exact chemist constitution of the buffer	D	-
Additives (SYBR Green I, DMSO, etc.)	E	-
Manufacturer of plates/tubes and catalog number	D	✓
Complete thermocycling parameters	E	✓
Reaction setup (manual/robotic)	D	-
Manufacturer of qPCR instrument	E	✓
qPCR Validation		
Evidence of optimization (from gradients)	D	-
Specificity (gel, sequence, melt, or digest)	E	✓
For SYBR Green I, C_q of the NTC	E	✓
Standard curves with slope and y-intercept	E	-
PCR efficiency calculated from slope	E	-
Confidence interval for PCR efficiency or standard error	D	-
R^2 of standard curve	E	-
Linear dynamic range	E	-
Cq variation at lower limit	E	-
Confidence intervals throughout range	D	-
Evidence for limit of detection	E	-
If multiplex, efficiency and LOD of each assay	E	N/A
Data Analysis		
qPCR analysis program (source, version)	E	✓
Cq method determination	E	-
Outlier identification and disposition	E	-
Results of NTCs	E	✓
Justification of number and choice of reference genes	E	✓
Description of normalisation method	E	✓
Number and concordance of biological relicates	D	✓
Number and stage(RT and qPCR) of technical replicates	E	✓
Repeatability (intra-assay variation)	E	✓
Reproducibility(inter-assay variation, %CV)	D	-
Power analysis	D	-
Statistical methods for result significance	E	✓
Software(source, version)	E	✓
Cq or raw data submission using RDML	D	N/A

Table A4-1 MIQE checklist for authors, reviewers and editors (cont.).

This MIQE checklist for authors, reviewers and editors was designed and produced by Bustin (Bustin et al., 2010). *Assessing the absence of DNA using a no RT assay is essential when first extracting RNA. Once the sample has been validated as DNA-free, inclusion of a no-RT control is desirable, but no longer essential.** Disclosure of the probe sequence is highly desirable and strongly encouraged. FFPE, formalin-fixed, paraffin-embedded; RIN, RNA integrity number; RQI, RNA quality indicator; GSP, gene-specific priming; dNTP, deoxynucleoside triphosphate.

A5 Appendix 5 : RNA Sequencing (See Chapter 6, p.206 and 210)

Table A5-1 Selected gene list of 3T3 cells after Co exposure at 1 and 10 µM.

Cluster	Up- and Down- regulated genes
C1	*Nfkbie*; nuclear factor of kappa light polypeptide gene enhancer in B cells inhibitor, epsilon *Shc4*; SHC (Src homology 2 domain containing) family, member 4 *Kcnk2*; potassium channel, subfamily K, member 2 *Eif3j1*; eukaryotic translation initiation factor 3, subunit J1 *Moap1*; Modulator of apoptosis 1 *Pcdha8*; Protocadherin alpha 8 *Mmrn2*; Multimerin-2
C2	*Ccl6*; chemokine (C-C motif) ligand 6 *Tfrc*; transferrin receptor *Bnip3*; BCL2/adenovirus E1B interacting protein 3 *Galnt4*; polypeptide N-acetylgalactosaminyltransferase 4 *Tlr6*; toll-like receptor 6 *Egr1*; early growth response *Apln*; apelin
C4	*Ddit3*; DNA-damage inducible transcript 3 *Gadd45b*; growth arrest and DNA-damage-inducible 45 beta *Pim1*; proviral integration site 1 *Rpl37*; ribosomal protein L37 *Rps29*; ribosomal protein S29 *Dpm3*; dolichyl-phosphate mannosyltransferase polypeptide 3 *St3gal6*; ST3 beta-galactoside alpha-2,3-sialyltransferase 6 *Ccl8*; chemokine (c-c motif) ligand 8 *Arrdc4;* arrestin domain containing 4 *Ung*; uracil dna glycosylase *Sdf2l1;* stromal cell-derived factor 2-like 1 *Siva1*; siva1, apoptosis-inducing factor *Galnt13;*polypeptide N-acetylgalactosaminyltransferase 13 *Hsd17b4*; hydroxysteroid (17-beta) dehydrogenase 4 *Tpi1*; triosephosphate isomerase 1 *Col4a6*; collagen type IV alpha 6 chain

Table A5-1 Selected gene list of 3T3 cells after Co exposure at 1 and 10 μM (cont.).

Cluster	Cluster	Cluster	Cluster
C3	*A4galt*; alpha 1,4-galactosyltransferase *Acadm*; acyl-Coenzyme A dehydrogenase, medium chain *Adam15*; a disintegrin and metallopeptidase domain 15 (metargidin) *Adam9*; a disintegrin and metallopeptidase domain 9 (meltrin gamma) *Adamts1*; a disintegrin-like and metallopeptidase (reprolysin type) with thrombospondin type 1 motif, 12 *Ak4*; adenylate kinase 4 *Asph*; aspartate-beta-hydroxylase *C1rb*; complement component 1, r subcomponent b *Calcrl*; calcitonin receptor-like *Ccl28*; chemokine (C-C motif) ligand 28 *Cdh2*; cadherin 2 *Cdon*; cell adhesion molecule-related/down-regulated by oncogenes *Cdsn*; corneodesmosin *Clec3b*; c-type lectin domain family 3, member b *Clstn1*; calsyntenin 1 *Col3a1*; collagen, type iii, alpha 1 *Col4a6*; collagen, type IV, alpha 6 *Col5a1*; collagen, type v, alpha 1 *Col5a3*; collagen, type v, alpha 3 *Csgalnact1*; chondroitin sulfate N-acetylgalactosaminyltransferase 1 *Cth*; cystathionase (cystathionine gamma-lyase)	C3	*Cx3cl1*; chemokine (c-x3-c motif) ligand 1 *Dhrs9*; dehydrogenase/reductase (SDR family) member 9 *Edil3*; egf-like repeats and discoidin i-like domains 3 *Egln1*; egl-9 family hypoxia-inducible factor 1 *Egln3*; egl-9 family hypoxia-inducible factor 3 *Ehd2*; EH-domain containing 2 *Ehd3*; EH-domain containing 3 *Emilin1*; elastin microfibril interfacer 1 *Eno1b*; enolase 1B, retrotransposed *Erbb3*; erb-b2 receptor tyrosine kinase 3 *Etv5*; ets variant gene 5 *Ext2*; exostoses (multiple) 2 *Fbln5*; fibulin 5 *Flrt2*; fibronectin leucine rich transmembrane protein 2 *Galnt13*; polypeptide N-acetylgalactosaminyltransferase 13 *Galnt7*; polypeptide N-acetylgalactosaminyltransferase 7 *Gamt*; guanidinoacetate methyltransferase *Gapdh*; glyceraldehyde-3-phosphate dehydrogenase *Gbe1*; glucan (1,4-alpha-), branching enzyme 1 *Gnpda1*; glucosamine-6-phosphate deaminase 1 *Gys1*; glycogen synthase 1, muscle *Hlcs*; holocarboxylase synthetase (biotin- [propriony-Coenzyme A-carboxylase (ATP-hydrolysing)] ligase) *Hsd17b4*; hydroxysteroid (17-beta) dehydrogenase 4 *Hsd17b7*; hydroxysteroid (17-beta) dehydrogenase 7 *Irak4*; interleukin-1 receptor-associated kinase 4

Table A5-1 Selected gene list of 3T3 cells after Co exposure at 1 and 10 μM (cont.).

Cluster	Cluster	Cluster	Cluster
C3	*Itgav*; integrin alpha V *Ldha*; lactate dehydrogenase A *Lepre1*; leprecan 1 *Leprel2*; leprecan-like 2 *Lgals3bp*; lectin, galactoside-binding, soluble, 3 binding protein *Man1c1*; mannosidase, alpha, class 1C, member 1 *Man2a1*; mannosidase 2, alpha 1 *Mgat2*; mannoside acetylglucosaminyltransferase 2 *Mmab*; methylmalonic aciduria (cobalamin deficiency) cblB type homolog (human) *Negr1*; neuronal growth regulator 1 *P4ha1*; procollagen-proline, 2-oxoglutarate 4-dioxygenase (proline 4-hydroxylase), alpha 1 polypeptide *P4ha2*; procollagen-proline, 2-oxoglutarate 4-dioxygenase (proline 4-hydroxylase), alpha II polypeptide *Pcdha12*; protocadherin alpha 12 *Pcdhb20*; protocadherin beta 20 *Pcdhb21*; protocadherin beta 21 *Pcdhb9*; protocadherin beta 9 *Pdk1*; pyruvate dehydrogenase kinase, isoenzyme 1 *Pfkl*; phosphofructokinase, liver, B-type *Pgam1*; phosphoglycerate mutase 1 *Pgm2*; phosphoglucomutase 2	C3	*Pip5k1c*; phosphatidylinositol-4-phosphate 5-kinase, type 1 gamma *Plcb3*; phospholipase C, beta 3 *Plod1*; procollagen-lysine, 2-oxoglutarate 5-dioxygenase 1 *Plod2*; procollagen lysine, 2-oxoglutarate 5-dioxygenase 2 *Polr3g*; polymerase (RNA) III (DNA directed) polypeptide G *Prkab2*; protein kinase, AMP-activated, beta 2 non-catalytic subunit *Pros1*; protein s (alpha) *Rcn2*; reticulocalbin 2 *Shc4*; SHC (Src homology 2 domain containing) family, member 4 *Sned1*; sushi, nidogen and egf-like domains 1 *Spon2*; spondin 2, extracellular matrix protein *St3gal5*; ST3 beta-galactoside alpha-2,3-sialyltransferase 5 *Stat6*; signal transducer and activator of transcription 6 *Stim2*; stromal interaction molecule *Suox*; sulfite oxidase *Tenm4*; teneurin transmembrane protein 4 *Tpi1*; triosephosphate isomerase 1 *Tpk1*; thiamine pyrophosphokinase *Tyk2*; tyrosine kinase 2 *Ugt1a6a*; UDP glucuronosyltransferase 1 family, polypeptide A6A *Wdr19*; wd repeat domain 19 *Wisp1*; wnt1 inducible signalling pathway protein 1